

Electronic Thesis and Dissertation Repository

8-3-2017 12:00 AM


Ultrasonic Techniques for Characterization of Oil-Water Emulsion and Monitoring of Interface in Separation Vessels

Embark Alshaafi
The University of Western Ontario

Supervisor
Anand Prakash
The University of Western Ontario

Graduate Program in Chemical and Biochemical Engineering
A thesis submitted in partial fulfillment of the requirements for the degree in Master of Engineering Science
© Embark Alshaafi 2017

Follow this and additional works at: <https://ir.lib.uwo.ca/etd>

 Part of the [Petroleum Engineering Commons](#), and the [Process Control and Systems Commons](#)

Recommended Citation

Alshaafi, Embark, "Ultrasonic Techniques for Characterization of Oil-Water Emulsion and Monitoring of Interface in Separation Vessels" (2017). *Electronic Thesis and Dissertation Repository*. 4738.
<https://ir.lib.uwo.ca/etd/4738>

This Dissertation/Thesis is brought to you for free and open access by Scholarship@Western. It has been accepted for inclusion in Electronic Thesis and Dissertation Repository by an authorized administrator of Scholarship@Western. For more information, please contact wlsadmin@uwo.ca.

Abstract

Emulsions created at different stages of crude oil production and processing present a number of problems and challenges. There is need to monitor emulsion layer in separation vessel to avoid its ingress into separated oil or water phases. It is also important to study role of different impurities and conditions on emulsion stability which determines the ease or difficulty on its breakup to separate the individual phases. There is also need to have a good understanding of emulsion rheology and effect of different variables on its flow behavior. There is currently a lack of suitable technique to monitor emulsion layer in separation vessels due to problems such as fouling, opacity and variable nature of crude oil composition and presence of impurities.

The first stage of this work, intended to develop an ultrasonic technique for on-line process monitoring to track and characterize emulsion phase generated during production and cleaning of crude oil. Ultrasonic based techniques have been explored to monitor interface position between water and emulsion layers and oil and emulsion layers in separation vessels. This study tested the potential of ultrasonic techniques for monitoring separation of water, oil and emulsion phases. The oil phase consisted of either mineral oil or crude oil and water content of their emulsion was between 20 to 40%. The tests were conducted in a 4-inch diameter and 20-inch tall column. Measurements of acoustic velocity, pulse attenuation were made with a 3.5 MHz frequency probe operating in through transmission mode. The presence of a phase a phase type at a probe location was easily and quickly identified by changes in either acoustic velocity, attenuation or their combination. In the emulsion layer, acoustic properties are observed to depend on droplet size and their

concentration. A significant change in signal either from oil to emulsion or from water to emulsion was observed and demonstrated the potential of the technique for such operations.

The second phase of this project, investigates potential of ultrasonic techniques to characterize water-in-oil emulsions using and compares with other methods. The emulsions were prepared with mineral oil and crude oil samples and the effects of different variables including mixing intensities, temperature, surfactant and fine solid particles concentrations have been observed. The emulsion mixtures prepared with samples of light and heavy crude oil investigated effects of asphaltene concentration on emulsion stability. The emulsions were characterized for their stability, droplet size distribution and rheology. Emulsion droplet structure is observed with optical microscopy and stability is examined by separation of water phase with time and its composition changes were tracked by ultrasonic techniques. The ultrasonic parameters recorded are changes in acoustic velocity, signal attenuation and its frequency spectrum. The ultrasonic probe captured the variation of droplet concentration of dispersed water phase in the emulsion with time.

The final stage of this investigation, studies the rheological behavior of various emulsions in terms of providing a better understanding. This rheological study consists of several factors including mixing speed, shear rate, shear stress, temperature, pH, salt content; solid particle, addition of surfactants concentration, and droplet average diameter have been studied. It has been designed in order to provide an understanding of water-in-oil emulsion flow behavior and contribute to technological developments to oil production problems specific to this crude.

Keywords

Ultrasonic techniques, Mineral Oil, Crude oil, Crude desalting, Emulsion characterization, Emulsion stability, Droplet size distribution, Mixing speed, Rheological behavior.

Co-Authorship Statement

Chapters 3, 4, and 5 are manuscripts to be submitted to peer-reviewed journals for consideration of publication. The contribution of each author is state below.

Chapter 3:

Ultrasonic based techniques to monitor interface position in oil, water and emulsion separation.

Authors: *Embark Alshaafi, Anand Prakash**

Status: To be submitted to **Fuel Processing Technology**

Embark Alshaafi and Hanning Lie performed experimental work and data analysis. Drs. Anand Prakash provided supervision and consultation regarding the experimental work and interpretation of the results. The manuscript was drafted by Embark Alshaafi, and reviewed and revised by Anand Prakash and Sean Mercer.

Chapter 4:

Characterization of water-in-oil emulsions by ultrasonic techniques

Authors: *Embark Alshaafi, Anand Prakash **

Status: To be submitted to **Petroleum Science and Engineering**

Embark Alshaafi performed experimental work and data analysis. Dr. Anand Prakash provided supervision and consultation regarding the experimental work and interpretation of the results. The manuscript was drafted by Embark Alshaafi, and reviewed and revised by Anand Prakash.

Chapter 5:

Characterization of rheological properties of Water-in-Oil Emulsion

Authors: *Embark Alshaafi, Anand Prakash* *

Status: To be submitted to **Journal of Petroleum Science and Engineering**.

Embark Alshaafi performed experimental work and data analysis. Dr. Anand Prakash provided supervision and consultation regarding the experimental work and interpretation of the results. The manuscript was drafted by Embark Alshaafi, and reviewed and revised by Anand Prakash.

Acknowledgments

First of all, all praise be to Allah, the most gracious and the most merciful, who gave me the strength and patience to achieve this effort.

I would like to express my sincere thanks to my supervisor Dr. A. Prakash, for his support and guidance on my thesis work and his enduring commitment and, without his deep trust and persistent help, this work would have never been possible.

I also acknowledge the efforts and support of the administrative staff, friends, and colleagues for their assistance and helpful discussion during my work at the Western University.

I extend further thanks to my parents, my brothers, and my sisters for their support, encouragement, and unconditional love. Finally, I want to thank my wife, my daughter “**Yaqeen**” for her incredible love, support, sacrifices and patience during my time as a master student.

I also would like to thank Libyan Scholarship program for providing a graduate studies scholarship.

Table of Contents

Abstract	i
Co-Authorship Statement.....	iii
Acknowledgments.....	v
Table of Contents	vi
List of Tables	xi
List of Figures	xii
List of Appendices	xviii
Nomenclature	xix
Greek Letters.....	xx
Chapter 1	1
1 General Introduction	1
1.1 Introduction.....	1
1.2 Thesis Objectives and Scopes	4
1.3 Overview of the present work.....	5
References.....	6
Chapter 2.....	7
2. Literature Review.....	7
2.1 Emulsion Formations and Classification	8
2.1.1 Emulsion Formation.....	8
2.1.2 Classification of Emulsions	9
2.2 Emulsion Stability.....	10
2.2.1 Creaming/Sedimentation.....	12
2.2.2 Flocculation.....	13

2.2.3	Coalescence.....	14
2.2.4	Phase Inversion	15
2.2.5	Ostwald Ripening (Disproportionation)	16
2.3	Emulsifying agents.....	17
2.3.1	Surfactants.....	17
2.3.2	Asphaltenes	19
2.3.3	Resins	20
2.3.4	Fine solid particles	20
2.4	Demulsification.....	23
2.4.1	Chemical demulsification	24
2.4.2	Electrical demulsification	26
2.4.3	Thermal demulsification	26
2.5	Types of Fluid Behavior	28
2.6	Emulsion characterization techniques.....	33
2.6.1	Microscopy	33
2.6.2	Light scattering	35
2.6.3	Nuclear Magnetic Resonance (NMR).....	36
2.6.4	Coulter Counter.....	37
2.6.5	Ultrasonic Techniques	38
	References	40
Chapter 3	45
3	Ultrasonic based techniques to monitor interface position in oil, water and emulsion separation.....	45
3.1	Introduction.....	46
3.2	Materials and Methods.....	47

3.3	Result and discussion	49
3.3.1	Selection of Probe Design and Configuration.....	49
3.3.2	Attenuation coefficient.....	55
3.3.3	Acoustic velocity	56
3.3.4	Tests with the probe to monitor interface position	59
3.3.4.1	Ultrasonic signals at water-emulsion interface.....	62
3.3.4.2	Ultrasonic signals at water-oil interface – no emulsion phase	63
3.3.5	Tests with Crude Oil Samples.....	66
3.3.6	Statistical Analysis.....	67
3.3.7	Local Variations inside the emulsion phase layer.....	69
3.3.8	Proposed probe configuration to monitor emulsion layer position.....	72
3.4	Conclusions.....	73
	References.....	74
	Appendix A.....	76
	Chapter 4.....	79
4.	Characterization of water-in-oil emulsions by ultrasonic techniques	79
4.1	Introduction.....	80
4.2	Experimental Details.....	83
4.2.1	Materials and Methods.....	83
4.2.2	Experimental Setup.....	84
4.3	Calculation of Acoustic Parameters	86
4.4	Results and Discussion	88
4.4.1	Emulsion Stability Tests with Mineral Oil	89
4.4.1.1	Effect of Agitation Intensity on Emulsion Stability	90
4.4.1.2	Average Droplet Size from Water Separation Rate.....	93

4.4.1.3	Acoustic Velocity in Emulsions	94
4.4.1.4	Effects of Fine Particles on Emulsion Stability	96
4.4.2	Investigations with Crude Oil Emulsions	97
4.4.2.1	Droplet Size Distribution.....	99
4.4.2.2	Calibration Curve to Determine Water Fraction from Velocity.....	101
4.4.2.3	Effect of de-emulsifier on water separation	102
4.4.2.4	Effects of Fine Particles on Light Crude Emulsion Stability	103
4.4.2.5	Comparison of Light and Heavy Crude Oils	105
4.4.2.6	Effect of Diluting Crude Oil with n-heptane	109
4.5	Conclusions.....	113
References	114
Appendix B	116
Chapter 5	125
5.	Characterization of rheological properties of Water-in-Oil Emulsion	125
5.1	Introduction.....	125
5.2	Materials and methods	126
5.2.1	Materials	126
5.2.2	Apparatus and experimental procedure.....	127
5.2.3	Asphaltene Extraction.....	129
5.2.4	Blending of crude oil samples.....	129
5.2.5	Preparation of Emulsion	131
5.3	Results and discussion	132
5.3.1	Rheological Properties of Mineral Oil Emulsions	132
5.3.2	Effect of mixing speed on droplet size	138
5.4	Rheological properties of crude oil emulsions.....	141

5.4.1	Emulsions of light and heavy crude oil mixtures.....	147
5.4.2	Effect of dispersed phase volume fraction.....	152
5.4.3	Effect of fine solid particles.....	153
5.4.4	Effect of Surfactant concentration.....	155
5.5	Modelling of emulsion flow behavior.....	157
5.5.1	Estimation of non-Newtonian models parameters.....	157
5.5.2	Comparison of predicted and experimental data.....	164
5.5.3	Validation of the Results.....	167
5.6	Conclusions.....	169
	References.....	170
	Appendix C.....	173
	Chapter 6.....	183
6	Conclusions and Recommendations.....	183
6.1	Conclusions.....	183
6.2	Recommendations.....	184
	Curriculum Vitae.....	185

List of Tables

Table 2-1 Some flow models for describing shear stress (τ) versus shear rate (γ).	32
Table 3-1 Acoustic impedance and reflection coefficient values for different materials used	51
Table 3-2 Ultrasonic properties in water, oil and emulsion phase	58
Table 4-1 Physical properties of different oil used for emulsion preparation.....	89
Table 5-1 Physicochemical properties of different oil samples	130
Table 5-2 Some flow models for describing shear stress (τ) versus shear rate (γ).	157
Table 5-3 Different types of water –in- oil emulsions used in this study	158
Table 5-4 Determination of n and k values for both model.	160
Table 5-5 Validation of the results of power law, HB, and Casson models.	168

List of Figures

Figure 2-1 W/O Emulsion (a), O/W Emulsion (b). (Khan et al., 2011).....	10
Figure 2-2 Emulsion destabilization mechanism (Binks and Horozov, 2006)	12
Figure 2-3 a schematic on the proposed phase inversion mechanism by Arirachakaran et al. (1989).	16
Figure 2-4 Schematic representation of (a) structure of surfactant, (b) surfactant molecules at the interface, and (c) spherical surfactant micelles. (Pichot, 2010)	18
Figure 2-5 Mechanism of emulsion stabilization by asphaltenes.	20
Figure 2-6 possible distributions of coarse and fine solids in an emulsion.	23
Figure 2-7 Shear stress vs Shear rate for various fluids behaviors.	28
Figure 2-8 Pseudo plastic fluid behavior (Pal et al, 1991).....	30
Figure 2-9 Plot of $(\dot{\gamma})^{0.5}$ versus $(\tau)^{0.5}$ for an emulsion that follows the Casson model.	31
Figure 3-1 Schematic diagram of interface position monitoring system with ultrasonic technique	49
Figure 3-2 Details of probe design selected for measurements	52
Figure 3-3 Comparison of acquired signal peak heights obtained in different media	53
Figure 3-4 Peak heights obtained in crude oil emulsions prepared at different mixing speeds	53
Figure 3-5 Photomicrographs of water-in-crude oil emulsions generated at different RPM: a) 500 rpm, b) 700 rpm, c) 800 rpm	55
Figure 3-6 Attenuation values based on peak heights of Figure 23	56

Figure 3-7 Variation of attenuation with location in the layer near the oil-emulsion interface (emulsion: 80% mineral oil in water)	60
Figure 3-8 Signal changes when probe moving from oil phase to emulsion	61
Figure 3-9 Variation of velocity with location in the layer near the oil-emulsion interface (emulsion: 60% mineral oil in water)	62
Figure 3-10 Variation of velocity with location in the layer near the water-emulsion interface (emulsion: 80% mineral oil in water)	63
Figure 3-11 Variation of acoustic velocity with location in the layer near the water-oil interface (Temp. = 21.5 °C)	64
Figure 3-12 Variation of attenuation with location in the layer near the water-oil interface	64
Figure 3-13 Records of amplitude (a) attenuation (b) obtained by raising and lowering of interface between water and emulsion phase	66
Figure 3-14 Variation of attenuation with location in the layer near the crude oil-emulsion	66
Figure 3-15 Variation of velocity with location in the layer near the oil-emulsion interface.....	67
Figure 3-16 Attenuation derived standard deviations in the emulsion and oil layers near the Oil-emulsion interface (emulsion: 80% oil).....	68
Figure 3-17 Acoustic velocity derived standard deviations in the two layers (emulsion: 80% oil).....	69
Figure 3-18 Pictographs of emulsion samples collected from top and bottom parts of emulsion layer	70
Figure 3-19 Droplet size distributions in top and bottom sections of emulsion layer.	70

Figure 3-20 Attenuations near top and bottom locations in emulsion layer	71
Figure 3-21 Acoustic velocity at top and bottom locations in the emulsion layer.....	72
Figure 3-22 Schematic of proposed ultrasonic based instrumentation to monitor emulsion layer position in a separation vessel.....	73
Figure 4-1 Range of acoustic frequencies used for different applications.....	83
Figure 4-2 Schematic diagram of the experimental setup for emulsion characterization.	86
Figure 4-3 Example of an ultrasonic signal captured by the receiver and displayed on screen.	87
Figure 4-4 Records of water separation and ultrasonic attenuation in water-mineral oil emulsions prepared with and without emulsifier	90
Figure 4-5 Records of separated water and ultrasonic attenuation over 24 hour period...	91
Figure 4-6 Droplet size distribution of emulsions prepared at different mixing speeds ...	92
Figure 4-7 Comparison of average droplet size and emulsion stability.....	93
Figure 4-8 Records of water resolution and ultrasonic velocity obtained with mineral oil emulsions	94
Figure 4-9 Effect of fine solid particles on water separation ultrasonic attenuation in emulsions of mineral oil.....	96
Figure 4-10 Effect of fine solid particles on water separation ultrasonic attenuation in emulsions of mineral oil.....	97
Figure 4-11 Records of water separation and ultrasonic attenuation in emulsions of light crude oil	98

Figure 4-12 Droplet size distribution in emulsions of water-in-light crude oil at different mixing speeds.....	100
Figure 4-13 Photomicrographs of freshly prepared water-in- light crude oil emulsions (at 10x)	100
Figure 4-14 Records of water separation and acoustic velocity in emulsions of light crude oil	101
Figure 4-15 Calibration curve to determine water fraction based on measured acoustic velocity in emulsions of crude oil	102
Figure 4-16 Records of water separation and ultrasonic attenuation in emulsions of light crude oil prepared with and without de-emulsifier.	103
Figure 4-17 Records of water separation and ultrasonic velocity in emulsions of light crude oil prepared with fine solid particles in crude oil.....	104
Figure 4-18 Comparison of water resolution and acoustic parameters in emulsions of light and heavy crude oil samples (a), attenuation and (b), acoustic velocity.	106
Figure 4-19 Comparison of water resolution and acoustic parameters in emulsions of light and heavy crude oil mixtures (a), attenuation and (b), acoustic velocity.....	107
Figure 4-20 Effect of asphaltene content on water resolution and acoustic parameters in crude oil (a), velocity and (b) attenuation.	108
Figure 4-21 Impact of diluting crude samples with heptane on water separation and attenuation (a), acoustic velocity (b).....	110
Figure 4-22 Photomicrographs of freshly prepared water-in-oil emulsions at 10x with different heptane dilutions	111
Figure 4-23 Droplet size distributions obtained in emulsions of crude oil and diluted crude with 25 wt % heptane	112

Figure 4-24 Effect of heptane addition on the viscosity of crude oil dispersions.....	113
Figure 5-1 Schematic diagram of the experimental setup for emulsion characterization.	128
Figure 5-2 Schematic diagram of the experimental setup for asphaltene extraction.	130
Figure 5-3 Rheo-gram of mineral oil at different temperatures.....	132
Figure 5-4 Relationship between viscosity and shear rate obtained in mineral oil.....	133
Figure 5-5 Shear stress versus shear rate for different types of fluids	134
Figure 5-6 Rheo-grams of water-in-mineral oil emulsions for different temperatures and mixing speed	136
Figure 5-7 Relationship between shear rate and viscosity in emulsions of mineral oil at different temperatures.	138
Figure 5-8 Droplet size distribution in water-in-mineral oil emulsions prepared at.....	139
Figure 5-9 Images of mineral oil emulsion samples prepared at different mixing speeds (20 wt% water in oil)	140
Figure 5-10 Effects of droplet size (mixing speed on mineral oil emulsion viscosity) ..	140
Figure 5-11 Rheogram of light crude oil at different temperatures.	141
Figure 5-12 Relationship between viscosity and shear rate obtained in light crude oil samples.....	142
Figure 5-13 Rheograms of water-in-crude oil emulsions at different temperatures and	144
Figure 5-14 Relationship between viscosity and shear rate for light crude oil emulsions	145
Figure 5-15 Droplet size distribution in water-in-crude oil emulsions prepared at	146

Figure 5-16 Images of crude oil emulsion samples prepared at different mixing speeds (20 wt% water in crude oil)	146
Figure 5-17 Effects of droplet size (mixing speed) on light crude oil emulsion viscosity	147
Figure 5-18 Rheogram of crude oil mixtures at different temperatures and shear rates.	149
Figure 5-19 Rheograms of water-in-heavy crude oil mixtures emulsions.....	150
Figure 5-20 Droplet size distribution in water-in- heavy crude oil emulsions prepared at different mixing speeds (20 wt% water in crude oil).....	151
Figure 5-21 Images of heavy crude oil emulsion samples at different mixing speed.....	151
Figure 5-22 Effects of droplet size (mixing speed) on heavy crude oil emulsion viscosity)	152
Figure 5-23. Effect of water volume fraction on W/O emulsion viscosity @ 1.223 s^{-1} W/O	153
Figure 5-24. Effect of water content on W/O emulsion shear stress @ 1.223 s^{-1} W/O ...	153
Figure 5-25 Effect of fine solid particles on LCO emulsions rheology	155
Figure 5-26 Estimation of non-Newtonian parameters for power law model	161
Figure 5-27 Estimation of non-Newtonian parameters for Herschel-Bulkley model.	162
Figure 5-28 Estimation of non-Newtonian flow behavior parameters for Casson model	163
Figure 5-29 Comparison of predicted and experimental data of power law model.....	164
Figure 5-30 Comparison of predicted and experimental data of HB model.	165
Figure 5-31 Comparison of predicted and experimental data of Casson model	166

List of Appendices

Appendix A 1 ultrasonic propagation wave in water.....	76
Appendix A 2 ultrasonic propagation wave in oil	76
Appendix A 3 Ultrasonic propagation wave in an emulsion prepared at agitation speed of 700 rpm	77
Appendix A 4 Measurements in crude oil.....	77
Appendix B 1 Stability mechanism.....	116
Appendix B 2 Compression of acoustic velocity of heavy and light crude oil.....	117
Appendix B 3 Compression of attenuation of heavy and light crude oil	117
Appendix B 4 Ultrasonic signal in light crude	118
Appendix B 5 Ultrasonic signal in water.	118
Appendix B 6 Ultrasonic signal in emulsion of 1200 Rpm.....	118
Appendix B 7 , Ultrasonic signal in fresh emulsion 1200 Rpm after 24 hr	118
Appendix B 8 Particles size distribution of Iron and clay	124
Appendix C 1 Asphaltene contents for different crude oil samples	173
Appendix C 2 Brookfield digital Rheometer calibration with fresh water	175
Appendix C 3 Shear rate and shear stress versus the time for fresh water sample.....	176
Appendix C 4 Brookfield digital Rheometer calibration with standard fluid of 49	177
Appendix C 5 Shear rate and shear stress versus the time for standard fluid of 49 cP...178	
Appendix C 6 Brookfield digital Rheometer calibration with standard fluid of 98 cP...179	

Nomenclature

LMO	Light Mineral Oil
LCO	Light Crude Oil
HCO	Heavy Crude Oil
W/O	Water-in-oil emulsion
O/W	Oil – in- water emulsion
HLB	Hydrophile-Lipophile Balance
Tween 20	Polyoxyethylene-20-sorbitan Monolaurate
Triton X-100	Polyethylene glycol octyl phenol ether
Rpm	Revolutions per minute
DSD	Droplet Size Distribution
d	droplet size (μm)
A_0	Initial amplitude
A	Final amplitude
c,v	Acoustic velocity (m.s^{-1})
ToF	Time of flight (s)
w_f	Fraction of FFT power spectrum
FFT	Fast Fourier Transforms
C_p	Specific Heat capacity (J/kg-K)
PL	Power Law Model
HB	Herschel – Bulkley Model
CM	Casson Model
UAS	Ultrasonic attenuation spectroscopy
NMR	Nuclear Magnetic Resonance
R^2	correlation coefficient (dimensionless)
SEE	Standard Error of Estimate
SSE	Sum of Square Errors
K	Consistency coefficient (Pa.s^n)
n	Flow behavior index (dimensionless)
y_i	Experimental results

Greek Letters

τ	Shear Stress (Pa)
γ	Shear rate (s^{-1})
β	Bulk modulus ($N.m^{-2}$)
ϕ	dispersed phase volume fraction (dimensionless)
η_c	viscosity of continuous phase (Pa. s)
η_d	viscosity of dispersed phase (Pa. s)
η_e	viscosity of emulsion (Pa. s)
η_r	relative viscosity of emulsion (dimensionless)
α	attenuation ($Np.m^{-1}$)
α_M	Measured attenuation ($Np.m^{-1}$)
α_a	Absorption attenuation ($Np.m^{-1}$)
α_v	Viscous attenuation ($Np.m^{-1}$)
α_t	Thermal attenuation ($Np.m^{-1}$)
α_s	Scattering attenuation ($Np.m^{-1}$)
\sum_a	Absorption surface area (m^2)
\sum_s	Scattering surface area (m^2)
$\varphi_d^{\mu,\sigma}$	Calculated volume fraction in log-normal distribution
κ	Compressibility ($m.N^{-1}$)
τ	Thermal conductivity ($W/m.K^0$)
μ_f	Fluid viscosity ($N.s.m^{-2}$)
μ	Geometric mean size (μm)
σ	Geometric standard deviation
λ	Wavelength (m^{-1})
δ_v	Viscous layer thickness (m)
f	ultrasonic frequency (MHz)
ρ	Density (kg/m^3)

To my beloved family

Chapter 1

1 General Introduction

1.1 Introduction

Emulsions are created by dispersion of one immiscible liquid into another in the form of fine droplets. Such dispersions are commonly encountered in a number of industrial processes more notably in crude oil production and processing, petrochemicals and food processing units. Crude oil which is a complex mixture of thousands of hydrocarbon compounds also contains impurities such as inorganic salts, suspended solids, and minerals. As the first major step in crude oil refining, the impurities of salts and suspended solids need to be removed. If these species are not removed from the oil, several issues could occur during the downstream process including excessive fouling of equipment, which affects the heat transfer rates in the exchangers and furnace tubes, equipment's corrosion, as well as catalyst deactivation.

The impurities of salt and suspended solids are removed by washing the crude oil with process water in the desalting operation. During desalting process, the water-in-oil emulsion (W/O) is generated must be eventually broken to achieve clean separation of oil and water streams. Heavy crude oils and bitumen usually hold large amounts of emulsion stabilizing species such as asphaltenes, resins, solid, clays and waxes (Bhardwaj and Hartland, 1988). Therefore, the gravity settling alone may not result in rapid separation of oil-water. Hence, in order to increase the rapidity and efficiency of water/oil separation a variety of heating and chemical demulsifying techniques have been utilized by oil producers. These kinds of treatment could be costly and require optimal control. Thus, it is

desirable to develop novel and less expensive techniques for emulsion characterization and monitoring. The emulsion phase is not expected in the cleaned oil and water outlet streams thus it is critical to optimizing the desalting process by monitoring the interfaces layers of (oil-emulsion- water). To do so, an appropriately designed and configured instrumentation scheme can avoid ingress of emulsion into desalted oil stream and loss of oil-containing emulsion into wash water exiting the vessel. Although a few techniques are commercially available for such applications, their shortcomings have been identified by the industry during long period tests (Meribout et al., 2004; Hauptmann et al., 2002; Astridge and Longfield, 1967). This can be attributed to rather difficult, dynamic and fouling environment of a crude oil desalter. On the other hand, ultrasonic based techniques have shown good potential for such challenging applications, based on initial testing with fouling and opaque conditions. An additional attractive feature of this technique is its potential to inspect emulsion layer composition changes which can provide important information for more reliable management of the unit.

The emulsion characters such as appearance, stability, and rheological behavior rely on their natures and droplet interactions as well (Derkach, 2009 and McClements, 1996). Various analytical techniques have been established to characterize the droplets in emulsions, e.g. electron microscopy, light microscopy, dynamic and static light scattering, neutron scattering and electrical conductivity, and Nuclear Magnetic Resonance (NMR) (Derkach, 2009; Coupland and McClements, 2001; McClements, 1996). However, most of these techniques have limitations, or they are appropriate only for dilute applications, while most emulsions of practical status are concentrated and optically opaque (Coupland and McClements, 2001). For example, NMR approach was utilized effectively to measure

droplet size distribution and volume fraction of the dispersed phase. However, NMR spectrometers are quite expensive to purchase and are not easily adapted for on-line measurements. Moreover, they are not suitable for smaller droplets characterization, as well require highly skilled operators.

Ultrasonic based technology offer several advantages to monitor changes in emulsion characteristics over time. Its advantageous features include lower power consumption, in-line measurement, long-term stability, non-invasiveness, high resolution and accuracy, and rapid response. The ultrasonic parameters usually recorded are changes in acoustic velocity, signal attenuation and its frequency spectrum. Emulsion droplet structure is observed with optical microscopy and stability is examined by tracking the changes in ultrasonic parameters with time. Ultrasonic attenuation spectroscopy (UAS) is becoming an attractive technique among other technologies to measure droplet size distributions in emulsions because of its ability to analyze concentrated and optically opaque emulsions. It depends on the conversion of the ultrasound measurements including the acoustic velocity and attenuation coefficient into droplet size information (Su et al., 2008 and McClements, 1996). The systematic monitoring of acoustic properties of an emulsion including sound velocity and sound absorption (attenuation) may offer insightful information regarding the droplet size distribution and emulsion stability (Shukla et al., 2010 and Atkinson and Kytomaa, 1992).

1.2 Thesis Objectives and Scopes

The main purposes of this thesis are summarized as follows:

- Development of ultrasonic technology based instrumentation to monitor and maintain emulsion layer position in separators like desalter operation and characterization of emulsion phase. Suitable probe design and configurations will be developed and tested for performance analysis, sensitivity, and accuracy.
- Development and testing of ultrasonic-based technology to monitor emulsion stability and changes in emulsion characteristics over time. Investigate effects of different variables on emulsion stability and characteristics. Utilizing ultrasonic propagation theory to study emulsion properties (i.e. water content and droplet sizes).
- Study rheological behavior of various emulsions for providing a better understanding of their stability and flow characteristics. Investigate effects of various parameters on rheological properties including mixing speed, droplet size, surfactant concentration, temperature, pH, salt content and solid particle etc.

1.3 Overview of the present work

The thesis entails of six chapters organized in the following categorization:

Chapter 1 provides a brief introduction to the emulsion formation and its challenges in the downstream processing. Limitations of the existing techniques used to characterize and monitor emulsions are discussed. While potentials of ultrasonic based techniques are pointed out.

Chapter 2 provides a detailed state-of-the-art literature review related to emulsion formations and classification. Emulsion stability mechanisms are discussed in details, the role of emulsifying agents is described, and emulsion destabilization phenomena is stated. Finally, the existing models which describe the flow behaviors of emulsions are mentioned.

Chapters 3 describes the results related to the development of ultrasonic technology based instrumentation to monitor and maintain desalter operation and characterization of emulsion phase. Suitable probe design and configurations have been developed and tested for performance analysis, sensitivity, and accuracy.

Chapter 4 discusses the development of ultrasonic-based technology to monitor emulsion stability and changes in characteristics with time. Acoustic parameters used for the purpose include sound velocity and sound absorption (attenuation). Potential of the technique is demonstrated through extensive testing with different conditions and contaminants.

Chapter 5 the effect of different factors and parameters on rheological behavior of various emulsions has been presented. Investigations are conducted to study effects of mixing speed, shear rate, temperature, pH, salt content; solid particle, surfactant concentration, and average droplet diameter. The existing models are tested against experimental data of this study.

Chapter 6 presents the general conclusions of the thesis work and recommendations for future studies.

References

- Ashrafizadeh, S.N., Kamran, M. 2010. Emulsification of Heavy Crude Oil in Water for Pipeline Transportation. *Journal of Petroleum Science and Engineering*, 71(3–4), 205–211.
- Clark, P., Pilehvari, A. 1993. Characterization of Crude Oil-in-Water Emulsions, *Journal of Petroleum Science and Engineering*, 9 (3), 165–181.
- Clausse, D., Gomez, F., Dalmazzone, C., *et al.* 2005. A method for the characterization of emulsions, thermogravimetry: Application to water-in-crude oil emulsion. *Journal of Colloid and Interface Science*, 287(2), 694-703.
- Ghanavati, M., Shojaei, M.J., Ramazani, S.A. 2013. Effects of Asphaltene Content and Temperature on Viscosity of Iranian Heavy Crude Oil: Experimental and Modeling Study. *Energy & Fuels*, 27(12), 7217–7232.
- Hauptmann, P., Hoppe, N., Puttmer, A. 2002. Application of Ultrasonic Sensors in the
- Lim, J.S., Wong, S.F., Law, M.C. 2007. A Review on the Effects of Emulsions on Flow Behaviours and Common Factors Affecting the Stability of Emulsions. *Journal of Applied Sciences*, 15(2), 167–172.
- Mcclements, D.J., Coupland, J.N. 1996. Theory of Droplet Size Distribution Measurements in Emulsions Using Ultrasonic Spectroscopy. *Colloids and Surfaces, A: Physicochemical and Engineering Aspects* 117, 161 170.
- Meribout, M., Habli, M., Al-Naamany, A. 2012. A New Ultrasonic-based device for Accurate Measurement of Oil, Emulsion, and Water Levels in Oil Tanks. *Instrument and Measurement Technology Conference*, 1942-1947.
- Meyer, S., Berrut, S., Goodenough, T., *et al.* 2006. A Comparative Study of Ultrasound and Laser Light Diffraction Techniques for Particle Size Determination in Dairy Beverages. *Measurement Science and Technology*, 17(2), 289–297.
- Process Industry, *Measurement Science and Technology*, 13(8), 73-83.
- Souleyman, A., Nour, A.H. 2015. Review on the Fundamental Aspects of Petroleum Oil Emulsions and Techniques of Demulsification. *Journal of Petroleum & Environmental Biotechnology*, 6(2), 1144-1163.
- Tharwat, F., Tadros. 2013. Emulsion Formation, Stability, and Rheology. *Emulsion Formation and Stability*, Chapter 1, 1–75.

Chapter 2

2. Literature Review

Emulsions play significant role in various industrial processes e.g. petroleum and industrial products (e.g. pharmaceuticals or cosmetic products and food products). Emulsion is a heterogeneous system, consisting of two or more immiscible liquid phases. It contains a minimum of one immiscible liquid thoroughly distributed in other liquid appearing as droplets, whose diameter may range from 0.1nm-20 μ m. Emulsions are thermodynamically unstable and kinetically stable systems. Usually, its stabilization is contributed by emulsifying agent, asphaltenes, resins and finely dispersed solids.

An emulsion system comprises of two phases; the dispersed droplets are the internal phase while the external phase (continuous phase) is the liquid surrounding the dispersed droplets. The emulsifying agent is responsible for the separation of these dispersed droplets from external phase ([Lissant, 1988](#)). Earlier, research on emulsions under deformation has resulted in significant and sequential theoretical and experimental studies. Many engineers and scientists participated in such investigations with a persistent interest in the understanding of nature and variance of the rheological properties of emulsions.

2.1 Emulsion Formations and Classification

2.1.1 Emulsion Formation

Schubert (1992), proposed three major criteria required for formation of crude oil emulsions;

1. Involvement of two immiscible liquids.
2. The presence of surface active compounds as an emulsifying agent.
3. Appropriate agitation to facilitate dispersion of one liquid into another as droplets.

When water and oil come into contact in the presence of an emulsifying agent and sufficient mixing, the crude oil emulsions are formed. For emulsion formation, the efficiency of agitation and emulsifier presence is very crucial. In oil production processes, there are multiple steps to create agitation, sometimes known as the shear level. These includes flow through reservoir rocks, well tubing, flow lines, production headers, valves, fittings, chokes; gas bubbles released because of phase change.

In general, more agitation results in small sized droplets distributed in oil, and as a consequence tighter emulsion is formed. The enormous studies on emulsion provided the fact that size of these water droplets may differ from less than one micrometer extending up to more than thousand micrometers. The presence of emulsifier is another element required for emulsion formation. The existence, quantity, and nature of emulsifier more considerably determine the emulsion type and its "tightness." In crude oils, natural emulsifiers exist in heavy fractions. Because of variation of heavier fractions in crude oils, the tendency of emulsification widely differs. Less stable emulsions are produced with crudes having a lower quantity of emulsifier, resulting in emulsions which separate quickly.

Much stable emulsions are formed in crudes which may have the proper type and adequate amount of emulsifier.

2.1.2 Classification of Emulsions

In a system, containing oil and water. Several emulsion classes could be distinguished:

- Oil-in-water Emulsion (O/W) as shown in **Figure 2-1 b**, is composed of oil globules dispersed into the water (Continuous phase).
- Water-in-oil Emulsion (W/O) as shown in **Figure 2-1a**, consists of the aqueous globules dispersed throughout the crude oil (Continuous phase).
- Oil-in-oil (O/O), this class can be illustrated as the emulsion having polar oil as internal phase dispersed in non-polar oil (continuous phase) or conversely, a non-polar oil as internal phase scattered in a polar oil (continuous phase).

In addition to principal styles, an unusual type of emulsion that is referred to as multiple emulsion can exist. Multiple emulsion is a complexed system, in which both water in oil emulsion (W/O) and oil in water emulsion (O/W) are dispersed throughout another immiscible phase; i.e. it includes water in- oil-in- water (W/O/W) emulsion and oil-in-water-in-oil (O/W/O) emulsion (Schramm, 2015; Pal, 1996).

Emulsions can also be categorized on the basis of the droplet size present in the continuous phase. The term macro-emulsion is used when these droplets are greater than 1 micrometer in size. Thermodynamically, such emulsions are not stable (with regard to time, these two phases split up due to the proneness of the emulsion to minimize its interfacial energy due to coalescence and separation). Although, a stabilization mechanism can minimize or even diminish the droplet coalescence. The majority of oilfield emulsions are of such types.

On the contrary, another class is known as micro-emulsions. In the presence of two immiscible phases, such emulsions are generated spontaneously due to their exceptionally minimal interfacial energy. Such type of emulsions have a relatively tiny size of droplets i.e. less than nanometer and are very stable thermodynamically. This class of emulsion differs very much from macro-emulsions in the account of their stability and formation.

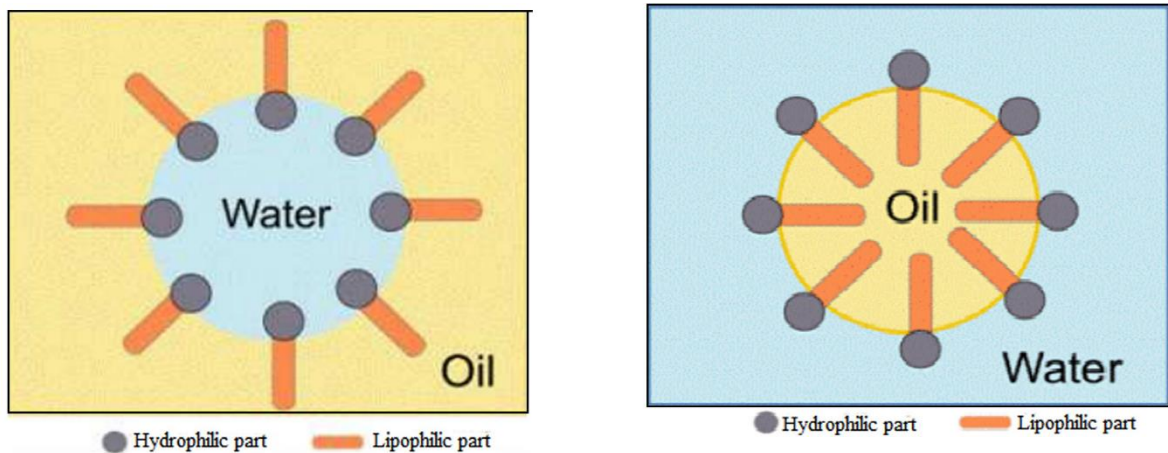


Figure 2-1 W/O Emulsion (a), O/W Emulsion (b). (Khan et al., 2011)

2.2 Emulsion Stability

Emulsion stability is a significant feature of water-in-oil emulsions and refers to the firmness and tenacity of an emulsion in the respective surrounding. Few types of emulsions, rapidly deteriorate into discrete phases (oil and water) but some are quite stable and can persist for days to years. Stable dispersions result due to the small size of drops with the existence of an interfacial film surrounding drops. For this reason, the suspended droplets do not float rapidly and also do not coalesce quickly.

The Emulsion stability is considered against three different procedures, which are:

1. Creaming (sedimentation)

2. Aggregation

3. Coalescence

The separation velocity relies on certain factors which include the difference in density between the two liquids, the viscosity of dispersed phase (droplet size) and the continuous phase. Variety of methods can be used to reduce separation i.e.

- Minimization of the density difference between phases.
- Reduction of the droplet size: Tiny droplets are formed due to increase in energy input of the system, which lessens interfacial tension between oil and water and therefore it prevents coalescence.
- Increase in viscosity of continuous phase: Elevating the viscosity of the surrounding liquid reduces the velocity at which the droplet moves up.
- Growth in the concentration of droplets: Due to substantially elevated concentration, droplets are compressed and become tightly packed, preventing their flow. Although, it may remain inflexible to raise the concentration of droplets due to physicochemical restrictions of the system.

Due to their thermodynamic nature, most emulsions tend to separate into two phases over time. Consequently, the emulsion characteristics such as droplet size distribution and other rheological properties will also change. The emulsion can reach to the stability level after examined different mechanisms that could take place during emulsification stage (emulsion breakdown), these mechanisms are summarized in **Figure 2-2**.

In most cases, the emulsion droplets and continuous phase have different densities. Droplets tend to move up or down through the continuous phase due to gravity. If the density of droplets is low, they have a tendency to move up high to produce a layer at the surface emulsion. This is referred to as creaming process. Conversely, if the density of droplets is high, then they have a tendency to settle down to produce a layer in the bottom. This is known as sedimentation process. Usually, the water density is higher than the density of oil. Thus droplets of W/O emulsions tend to sediment, while O/W emulsions are more likely to cream.

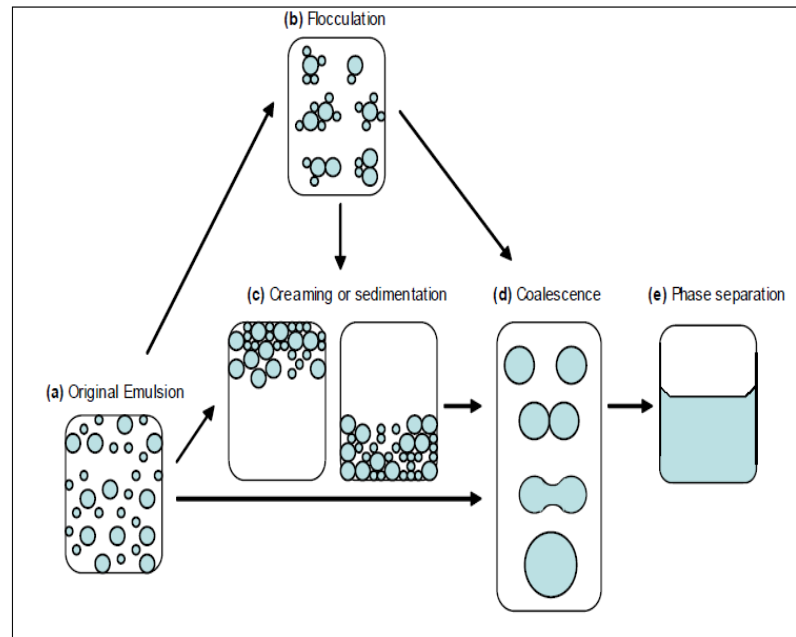


Figure 2-2 Emulsion destabilization mechanism (modified from Binks and Horozov, 2006).

2.2.1 Creaming/Sedimentation

Certain exterior forces are responsible for Creaming and Sedimentation. These can be gravitational force or centrifugal phenomena. At times, when these external forces overreach the Brownian motion of droplets (Thermal motion), a concentration gradient is

generated. This results in either creaming of large droplets, shifting rapidly up at the surface (density of droplets $<$ density of medium) or to the sedimentation phenomena in which droplets rest in the bottom of the container (density of droplets $>$ density of medium). In the limiting cases, the droplets may get assembled in a close-packed (random or ordered) array at the top or bottom of the container with the remaining volume of container occupied by the continuous liquid phase.

Creaming is an opposite of sedimentation, resulting from density difference between the two liquid phases. The term Sedimentation is used if the particles show movement in the direction in which gravity acts ($\Delta\rho > 0$). Alternatively, in the case of the flow against gravity ($\Delta\rho < 0$), the process refers to Creaming. The sedimentation process applies to most water-in-oil emulsions and solid dispersions, whereas the creaming process applies to most oil-in-water emulsions and bubbles dispersed in liquids.

2.2.2 Flocculation

Flocculation refers to the accumulation of droplets (without any change in the size of the droplet) into larger units. It occurs due to the presence of Vander Waals forces, usually prevailing in all dispersive systems. Flocculation occurs when the repulsive forces to retain the droplets at a distance is not enough due to weak Vander Waals forces. The flocculation intensity either strong or weak may depend on the intensity of attractive energy involved in the system.

In the account of controlling the texture and structure of emulsions, the understanding of flocculation process is very significant. Mathematical models have been progressed to clarify the process occurring during the formation of droplet flocs (frequency and efficiency

of collisions) to foresee the effects of flocculation on the stability of emulsions, but these will not be described here. Relying on the need and choice of final products, different methods can be applied to control flocculation. The particular method can be chosen as directed by the components and nature of emulsion to be developed (it includes texture, structure, appearance, etc.). The method which is highly productive in restraining the rate and intensity of flocculation is to control the colloidal interactions among droplets (these interactions may include steric, electrostatic, hydrophobic, etc.).

2.2.3 Coalescence

Coalescence is defined as disintegrative phenomena of the liquid film between small droplets, resulting in merging. The combination of these little droplets outcomes into bigger droplets. The limiting case for coalescence is the complete separation of the emulsion into two distinct liquid phases. The driving force for coalescence is the surface or film fluctuations which result in close approach of the droplets whereby the van der Waals forces are strong thus preventing their separation.

The combination of droplets occurs when the thin film of continuous phase between two drops breaks and they fuse quickly to form a single large drop. Therefore, the rate of coalescence is a key factor on which the stability of an emulsion system depends. It is clear that the properties of this film will dictate the stability of the emulsion.

The merger of these droplets to form a massive drop is followed by the emergence of an oil layer at the surface of emulsion (Oil-in-water emulsions). It only occurs due to the breakup of thin film between two droplets. When droplets are in close neighbourhood, their shape may get distorted, and the surface of droplets in contact may get flattened. This

deformation increases the surface area between droplets in contact, and as a consequence, droplets shows more proneness for coalescence. The estimation of coalescence can be significantly predicted by the rate of rupture of the thin film. Droplets are always in continuous motion with very brief collision time with each other. However, if this period is long enough in contrast to the time needed for the film to form stable emulsion, coalescence can occur. For prevention and control of coalescence, few methods have been established. Since the coalescence greatly relies on colloidal and hydrodynamic interactions among droplets, and the physicochemical properties of the components used in the emulsion (specifically continuous phase and the emulsifier), minimization or restriction in contact of droplets and breakup of thin interfacial film are key factors where much research and efforts are required. The coalescence of the droplet is majorly contributed by the emulsifiers adsorbed at the oil-water interface. The ability of surfactants in restricting coalescence relies on their physicochemical features. Such as, the electrostatic repulsion between the droplets is induced by the presence of charged (positive or negative) emulsifiers at the droplet interface, which tend to prevent droplet contact.

2.2.4 Phase Inversion

This inversion phenomenon is very much evident in dispersed liquid-liquid mixtures (e.g. in pipe flow or stirred vessels), but the mechanism behind it is still not well comprehended. Two modes of dispersion are observed on the basis of phase fraction and initial circumstances, these are oil-in-water and water-in-oil. The phase inversion is usually observed when mixture go through some changes in the phase distribution, as the phase fraction accomplishes certain critical values (Yeh *et al.*, 1964; Arirachakaran *et al.*, 1989; Pal, 1993; Piela *et al.*, 2008). It is a phase inversion point when inversion occurs at critical

phase fraction. The dispersion undergoes continuous coalescence i.e. breakup of the thin film between dispersed droplets. This dynamic process may reach equilibrium at low dispersed phase fractions. When dispersed phase fraction elevates, the phenomena may get unstable, resulting in much dominant coalescence due to the closeness of dispersed droplets. Ultimately, when these two phases swap their continuity resulting in phase inversion. This phase inversion and variation in phase continuity may lead to significant reformations in rheology of the mixture resulting in higher fluctuations in pressure gradient during pipe flow (Angeli, 1996; Nädler, 1995).

2.2.5 Ostwald Ripening (Disproportionation)

Ostwald Ripening or disproportionation appears due to the limited solubility of liquid phases. Immiscible liquids have mutual solubility which cannot be negated. For poly-dispersive emulsions, tiny droplets will have comparatively higher solubility than huge droplets because of the curvature effects. These tiny droplets may vanish with a certain time interval, and their molecules diffuse to the bulk and get deposited on the larger droplets resulting in a distribution of droplet size to larger values.

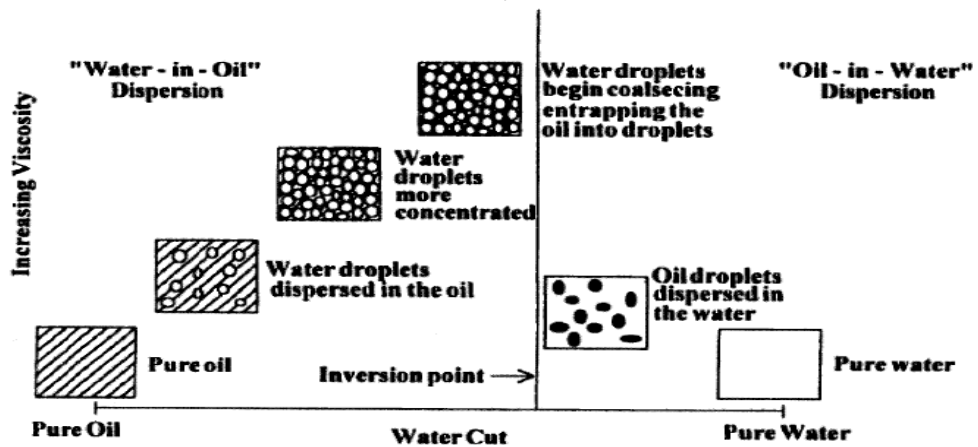


Figure 2-3 a schematic on the proposed phase inversion mechanism by Arirachakaran et al. (1989).

2.3 Emulsifying agents

Emulsifying agent refers to the substances which aim to maintain the stability of the emulsion thus to prevent the disperse phase from coalesce flocculation etc. The mechanism of each emulsifying agent is different. For instance, surfactant, as one broad kind of emulsifying agent, aims to lower the interfacial tension at the interface. The other agent, such as solid particles, create mechanical barriers at the interface.

2.3.1 Surfactants

Surfactants are a prevalent emulsifying agents, having adsorbing characteristics on interfaces and they can significantly change their interfacial free energy. In general, surfactants contain polar hydrophilic “heads” and non-polar hydrophobic “tails.” The polar “heads” would be the major classification of the surfactant. The most common species are non-ionic surfactants of polyoxyethylene moieties, such as polyoxyethylene alcohol or alkylphenol ethoxylate. Other non-ionic surfactants include sorbitan esters of oleic or lauric acids, ethoxylated sorbitan esters of oleic or lauric acids, as well as polyethylene glycol esters of oleic acids. (Sztukowski, 2005) The nature of “head” and “tail” of surfactants differs, directing too many variations in properties of surfactant. Surfactant solubility in the aqueous medium is also established by the affinity of the hydrophilic part of surfactant with water. Surfactants are classified on the basis of the type of hydrophilic group present:

- *Anionic*: the presence of negative charge as head moiety
- *Cationic*: the presence of positive charge as head moiety
- *Non-ionic*: no apparent charge observed in head moiety
- *Zwitterionic*: both negative and positive charge observed in head moiety

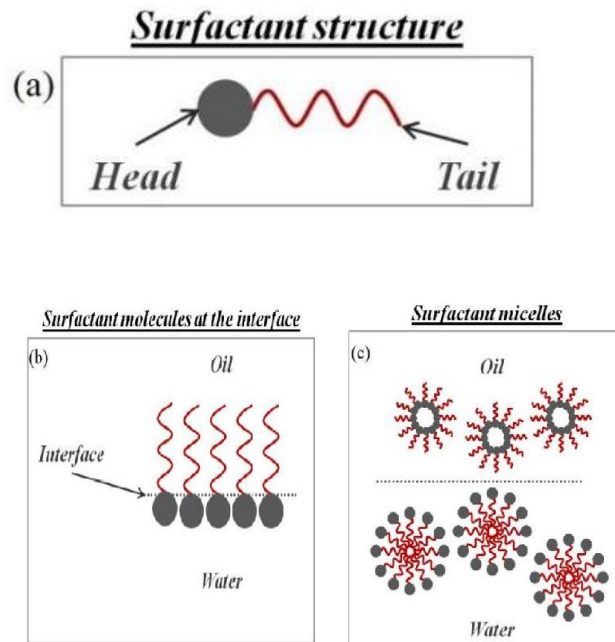


Figure 2-4 Schematic representation of (a) structure of surfactant, (b) surfactant molecules at the interface, and (c) spherical surfactant micelles. (Pichot, 2010)

After surfactants dissolve in liquid, micelles would be formed by either adsorption at the interface or self-assembly. A micelle is an aggregate of surfactant molecules dispersed in a liquid colloid. The adsorption of surfactants at the interface provides an expanding force against the natural tension between the continuous phase and dispersed phase which provides a reduction of the interfacial tension. The decline in the interfacial tension also reduces the free energy associated with the interface and increases the probability that continuous and dispersed phase remain emulsified. Nevertheless, besides decreasing interfacial tension, in this way, surfactants could also potentially increase the interfacial viscosity which results in a mechanical resistance to coalescence. Furthermore, it would create an electrostatic repulsion force among each micelle and reduce the chances of flocculation. The combination of these effects would thus essentially result in emulsion stabilization.

2.3.2 Asphaltenes

Asphaltenes are large, polar; polynuclear molecules contain condensed aromatic rings, aliphatic side chains (Strausz *et al.*, 1992; Watson *et al.*, 1994). They are the highest molecular weight fraction in crude oil. The density of asphaltenes has a range of 1132 to 1193 kg/m³ (Akbarzadeh *et al.*, 2004). The chemical characteristics of asphaltenes cause them to be amphiphilic and therefore exhibit surface activity (Rogacheva *et al.*, 1980).

Asphaltenes have surface active characteristics which prove them suitable emulsifiers. The collection of asphaltene molecules at the interface leads to the formation of a rigid film, which restricts the coalescence. For coalescence in between two droplets, the thin film needs to break up and drained off. However, this drainage of the film is prevented due to the natural presence of asphaltene. The principle feature for such restraint is steric repulsion exhibited by high molecular weight components of asphaltene present in thin film.

The physical state of asphaltenes existing in crude has a remarkable effect on its emulsion stability properties. Asphaltenes in colloidal state stabilize the emulsions, but it is strongly evident that its stabilizing properties are notably intense when it occurs in the solid state as precipitated from crude.

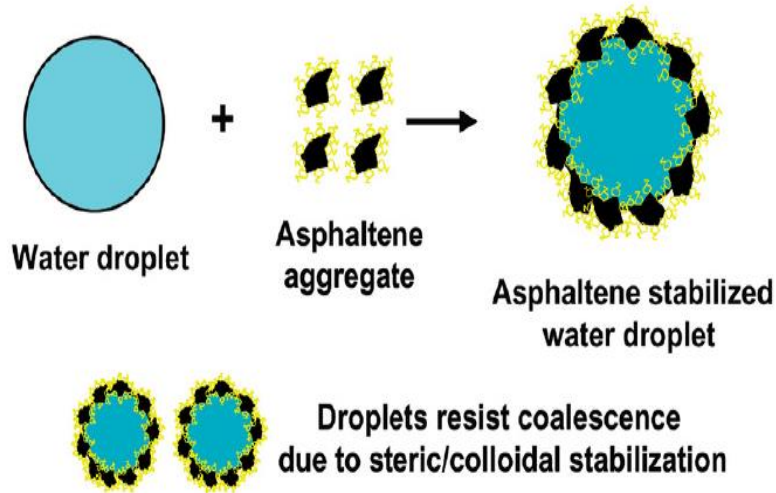


Figure 2-5 Mechanism of emulsion stabilization by asphaltenes.

2.3.3 Resins

Similar to asphaltenes, resins are also large molecules which are complex compounds with high molecular weight and are insoluble in ethyl acetate but are soluble in n-heptane. It has great tendency to couple with asphaltenes, resulting in the formation of the asphaltene-resin micelle. It plays a vital part in stabilizing emulsions. The asphaltene: resin ratio in the crude oil reveals the type of film formed (solid or mobile), and emulsion stability directly depends on it.

2.3.4 Fine solid particles

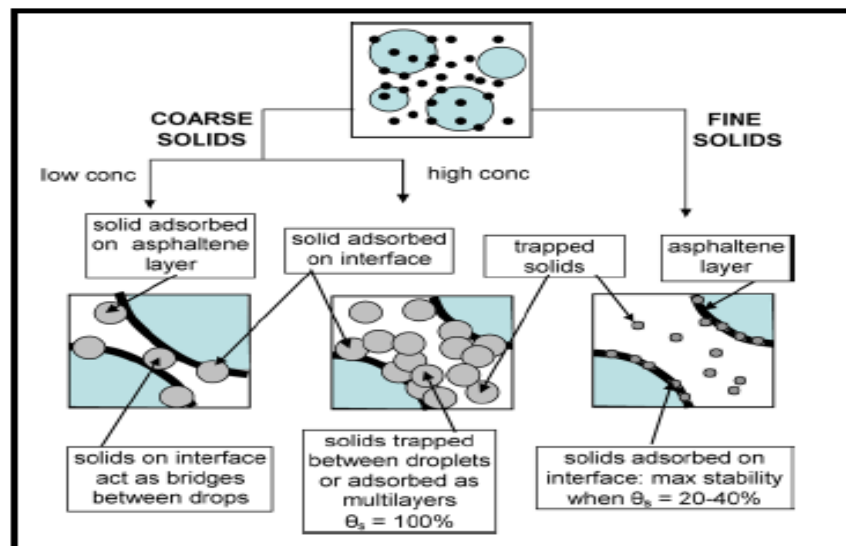
The fine solid particles are non-asphaltenic solids which are fine clays, silicates or ash present in the crude oil/bitumen, or corrosion products and precipitated material that becomes insoluble, (Bensebaa *et al.*, 2000). The role and efficiency of these solids in stabilizing emulsions relies on several features, including their concentration, density, size distribution, and surface properties. The interaction of asphaltenes with solids, i.e., the

adsorption or desorption of asphaltenes on these surfaces also contributes to their effectivity in stabilizing emulsions.

These fine solids particles can stabilize an emulsion by getting adsorbed directly on water/oil interface or adsorption on an existing surfactant film. These solids adsorbed in either way can generate a steric hindrance in between neighbouring water droplets, resisting droplet collisions, film drainage, and coalescence (Tambe *et al*, 1993; Tadros *et al*, 1983). In the case where strong particle-particle interaction exists, these particles can majorly contribute to the mechanical rigidity of the film forming a compact network structure (Tambe *et al*, 1993; Abend *et al.*, 1998; Binks, 2002). It is also noticeable that partial surface coverage by these fine solids particles can be enough in stabilizing emulsions (Binks *et al*, 2002). When these fine solid particles are confined between the droplets, they may have the ability to decrease aggregation and creaming/sedimentation of an emulsion phase and also minimizes the probability of coalescence. The overall emulsion viscosity may also increase (Aveyard *et al.*, 2003; Yan *et al*, 1993) and minimizes the probability of discrete separation of water and oil. The mechanisms linked with solids-stabilized emulsions and intensity at which solids elevate emulsion stability relies on features like size, shape, the morphology of particle, and density, concentration, surface interaction, and wettability of system. It can be established that stability of an emulsion maximizes in the case of minimum size of particle and density and elevating particle concentrations. In fact, for being potent emulsion stabilizers, solid particles must be at least ten times smaller than the droplet (Aveyard *et al.*, 2002; Binks *et al*, 2002) and should also be locally bi-wettable, i.e., they should contain few surfaces majorly wetted by water and some of the oil. A “water-wet” solid implies to the particle preferably wetted by water whereas oil more easily

wets an “oil-wet” solid particle. The apparent contact angle, θ , as measured through the water phase, is smaller than 90° in a water-wet solid particle and an oil-wet solid, the apparent contact angle is larger than 90° . For the formation of adequately thick and strong mechanical barrier between the droplets, the majority of the solid should come through into the continuous phase. It is to be noted that the measured contact angle does not involve the molecular orientation of water-wet and oil-wet regions on the solid, but an apparently evident contact angle is considered for measurements. Therefore, a possible arrangement of these fine solid particles at the interface is such that oil-in-water emulsions are stabilized by water-wet solids, whereas water-in-oil emulsions are stabilized by oil-wet solids, as illustrated in **Figure 2.6 a and b**. Usually, the reduction in interfacial tension is not caused by adsorbed solids, while the contrary has been observed by Nushtaeva and Kruglyakov (2004). Solids cause a mechanical barrier at the interface.

(a)



(b)

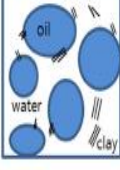
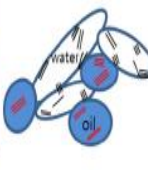

Combination of clay	Hydrophilic clay	← Mixture of clays →	Hydrophobic clay
Location of clay	Water phase/interface	Interface/phases	Oil phase
Effect of clay	Increase of interfacial area	Formation of complex interface	Increase of oil viscosity
Microstructure of Emulsion			

Figure 2-6 a,b possible distributions of coarse and fine solids in an emulsion.

2.4 Demulsification

Application of certain procedures accomplishes demulsification of water-in-crude oil emulsion. It can be a mechanical process, chemical procedures, thermal process, or electrical application. Several other techniques may also be applied to attain demulsification, like pH adjustment, membrane separation technique, filtration process, and heat treatment applications (Gafonova, 2000). For fast and quick separation, vast understanding of salient features of the emulsion is needed with knowledge of mechanisms that are intricated during coalescence of water droplets (Ese *et al.*, 1999). Demulsification is a breakdown phenomenon of emulsion into distinct phases, majorly water and oil. The initial process needed compulsorily in oil refining is the segregation of water from the crude oil. It is a common requirement for either a petrochemical industry or an oil refinery. Presently, certain emulsion breakers are widely used as chemical additives to break the water-in-oil emulsions.

The demulsification methods like thermal, mechanical, electrical or chemicals depend preferably on the physicochemical structure of oil from which they are formed, emulsification conditions, and aging. It concludes that the approach of demulsification for treating the water in oil emulsion may differ in respective industries.

Demulsification is splitting of an oil emulsion into two phases i.e. oil and water. For an oil refinery, the processes are carried out to ensure following aspects,

(a) Rate of separation

(b) Residual amount of water after demulsification

The aspects that escalate the emulsion breaking phenomena includes:

- Removal of solid particles
- Reduced agitation
- High temperature
- Increased retention time
- Control of emulsifying agents

The most common methods for emulsion treatment are:

2.4.1 Chemical demulsification

The addition of chemicals, called as demulsifiers is very familiar procedure of treating emulsions. Such additives intend to counteract on emulsifying agents that stabilize emulsions. Demulsifiers are surface active compounds, they act on the oil-water interface to destabilize and breaks hard film to speed up coalescence of water droplets. Following steps are needed for optimal demulsification:

- Proper selection of demulsifier and appropriate amount of demulsifier
- Sufficient agitation
- Enough retention time within treaters to settle water droplets
- Facilitating the system with thermal application, electric grids, coalescers, etc. as per requirement

Demulsifiers consists of various solvents (benzene, toluene, xylene, short-chain alcohols, and heavy aromatic naphtha), surfactants, flocculants and wetting agents. It functions by partial or complete dismissal of stabilizing polar interfacial film surrounding emulsion droplets. This removal of film may lead to various changes in properties like interfacial viscosity or elasticity of the protecting film, promoting destabilization. Certain demulsifiers perform as wetting agents and modify the wettability of the stabilizing particles, resulting in the rupture of film.

Dosage: Insufficient amount of demulsifier leaves the emulsion unresolved, and high dosage may be disastrous to the process because these are also surface active agents like emulsifiers and it may produce stable emulsions if dosed excessively. It substitutes the natural emulsifiers at the interface.

Since various components exist in crude, the efficiency of demulsifier is majorly contributed by crude oil nature. Adsorption and displacement process relies on pH, salt content & temperature. The demulsifiers which quickly displaces the preformed rigid films and leave a mobile film (which shows minimal resistance to coalesce) as a substitute are the most efficient ones.

2.4.2 Electrical demulsification

Demulsification can also be done through application of high voltage electricity. It is commonly accepted that water droplets are charged, and in an electric field, the droplets move quickly, the collisions between them lead to coalescence. Electric field also interrupts the interfacial film by relocating polar molecules. It weakens the rigid film and enhances coalescence. The electrical system comprises a transformer with electrodes which supply high voltage alternating current. These electrodes are positioned as to facilitate an electric field which is perpendicular to the direction of flow. In some designs, distance in between electrodes is adjustable. It helps to variate the voltage to meet the need of emulsion being treated (Issaka, 2015; Reza, 2016).

This type of demulsification is rarely used alone. It is used in synchronicity with the addition of chemical and application of heat. However, at all times, the usage of electrostatic dehydration technique is useful in terms of reducing the need of thermal application. Minimal temperature requirements results in reduced consumption of fuel, less troubles caused due to scale formation and corrosion and a decrease in losses of lighter fractions. Additionally, it may reduce the use of emulsion breaking chemicals.

2.4.3 Thermal demulsification

The heating process enhances the breakage and separation of emulsions. It decreases the oil viscosity and elevates the rate of settling for water. Low interfacial viscosity caused by elevated temperatures may also result in destabilizing rigid films. Additionally, the higher thermal energy of droplets promotes the coalescence frequency among water droplets i.e.

heat promotes demulsification. Despite above facts, thermal demulsification rarely fixes emulsion issue alone. High temperatures may have some damaging impacts as well.

Primarily, heating the stream costs much. Secondly, it may lead to loss of lighter fractions of crude oil minimizing its volume and API gravity. Lastly, due to increased temperatures, treating vessels are more prone to corrosion and scale deposition. So, the decision to use heat for demulsification should be made after investigating overall economic analysis of the treatment facility (Issaka, 2015; Reza, 2016).

2.5 Types of Fluid Behavior

Due to their natures, most fluids may experience different behaviors when the measured values of viscosity or shear stress are plotted as a function of shear rate as shown in **Figure 2-7**. Those curves can be used to fit the rheological patterns. For example, the Newtonian behavior represents the fluid with independent of the shear rate. However, a straight line can describe the relation of shear stress vs. shear rate. Newtonian fluids obey the Newton law of viscosity, given by:

$$\tau = \eta \gamma \quad (2.1)$$

Where τ is the shear stress (Pa), γ is the shear rate exerted on the fluid (s^{-1}), and η is fluid viscosity (Pa. s).

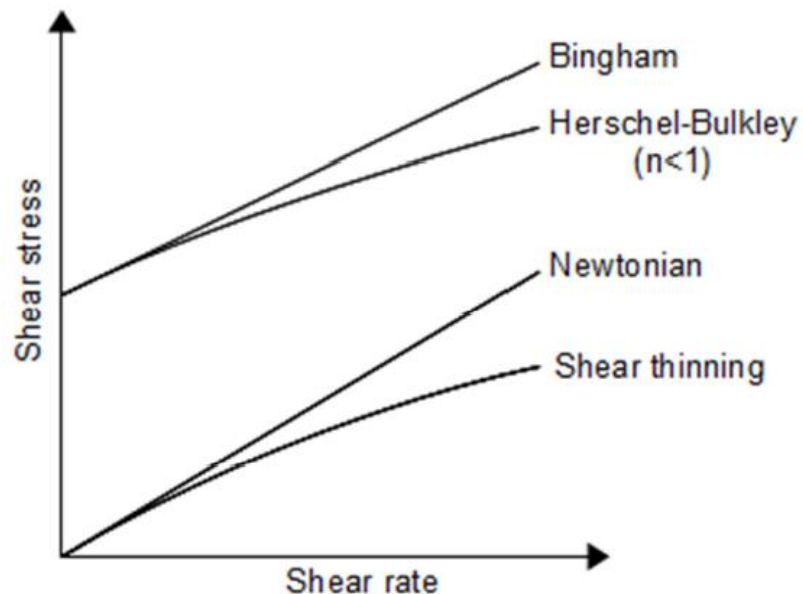


Figure 2-7 Shear stress vs Shear rate for various fluids behaviors.

The most common pattern observed when the apparent viscosity declines with the increasing of shear rate, this phenomenon is called shear thinning where the fluids do not obey the Newton law of viscosity. As can be shown below in **Figure 2-8** the plot of τ versus $\dot{\gamma}$ is linear at very high or low shear rates. The slope of the linear portion of the curve at high shear rates gives the viscosity at infinite shear (η_{∞}). The slope at very low shear rates gives the viscosity at zero shear rate (η_0). The power law, which is used to correlate the shear stress and shear rate, can represent this behavior (Pal et al., 1992; Darby, 1996; Wilkes, 1999) by applying log-log plot of $\dot{\gamma}$ versus τ gives a straight line with a slope of n . The power law was given as:

$$\tau = k \dot{\gamma}^n \quad (2.2)$$

Where

k, the consistency coefficient [Pa.sⁿ]

n, the flow behavior index, ($n < 1$ shear-thinning fluids, $n = 1$ Newtonian fluids, and Dilatant behavior occur when n greater than 1).

The Dilatant behavior is rarely occurring when the viscosity of system increases as the shear rate increased.

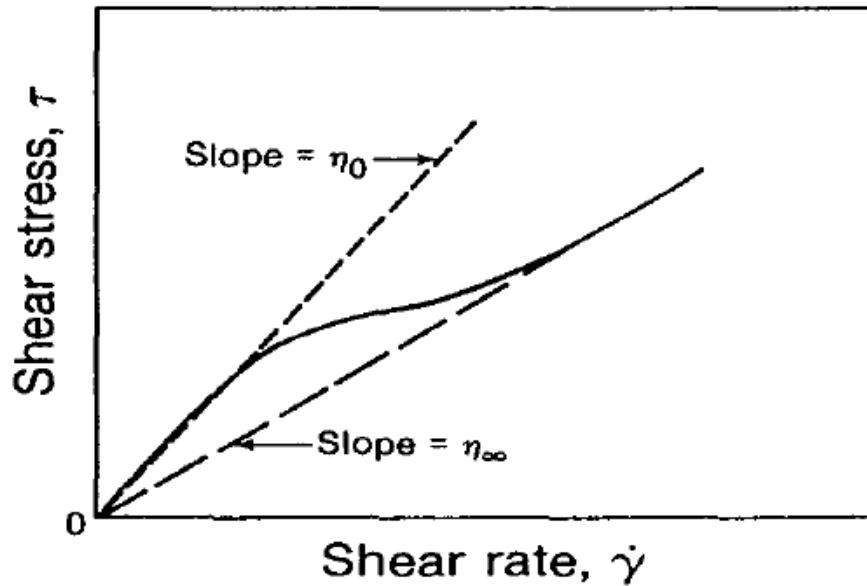


Figure 2-8 Pseudo plastic fluid behavior (Pal et al, 1991)

Herschel – Bulkley model (HB) can be introduced when the yield stress of emulsion is measurable; this model is appropriate for a fluid which requires a little stress during flow as a function of shear rate and yield stress. HB model equation is quite similar to power law model with including the yield stress term. According to (Barnes, 1989), “the concept of yield stress has been challenged because a fluid may deform minutely at stress values lower than the yield stress.”

$$\tau = \tau_0 + k(\dot{\gamma})^n \quad (2-3)$$

Where τ is shear stress (Pa), τ_0 is yield stress, k is the consistency index, $\dot{\gamma}$ is the shear rate (s^{-1}), and n is the flow behavior index. Both parameters k and n can be determined from linear regression of $\log \tau - \tau_0$ versus $\log \dot{\gamma}$ as the intercept and slope, respectively, only when the yield stress of the sample is experimentally known. Rao and Cooley (1983) stated that

nonlinear regression technique was used to estimate τ_0 , k , and n . This technique is used only when the rheological parameters are not available experimentally.

The Casson model has been proposed to characterize the emulsion dispersions; for instance, the emulsion whose flow behavior follows the Casson model, a straight-line results of plotting the square root of shear rate $(\dot{\gamma})^{0.5}$ against the square root of shear stress $(\tau)^{0.5}$, with slop K_c and intercept K_{0c} . Additionally, the Casson yield stress is calculated as the square of the intercept, $\tau_0 = (K_{0c})^2$ and the Casson plastic viscosity as the square of the slop, $\eta_{ca} = (K_c)^2$ as shown in **Figure 2-8**.

$$\tau^{0.5} = K_{0c} + K_c (\dot{\gamma})^{0.5} \quad (2-4)$$

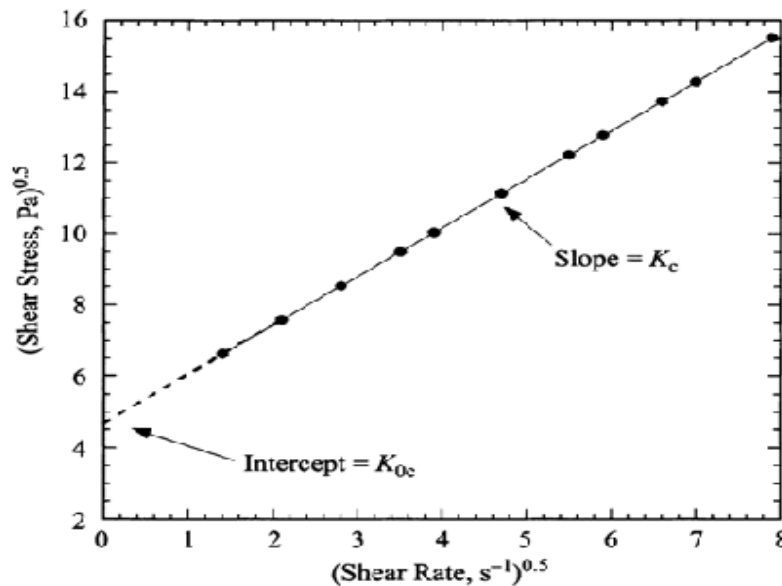


Figure 2-9 Plot of $(\dot{\gamma})^{0.5}$ versus $(\tau)^{0.5}$ for an emulsion that follows the Casson model.

Table 2-1 some flow models for describing shear stress (τ) versus shear rate ($\dot{\gamma}$).

$\tau = \eta \dot{\gamma}$	Newtonian model
$\tau = [\eta_{\infty} \dot{\gamma} + K_s \dot{\gamma}^{n_s}]$	Sisko model for high shear rate with respect to η_{∞}.
$\tau = k\dot{\gamma}^n$	Power model used for Non-Newtonian
$\tau - \tau_0 = \eta \dot{\gamma}$	Bingham model
$\tau - \tau_0 = k\dot{\gamma}^n$	Herschel- Bulkley model
$\tau^{0.5} = k_{0c} + k_c(\dot{\gamma})^{0.5}$	Casson model
$\tau^{0.5} - \tau_{0m} = k_M \dot{\gamma}^n$	Mizrahi and Berk (1972) model is a modification of the Casson model

2.6 Emulsion characterization techniques

Various analytical techniques have been established to characterize the droplets in emulsions, e.g. electron microscopy, light microscopy, dynamic and static light scattering, neutron scattering and electrical conductivity, and Nuclear Magnetic Resonance (NMR). However, most of these techniques have limitations, or they are appropriate only for dilute applications, while most emulsions of practical status are concentrated and optically opaque.

2.6.1 Microscopy

Microscopy techniques basically involve the generation of visible images from complex or simple structures that cannot be seen with naked eyes using microscopes for easy comprehension. There are three major categories of microscopy, classified according to their working principles: optical, electron and scanning probe microscopy. Optical and electron microscopies entail the interpretation of transmitted, reflected or refracted electromagnetic radiation or electron beams resulting from interactions with a specimen to give magnified versions of its image (Aguilera and Stanley, 1990; McClements, 1999). Whereas in scanning probe microscopy, the surface of a specimen is scanned with probes and the resulting interactions used to generate its shapes and surface characteristics. Depending on the adopted microscopy technique, one could have insights on the structural organization of an emulsion. Modern microscopes usually come with a computer system for data capture, acquisition and subsequent image processing via suitable software, allowing more information on an emulsion microstructures (Russ 2004). This information includes floc size, fractal dimensions and particle size distribution.

Optical microscopes can be equipped with a variety of special measurement cells. For instance, cells with provision for controlling temperature rate allow for the investigation of phase transition properties of an emulsion. More so, there are special cells for studying the behaviour of droplets under mechanical stress (Linden *et al.*, 2003) and for estimating forces between droplets in concentrated emulsions (Brujic *et al.* 2003). However, there are often issues relating to phase contrast, which is usually caused by the poor contrast of the major components of an emulsion (Van Dalen, 2002). To enhance the phase contrast and ensure image improvement, various strategies have been adopted which include staining and changing light intensity. The staining is usually carried out with chemical dyes or lipid stains which either bind to specific components of an emulsion or preferentially partition into a single phase, as long as the emulsion microstructures remain undistorted (Murphy 2001). Examples of these stains include Nile red, Sudan Black B and Rhodamine B. Alternatively, fluorescent materials can be used as stains and in such case, a fluorescent-based microscope should be used for detection. The second strategy basically improves on phase contrast by adjusting light intensity based on the difference in refractive index across the microstructure using specialty lenses. This strategy is adopted in differential interference contrast microscopy and interference reflection microscopy. Confocal laser scanning microscopy is one of the most advanced microscopic techniques for characterizing an emulsion. It constructs three-dimensional images of an emulsion by obtaining sets of 2D images at different depths without the need for physical sectioning (Plucknett *et al.*, 2001). Thereby, providing insights on the spatial locations and fates of components within an emulsion, as well as the organization of its microstructure.

Despite modern microscopes being linked to computer systems for ease and fast image processing, obtaining quality and statistically reliable results remains time-consuming because randomly selected, large number of spatially different regions within an emulsion are needed for the analysis. Another major drawback is the distortion in structural properties of an emulsion (especially flocculated samples) during sample preparation.

2.6.2 Light scattering

Static light scattering techniques, also known as laser diffraction techniques for particle size characterization rely on the principle that the scattering pattern produced when a laser beam is focused on a dilute emulsion correlates with the particle size distribution of the emulsion. Instruments utilizing this technique are usually incorporated with software that comprises mathematical models which are often based on “Mie theory.” The models predict the scattering pattern from the particle characteristics: refractive index ratio, absorption coefficient, and diameter. After which, the software using the measured scattering pattern and the predicted one establish the best-fit and then generate reports as a data table or plots (particle concentration versus particle size. It should be noted that the concentration can either be in volume or number, while the size in either diameter or radius. Light scattering instruments that are commercially available are well suited for particle size ranging from ca. 0.1 to 1000 μm . Typically, the instrument requires sample preparation to a relatively low concentration (≤ 0.1 wt. %) to ensure the translational passage of a light beam while avoiding multiple scattering effects. Therefore, emulsion samples need to be carefully and sufficiently diluted without compromising its microstructural properties (Alexander *et al*, 2006; McClements, 1996).

Dynamic light scattering (DLS) techniques exploit the temporal fluctuations in intensity, when a light is scattered by particles whose spatial locations change frequently owing to Brownian motion, for particle size characterization. The frequency of the fluctuations depends on the speed of the particle which is influenced by the particle size. Smaller particles move faster than bigger counterparts, thus would result in more relatively rapid intensity fluctuations. The particle size distribution of an emulsion is determined from the change in intensity of scattered waves over time at a scattering angle using suitable mathematical models. Commercially available DLS instruments are suitable for particles whose diameters range from 0.003 to 5 μm . However, the concentration requirement varies with the method used for determining the intensity fluctuations. Some instruments measure transmitted light through an emission, thus limiting their suitability to sufficiently dilute emulsions (< 0.1 wt %); while others measure back-scattered light instead, thereby making them suitable for both concentrated and dilute emulsions (0.001 – 10 wt %). Moreover, diffusing wave spectroscopy (DWS) is an advanced DLS technique which extends the analytical capacity of light scattering to opaque samples (Alexander *et al*, 2006; McClements, 1996). The working principle of DWS is like DLS except that detected photons follow diffusive paths because of the highly multiple scattering in the opaque media, as opposed to single scattering. DWS technique is particularly suited for analyzing the mean size of particles or aggregates.

2.6.3 Nuclear Magnetic Resonance (NMR)

NMR-based particle sizing employs the interactions that exist between the proton nuclei and radio waves to provide insight on the microstructure of emulsions. The working principle is such that an emulsion is subjected to a static magnetic field gradient and a series

of radio frequency pulses, which excited some of the nuclei to higher energy levels. The excitation, in turn, leads to a detectable signal whose amplitude depends on the motion of the nuclei in the sample. The amplitude has an inverse relationship with the motion of the nucleus. Hence, the rate of reduction in the signal amplitude is used for studying the molecular motion. Unlike in a bulk liquid, the motion of a liquid within an emulsion droplet undergoes restricted diffusion owing to the presence of interfacial boundaries. However, this phenomenon is not apparent within a short-time domain given the distance covered. The attenuation in NMR signals at different instances is used to determine when the diffusion is restricted, which is in turn utilized to estimate the droplet size distribution via suitable mathematical models. Commercially available NMR-based instruments are appropriate for particles between 0.2 to 100 μm in size, whose concentrations in an emulsion may range from 1 to 80 wt %; thus, in most cases, dilution is not necessary. This technique determines the actual size of individual droplets in flocculated emulsion (not floc size) because the restricted diffusion is not affected by flocculation process. Furthermore, using NMR techniques for a continuous phase of emulsions (flocs) provide insights into the structural organization of droplets within flocs. NMR techniques for particle size distribution are non-destructive and suitable for concentrated and optically opaque emulsions (Carey, 2011, Opedal, 2009, McClements, 1996).

2.6.4 Coulter Counter

Coulter counter techniques, also known as electrical pulse counting techniques relied on the difference in electrical conductivities when a dilute emulsion passed through a small orifice to count and size particles. In simple form, the emulsion to be analyzed are contained in a beaker containing two dipping electrodes, one of which is housed in a glass tube with

a tiny hole for the suction of the emulsion. Upon the passage of each particle through the orifice, a transient drop in electrical current is observed, owing to the relatively lower electrical conductivity of oil. The instrument records the transient drop as an electrical pulse, which in turn is converted to another useful parameter such as droplet concentration and particle size distribution (PSD). The concentration of droplets is estimated as the number of pulses through the hole per unit volume of emulsion, while the PSD is analogous to the distribution of individual pulse height since the height of an electrical pulse depends on the particle volume. Commercially available coulter counter determines the PSD for particle size ranging from 0.4 to 1200 μm . Typically, such large range of particle size is usually covered by using a series of glass tubes with varying sizes of holes. For sample preparation, the instrument requires a relatively low concentration (≤ 0.1 wt. %) to ensure the passage of a single particle through the hole at a time. Hence prior to analysis, emulsion samples need to be well-diluted without compromising its microstructural properties (McClements, *et al*, 1996).

2.6.5 Ultrasonic Techniques

Ultrasonic waves are high frequency acoustic waves in the form of mechanical vibrations. Experimental techniques commonly used to measure ultrasonic properties can be divided into three categories: pulse echo, through transmission and interferometric methods (McClements, 1996). Acoustic signals acquired from oil, emulsion and water phases can differ due to differences in phase properties. Ultrasonic techniques possess several desirable qualities for a monitoring system. The analysis is non-destructive and minimally invasive, hardware can be compact, the results are robust and reliable, and the data can be seen in real time. An additional attractive feature of this technique is its potential to inspect

emulsion layer composition changes using acoustic spectroscopy which can provide important information for more reliable management of the unit.

Ultrasonic spectrometry is based on the change in ultrasonic attenuation relative to frequency, and the shape of its spectra is a function of particle concentration and size distribution. Typically an emulsion sample is positioned in a controlled chamber (temperature monitored) with provision for ultrasonic spectrum measurement, typically 0.1 – 150 MHz. Ultrasonic spectrometry instruments are usually incorporated into software (e.g. ECAHtheory) that allows the prediction of ultrasonic spectra of emulsions from the particle characteristics and the physical properties of dispersed and continuous phases. Particle characteristics include concentration, size and size distribution, while the useful physical properties of the phases are ultrasonic velocity, ultrasonic attenuation, thermal conductivity, density, viscosity, specific heat capacity and thermal expansion coefficient. The software determines the best-fit particle size distribution by comparing measured ultrasonic spectra and theoretically predicted ones and then generate suitable data which are presented as tables or plots of particle size (diameter/radius) against particle concentration (number/volume). Most commercial ultrasonic spectrometers have a measurement range of 0.01 to 1000 μm for particle diameter, which in principle work for emulsions within the range of 1 – 50 wt % (particle concentration). However, at higher droplet concentrations or flocculated emulsion, the governing principle becomes non-applicable, and as such any data obtained outside the earlier specified range become inaccurate. (McClements, 2000a; Chanamai, *et al*, 1999). Noteworthy, ultrasonic spectrometry measurements are non-destructive and can be performed *in situ* for optically opaque emulsions.

References

- Abdel-Raouf, M. 2012. Factors Affecting the Stability of Crude Oil Emulsions. *Egyptian Petroleum Research Institute*, 2012, 183–204.
- Abend, S., Bonnke, N., Gutschner, U. *et al.* 1998. Stabilization of emulsions by heterocoagulation of clay minerals and layered double hydroxides. *Colloid Polym Sciences*, 276, 730-737.
- Aichele, C.P., Chapman, W.G., Rheyn, L.D., *et al.* 2014. Characterization of Water-in-Crude-Oil Emulsions in a Complex Shear Field. *Experimental Thermal and Fluid Science*, 53 (2014), 190–96.
- Alba, F., Crawley, G.M., Fatkin, J. 1999. Acoustic Spectroscopy as a Technique for the Particle Sizing of High Concentration Colloids , Emulsions, and Suspensions. *Colloids and Surfaces A: Physicochemical and Engineering Aspects*, 153 (1-3), 495–502.
- Alexander, M., Dalgleish, D.G. 2006. Dynamic Light Scattering Techniques and Their Applications in Food Science. *Food Biophysics*, 2-13.
- Al-Sabagh, A.M., Nasser, N.M., Abd El-Hamid, T.M. 2013. Investigation of Kinetic and Rheological Properties for the Demulsification Process. *Egyptian Journal of Petroleum*, 22 (1), 117–127.
- Al-wahaibi, T., Angeli, A. 2008. Droplet Size and Velocity in Dual Continuous Horizontal Oil – Water Flows. *Chemical Engineering Research and Design*, 86 (1), 83–93.
- Al-Yaari, M., Husseinb, A., Al-Sarkhic, A. 2015. Effect of Water Salinity on Surfactant-Stabilized Water-Oil Emulsions Flow Characteristics. *Experimental Thermal and Fluid Science*, 64 (2015), 54–61.
- Anisa, I.N., Nour, H.N. 2010. Effect of Viscosity and Droplet Diameter on Water-in-Oil Emulsions: An Experimental Study. *Engineering and Technology*, 38 (2), 213–216.
- Ariffin, T., Yahya, E., Hazlina, H. 2016. The Rheology of Light Crude Oil and Water-in-Oil-Emulsio. in *Procedia Engineering*, 2016, cxlviii, 1149–55
- Arirachakaran, S., Oglesby, K.D., Shoulam, O., *et al.* 1989. An investigation of oil water flow phenomena in horizontal pipes. Paper SPE 18836, *Society of Petroleum Engineers*.
- Artur J Jaworski and Guangtian Meng, 'Journal of Petroleum Science and Engineering On-Line Measurement of Separation Dynamics in Primary Gas / Oil / Water Separators : Challenges and Technical Solutions — A Review,' *Journal of Petroleum Science and Engineering*, 68.1–2 (2009), 47–59.
- Ashrafizadeh, S.N., Kamran, M. 2010. Emulsification of Heavy Crude Oil in Water for Pipeline Transportation. *Journal of Petroleum Science and Engineering*, 71 (3-4), 205–11.

Ashrafizadeh, S.N., Kamran, M. 2010. Emulsification of Heavy Crude Oil in Water for Pipeline Transportation. *Journal of Petroleum Science and Engineering*, 71 (3–4), 205–211.

Aveyard, R., Binks, B.P., Clint, J.H. 2003. Emulsions Stabilized Solely by Colloidal Particles. *Advances in Colloid and Interface Science*, 100-102, 503-546.

Bensebaa, F., Kotlyar, L.S., Sparks, B.D., *et al.* 2000. Organic coated solids in athabasca bitumen: Characterization and process implications. *The Canadian Journal of Chemical Engineering*, 78 (4), 610-616.

Binks, B.P., Horozov, T.S. 2008. *Colloidal Particles at Liquid Interfaces*, Cambridge University Press, Cambridge, 1-520.

Binks, B.P., Kirkland, M. 2002. Interfacial structure of solid-stabilised emulsions studied by scanning, *Physical Chemistry Chemical Physics*, 4 (15), 3727–3733.

Binks, B.P., Kirkland, M. 2002. Interfacial Structure of Solid-Stabilized Emulsions Studied by Scanning Electron Microscopy. *Physical Chemistry Chemical Physics*, 4, 3727-3733.

Binks, B.P., Tyowua, A.T. 2016. Particle-Stabilized Powdered Water-in-Oil Emulsions. *Langmuir*, 32 (13), 3110–3115.

Chanamai, R., Alba, F., McClements, D.J. 2000. Ultrasonic Spectroscopy Study of Salad Dressings. *Journal of Food Science*, 65,507–513.

Chanamai, R., Herrmann, N., McClements, D.J. 1999. Influence of thermal overlap effects on the ultrasonic attenuation spectra of polydisperse oil-in-water emulsions. *Langmuir*, 15 (10), 3418–3423.

Clausse, D., Gomez, F., Dalmazzone, C. 2005. A Method for the Characterization of Emulsions, Thermogravimetry : Application to Water-in-Crude Oil Emulsion A Method for the Characterization of Emulsions. *Journal of Colloid and Interface Science*, 287 (2), 694-703.

Coupland, J.N., McClements, J.D. 2015. Droplet Size Determination in Food Emulsions: Comparison of Ultrasonic and Light Scattering Methods. *Journal of Food Engineering*, 50 (2), 117–20. Dalen, G.V. 2002. Determination of the water droplet size distribution of fat spreads using confocal scanning laser microscopy. *Journal of Microscopy*, 208: 116–133.

El-Gamal, M., Mohamed, A.M., Zekri, A.Y. 2005. Effect of Asphaltene, Carbonate, and Clay Mineral Contents on Water Cut Determination in Water – Oil Emulsions. *Journal of Petroleum Science and Engineering*, 46 (3), 209-224.

Ese, M.H., Galet, L., Clause, D. 1999. Properties of Langmuir Surface and Interfacial Films Built up by Asphaltenes and Resins: Influence of Chemical Demulsifiers. *Journal of Colloid and Interface Science*, 220, 293-301.

Gafonova, O.V. 2000. Role of Asphaltenes and Resins in the Stabilization of Water-in-Hydrocarbon Emulsions. M.Sc. Thesis, University of Calgary.

Issaka, S.A., Nour, A.H., Yunus, R.M. 2015. Review on the Fundamental Aspects of Petroleum Oil Emulsions and Techniques of Demulsification. *Journal of Petroleum & Environmental Biotechnology*, 6 (2), 1-15.

Issaka, S.A., Nour, A.H., Yunus, R.M. 2015. Review on the Fundamental Aspects of Petroleum Oil Emulsions and Techniques of Demulsification. *Journal of Petroleum & Environmental Engineering*, 6 (2), 1144-1163.

Khan, B.A. 2011. Basics of Pharmaceutical Emulsions: A Review. *African Journal of Pharmacy and Pharmacology*, 525 (25), 2715-2725.

Kilpatrick, P.K. 2012. Water-in-Crude Oil Emulsion Stabilization: Review and Unanswered Questions. *Energy Fuels*, 26 (7), 4017-4026.

Kruglyakov, P.M., Nushtaeva, A.V. 2004. Emulsion Stabilized by Solid Particles: Influence of the Capillary Pressure. In: Petsev, D.N., Ed., Emulsions: Structure, Stability and Interactions, Elsevier, Amsterdam, 641-676.

Langevin, D., Argillier, J.F. 2016. Interfacial Behavior of Asphaltenes. *Advances in Colloid and Interface Science*, 233, 83-93.

McClements, J.D. 1996. Principles of Ultrasonic Droplet Size Determination in Emulsions. *Langmuir*, 12 (14), 3454-3461.

McClements, J.D. 2007. Critical Review of Techniques and Methodologies for Characterization. *Crit Rev Food Sci Nutr*, 67 (7), 611-649.

McLean, J.D., Kilpatrick, P.K. 1997. Effects of Asphaltene Aggregation in Model Heptane-Toluene Mixtures on Stability of Water-in-Oil Emulsions. *Journal of Colloid and Interface Science*, 34 (196), 23-34.

Nadirah, L., Abdurahman, H.N., Rizauddin, D. 2014. Rheological Study of Petroleum Fluid and Oil-in-Water Emulsion. *Nadirah International Journal of Engineering Sciences & Research Technology*, 3 (1), 129-134.

Nädler, M., Mewes, D. 1995. Effects of the liquid viscosity on the phase distributions in horizontal gas-liquid slug flow, *International Journal of Multiphase Flow*, 21 (2), 253-266.

Opedal, N.V., Sørland, G., Sjöblom, J. 2009. Methods for Droplet Size Distribution Determination of Water-in-Oil Emulsions Using Low-Field NMR. *Diffusion-Fundamentals.org*, 9 (7), 1-29.

Pal, R. 1993. Pipeline Flow of Unstable and Surfactant Stabilized Emulsions, *AIChE J*, 39 (11), 1754-1764.

- Pal, R. 1996. Multiple O/W/O Emulsion Rheology. *Langmuir*, 12 (9), 2220-2225.
- Pal, R., Yan, Y., Masliyah, J. 1992. Rheology of emulsions. *Advances in Chemistry*, Vol. 231, Chapter 4, 131–170
- Piela, K., Delfos, R., Ooms, G., *et al.* 2008. On the Phase Inversion Process in an Oil-Water Pipe Flow. *International Journal of Multiphase Flow*, 34 (7), 665–677.
- Puerto, M.C. 2003. Surfactants: Fundamentals and Applications in the Petroleum Industry. *Chemical Engineering Journal*, 83 (1), 63.
- Rogacheva, O.V., Rimaev, R.N., Gubaidullin, V.Z., *et al.* 1980. Investigation of the Surface-Activity of the Asphaltenes of Petroleum Residues. *Colloid J USSR*, 42 (3), 490-493.
- Santos, R.G., Bannwart, A.C., Loh, W. 2014. Phase Segregation, Shear Thinning and Rheological Behavior of Crude Oil-in-Water Emulsions. *Chemical Engineering Research and Design*, 92 (9), 1629–1636.
- Schramm, L.L. 1992. Emulsions Fundamentals and Applications in the Petroleum Industry, *Advances in Chemistry*, Washington, DC: *American Chemical Society*, CCXXXI.
- Schubert, H., Armbruster, H. 1992. Principles of Formation and Stability of Emulsions. *Chemie Ingenieur Technik*, 32 (1), 14-28.
- Souza, W.J., Santos, K.M., Cruz, A.A. 2015. Effect of Water Content, Temperature and Average Droplet Size on the Settling Velocity of Water-in-Oil Emulsions. *Brazilian Journal of Chemical Engineering*, 32 (2), 455–464.
- Spedding, P.L., Donnelly, G.F., Cole, J.S. 2005. Three Phase Oil-Water-Gas Horizontal Co-Current Flow: I. Experimental and Regime Map. *Chemical Engineering Research and Design*, 83 (4), 401–411.
- Strausz, O.P., Mojelsky, L.T., Lown, E.M. 1992. The Molecular Structure of Asphaltene:an Unfolding Story. *Fuel*, 71 (12), 1355-1363.
- Sztukowski, D.M., Yarranton, H.W. 2005. Oilfield Solids and Water-in-Oil Emulsion Stability. *Journal of Colloid and Interface Science*, 285 (2), 821–833.
- Tadros, T.F., Vincent, B. 1983. Encyclopedia of emulsion technology Edited by: Becher, P. Vol. 1, 129New York: Marcel Dekker.
- Tambe, D.E., Sharma, M.M. 1993. Factors Controlling the Stability of Colloid-Stabilized Emulsions. I. An Experimental Investigation. *Journal of Colloid and Interface Science*, 157 (1), 244-253.

Wang, W., Cheng, W., Chen, L. 2013. Flow Patterns Transition Law of Oil-Water Two-Phase Flow under a Wide Range of Oil Phase Viscosity Condition. *Journal of Applied Mathematics*, 2013, 1–8.

Watson, B. A., & Barteau, M. A. (1994). Imaging of petroleum asphaltenes using scanning tunneling microscopy. *Industrial and Engineering Chemistry Research*, 33(10), 2358-2363.

Yan, Y., Masliyah, J.H. 1993. Solids-Stabilized Oil-in-Water Emulsions : Scavenging of Emulsion Droplets by Fresh Oil Addition. *Colloids and Surfaces A: Physicochemical and Engineering Aspects*, 15 (1), 123–132.

Yeh, G.C., Haynie J., Moses, R.A. 1964, Phase-volume relationship at the point of phase inversion in liquid dispersions. *AIChE J.*, 10 (2), 260-265.

Zolfaghari, R., Ahmadun, F., Abdullah, L., et al. 2016. Demulsification Techniques of Water-in-Oil and Oil-in-Water Emulsions in Petroleum Industry. *Separation and Purification Technology*, 170 (1), 377–407.

Chapter 3

3 Ultrasonic based techniques to monitor interface position in oil, water and emulsion separation

Abstract

Ultrasonic based techniques have been explored to monitor interface position between water and emulsion layers and oil and emulsion layers in separation vessels. Oil and water emulsion formation is a common occurrence in the oil and gas processing and several other commercial operations. This study tested the potential of ultrasonic techniques for monitoring separation of water, oil and emulsion phases. The oil phase consisted of either mineral oil or crude oil and water content of their emulsion was between 20 to 40%. The tests were conducted in a 4-inch diameter and 20-inch tall column. Measurements of acoustic velocity, pulse attenuation were made with a 3.5 MHz frequency probe operating in through transmission mode. The presence of a phase a phase type at a probe location was easily and quickly identified by changes in either acoustic velocity, attenuation or their combination. In the emulsion layer, acoustic properties are observed to depend on droplet size and their concentration. A significant change in signal either from oil to emulsion or from water to emulsion was observed and demonstrated the potential of the technique for such operations.

Key words: Ultrasonic techniques; Phase separation; Emulsion layer; Pulse attenuation

3.1 Introduction

Oil-water separations form an integral part of a number of operations such as crude oil processing, discharge from electrical substations and waste oil/grease separation from the effluent of food processing facilities. The presence of water with oil will almost invariably lead to emulsion formation which often requires additional treatment steps. This is the case during crude oil production steps where comingled water generates water-in-oil emulsions (Kokal, 2005; Yan et al., 2001). The crude oil collected from the ground also contains high levels of salts such as chlorides of calcium, sodium and magnesium. If these compounds are not removed from the oil, several problems can arise in the downstream refining processes such as heat exchanger fouling and deposits and catalyst poisoning. The impurities of salts and sand in crude oil are removed in a desalter unit in an oil refinery. Here process water is mixed with incoming crude oil to dissolve out the salts from crude oil and the mixture then enters separation vessels where the cleaned oil leaves from top and water containing dissolved salts leave from the bottom. The emulsion phase created by oil-water mixing is in the middle from which water droplet settle out. The emulsion phase is generated by the dispersion of water-droplets into oil phase and stabilized by impurities associated with crude oil. The emulsion phase characteristics can vary with crude composition and type of impurities present in oil. The emulsion phase is not expected in the cleaned oil and water outlet streams thus monitoring the emulsion layer is crucial for successful operation of the desalter. A properly designed and configured instrumentation scheme can avoid ingress of emulsion into desalted oil stream and loss of oil-containing emulsion into wash water exiting the vessel. Although a few techniques are commercially available for such applications, their shortcomings have been identified by the industry

during long period tests (Meribout et al., 2004; Hauptmann et al., 2002; Astridge and Longfield, 1967). This can be attributed to rather difficult, dynamic and fouling environment of a crude oil desalter. On the other hand, ultrasonic based techniques have shown good potential for such challenging applications, based on initial testing with fouling and opaque conditions. An additional attractive feature of this technique is its potential to inspect emulsion layer composition changes which can provide important information for more reliable management of the unit.

3.2 Materials and Methods

Mineral oil used for the experiments was purchased from VWR International and crude oil samples were provided by Imperial Oil Ltd. Deionized water was used to prepare water-in-oil emulsions and the oil content in emulsions was varied from 60 to 80%. Tween 20 (from Sigma Aldrich) was used as surfactant or emulsifier at concentration in the range 0.2 to 1 vol. % of oil for the preparation of water-in-oil emulsion. To prepare the emulsion, surfactant was added to the oil phase and dissolved in it by gentle agitation in batches of about 700 ml. A variable speed agitator (ARROW 850, Arrow Engineering Co) was used to provide agitation and shearing of emulsion fluids. The droplet sizes of the emulsions were determined by taking photomicrographs with Boreal optical microscope equipped with a camera. The images of the photomicrographs were analyzed to obtain droplet size distribution by using image processing software (Motic Images Plus 2.0).

A schematic diagram of the experimental set up used for the tests is shown in **Figure 3-1**. To study ultrasonic signal in different layers (i.e. oil, emulsion, water), tests were conducted in a 4" ID and 20" tall Plexiglas column equipped with ports to insert the probes. The test column contained different combinations of oil, emulsion and water phases and the height

of each layer was between 4 to 6". To start a test, a prepared emulsion was placed into the test column and water was filled in the test column slowly from bottom by opening the valve connecting the column to a nearby water tank. The height of water phase was raised or lowered to bring the probe into water, emulsion or oil phase. For a typical run, the probe was initially in the water phase and then moved into the emulsion and oil phases crossing the water/emulsion and emulsion/oil interfaces. The probe was connected to an ultrasonic pulser-receiver unit (UTEX Inc.). It was controlled by a software interface which allowed remote control and configuration of the instrument. Transducer excitation was achieved with an ultra-fast square wave pulse featuring adjustable pulse width and adjustable pulse voltage. The amplifiers in the instrument were directly gain controllable eliminating the need for attenuators that contribute to receiver noise. For the initial tests, a commonly used probe design used for liquid level detection was used. The interface position is determined by acoustic pulses reflected from interface due to differences in acoustic impedance. The intensity of reflected wave depends on the acoustic impedance mismatch between the materials across the boundary (Hauptmann et al., 2002). The distance of the interface from the probe can be determined by the following equation.

$$\mathbf{d}_{intf} = \mathbf{0.5} \times \mathbf{C} \times \mathbf{ToF} \quad (3.1)$$

Where C is acoustic velocity (m/s) in the water phase and ToF is time of flight recorded by the instrument for the wave to travel from transducer to the interface and back. The multiplication factor of 0.5 accounts for the fact that the wave traversed the distance twice from transducer to the interface.

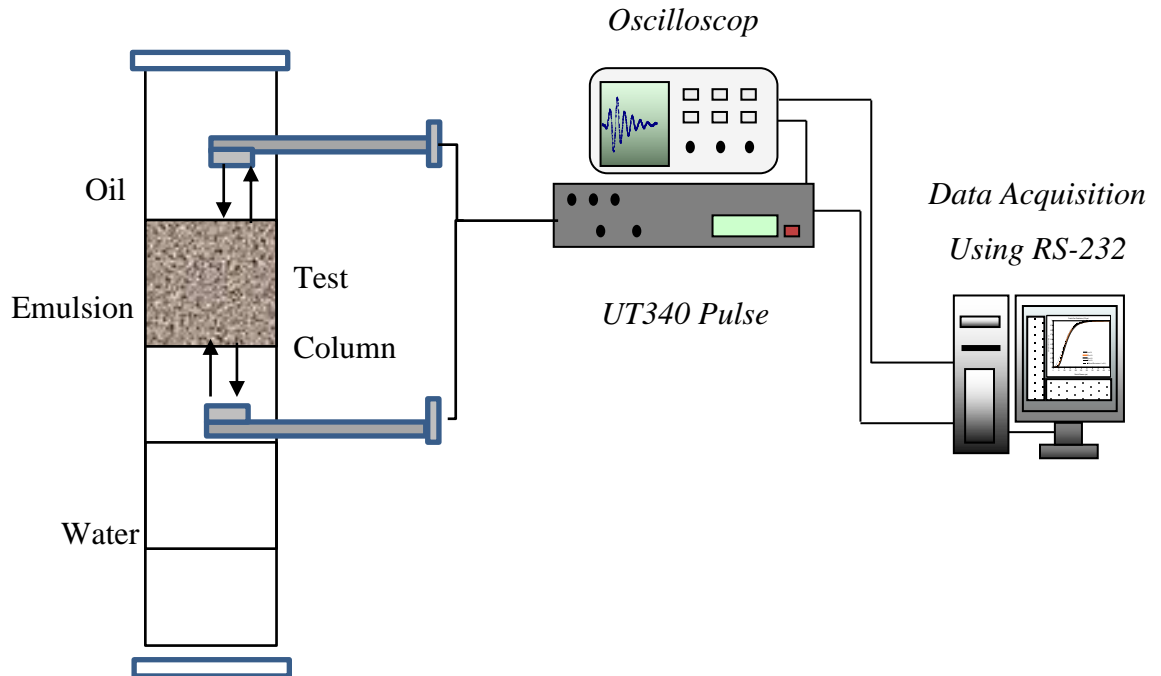


Figure 3-1 Schematic diagram of interface position monitoring system with ultrasonic technique

3.3 Result and discussion

3.3.1 Selection of Probe Design and Configuration

Tests with the initial probe design based on capture of reflected signal from interface (**Figure 3-1**) found that the reflected signal strength from emulsion interface was very weak making it difficult to isolate from signal noise. This indicated that the amount of energy reflected from the interface was quite low. The strength of the reflected signal depends on difference in acoustic impedance of the materials in contact at the boundary (Hoyle, 1996; Ensminger and Bond, 2012) as well the relative size and type of the contact boundary. The amount of energy reflected from the boundary (hence signal strength) can be estimated by the following equation;

$$R = \left[\frac{Z_2 - Z_1}{Z_2 + Z_1} \right] \quad (3.2)$$

Where Z_1 is the acoustic impedance of the medium from which the wave is propagating to the other side and Z_2 is the acoustic impedance of the material on the other side of the interface. For plane waves, this is equal to the product of medium density ρ and acoustic velocity c ($Z = \rho c$). The reflection coefficients for different interfaces are tabulated below for comparison (**Table 3-1**). It can be seen that reflection coefficient for oil-water interface is low compared to water and steel interface which is the main reason for weaker signal from oil-water interface. Metal boundaries generally provide higher reflection due to their high acoustic impedance.

Table 3-1 Acoustic impedance and reflection coefficient values for different materials used

Material	Acoustic velocity (m.s ⁻¹)	Density (kg.m ⁻³)	Acoustic impedance (kg.m ⁻² s ⁻¹)	Reflection coefficient	Remarks
Water	1450.0	998	1.447x10 ⁶	Oil-to-Water: 16%	No reflection for wave travelling from water to oil
Mineral Oil	1262.5	830	1.05x10 ⁶	Water-to-Oil: -16%	
Emulsion (water-mineral oil)	1288.5	863	1.1x10 ⁶	Water-to-Emulsion Oil-to-Emulsion: 3%	No reflection expected from water to emulsion and weak reflection from oil to emulsion
Steel	5800	7800	45.24 x10 ⁶	Water-to-Steel: 93.7 % Oil-to-Steel: 95.4%	Strong reflection expected from water to steel or oil to steel

In order to overcome the limitations due to weak reflected signals from the interfaces, it was decided to test through transmission mode to monitor interface position. For the test of this configuration, there is need to mount two transducers on a probe. One of the transducers generates the pulse and the transmitted signal is received by the other transducer. To make it work for the intended applications, two sets of such probes are needed. One placed in the aqueous phase below the emulsion-water interface and the second placed in the oil phase at a suitable distance above the emulsion-oil interface. Other considerations for capture of a high strength signal include good alignment between pulse generator and receiver and an optimal distance between the two. A distance of about 52 mm was selected between the

generator and receiver based on considerations of near field effect and pulse divergence. The probe design shown in **Figure 3-2** was used to test the response indifferent media.

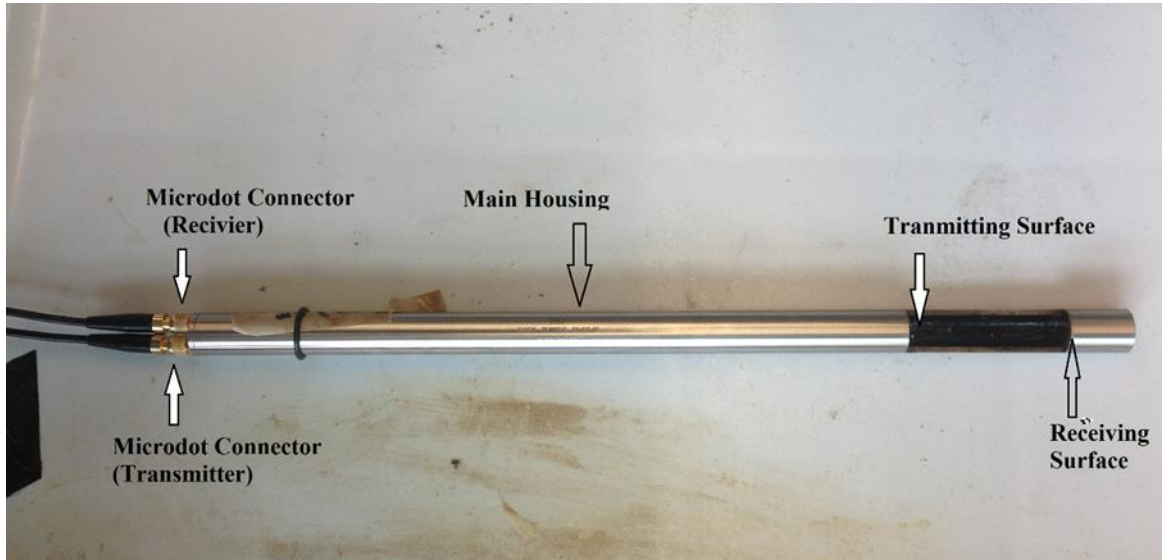


Figure 3-2 Details of probe design selected for measurements

Figure 3-3 compares strengths of the acquired signals (signal peak-height) obtained in water, oil and emulsion. Acoustic signals acquired from oil, emulsion and water phases can differ due to differences in phase properties. It is seen from **Figure 3-3** that the signal strength is highest in water and lowest in the emulsion. Lower peak height indicated more energy loss in the medium for the travelling wave. However, the acquired signal in the emulsion phase too was well above the noise and easy to detect. The difference in the received signal strengths can be attributed to a number of factors such as viscosity, presence of suspended particle/droplets and degree of system heterogeneity (Hogendoorn 2009; Kalivoda, 2011; Chen et al., 2013).

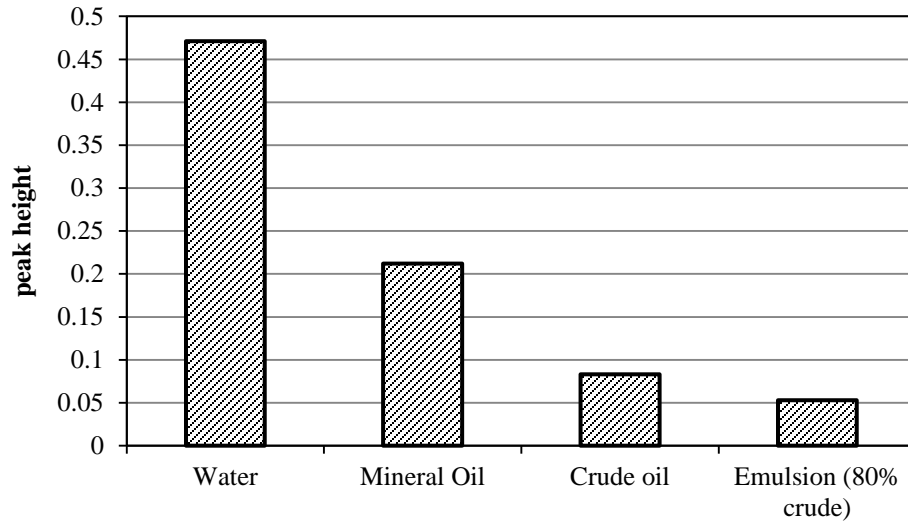


Figure 3-3 Comparison of acquired signal peak heights obtained in different media

Variation of peak heights in emulsions of water in crude oil prepared with different mixing speed are compared in **Figure 3-4**. It is observed that the peak heights decrease or energy loss increases with increase in mixing speed.

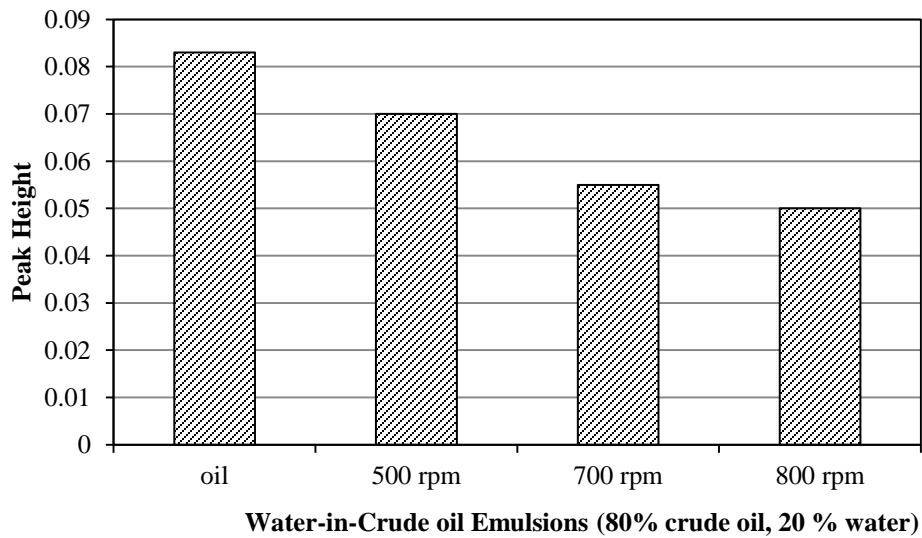
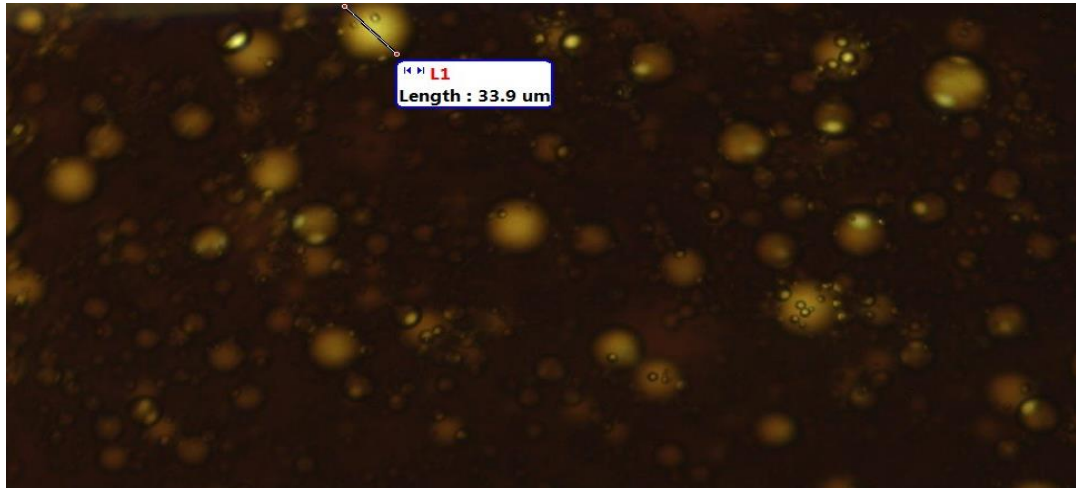


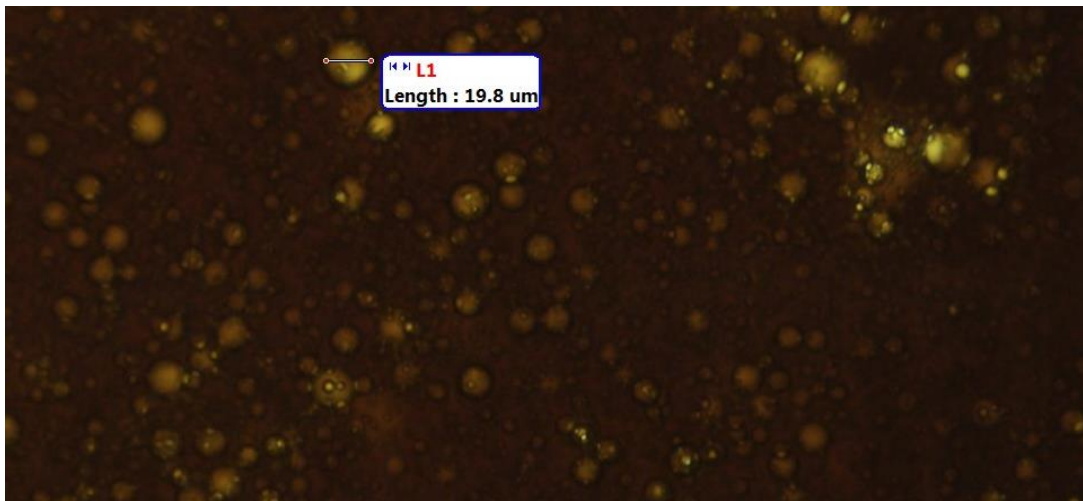
Figure 3-4 Peak heights obtained in crude oil emulsions prepared at different mixing speeds

The photomicrographs of the emulsion samples for the three rpms are presented in **Figures 3-5a to c**. It can be seen that droplet size decreases with increasing rpm although change in droplet size is less significant from 700 to 800 rpm thus. This behaviour of emulsions would require further considerations.

(a)



(b)



(c)

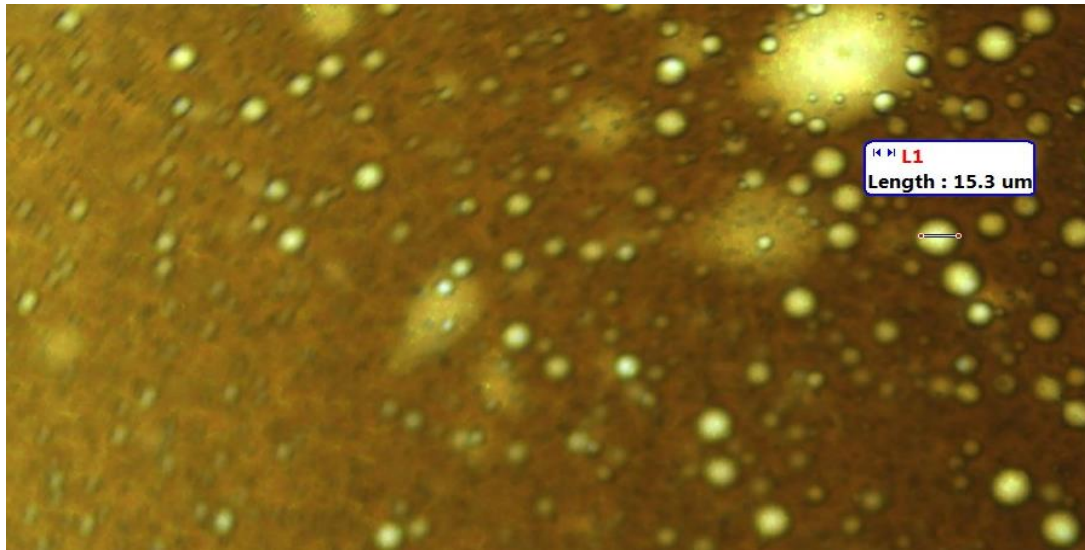


Figure 3-5 Photomicrographs of water-in-crude oil emulsions generated at different RPM: a) 500 rpm, b) 700 rpm, c) 800 rpm

3.3.2 Attenuation coefficient

While peak height measurements used above provide a quick comparison of signal strength in different systems, there is need to maintain a constant initial signal strength and a constant distance between signal generator and receiver. These limitations can be avoided by the more generalized approach based on calculation of attenuation coefficient. Acoustic energy is diminished or attenuated exponentially with distance as it travels from its source. Attenuation is usually reported using the attenuation coefficient (α), which has units of $\text{dB}\cdot\text{cm}^{-1}$ or simply cm^{-1} . In practice, this figure can be computed using the experimental and initial (or reference) values of amplitude, intensity, or pressure (Szabo, 2004).

$$\alpha = \frac{1}{d} \ln \left[\frac{A_{ref}}{A} \right] = \frac{1}{d} \ln \left[\frac{P_0}{P} \right] = \frac{1}{d} \ln \left[\frac{I_0}{I} \right] \quad (3.3)$$

Where d is the path length from transmitter to receiver (use 2d for pulse-echo techniques)

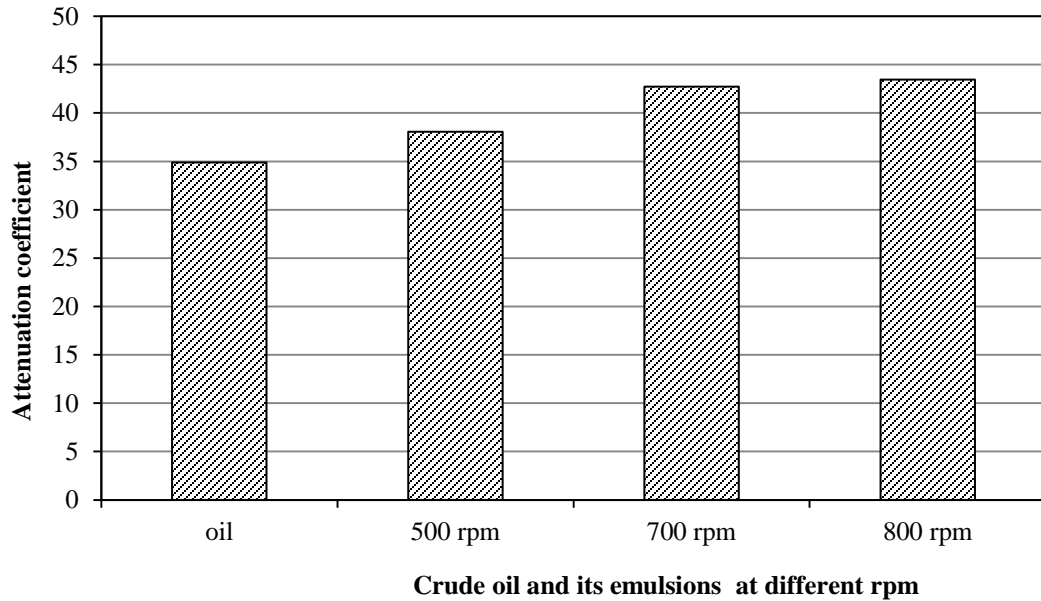


Figure 3-6 Attenuation values based on peak heights of Figure 23

3.3.3 Acoustic velocity

Acoustic velocity (v) is governed by the thermodynamic properties of the medium through which it is traversing. Based on the concept that sound is propagated as a harmonic longitudinal compression wave, the Newton-Laplace equation presents acoustic velocity through a given medium as a function of its bulk modulus (β) and density (ρ) (Ament, 1953; Urick, 1947).

$$v = \sqrt{\frac{\beta}{\rho}} = \frac{1}{\sqrt{\rho\kappa_s}} \quad (3.4)$$

If bulk modulus and density data are available, values for acoustic velocity can be predicted for different media using equation 3.4. Likewise, the equation can be used to draw conclusions about a fluid's density or isentropic compressibility (the reciprocal of bulk modulus) from experimentally obtained values of acoustic velocity. In practice however, bulk modulus is difficult to obtain specially for liquid mixtures like mineral oil and crude oil while density is easily measured by available methods. Using measured acoustic velocity and density equation 3.4 can be used to obtain bulk modulus for the liquid phase. The calculated values for bulk modulus are listed in **Table 3-2**

Equation 3.4, however is valid only for homogenous fluids. For application to non-homogenous mediums such as emulsions, this equation can be modified by calculating the effective density and elasticity of the suspension (Pinfield and Povey, 1997, Kuster and Toksoz, 1974; Urick, 1947). A simple modification is calculation of density and elasticity of the suspension based on their volumetric fractions.

$$\beta_{\text{eff}} = (1-\phi)\beta_{\text{Oil}} + \phi\beta_w \quad (3.5)$$

$$\rho_{\text{eff}} = (1-\phi)\rho_{\text{Oil}} + \phi\rho_w \quad (3.6)$$

Substituting these values of density and elasticity in equation 3.4 will give the velocity of ultrasound in suspensions. **Table 3.1** presents measured and calculated values of acoustic parameters in different media. Following observations can be made.

- Attenuation increases with decrease in droplet size due to increase in rpm used for emulsion preparation
- Acoustic velocity, however is nearly independent of droplet size in emulsions prepared by agitation speeds of 500 rpm and 700 rpm.

Table 3-2 Ultrasonic properties in water, oil and emulsion phase

Medium	Measured Acoustic Velocity (m/s)	Attenuation (1/m)	Measured avg. droplet size (μm)	Density (kg/m ³)	Calculated Bulk Modulus- (N/m ²)
Water	1450	Reference	NA	998	2.2x10 ⁹
Mineral oil	1340	7.3	NA	830	1.35x10 ⁹
Emulsion 1 (500 rpm)	1368.5	10.17	85.38	863	1.51x10 ⁹
Emulsion 2 (700 rpm)	1370	16.75	54.53	863	1.51x10 ⁹

From equations 3.3 to 3.5 and observations in **Table 3-2**, it is possible to estimate water fraction in the emulsion phase using measured acoustic velocity in emulsion phase, measured density of each phase and calculated bulk modulus from measured acoustic velocity in each phase. The resulting equation shown below could predict the water fraction of the emulsion phase within 5% for the data of this study.

$$\phi = \frac{[V_{emu}^2 \rho_{oil} - \beta_{oil}]}{[V_{emu}^2 (\rho_{oil} - \rho_w) + (\beta_w - \beta_{oil})]} \quad (3.7)$$

3.3.4 Tests with the probe to monitor interface position

These tests were conducted by raising/lowering the interface position with respect to the probe by adding or draining water from column bottom. The change in signal was recorded as the interface moved across the probe. Variation of attenuation near the oil-emulsion interface is shown in **Figure 3-7**. The probe was initially in the oil phase, about 4 cm beyond the interface and it was brought into the emulsion phase by slowly draining water from the column. On the diagram location '0' indicates beginning of emulsion phase layer. It can be seen that the probe clearly and quickly captured the change in attenuation moving from oil to emulsion phase. As expected, the attenuation in emulsion phase is higher than in oil phase, which can be attributed to the heterogeneity of the emulsion phase. It is also observed from **Figure 3-7** that as the probe approached the interface from the oil phase, there is a steady increase in attenuation before dropping quickly in the emulsion phase. The increase in attenuation near the interface can be attributed to the presence of both oil and emulsion phase in the active area of the probe.

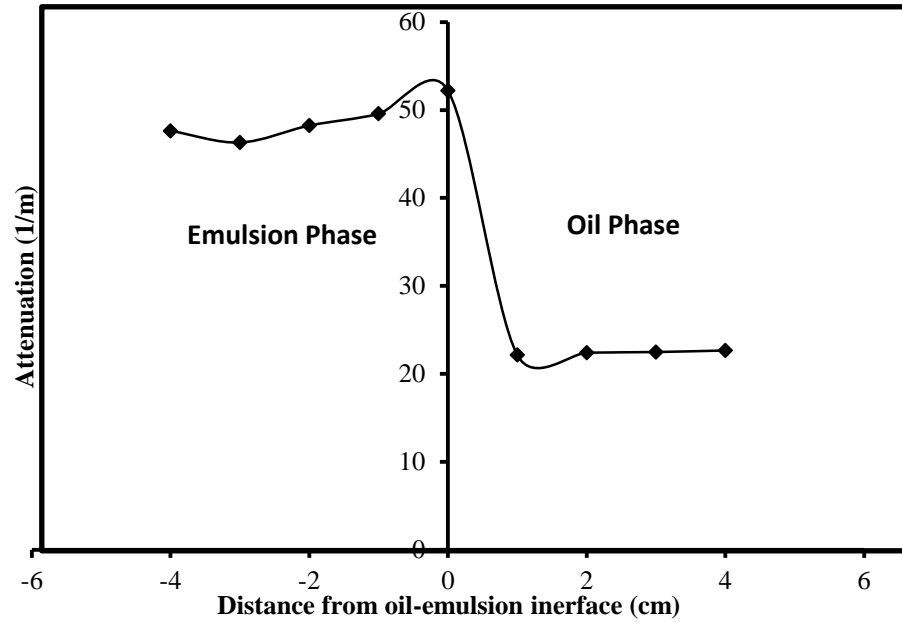


Figure 3-7 Variation of attenuation with location in the layer near the oil-emulsion interface (emulsion: 80% mineral oil in water)

Figure 3-8 shows how the signal-shaped changed when the probe moved from oil phase into the emulsion phase. A significant change in acquired signal height is clear to observe. Such visual observations can provide easy detections for tracking the operation.

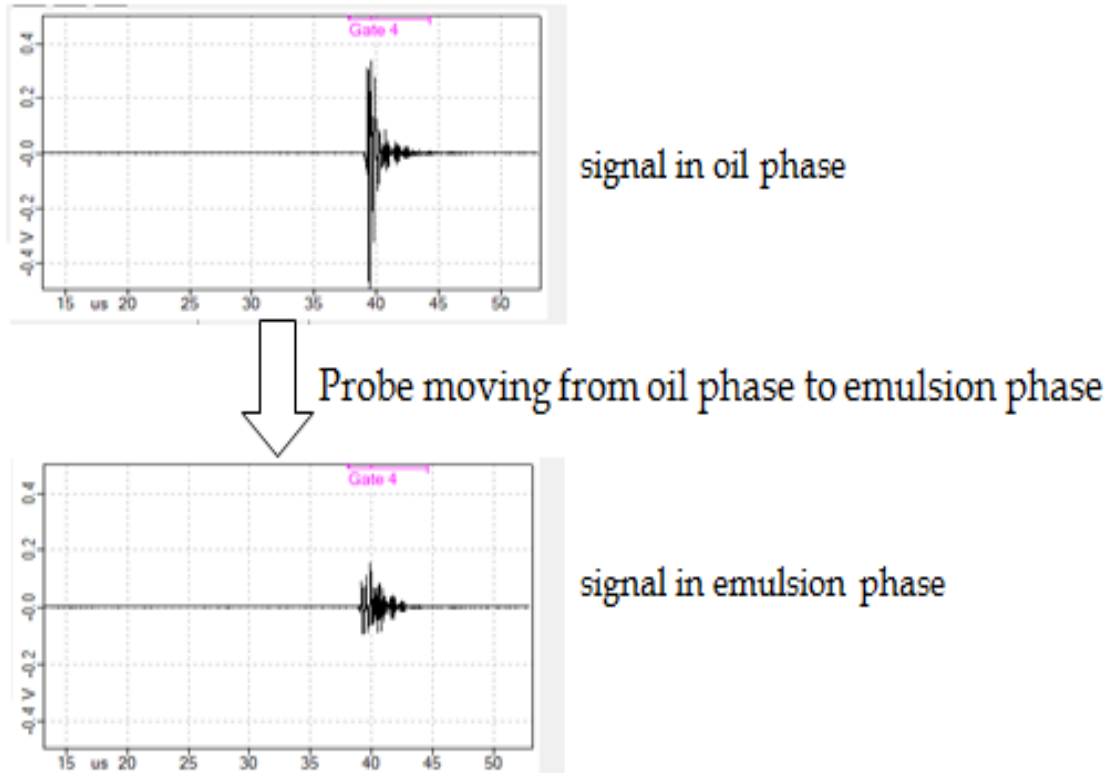


Figure 3-8 Signal changes when probe moving from oil phase to emulsion

Figure 3-9 presents variation of acoustic velocity as the probe moved from oil to the emulsion phase prepared with mineral oil. It can be seen that acoustic velocity increases quickly near the interface as the probe moves into the emulsion phase. Since the probe was fixed at one location, it moved down relative to interface as the oil-emulsion moved up as water entered from column bottom. Initial measurement is made at location 4 cm beyond the interface (represented by 4cm) and then stepping 1 cm toward the interface until -4 cm below the interface. Simultaneous acoustic velocity measurements with attenuation measurements can provide confirmation tests.

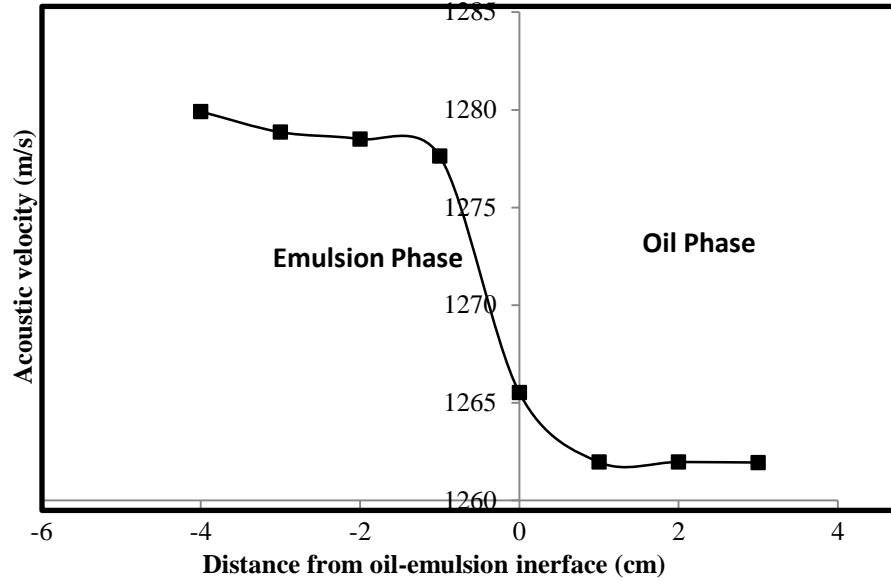


Figure 3-9 Variation of velocity with location in the layer near the oil-emulsion interface (emulsion: 60% mineral oil in water)

3.3.4.1 Ultrasonic signals at water-emulsion interface

Variation of attenuation recorded as the probe moved from water to emulsion phase is shown in **Figure 3-10**.

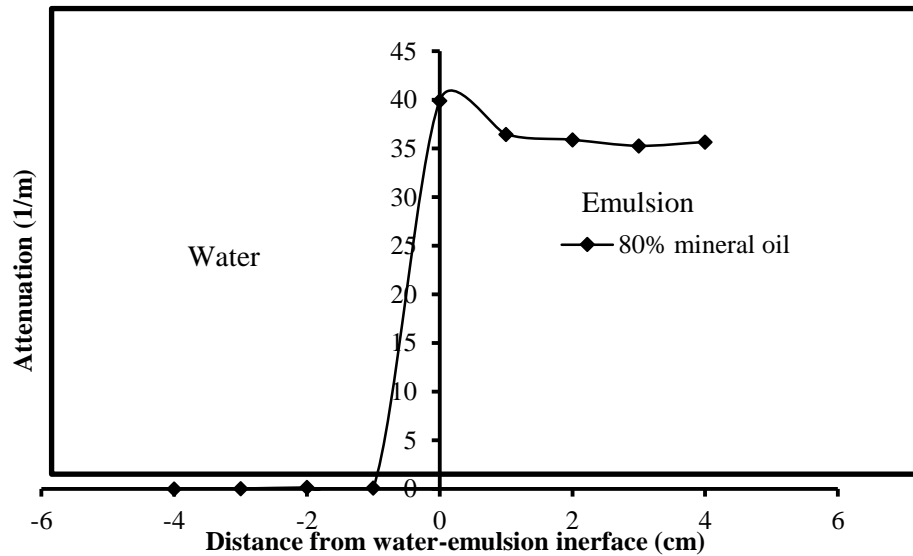


Figure 3 10 Variation of attenuation with location near the water-emulsion interface.

It can be seen that attenuation increases significantly as the probe moves closer to the interface. Once inside the emulsion phase, there is only very little variation in attenuation. As expected acoustic velocity decreases significantly as the probe moved from aqueous phase to the emulsion phase (**Figure 3-11**).

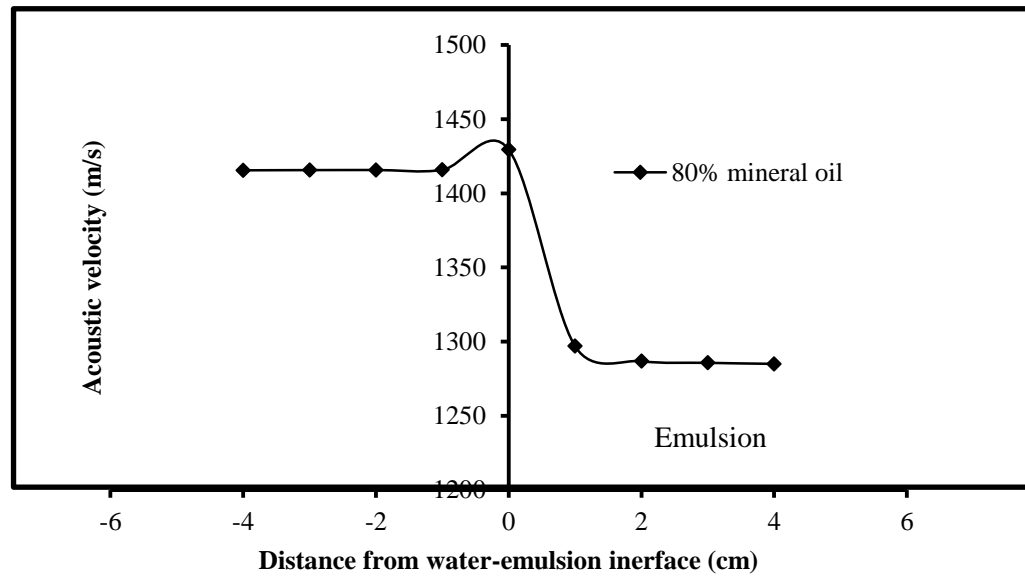


Figure 3-10 Variation of velocity with location in the layer near the water-emulsion interface (emulsion: 80% mineral oil in water)

3.3.4.2 Ultrasonic signals at water-oil interface – no emulsion phase

Experiments were also conducted with oil-water interface in absence of the emulsion layer. The effect of oil-water interfacial layer is also observed, as shown in **Figures 3-12** and **3-13**. When probe is moved from water phase into mineral oil phase, acoustic velocity is reduced and attenuation is increased. At interface location, the velocity is between velocities in bulk oil and water phases. The attenuation in the interface exhibits a maximum value, which is a similar to the phenomenon observed in oil-emulsion and water-emulsion interfaces. At the interface location, the transducer is partially immersed in each phase. The propagating wave experienced a sudden discontinuity due to significant differences in

phase properties. This would lead to significant lower loss amplitude of the traveling wave as recorded by higher attenuation on the interface.

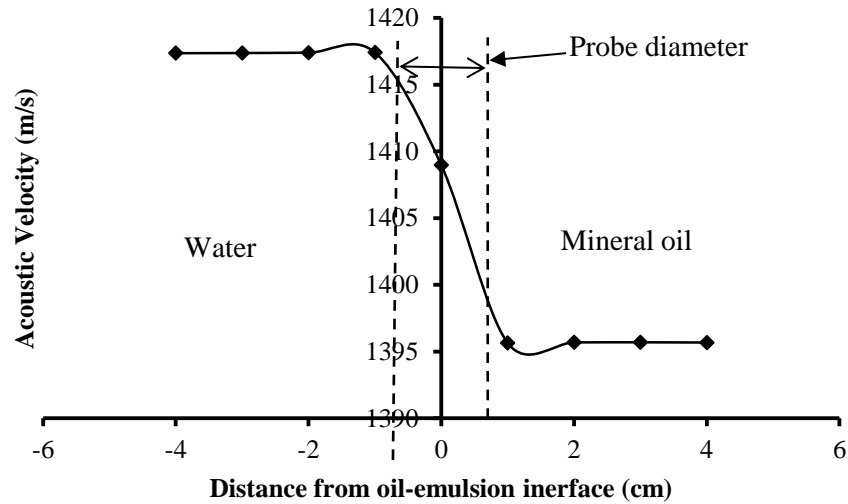


Figure 3-11 Variation of acoustic velocity with location in the layer near the water-oil interface (Temp. = 21.5 °C)

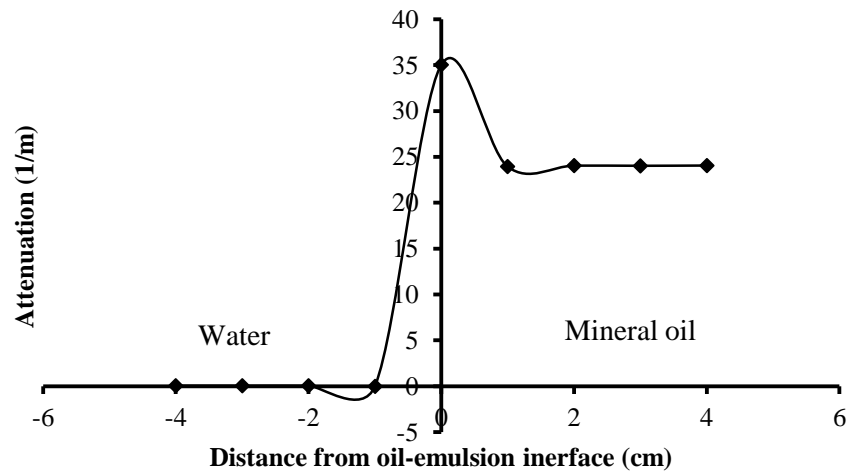
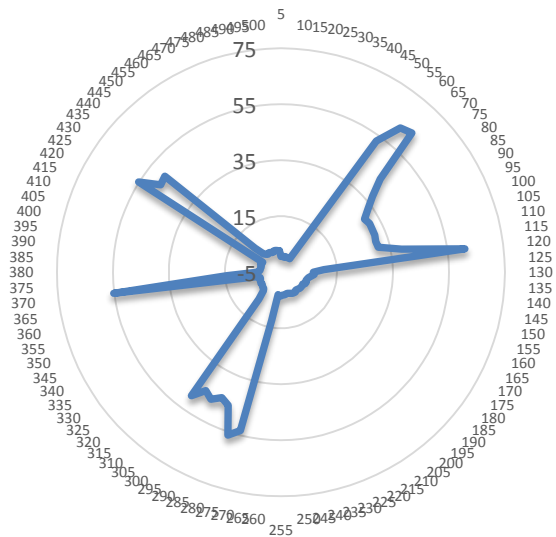
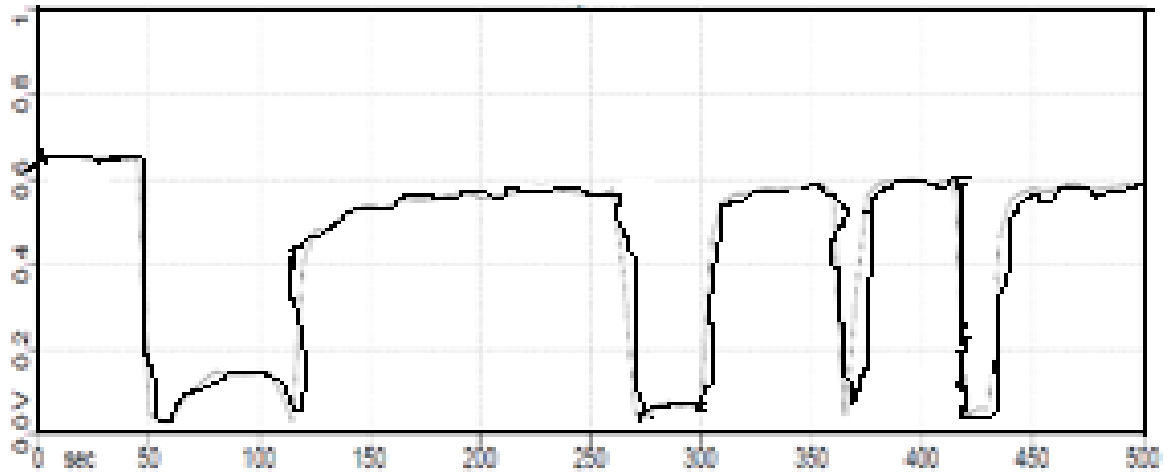


Figure 3-12 Variation of attenuation with location in the layer near the water-oil interface

To further test the techniques to monitor the interface position, test was conducted by raising and lowering the interface position repeatedly. The recorded signal values are plotted in **Figure 3-14** on a rectangular and a circular chart to duplicate commonly used practice in industry. The dip in recorded value indicates that probe has moved into the emulsion phase.



3.3.5 Tests with Crude Oil Samples

After demonstrating the ability of the technique with mineral oil, a few tests were also conducted with crude oil samples and emulsions of water-in-crude oil. As shown in **Figures 3-15** and **3-16**, the probe response was similar to those observed with mineral oil, although differences were noticed with respect to probe response rate which can be attributed to differences in composition and rheology of the two oils. The probe design may require alterations, if a faster response rate is required.

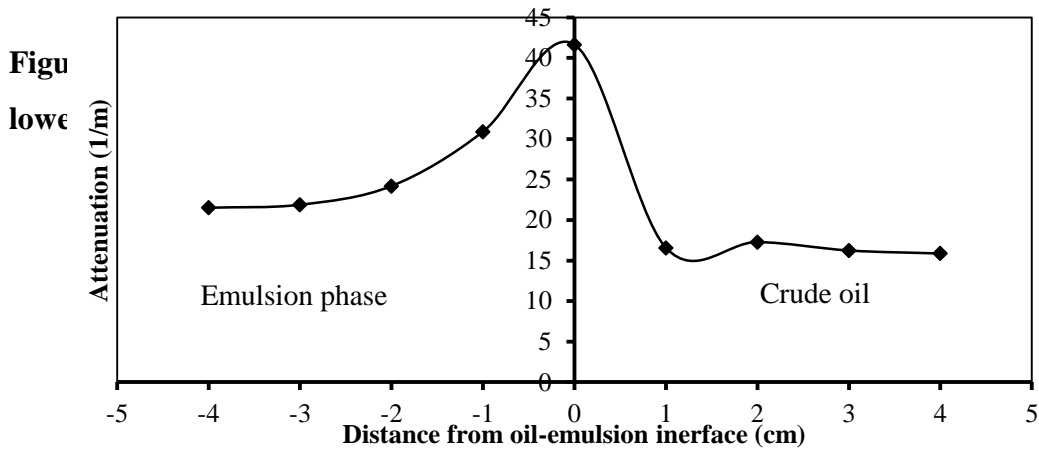


Figure 3-14 Variation of attenuation with location in the layer near the crude oil-emulsion

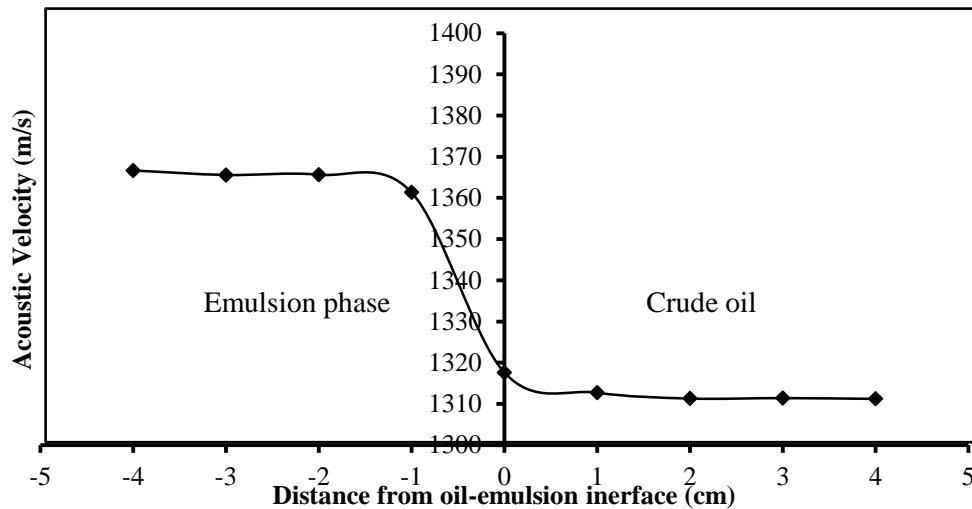


Figure 3-15 Variation of velocity with location in the layer near the oil-emulsion interface

3.3.6 Statistical Analysis

Each data point in the Figures above is an average of 400 data points recorded. The data set was also used to calculate standard deviations and values were plotted to look for trends.

Figures 3-17 shows that standard deviations (S.D.) derived from attenuation are significantly higher in the emulsion phase than in oil and water phases. This can be attributed to the heterogeneous nature of the emulsion phase due to the presence of droplets of different sizes in the dispersion.

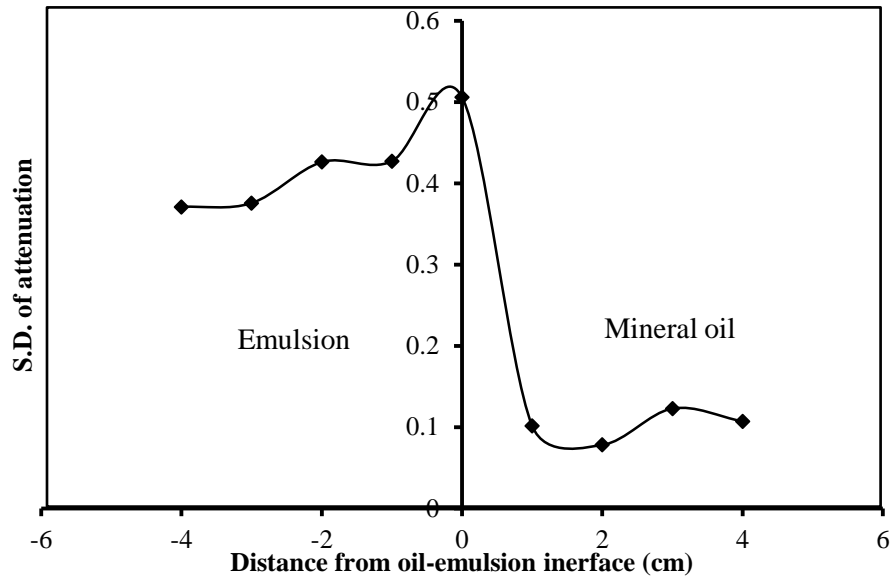


Figure 3-16 Attenuation derived standard deviations in the emulsion and oil layers near the Oil-emulsion interface (emulsion: 80% oil)

Standard deviations (S.D.) derived from acoustic velocity measurements in the two layers are presented in **Figure 3-18**. It is observed that the standard deviations are significantly smaller and the difference in values between the emulsion and oil phases are also lower compared to attenuation data. These observations can be related to earlier measurements of acoustic velocity in emulsions prepared at different agitation speeds. It was found that although droplet size distribution changed with increase in rpm, there was little effect on measured acoustic velocity.

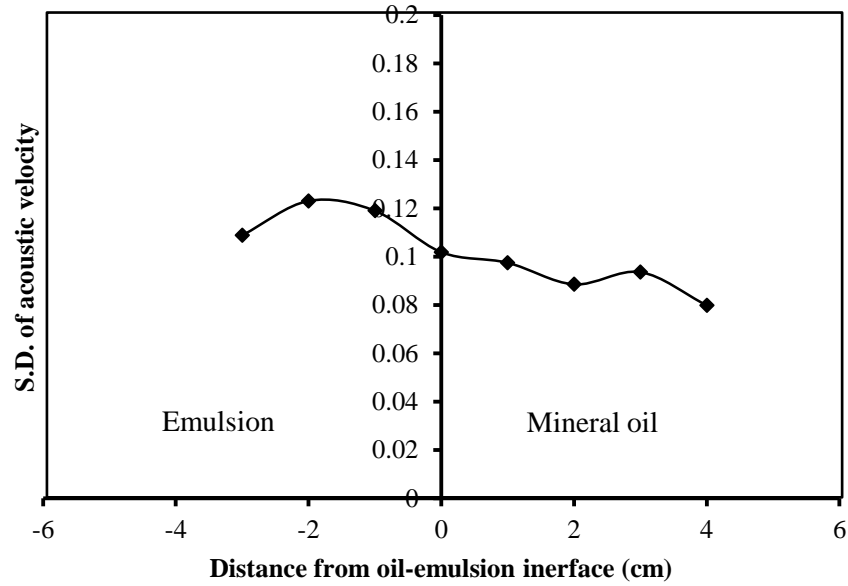


Figure 3-17 Acoustic velocity derived standard deviations in the two layers (emulsion: 80% oil)

3.3.7 Local Variations inside the emulsion phase layer

The emulsion layer can easily undergo local variations with respect to the dispersed phase composition. This can be result of droplet settling, coalescence or flocculation processes (Yan et al., 2001; Kokal, 2005). The sensitivity of the probe to capture local variations inside the emulsion phase was tested by measurements near the top and bottom of the emulsion layer. The probe was placed about 10 mm below oil-emulsion interface and 10 mm above water-emulsion interface, as shown in **Figure 3-19**. At the same time, emulsion samples were collected from these locations to determine droplet size distributions. The pictographs of the top and bottom point samples are also shown in **Figure 3-19**. It can be seen that there is higher concentration of smaller droplets at the top and their density is significantly lower near the bottom where larger droplets dominate. The cumulative droplet

size distribution at the two locations is plotted in **Figure 3-20** which confirms higher concentration of smaller droplets in the top region of emulsion layer.

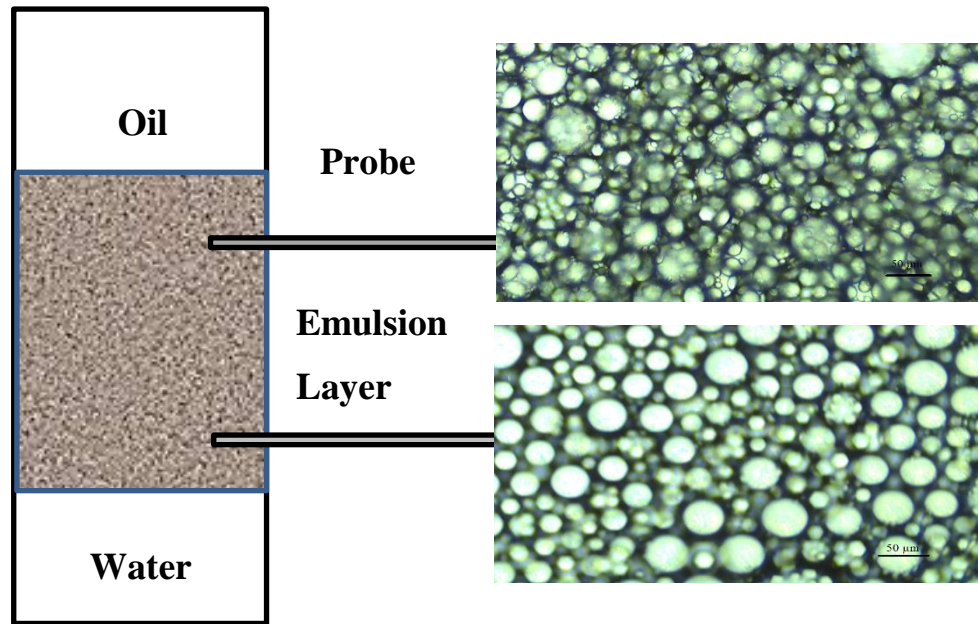


Figure 3-18 Pictographs of emulsion samples collected from top and bottom of emulsion layer

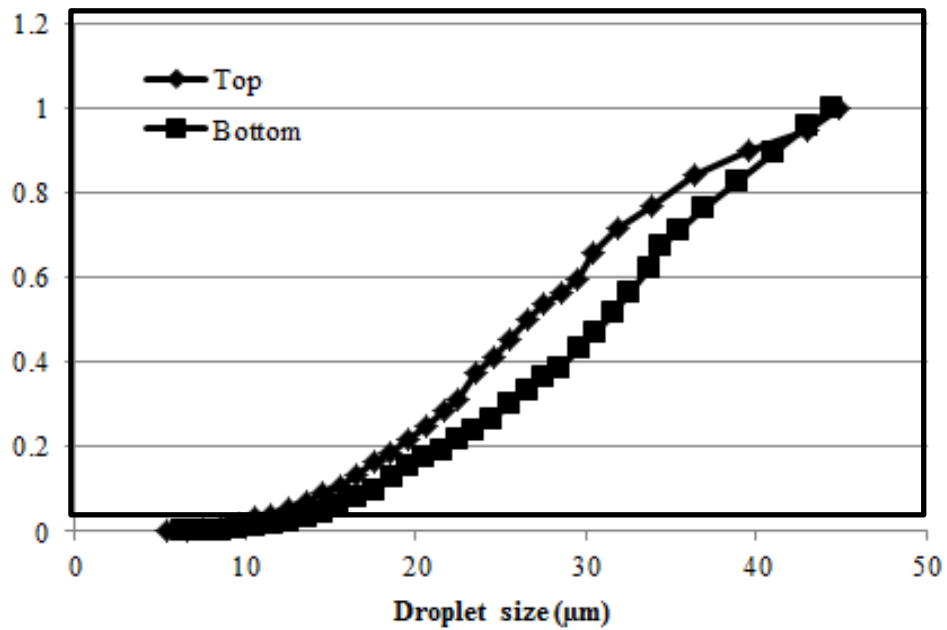


Figure 3-19 Droplet size distributions in top and bottom sections of emulsion layer.

Measured values of attenuation and acoustic velocity recorded at the two locations are compared in **Figure 3-21** and **3-22**. The higher attenuation at the top can be attributed to larger concentration of smaller droplets which can enhance dynamic viscosity of the emulsion (Pal, 1996). It was demonstrated by Pal (1996) that the viscosity of emulsion with fine droplet (12 μm) is significantly higher than of emulsion with coarse droplets (30 μm). The higher concentration of larger droplets in the bottom section would lower emulsion viscosity.

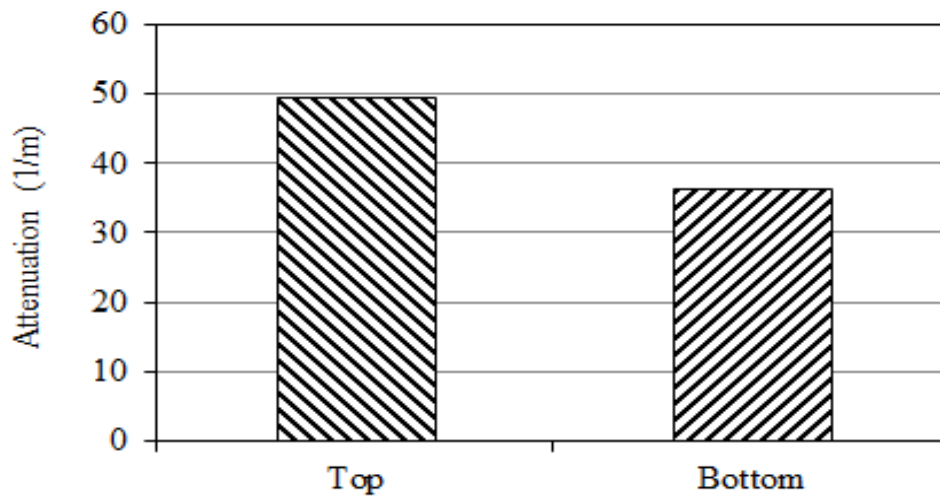


Figure 3-20 Attenuations near top and bottom locations in emulsion layer

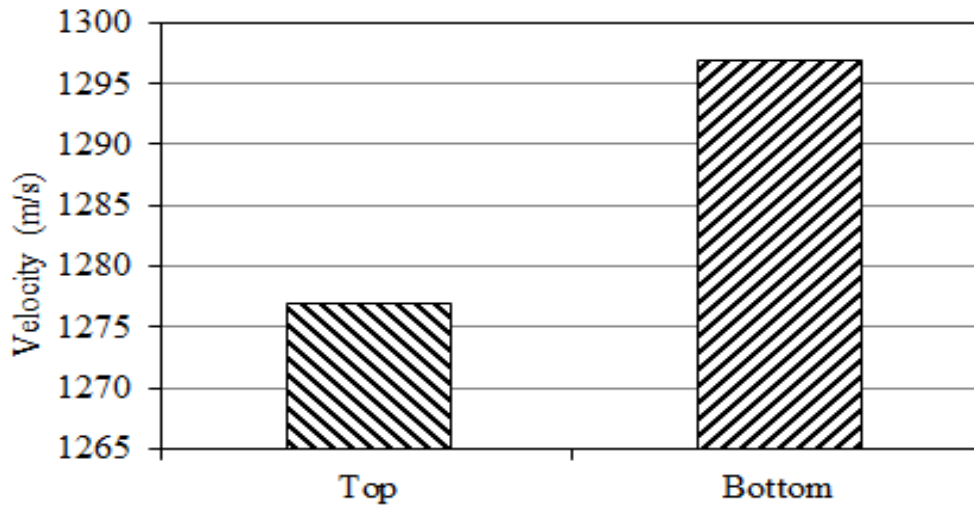


Figure 3-21 Acoustic velocity at top and bottom locations in the emulsion layer

Figure 3-22 shows that the velocity in bottom section is higher than in top section, indicating a lower concentration of mineral oil at bottom section in the emulsion phase. This is a result of settling out of water droplets from the emulsion building up concentration of water in the dispersion at the bottom location.

3.3.8 Proposed probe configuration to monitor emulsion layer position

Based on above tests and observations, a probes configuration shown in **Figure 3-23** was proposed to monitor emulsion layer in crude oil desalter operation. For the proposed approach, two ultrasonic probes are included, one in oil layer (S1) and other in water layer (S2). These probes are designed to operate in through transmission mode. Probe S1 is normally located in the oil layer and S2 in the water layer. If emulsion layer moves up into S1 location, the signal from probe S1 will change from oil layer to emulsion layer.

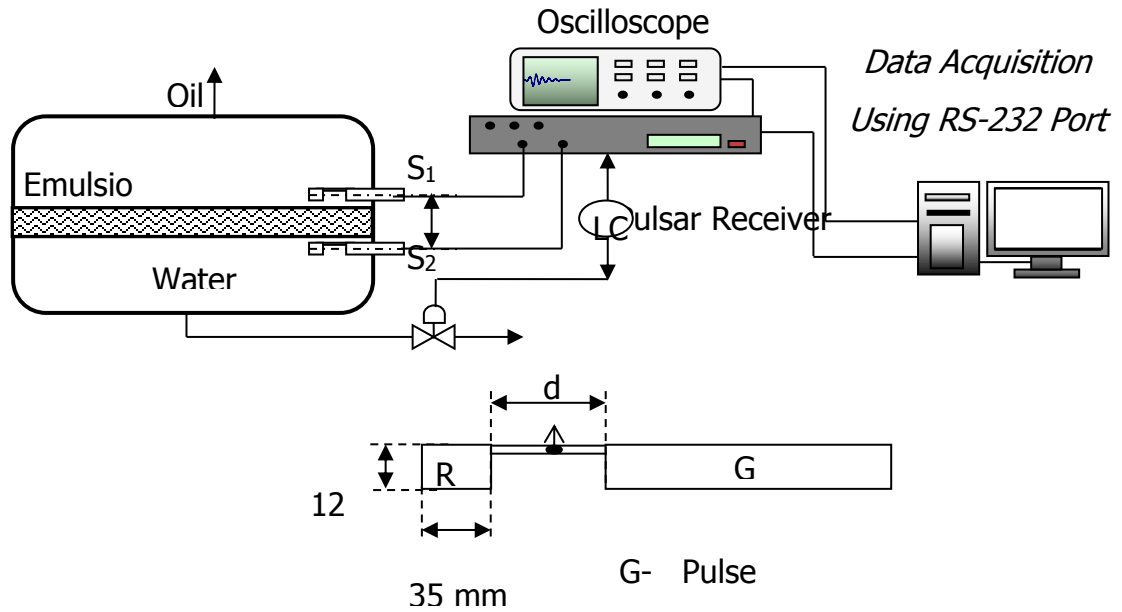


Figure 3-22 Schematic of proposed ultrasonic based instrumentation to monitor

If emulsion layer moves down into S2 location, the signal from S2 will be identified from water layer to emulsion layer. Series of experiments conducted in this study demonstrate the technical viability of this approach since ingress of emulsion layer into the probe space resulted in a significant change of wave parameters including acoustic velocity, attenuation and statistical properties of the signal.

3.4 Conclusions

The potential of utilizing based techniques to monitor emulsion layer in separation vessels such as crude oil desalter operation has been demonstrated through a series of tests and detailed analysis of data. It is demonstrated that a high degree of confidence in the measurements is achievable with simultaneous measurements of acoustic velocity,

attenuation and statistical analysis of the acquired data. An instrumentation scheme to monitor and control crude oil desalter operation has been proposed. This scheme utilizes two probes, one placed in the oil phase, just above the maximum height allowable for emulsion layer and other placed just below the lowest level for the emulsion phase. A suitably planned algorithm can further improve the performance and utilization of the proposed scheme.

References

- Ament, W. 1953. Sound Propagation in Gross Mixtures. *The Journal of The Acoustical Society of America*, 25 (4), 638-641.
- Astridge, D.G., Longfield, M.D. 1967. Capacitance Measurement and Oil Film Thickness in a Large Radius Disc and Ring Machine. *Proc. Inst. Mech. Engrs*, 182 (14), 89-96.
- Ammann, J., Galaz, B. 2003. Sound velocity determination in gel-based emulsion. *Ultrasonics*, 41(7) , 569-579.
- Chen, Y., Huang, Y., Chen, X. 2013. Acoustic propagation in viscous fluid with uniform flow and a novel design methodology for ultrasonic flow meter. *Ultrasonics*, 53 (2), 595–606.
- Filho, D.C., Ramalho, J.B., Spinelli, L.S., *et al.* 2012. Aging of water-in-crude oil emulsions: Effect on water content, droplet size distribution, dynamic viscosity and stability. *Colloids and Surfaces A: Physicochemical and Engineering Aspects*, 396 (20), 208–212.
- Filho, D.C., Ramalho, J.B., Spinelli, L.S., *et al.* 2012. Aging of water-in-crude oil emulsions: Effect on rheological parameters. *Colloids and Surfaces A: Physicochemical and Engineering Aspects*, 405 (3), 73-78.
- Hauptmann, P., Hoppe, N., Puttmer, A. 2002. Application of Ultrasonic Sensors in the Process Industry. *Measurement Science and Technology*, 13 (2), 73-83.
- He, P., Zheng, J. 2001. Acoustic dispersion and attenuation measurement using both transmitted and reflected pulses. *Ultrasonics*, 39 (1), 27-32.
- Hoyle, B.S. 1996. Process tomography using ultrasonic sensors. *Measurement Science and Technology*, 7 (3), 272-280.

Khatri, N.I., Andrade, J., Baydak, E.N., *et al.* 2011. Emulsion layer growth in continuous oil-water separation. *Colloids and Surfaces A: Physicochemical and Engineering Aspects* 384 (2011) 630-642.

Kokal, S. 2005. Crude-oil Emulsions: A state-of-the-art review. *SPE Production and Facilities*, 20 (1), 5-13.

Kuster, G.T., Toksöz, M.N. 1974. Velocity and attenuation of seismic waves in two-phase media: Part II. Experimental results. *Geophysics*, 39 (5), 607-618.

Meribout, M., Habli, M., Al-Naamany, A., *et al.* 2004. A New Ultrasonic-based device for Accurate Measurement of Oil, Emulsion, and Water Levels in Oil Tanks. *Instrument and Measurement Technology Conference*, (3), 1942-1947.

Pal, R. 1996. Effect of Droplet Size on the Rheology of Emulsions. *AIChE Journal*, 42 (11), 3181-3190.

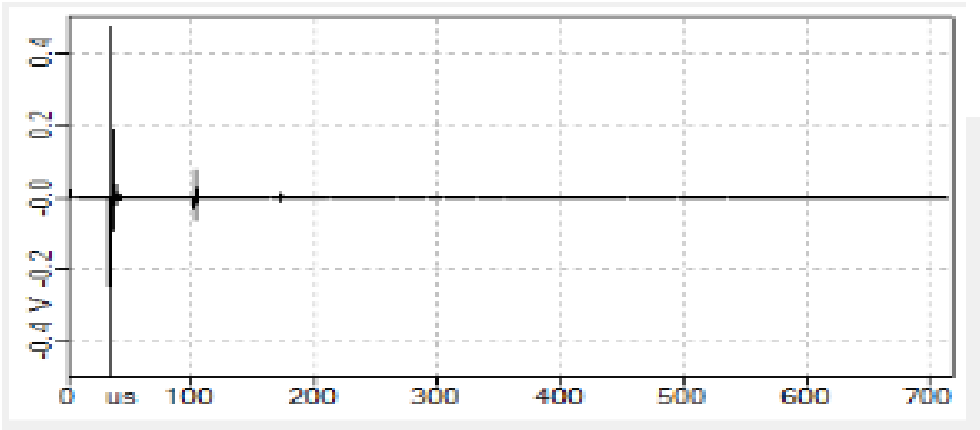
Pinfield, V.J., Povey, M.J. 1997. Thermal scattering must be accounted for in the determination of adiabatic compressibility. *The Journal of Physical Chemistry B*, 101 (7), 1110-1112.

Szabo, T. 2004. Attenuation. In T. Szabo, *Diagnostic Ultrasound Imaging - Inside Out*". London: *Elsevier* , 71-95.

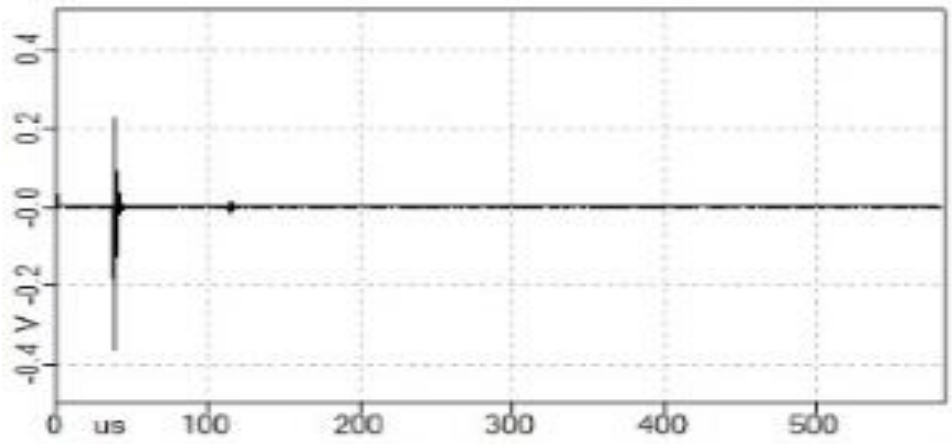
Urlick, R. 1947. A sound Velocity Method for Determining the Compressibility of Finely Devided Substances. *Journal of Applied Physics*, 18 (11), 983-987.

Yan, N., Gray, M.R., Maslihah, JH. 2001. On Water—in-oil emulsions stabilized by fine solids. *Colloids and Surfaces, A: Physicochemical and Engineering Aspects*, 193 (1), 97-101.

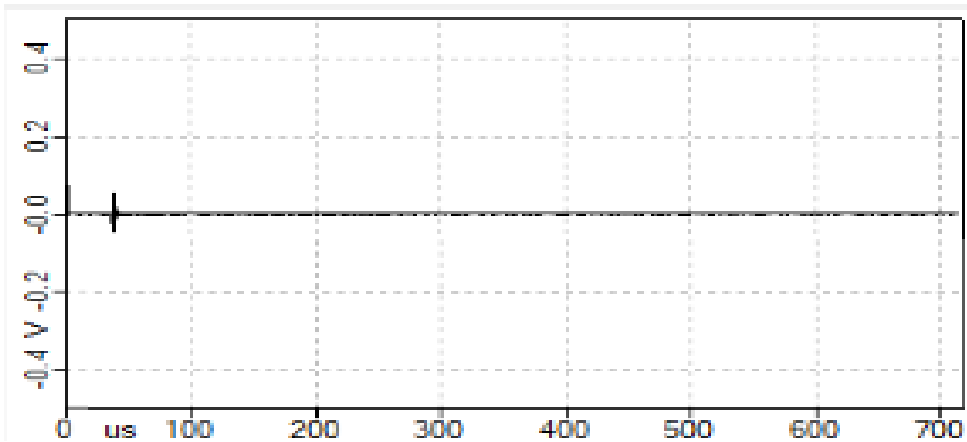
Appendix A



Appendix A 1 ultrasonic propagation wave in water

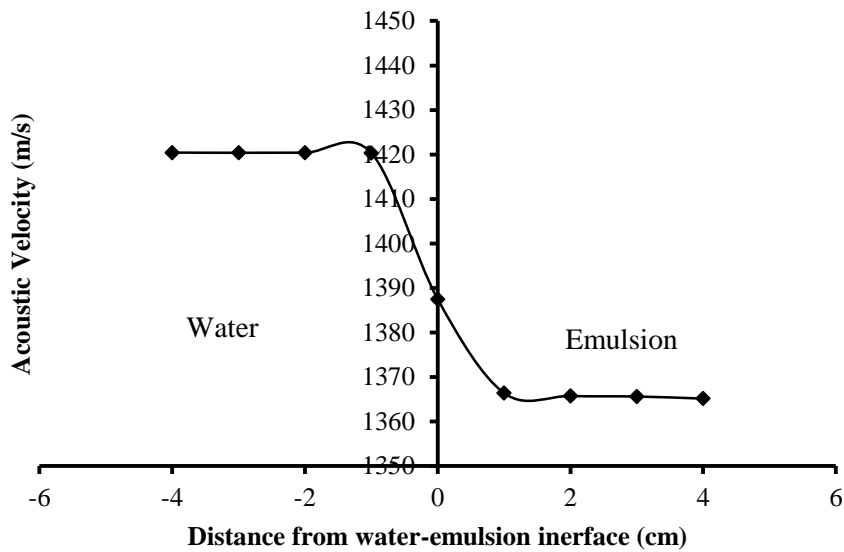


Appendix A 2 ultrasonic propagation wave in oil

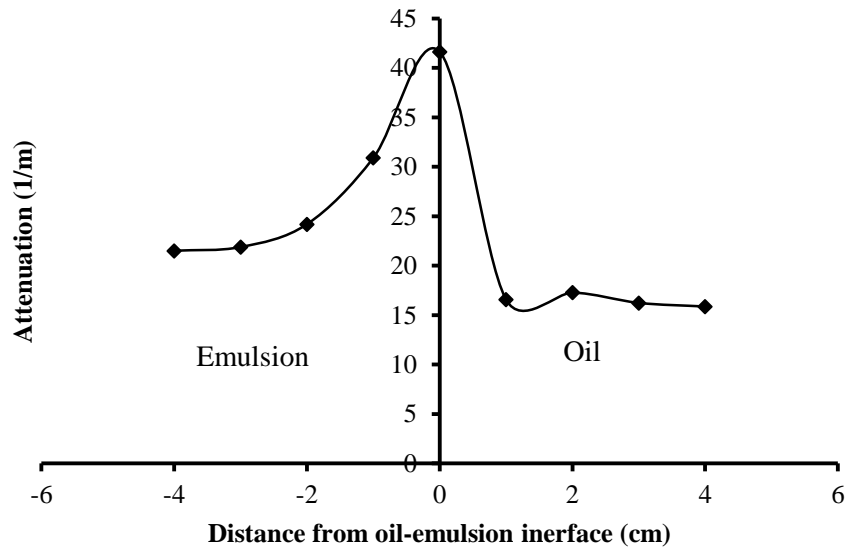
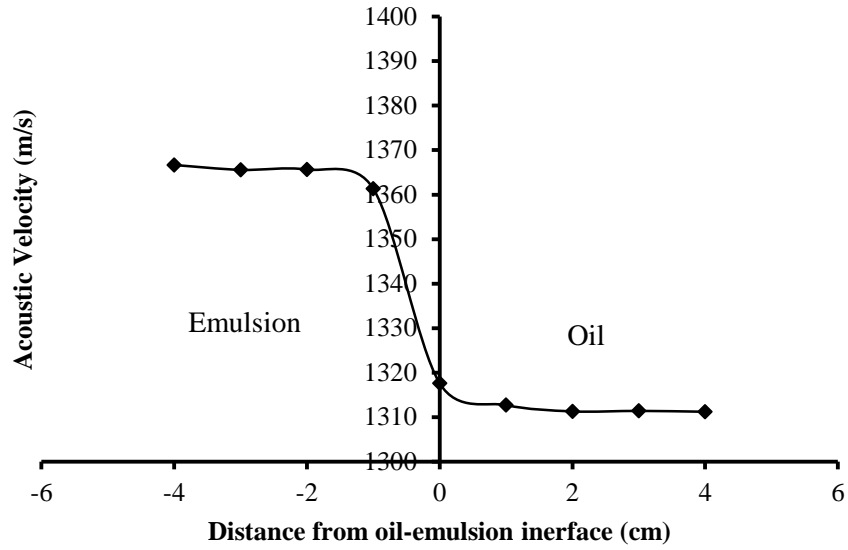


Appendix A 3 Ultrasonic propagation wave in an emulsion prepared at agitation speed of 700 rpm

Measurements in crude oil



Appendix A 4 Measurements in crude oil



Appendix A 5 Measurements in crude oil Emulsion

Chapter 4

4. Characterization of water-in-oil emulsions by ultrasonic techniques

Abstract

This study investigates potential of ultrasonic techniques to characterize water-in-oil emulsions using and compares with other methods. The emulsions were prepared with mineral oil and crude oil samples and the effects of different variables including mixing intensities, temperature, surfactant and fine solid particles concentrations have been observed. The emulsion mixtures prepared with samples of light and heavy crude oil investigated effects of asphaltenes concentration on emulsion stability. The emulsions were characterized for their stability, droplet size distribution and rheology. Emulsion droplet structure is observed with optical microscopy and stability is examined by separation of water phase with time and its composition changes were tracked by ultrasonic techniques. The ultrasonic parameters recorded are changes in acoustic velocity, signal attenuation and its frequency spectrum. The ultrasonic probe captured the variation of droplet concentration of dispersed water phase in the emulsion with time.

4.1 Introduction

Formation of emulsions specially water-in-oil emulsion present challenging problems in a number of industrial operations more notably in crude oil production and its refining and petrochemical processes. The emulsions are created as a result of intimate contact between hydrocarbon and aqueous phases involved. This is the case during crude oil production steps where comingled water generates water-in-oil emulsions (Kokal, 2005; Yan et al., 2001). The crude oil collected from ground also contains high levels of salts which can give rise to several problems such as heat exchanger fouling and catalyst poisoning in the downstream refining processes. The impurities of salts and sand in crude oil are removed in a desalter unit in an oil refinery. Here process water is mixed with incoming crude oil to dissolve out the salts, and the emulsified mixture then enters separation vessels where the cleaned oil leaves from top and water containing dissolved salts leave from the bottom. However, the separation rate of the emulsion into the individual phases is affected by a number of factors such as crude oil composition, asphaltene content, droplet size distribution, presence of fine particles, etc. Emulsion destabilization process involves several steps which include flocculation, sedimentation, coalescence and finally phase separation due to density difference between oil and water. Flocculation of water globules involves aggregation of droplets to form clusters which sediment under the influence of gravity. During the coalescence step, flocculated droplets fuse to form larger one leading to phase separation (Graham et al., 2008). The coalescence step can be slowed down by the presence of stabilizing agents such as clay particles and crude oil components such as asphaltenes, resins and acids (Moradi et al., 2011; Graham et al., 2008). Emulsion stability can be determined by several methods such as bottle tests and electrical methods (Wang and Alvarado, 2009). Bottle tests which rely on water resolution are more common due to

low cost and ease of tracking. It can be combined with other methods such as electrical and acoustic techniques.

The emulsion characters such as appearance, stability, and rheological behavior rely on their natures and droplet interactions as well (Derkach, 2009 and McClements, 1996). Various analytical techniques have been established to characterize the droplets in emulsions, e.g. electron microscopy, light microscopy, dynamic and static light scattering, neutron scattering and electrical conductivity, and Nuclear Magnetic Resonance (NMR) (Derkach, 2009; Coupland and McClements, 2001; McClements, 1996). However, most of these techniques have limitations or they are appropriate only for dilute applications, while most emulsions of practical status are concentrated and optically opaque (Coupland and McClements, 2001). For example, NMR approach was utilized effectively to measure droplet size distribution and volume fraction of the dispersed phase. However, NMR spectrometers are quite expensive to purchase and are not easily adapted for on-line measurements. Moreover, they are not suitable for smaller droplets characterization, as well require highly skilled operators.

Ultrasonic attenuation spectroscopy (UAS) is becoming an attractive technique among other technologies to measure droplet size distributions in emulsions because of its ability to analyze concentrated and optically opaque emulsions. It depends on the conversion of the ultrasound measurements including the acoustic velocity and attenuation coefficient into droplet size information (Su et al., 2008 and McClements, 1996). Ultrasonic waves have frequencies ranging from 20 kHz to 10000 GHz (Ensminger and Bond, 2012). However, ultrasonic frequencies below 20MHz are the most commonly used in industrial applications. Attenuation coefficient of the propagating wave is affected by fluid viscosity

and frequency (Atkinson and Kytomaa, 1992). The systematic monitoring of acoustic properties of an emulsion including sound velocity and sound absorption (attenuation) may offer insightful information regarding the droplet size distribution and emulsion stability (Shukla et al., 2010 and Atkinson and Kytomaa, 1992).

The main focus of the present work is development and testing of ultrasonic based technology to monitor changes in emulsion characteristics over time. The ultrasonic parameters recorded are changes in acoustic velocity, signal attenuation and its frequency spectrum. The ultrasonic techniques were selected for their several advantageous features including; lower power consumption, in-line measurement, long-term stability, non-invasiveness, high resolution and accuracy, and rapid response. The technique provided good information regarding emulsion stability, changes in droplet size distribution and concentration. Emulsions were prepared with mineral oil and crude oil samples and the effects of various factors including mixing speed, temperature, surfactant, and solid particles concentrations were investigated. The applied frequency for ultrasonic waves has been varied from 1 to 5 MHz to carry out a sensitivity analysis. Emulsion droplet structure is observed with optical microscopy and stability is examined by tracking the changes in ultrasonic parameters with time. A model based on ultrasonic attenuation spectroscopy is tested to track changes in droplet size distribution with time.

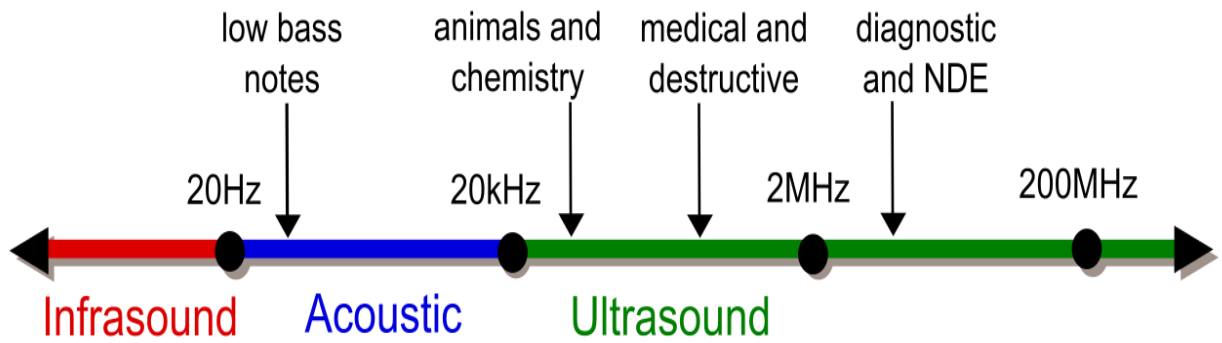


Figure 4-1 Range of acoustic frequencies used for different applications (Ref)

4.2 Experimental Details

4.2.1 Materials and Methods

The light mineral oil (LMO) used in the experiments was purchased from VWR International. Its density was measured at 858.8 kg/m^3 and viscosity $60 \text{ mPa}\cdot\text{s}$ (cP) at room temperature. The crude oil (CO) samples were provided by Imperial Oil Ltd. The density of crude oil sample was measured to be 866.7 kg/m^3 , API gravity 31.17 and viscosity 11 cP at room temperature. The commercial Triton X-100 (polyethylene glycol octylphenol ether) purchased from VWR International, chemical formulation of $\text{C}_{33}\text{H}_{60}\text{O}_{10}$, was used as emulsifier. This surfactant is a non-ionic hydrophilic, it has density of 1065 kg/m^3 , HLB (Hydrophile-Lipophile Balance) 13.5, viscosity of $240 \text{ mPa}\cdot\text{s}$ at 25°C , and the surface tension is about 3100 dyne/cm . The commercial non-ionic hydrophilic surfactant Tween 20 (Polyoxyethylene-20-sorbitan Monolaurate) with chemical formulation of $\text{C}_{58}\text{H}_{114}\text{O}_{26}$, was used as de-emulsifier. It has density of 1100 kg/m^3 , viscosity of 450 cP at 25°C , and HLB of 16.5. Fine solid particles used included Iron and Kaolin clay with average diameter size of $10 \mu\text{m}$. These were supplied by Fisher Scientific. The clay has chemical formulation

of $\text{H}_2\text{Al}_2\text{Si}_2\text{O}_8\text{-H}_2\text{O}$ (hydrated Aluminum Silicate), density of 1800 kg/m^3 , and its physical state is Beige solid powder.

Brookfield digital Rheometer was employed to determine the rheology of the emulsion at different temperatures controlled by water bath thermostat. Density measurements were conducted using SG-Ultra Max Ex Petrol Density Meter, by Eagle Eye Power Solutions. IKA mechanical mixer (model RW 20D), with a four blade stainless steel propeller type stirrer was used to prepare the emulsion mixture. A Seven Excellence PH meter supplied from Mettler Toledo Company was used to monitor and adjust the PH of aqueous solution. Dispersed water droplets in the oil phase for different emulsions were visualized using optical microscope (OMAX) with 10x objective, the diameter of droplets were measured using Impulse 7 software. Measurements of acoustic parameters were carried out over a frequency range of 1.5, to 5 MHz with specially designed ultrasonic these probes.

4.2.2 Experimental Setup

A schematic of experimental set up used for emulsion preparation and testing is shown in **Figure 4-2**. It consists of an ultrasonic pulser-receiver (UTEX Inc.), a probe mounted on a float and placed in a tank containing the liquid media. The transducer was connected to the pulse-receiver capable of exciting ultrasonic transducers with center frequencies from 1MHz to 150MHz. Data was collected over 10 seconds at a sampling frequency of 100Hz, yielding 1000 values of time-of-flight and amplitude per run. The arithmetic average of each set of values was calculated and subsequently used to calculate acoustic velocity and attenuation, respectively. The standard deviation of each set was also calculated to ensure the data was fairly uniform and more or less free of outliers. It was controlled by a software interface which allowed remote control and configuration of the instrument. Transducer

excitation was achieved with an ultra-fast square wave pulse featuring adjustable pulse width and adjustable pulse voltage. The amplifiers in the instrument were directly gain controllable eliminating the need for attenuators that contribute to receiver noise.

Emulsions were prepared in a beaker or a jacketed container at different stirring speeds (600 to 1200 rpm) with the help of IKA mixer. To prepare water-in-oil emulsions, a measured volume of the oil sample was placed in a 1000 ml beaker, then about 0.2 wt% of Triton X-100 surfactant was added to the oil phase. The mixture was stirred for about 5 minutes to ensure homogenous solution. This was followed by gradual addition of aqueous phase while maintaining constant stirring speed for about 30 minutes. The pH of the aqueous phase was adjusted with pH buffer solutions and it was monitored with pH meter.

Brookfield Rotational Digital Rheometer model LV/DV-III with ULA spindle was used to determine the rheological measurements for all the samples at different temperatures controlled by water bath thermostat connected to Rheometer, spindle type ULA was used for all measurements, this device was capable to afford the shear rate, shear stress, and apparent viscosity. The Rheometer was calibrated using Brookfield Standards fluid (4.9 – 48- 98 – 490 cP at 25°C) and systematically cleaned between measurements of different samples.

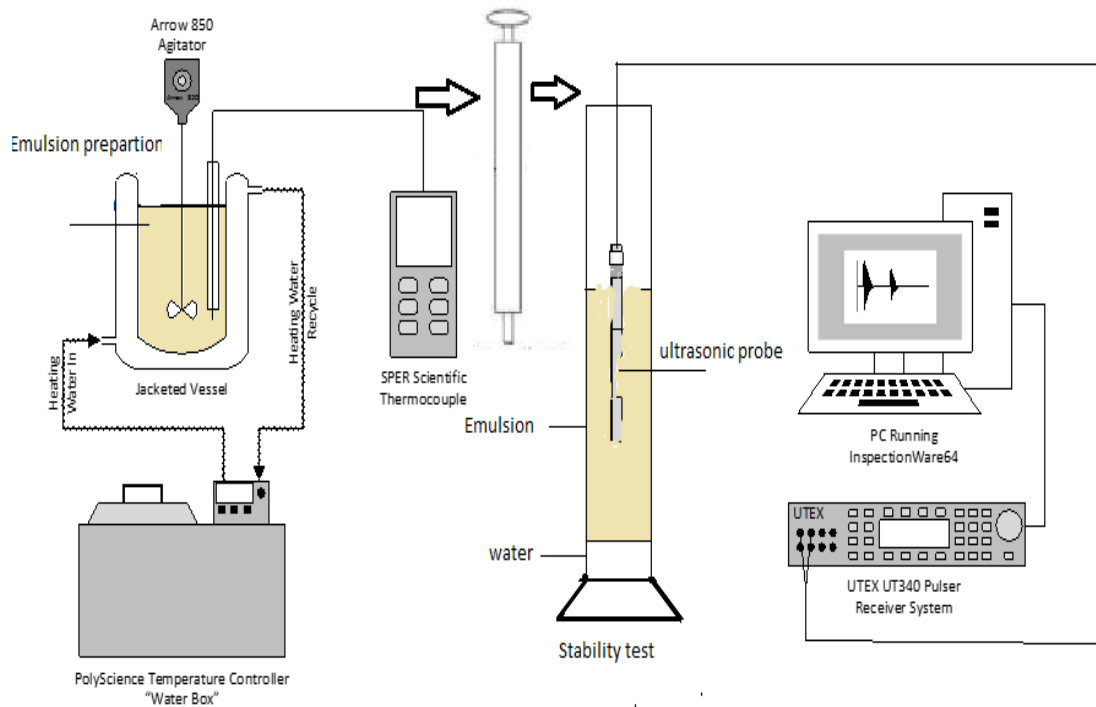


Figure 4-2 Schematic diagram of the experimental setup for emulsion characterization

4.3 Calculation of Acoustic Parameters

The ultrasonic parameters used to characterize the emulsions are the velocity and attenuation of the propagating wave. The ultrasonic probe used for the measurements operated in through transmission mode. It consists of a transmitter and receiver separated by a fixed distance, d . The time it took for the wave to travel and be picked by the receiver is known as the time of flight (ToF). The distance between the transducer and the receiver, along with the ToF can then be used to calculate the speed of sound in a given medium by equation 4.1. Figure 4-3 shows a typical waveform captured by the receiver, the time of

flight is recorded on the x axis while signal strength or amplitude (voltage) is shown on y axis

$$v = \frac{d}{TOF} \quad (4.1)$$

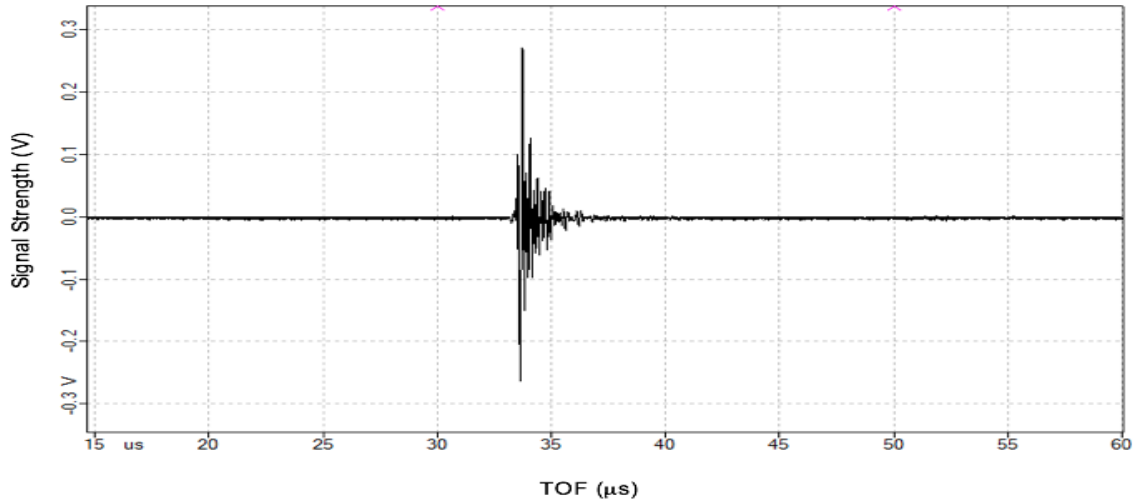


Figure 4-3 Example of an ultrasonic signal captured by the receiver and displayed on screen.

The attenuation coefficient (α) was estimated by measuring the decline in amplitude of an ultrasonic wave, travelling a known distance through the sample.

$$\alpha = -\frac{1}{d} \ln \left(\frac{A}{A_0} \right) \quad (4.2)$$

A_0 , is reference amplitude and A ,is the final amplitude of the transmitted signal. In this study reference amplitude selected is the amplitude of transmitted signal in deionized water sample.

Physical properties of different oil samples used in the study are tabulated below. The asphaltene content in crude oil samples was determined based on ASTM D2007-80

procedure with some modifications. *N*-heptane was added to each crude oil sample in a 1000 ml conical flask using a solvent-to- crude oil ratio of 5:1. The flask was covered with an aluminum foil to prevent solvent evaporation and its content agitated for 45 minutes using a magnetic stirrer. The mixture was then left in the fume-hood for 48 hours, after which it was slowly vacuum-filtered through a 0.22µm filter paper funnel assembly. The filter paper containing the asphaltene residue was allowed to dry in the fume-hood until a constant weight was accomplished (~5 days). The dried asphaltene transferred into a glass vial. A multispeed pump was used to transfer the filtrate to another container, from which the *n*-heptane was recovered via a rotavap. The weight of the asphaltenes calculated by:

$$\text{Asphaltene content (g/100ml)} = \frac{\text{weight of dried asphaltene (g)}}{\text{crude oil volume (ml)}} \quad (4.3)$$

4.4 Results and Discussion

Due to their thermodynamic instability, most emulsions tend to separate out into individual phases over time. The destabilization process usually occurs in several steps which include flocculation, sedimentation, and coalescence and finally phase separation. Consequently, the emulsion characteristics such as composition, drop size distribution and other rheological properties also change with time. In this study, the stability of emulsion is evaluated according to amount of water separated out from the prepared emulsion over a period of 24 hours. The prepared emulsions were placed in graded 1000 ml cylinder and left for settling by gravity. The changes in emulsion characteristics were examined with the ultrasonic probe inserted in the emulsion layer. Thus changes in attenuation and acoustic velocity were recorded to better describe the de-emulsification process.

Table 4-1 Physical properties of different oil used for emulsion preparation

Physical property	Light Mineral Oil (LMO)	Light Crude Oil (LCO)	Heavy Crude Oil (HCO)
Sp. gravity @ 60 F ⁰	0.8688	0.8699	0.9129
Density (kg/cm ³)	868.8	869.9	912.9
API ⁰	31.51	31.17	23.5
Kinematic viscosity (cP) @ 25 ⁰ C	60	11	33.60
Asphaltene content (wt %)	0	1.45	9.01

4.4.1 Emulsion Stability Tests with Mineral Oil

Initial tests for emulsion characterization were first conducted with mineral oil samples and response of ultrasonic probe was recorded together with measurements of water resolution and droplet size distributions. To begin with, emulsion stability tests were conducted with and without emulsifier added to the oil phase. It can be seen in **Figure 4-4** that there was quick separation of oil and water phases without the emulsifier added to the oil phase. The emulsion stability, however improved significantly with the addition of emulsifier. It is also observed from the figure that the water resolution process was captured easily by the measurement of ultrasonic attenuation in the system. Subsequently most of the emulsions were prepared with the emulsifier added to the oil sample for improved stability and more detailed analysis of the emulsion phase.

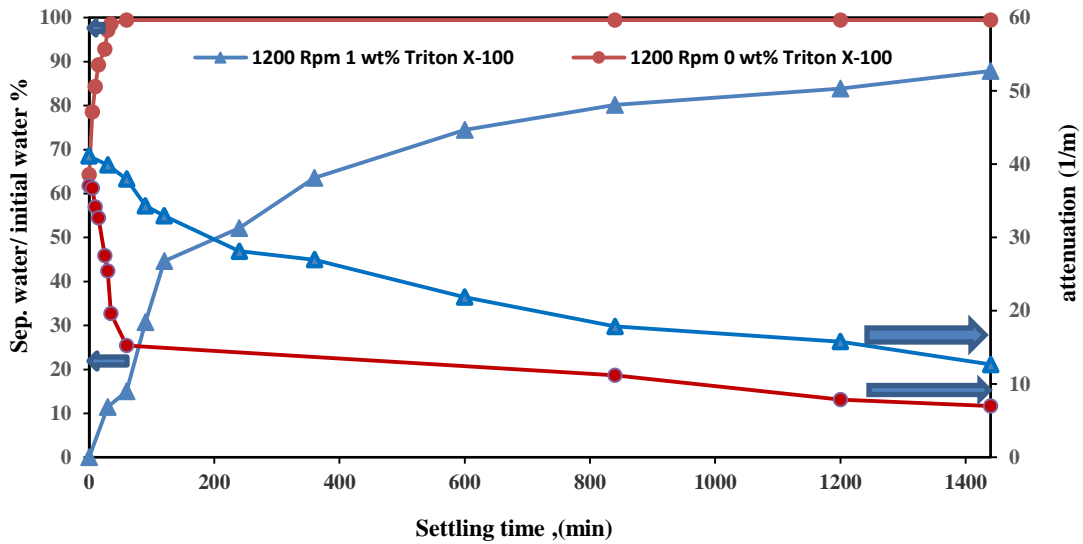


Figure 4-4 Records of water separation and ultrasonic attenuation in water-mineral oil emulsions prepared with and without emulsifier

4.4.1.1 Effect of Agitation Intensity on Emulsion Stability

Figure 4-5 compares the water resolution rate and corresponding attenuation in emulsions prepared at rpms' of 600 and 1200. The water resolution curve can be approximately divided into three zones. It can be seen that there is quick separation of the aqueous phase until about 100 minutes followed by a slower rate until about 600 minutes and a significantly slower rate thereafter. It is seen that in zone 1 there is little difference between the emulsions prepared at different rpms. During the initial separation phase about 45% of water separates out. For higher durations, there is difference and observed rates of water resolution are lower with emulsions prepared at the higher rpm. It can be seen that attenuation decreases gradually with the separation of water. The faster decline at the beginning coincides with the faster separation rate of water. Also attenuation is higher in emulsion prepared at higher rpm and remains higher until the end of the run.

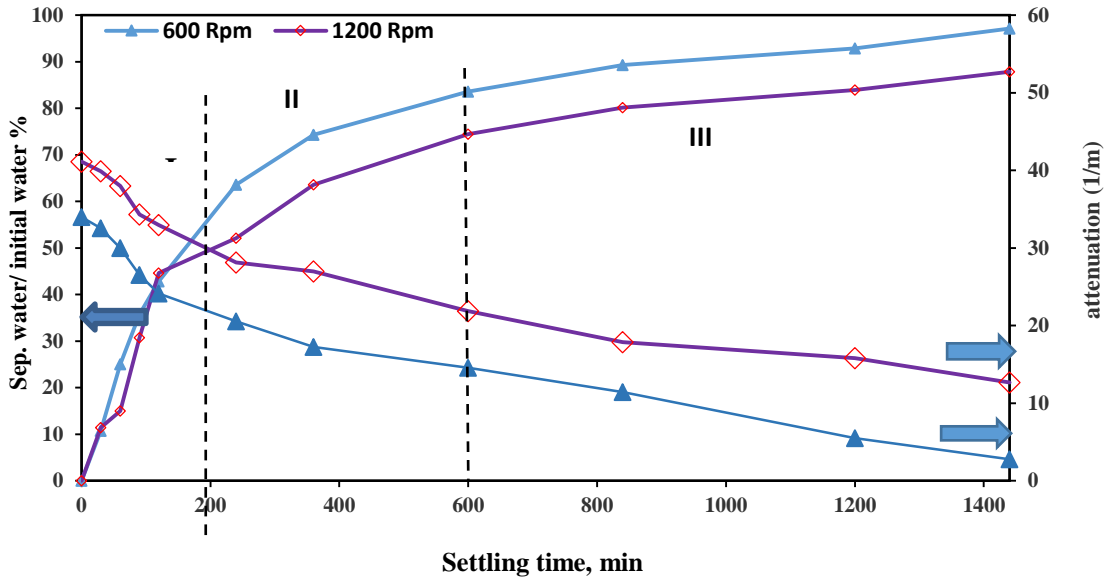


Figure 4-5 Records of separated water and ultrasonic attenuation over 24 hour period

Lower water volume separated at higher mixing speed indicates more stable emulsion which also leads to higher ultrasonic attenuation. This can be related to a decrease in droplet size of the dispersed phase due to increase in mixing intensity. The change in droplet size distribution with mixing speed was examined using optical microscope the diameter of droplets in the dispersion was determined using Impulse 7 software. **Figure 4-6** compares the cumulative distribution of droplet size for different mixing speeds. A decrease in droplet size with increasing rpm is clearly seen. It is also observed that there is a large decline going from 600 and 800 rpm followed by a slower decrease for higher rpm. The average size of emulsion droplets decreased from 160 to 29 micron with increase in the mixing speed from 600 to 1200 rpm. Higher water resolution obtained in emulsion prepared at lower rpm can be directly linked to higher droplet size in the dispersion and vice versa. However droplet size effect cannot explain similar rate of water separation observed in the

initial period (**Figure 4-5**). A possible explanation is that higher rpm is creating flocs of smaller droplets and these clusters coalesce and sediment together. Once the concentration of smaller droplets decreases in the dispersion due to sedimentation, there is less probability of clustering.

Figure 4-7 summarizes the influence of mixing speed on average droplet size and emulsion stability shown by percent water resolution. As expected there is increase in emulsion stability with decrease in droplet size but the effect is relatively small compared to large decrease in droplet size. This also indicates the role of droplets flocculation in the dynamics of emulsion stability.

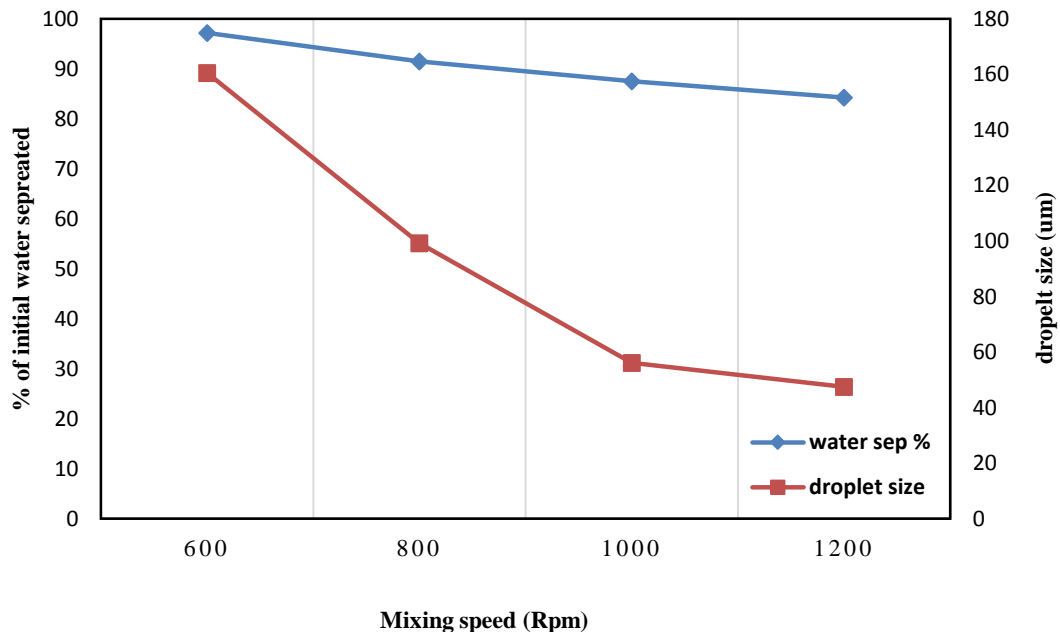


Figure 4-6 Droplet size distribution of emulsions prepared at different mixing speeds

4.4.1.2 Average Droplet Size from Water Separation Rate

The average sedimentation or settling velocity of droplets in a dispersion can also be estimated from the plot of water resolution as a function of time. The settling velocity is slope of this curve at any given time. It can be seen in **Figure 4-5** that the slope is nearly constant in zone 1 indicating essentially constant settling flux of similar size droplets. This settling velocity could be used to estimate average droplet size using Stokes' law equation given below.

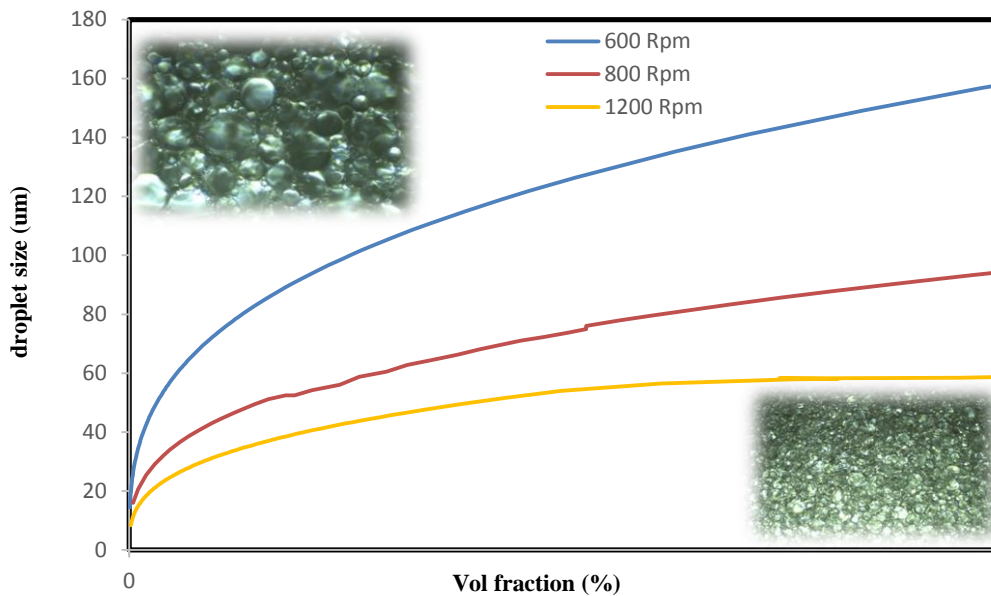


Figure 4-7 Comparison of average droplet size and emulsion stability

$$V_d = \frac{d_d^2(\rho_w - \rho_{oil})g}{18\mu} \quad (4.4)$$

Here d_d is droplet size, ρ_w and ρ_{oil} are densities of water and oil phases and μ is dynamic viscosity of the continuous phase. This procedure estimated a droplet size of 50 μm for the initial separation phase. While there is large fraction of larger droplets in emulsions

prepared at 600 rpm, the fraction is much smaller in emulsion of 1200 rpm. Thus there is more likelihood of settling of flocculated droplets in this emulsion prepared at higher rpm.

4.4.1.3 Acoustic Velocity in Emulsions

Acoustic velocity was the other important ultrasonic parameter measured and tracked during emulsions stability tests. **Figure 4-8** records a decrease in acoustic velocity as the water resolution progressed during the stability tests.

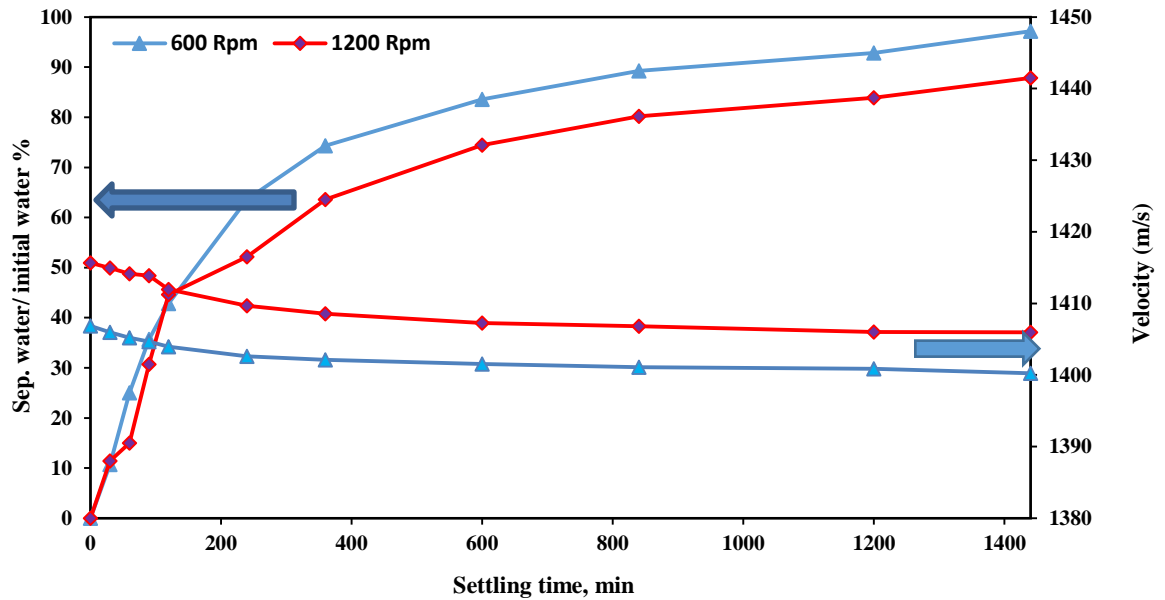


Figure 4-8 Records of water resolution and ultrasonic velocity obtained with mineral oil emulsions

The decrease in measured acoustic velocity can be attributed to removal of water from the dispersion. Acoustic velocity (v) is governed by the thermodynamic properties of the medium through which it is traversing. Based on the concept that sound is propagated as a harmonic longitudinal compression wave, the Newton-Laplace equation presents acoustic velocity through a given medium as a function of its bulk modulus (β) and density (ρ) (Ament, 1953 ; Urick, 1947).

$$v = \sqrt{\frac{\beta}{\rho}} = \frac{1}{\sqrt{\rho\kappa_S}} \quad (4.5)$$

If bulk modulus and density data are available, values for acoustic velocity can be predicted for different media using above equation. Equation **4.5**, however is valid only for homogenous fluids. For application to non-homogenous mediums such as emulsions, this equation can be modified by calculating the effective density and elasticity of the suspension (Pinfield and Povey, 1997, Kuster and Toksoz, 1974; Urick, 1947). A simple modification is calculation of density and elasticity of the suspension based on their volumetric fractions.

$$\beta_{\text{eff}} = (1-\phi)\beta_{\text{Oil}} + \phi\beta_{\text{W}} \quad (4.6)$$

$$\rho_{\text{eff}} = (1-\phi)\rho_{\text{Oil}} + \phi\rho_{\text{W}} \quad (4.7)$$

Substituting these values of density and elasticity in equation **4.5** will give the velocity of ultrasound in suspensions. As the water fraction decreases in the dispersion due to separation, the measured acoustic velocity would get closer to that in mineral oil. Since acoustic velocity is higher in water (1460 m/s) and lower in mineral oil (~ 1340 m/s), the

measured acoustic velocity in the water-mineral oil emulsion is expected to decrease with the separation of water.

4.4.1.4 Effects of Fine Particles on Emulsion Stability

Fine solid particles present in oil phase can affect the emulsion stability due to their interactions with the sedimentation or coalescence process. These particles can vary in size from a few microns to nano size depending on the source of oil. A preliminary investigation on the effect of micron size particles was conducted in emulsions of water in mineral oil. The results presented in Figure 4-9 and 4-10 show that water separation was hindered in presence of particles of iron and clay and the iron particles had bigger effect. It may be noted that the particles size of 10 micron was significantly smaller than average droplet size in the dispersion (~ 40 micron). Thus the particles could be easily trapped between the droplets, thus preventing their coalescence.

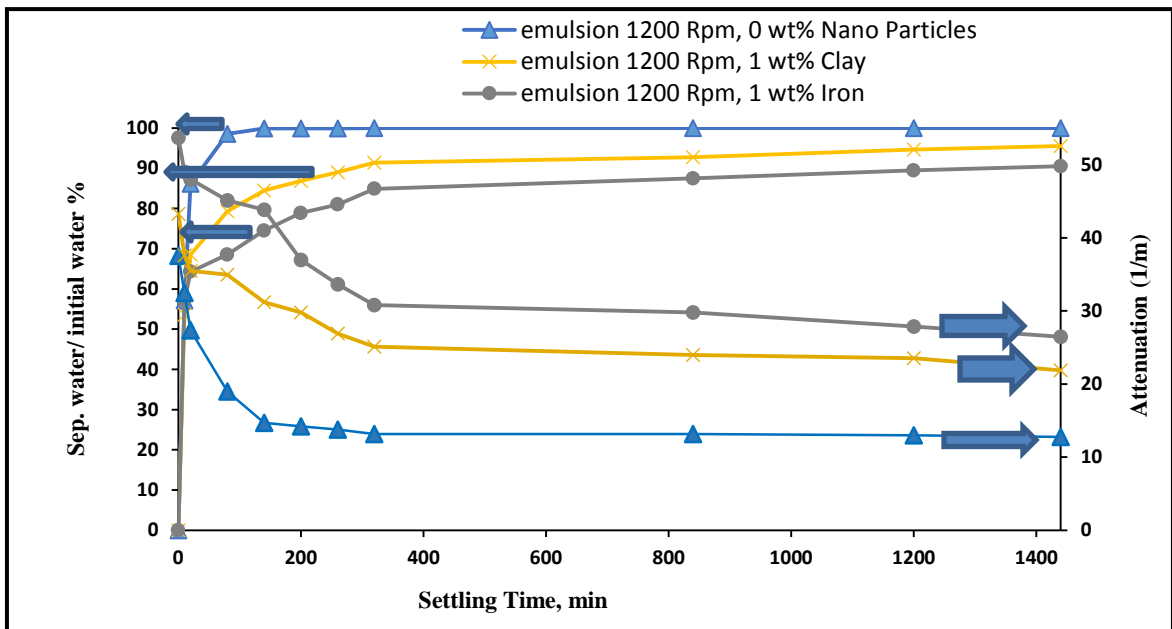


Figure 4-9 Effect of fine solid particles on water separation ultrasonic attenuation in emulsions of mineral oil

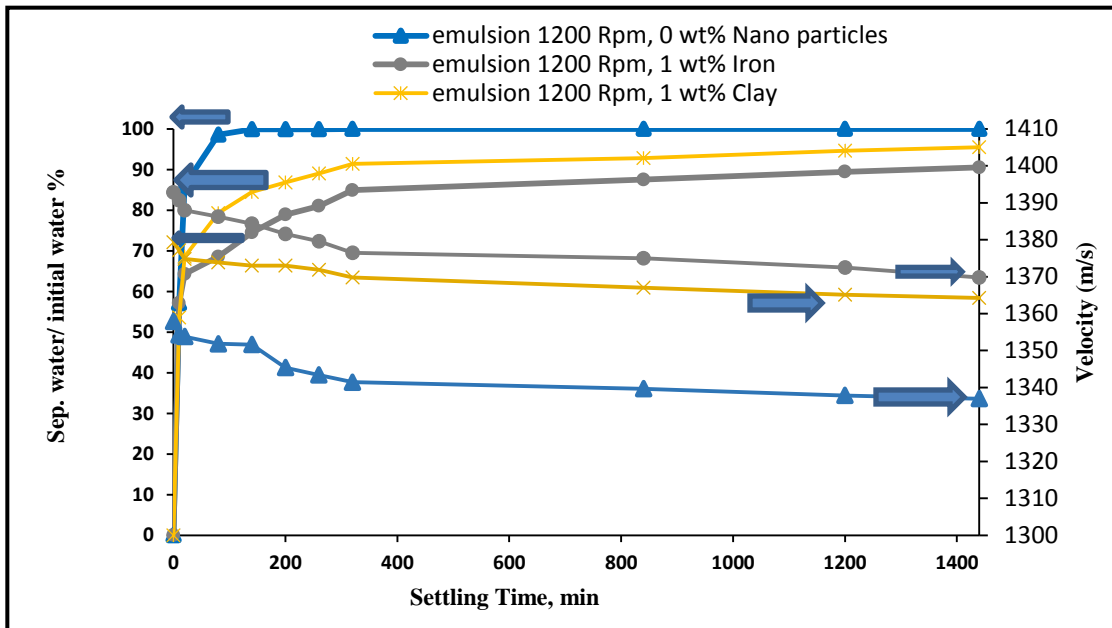


Figure 4-10 Effect of fine solid particles on water separation ultrasonic attenuation in emulsions of mineral oil

4.4.2 Investigations with Crude Oil Emulsions

For these tests a light crude oil (LCO) and a heavy crude oil (HCO) samples obtained from industry partner were used. The procedure for the preparation of emulsions and stability tests is similar to that used for mineral oil. Emulsions were prepared with higher mixing speeds of 1200 and 1400 rpm without emulsifier added to simulate conditions commonly encountered in industrial operations. The results of water resolution and measured attenuation are presented in **Figure 4-11**.

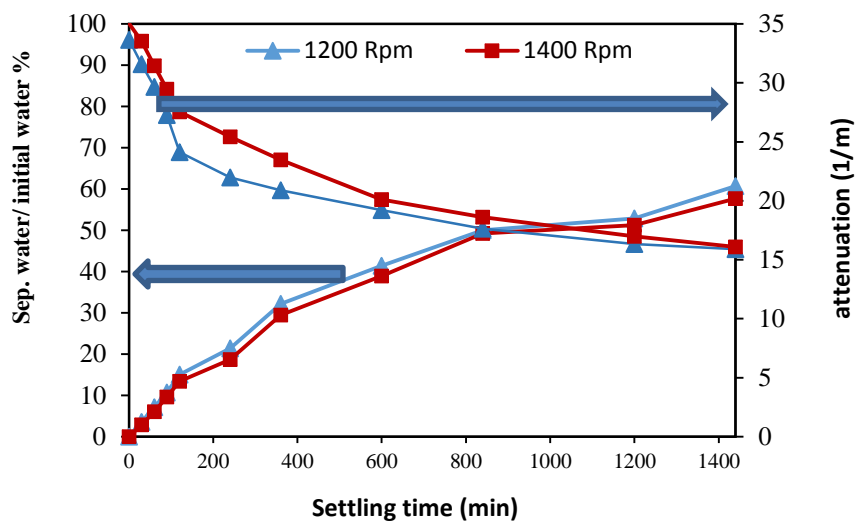


Figure 4-11 Records of water separation and ultrasonic attenuation in emulsions of light crude oil

It is observed from **Figure 4-11** that about 60% of initial water separated out at the end of 24 hours and the value is only slightly higher with emulsion prepared at 1200 rpm. The rate of water droplet separation is higher for the initial period (for about 2 hours) and more gradual subsequently. The attenuation curves shown on the figure provide a better picture of the water droplets settling/separation process for the two rpm. There is fast drop in attenuation for the initial period of about 120 minutes which corresponds to high initial rate of separation. However, the rate of drop is clearly higher with 1200 rpm emulsion. This can be attributed to presence of higher concentration of larger drops with 1200 rpm emulsion. There is a clear decrease in slope above 100 minutes and the two curves have a different slopes for the period 100 to 600 minutes. During this period, flocculation and coalescence of smaller droplets are likely dominating. The slope of the two curves becomes much smaller and similar for separation period higher than 600 minutes. The separation process

during this period is mainly controlled by slow settling rate of remaining smaller droplets in the emulsion.

Comparison of **Figures 4-5** and **4-11** shows that total water separated out with crude oil emulsion is significantly lower (60%) compared to mineral oil emulsion where nearly 90% of water separated out. It may also be pointed out that the crude oil emulsions were prepared without any emulsifier added. This can be attributed to complex composition of crude oil with presence of long chain molecules such as resins and asphaltenes which can act as emulsifiers or coalescence inhibitors. As discussed below, there is significant difference in droplet size distribution between the two oil.

4.4.2.1 Droplet Size Distribution

It can be seen in **Figure 4-12** that the droplet size decreased and distribution became narrower with an increase in the mixing speed from 1000 to 1400 rpm. A comparison with droplet size distribution obtained in mineral oil emulsions (**Figure 4-6**) reveals significantly smaller droplets in emulsions of crude oil. The smaller droplets will slow down the separation of water and improve emulsion stability as observed above.

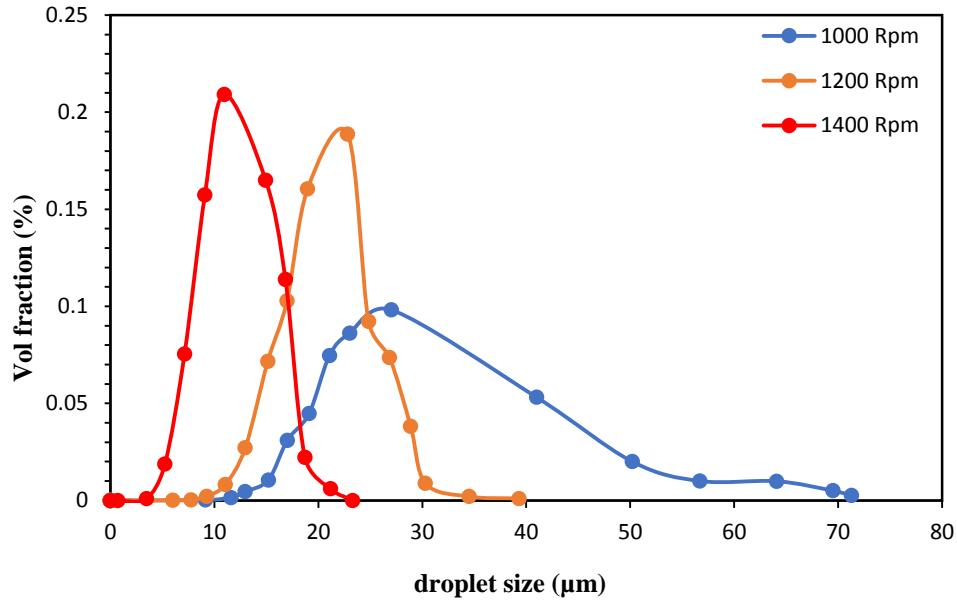


Figure 4-12 Droplet size distribution in emulsions of water-in-light crude oil at different mixing speeds

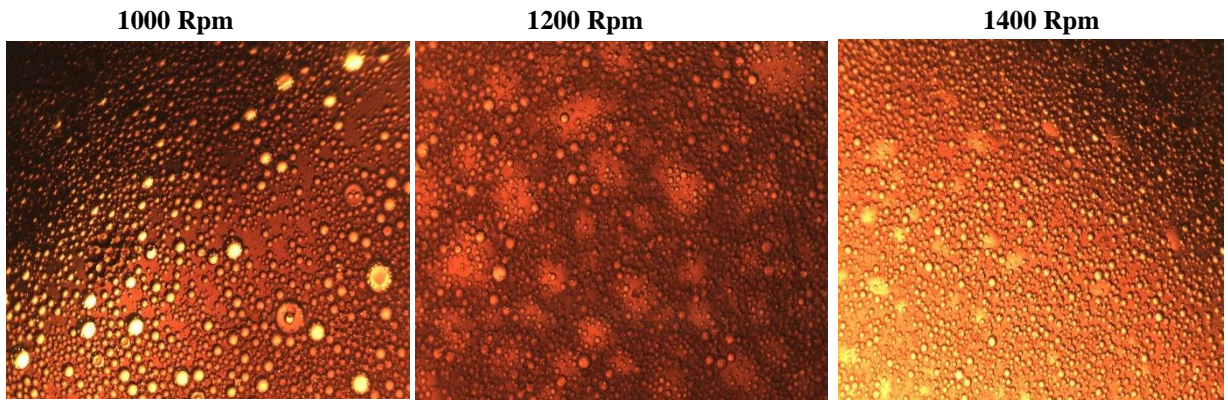


Figure 4-13 Photomicrographs of freshly prepared water-in- light crude oil emulsions (at 10x)

Figure 4-14 tracks changes in acoustic velocity during the droplet settling process. The variations are similar to those observed with attenuation measurements over different settling periods. The acoustic velocity decreases with time as the water droplets settle out

and would approach values closer to crude oil. It can be noted that the measured acoustic velocities are higher with emulsion prepared at 1400 rpm compared to 1200 rpm. This can be attributed to slower rate of settling of finer droplets in the emulsion.

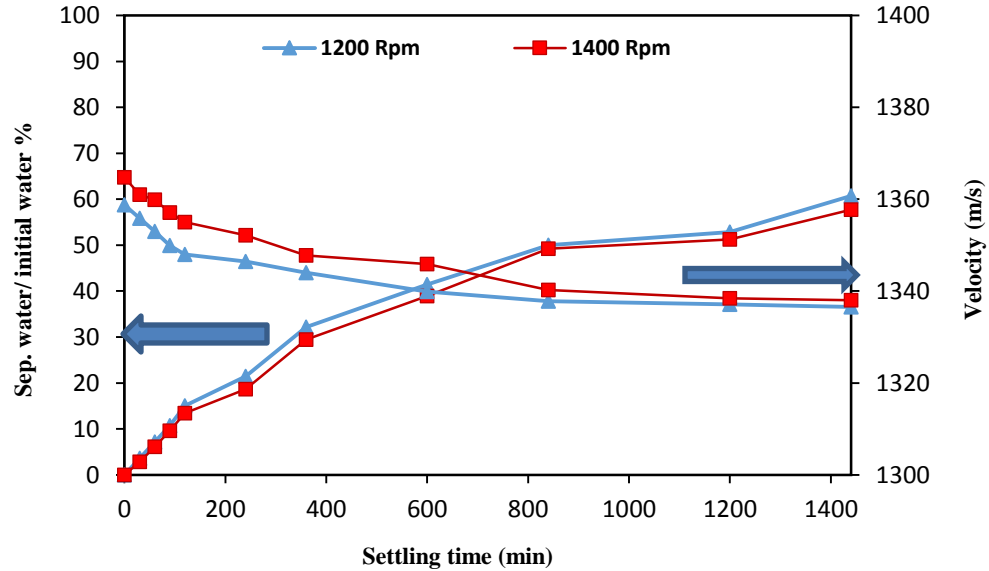


Figure 4-14 Records of water separation and acoustic velocity in emulsions of light crude oil

4.4.2.2 Calibration Curve to Determine Water Fraction from Acoustic Velocity

Equations 4.5 to 4.7 can be combined and rearranged to estimate water fraction in the emulsion phase using measured acoustic velocity in the emulsion phase, and known density and bulk modulus in each phase. The resulting equation shown below can be used to develop a calibration curve shown in **Figure 4-15**.

$$\phi = \frac{[V_{emu}^2 \rho_{oil} - \beta_{oil}]}{[V_{emu}^2 (\rho_{oil} - \rho_w) + (\beta_w - \beta_{oil})]} \quad (4.8)$$

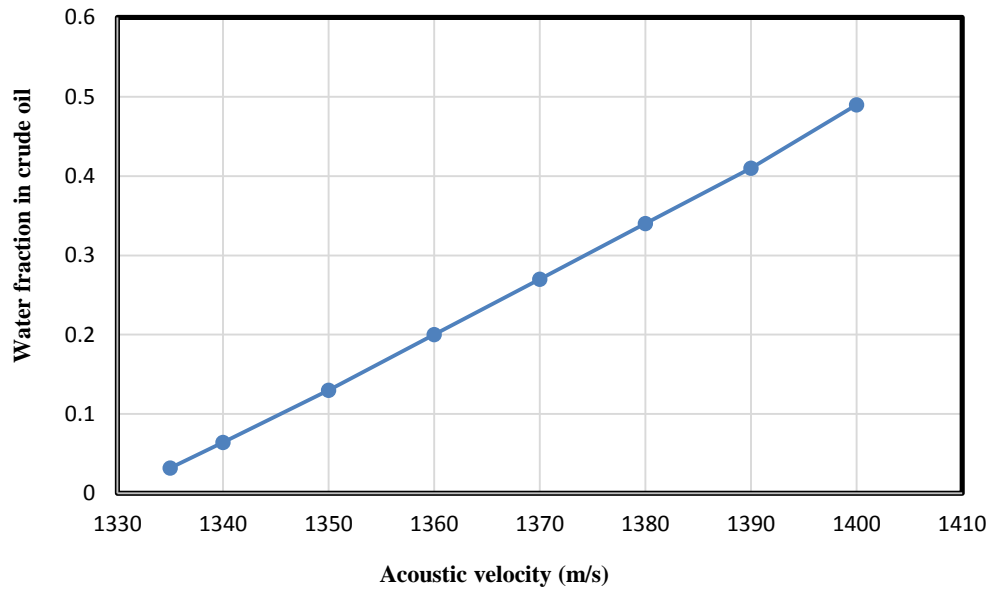


Figure 4-15 Calibration curve to determine water fraction based on measured acoustic velocity in emulsions of crude oil

4.4.2.3 Effect of de-emulsifier on water separation

As observed above, the water separation rate in emulsions of water-in-light crude oil was slow. This slow rate may not be acceptable for some industrial operations. In order to enhance the settling out of water droplets, emulsion of light crude oil was prepared with 1wt% de-emulsifier (Tween-20).

It can be seen from **Figure 4-16** that water separation improved from about 60% to 70%. The de-emulsifier would act by enhancing droplet coalescence leading to their faster separation. This operation can be further optimized.

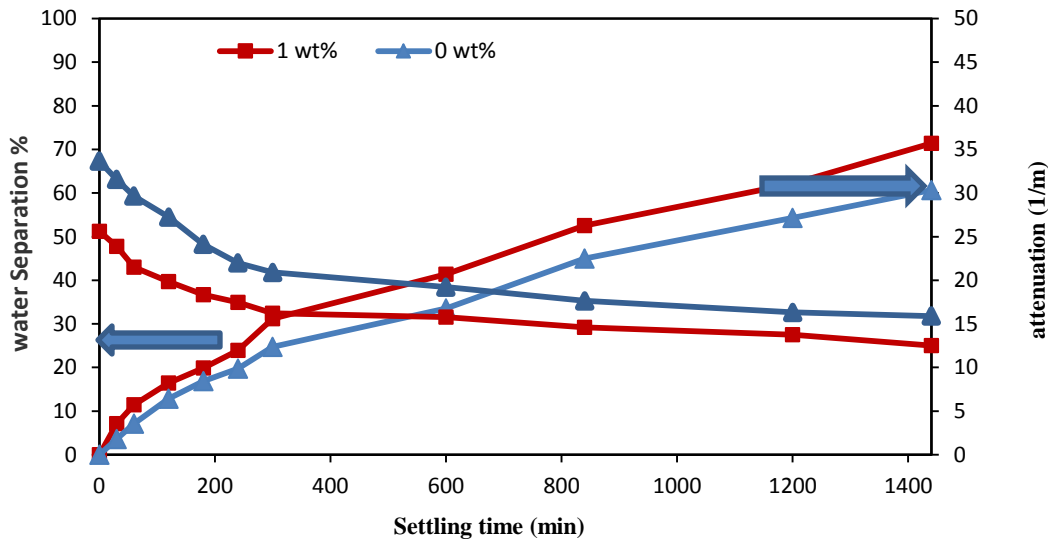


Figure 4-16 Records of water separation and ultrasonic attenuation in emulsions of light crude oil prepared with and without de-emulsifier.

4.4.2.4 Effects of Fine Particles on Light Crude Emulsion Stability

It was pointed out earlier that fine solid particles present in oil phase can affect the emulsion stability due to their interactions with the sedimentation or coalescence process. These particles can vary in size from a few microns to nano size depending on the source of oil. The effect of selected micron size particles was conducted in emulsions of light crude oil. The results presented in **Figure 4-17** show that water separation was enhanced in presence of particles of iron and clay and the iron particles had bigger effect. It may be noted that the particles size of 10 micron was larger than average droplet size in the dispersion. To be potent emulsion stabilizers, solid particles must be at least ten times tinier than the droplet

(Aveyard *et al.*, 2002; Binks and Kirkland, 2002). Thus particles could not be trapped between droplets and their faster settling accelerated droplets separation as well. Presence of smaller particles (~ 1 micron) will likely hinder the droplet settling rate. Faster separation observed with iron particles can be attributed to their higher density.

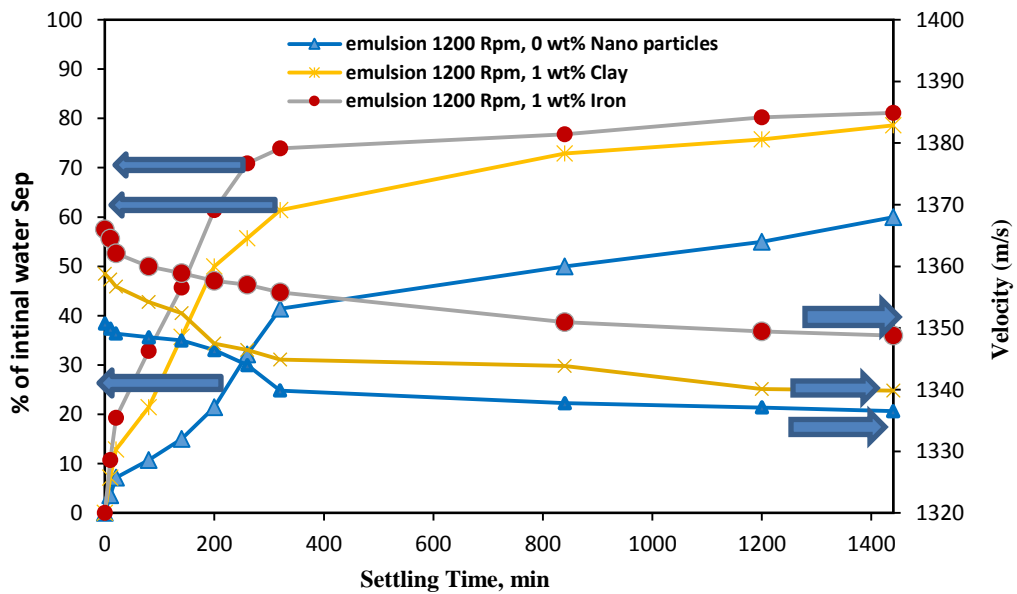
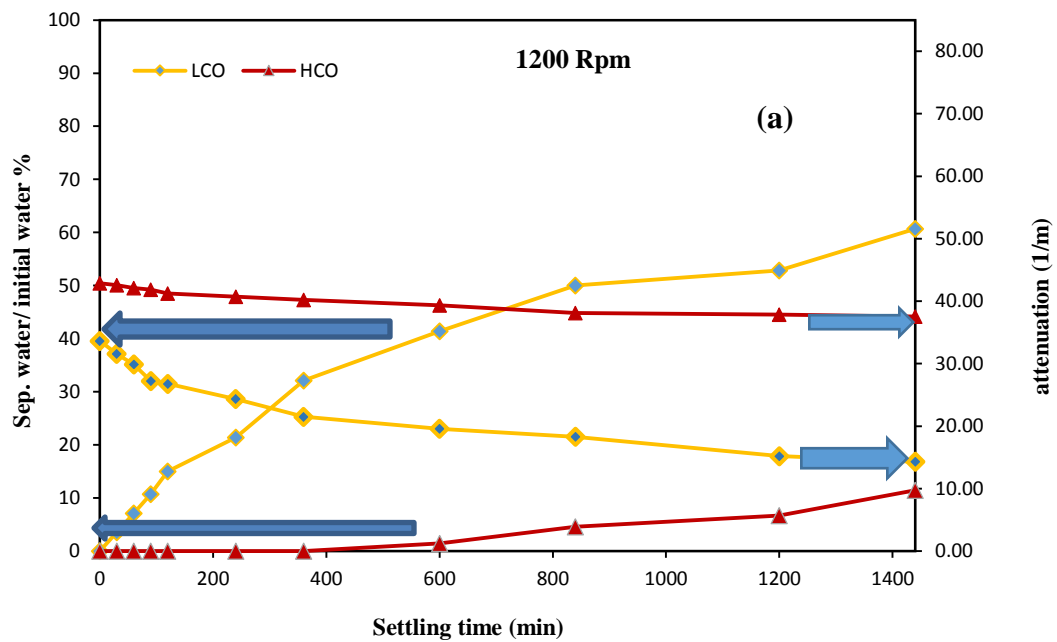


Figure 4-17 Records of water separation and ultrasonic velocity in emulsions of light crude oil prepared with fine solid particles in crude oil

4.4.2.5 Comparison of Light and Heavy Crude Oils

Stability of emulsions prepared in light and heavy crude oil samples and their mixtures were compared and monitored with the measurements of the two acoustic parameters. As observed in **Figure 4-18**, the water resolution rate is significantly slower in the heavy crude oil as compared to the light crude. This is also reflected in the slow variations of attenuation and acoustic velocity in the emulsion of heavy crude oil. The higher stability of heavy crude oil emulsion can be mainly attributed to its significantly higher asphaltene content (9 % vs 1.45%). The condensed aromatic ring structure of asphaltene molecules have tendency to accumulate at the droplets interface, preventing their coalescence process.



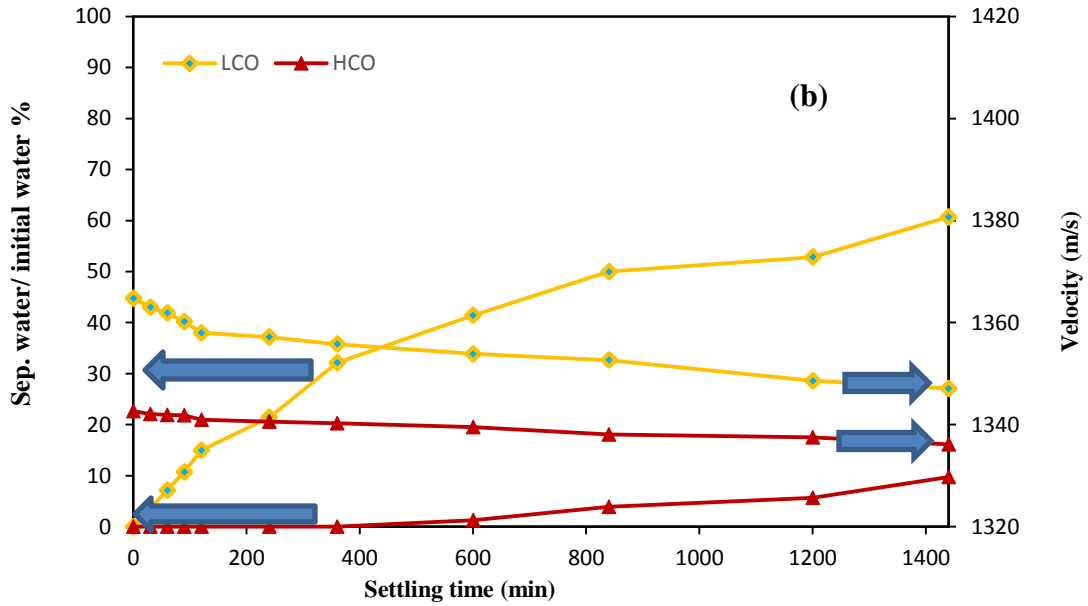


Figure 4-18 Comparison of water resolution and acoustic parameters in emulsions of light and heavy crude oil samples (a), attenuation and (b), acoustic velocity.

The effect of asphaltene content in crude oil emulsions stability was further investigated with mixture of light and heavy crude oil samples. The results obtained with 50 and 70% heavy crude oil in the mixture are presented in **Figure 4-19a** and **b**. It can be seen that the mixture with 50% heavy crude oil had much improved water separation compared to the mixture with higher heavy oil content.

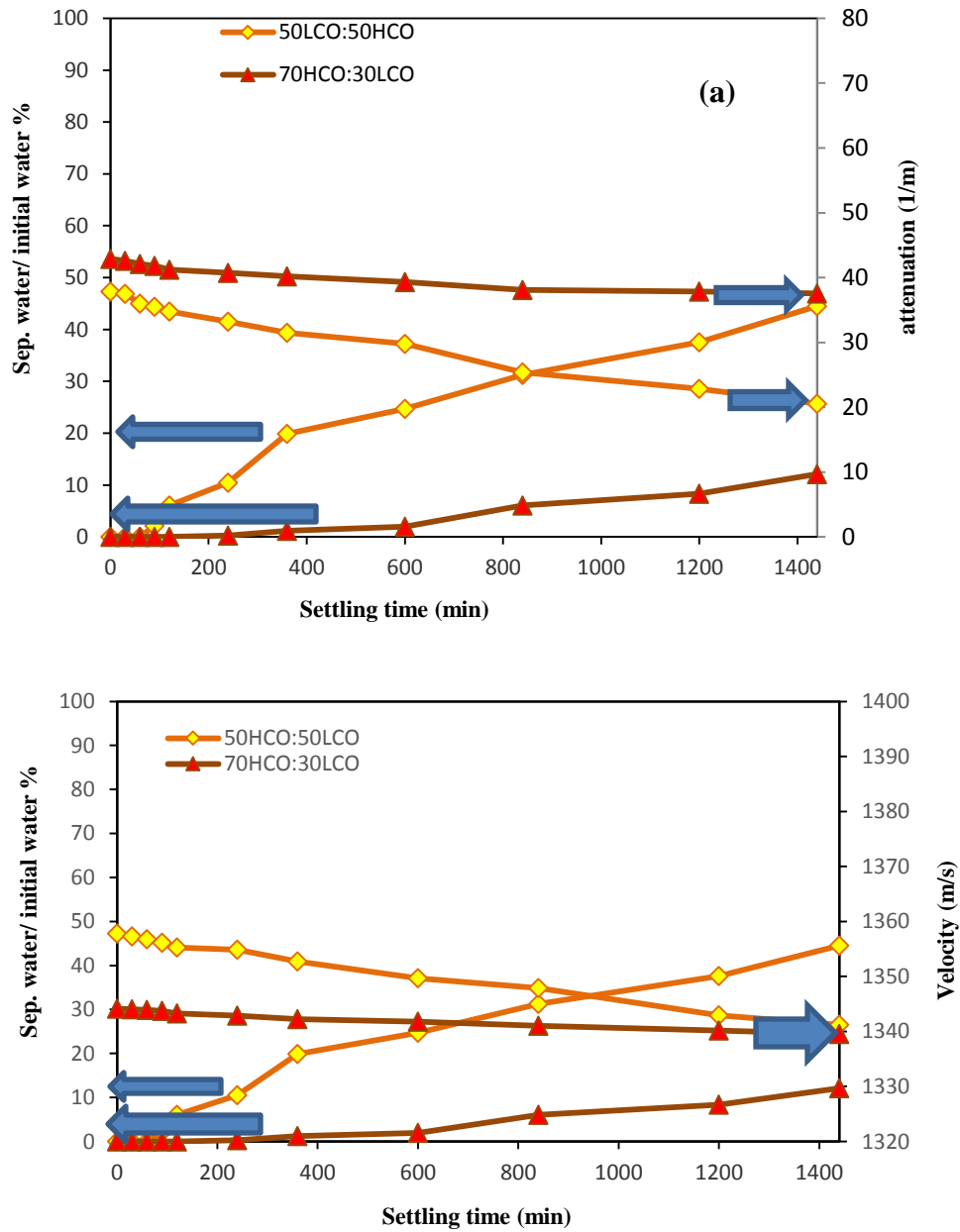


Figure 4-19 Comparison of water resolution and acoustic parameters in emulsions of light and heavy crude oil mixtures (a), attenuation and (b), acoustic velocity

Based on the results of this study, **Figure 4-20a** and **b** presents water separation obtained as a function of asphaltene content. It can be observed that for good water separation, asphaltene content in the crude should be less than 2 wt%.

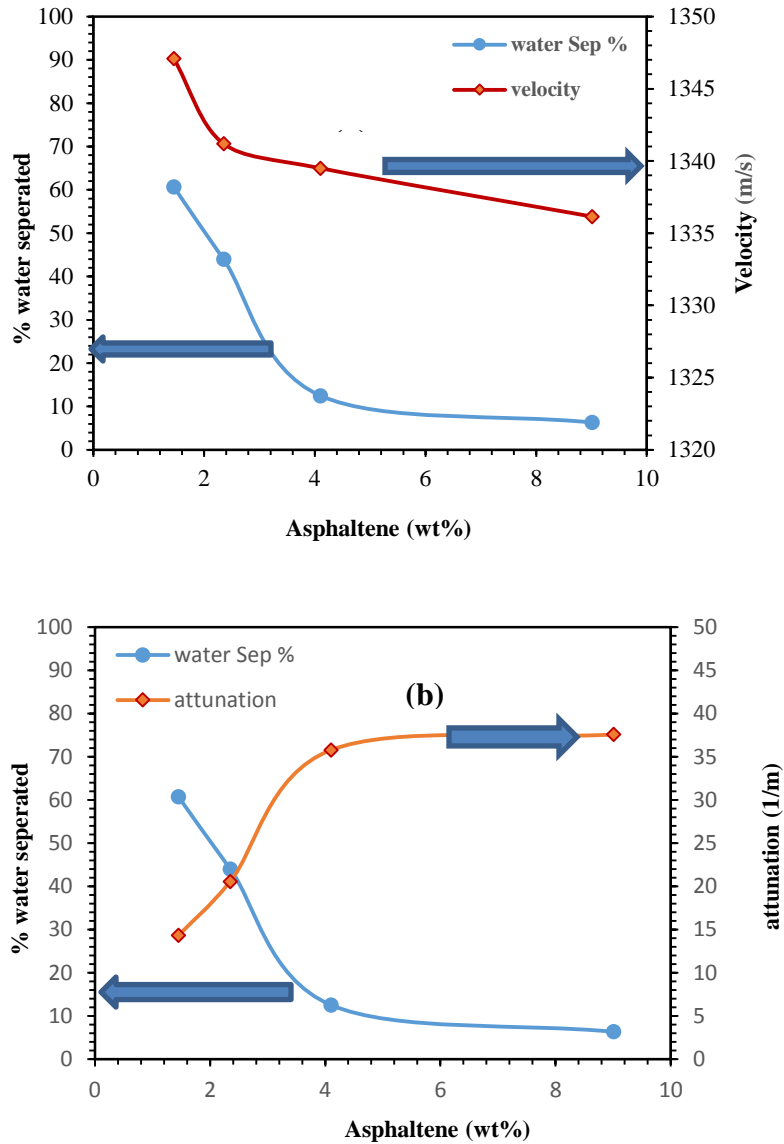
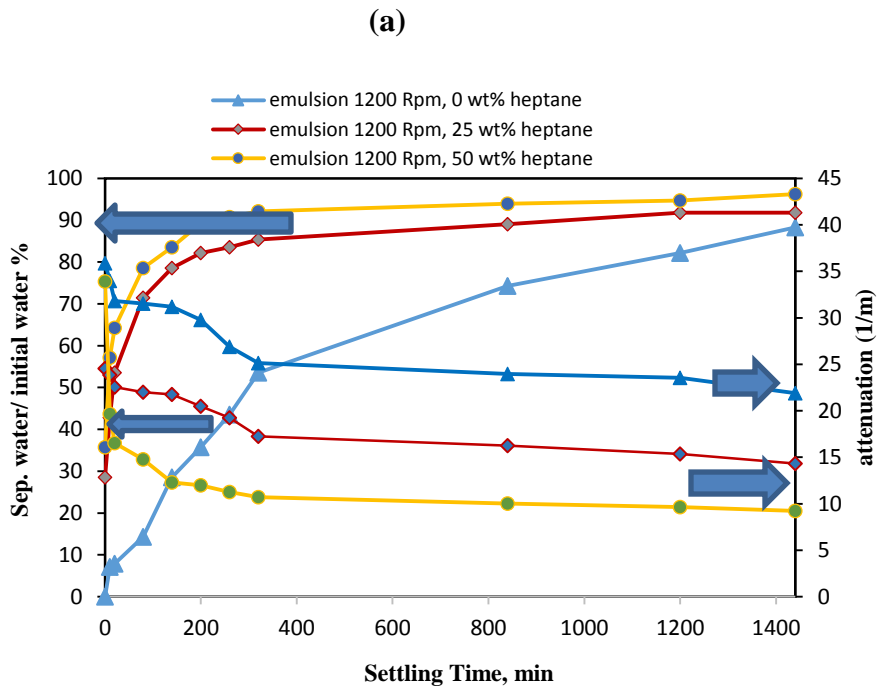


Figure 4-20 Effect of asphaltene content on water resolution and acoustic parameters in crude oil (a), velocity and (b) attenuation.

4.4.2.6 Effect of Diluting Crude Oil with n-heptane

Diluting crude oil with n-heptane would have the effect of lowering the viscosity and asphaltene content of the crude oil. The effects of these dilutions were investigated with 25 and 50 wt. % heptane addition to the light crude oil samples. The results of these tests are presented in **Figures 21a** and **b**. It can be observed that water resolution rate was much faster in the emulsions prepared with diluted samples compared to undiluted crude oil emulsions. Also rate of separation jumped significantly with the addition of 25% heptane while the increase from 25 to 50% was less significant. These observation can be attributed to the dual effects: lowering of viscosity and asphaltene content as a result of heptane dilution.



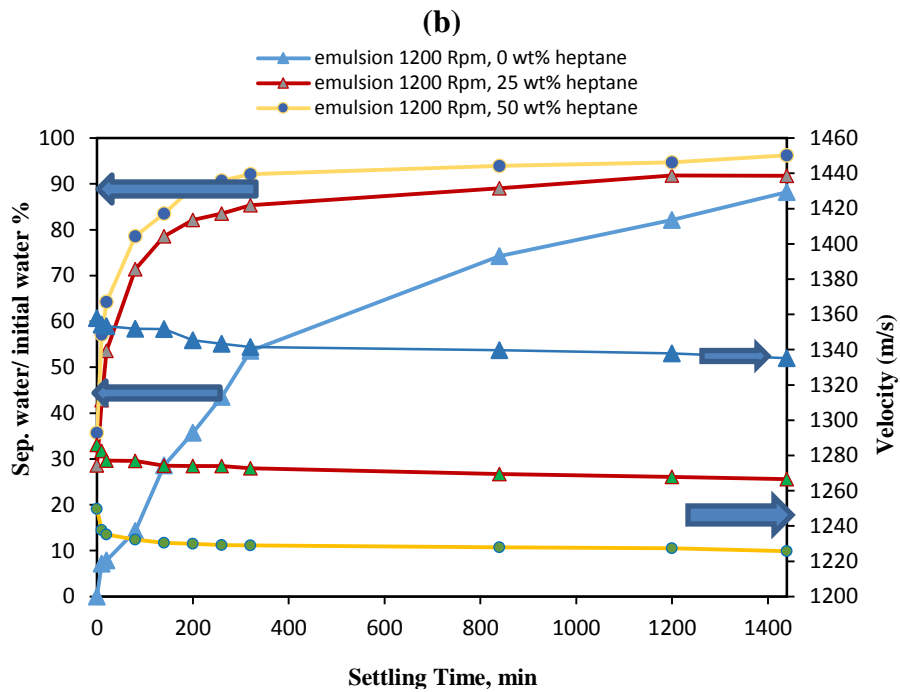


Figure 4-21 Impact of diluting crude samples with heptane on water separation and attenuation (a), acoustic velocity (b)

It is also noted from these figures that both attenuation and velocity decreased with increasing amount of heptane in the mixture. The influence of heptane dilution was further investigated with the measurement of rheological properties and droplet size distribution in water-in-oil emulsions. It can be seen from photos in **Figure 4-22** that fraction and size of larger droplets decreased with the addition of heptane.

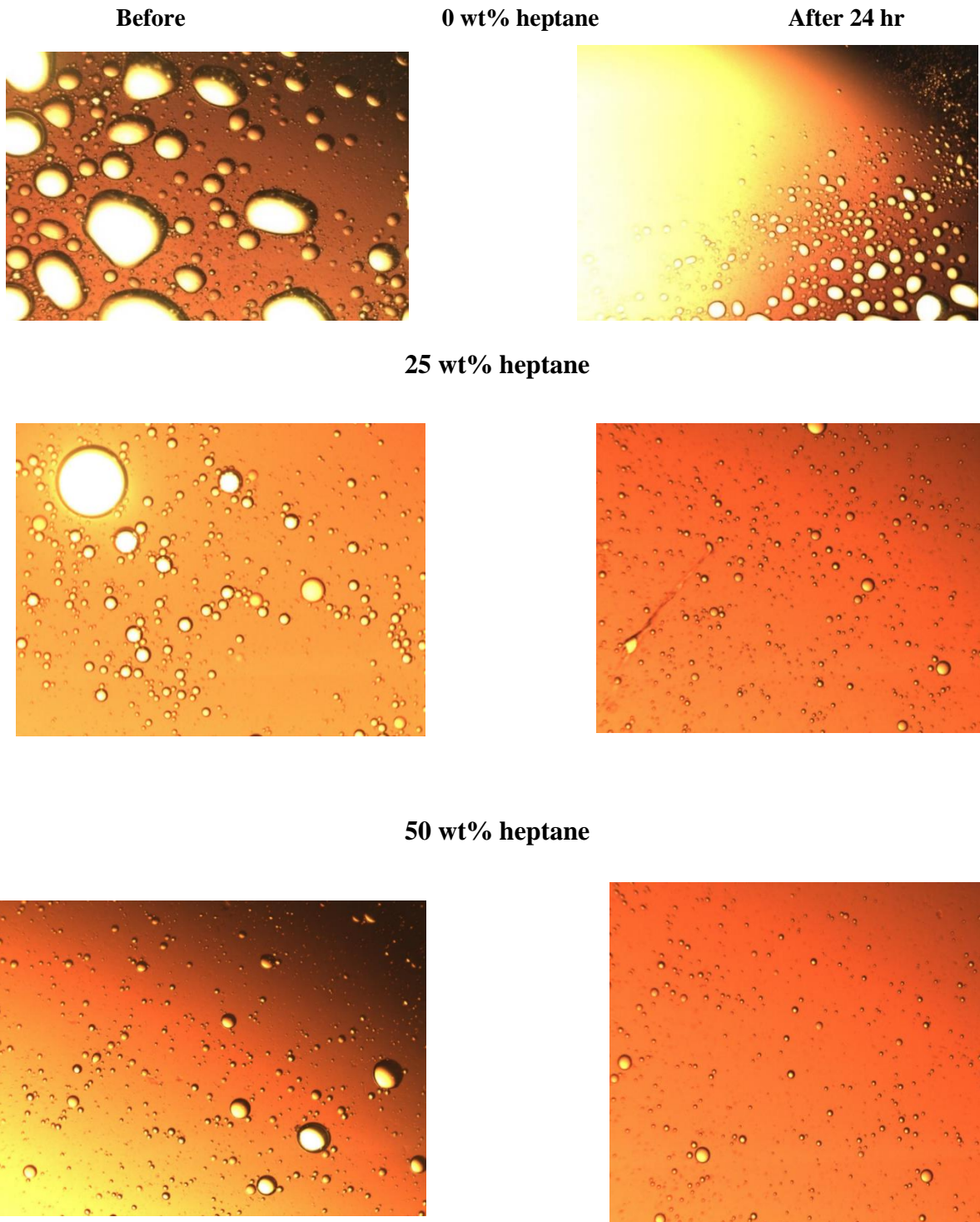


Figure 4-22 Photomicrographs of freshly prepared water-in-oil emulsions at 10x with different heptane dilutions

The droplet size distribution plotted in **Figure 4-23** shows that the size of highest fraction decreased from 35 to 20 microns and the distribution became narrower with the addition of 25 wt% heptane in crude.

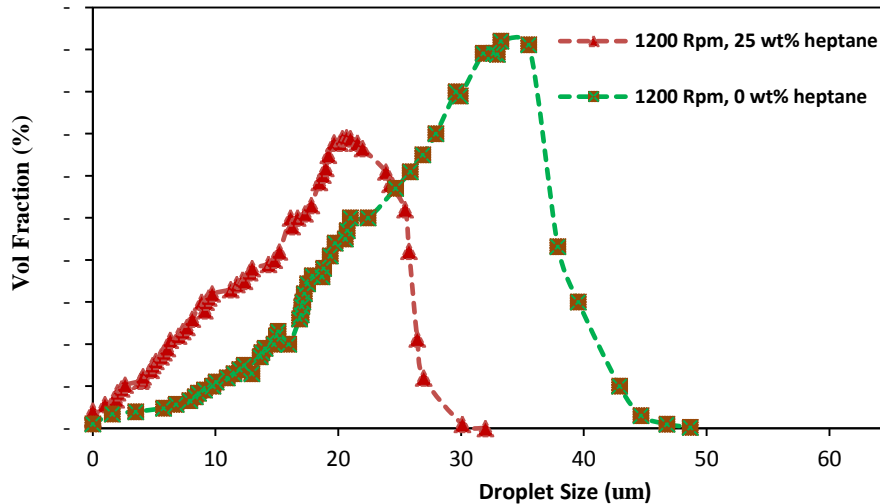


Figure 4-23 Droplet size distributions obtained in emulsions of crude oil and diluted crude with 25 wt % heptane

The addition of n-heptane has a major influence on the crude oil emulsion viscosity. It can be seen in **Figure 4-24** that there is significant decrease in dispersion viscosity due to the addition of low viscosity heptane to the mixture. It may be noted that while decrease in droplet size is expected to slow down the water separation, there will be opposite effect due to reduction of dispersion viscosity and density difference as per droplet settling equation 4.4. When this equation is used to estimate the settling velocities of droplet size with the highest fraction, the smaller droplet in dispersions of crude oil and 25 wt% heptane have larger settling velocity.

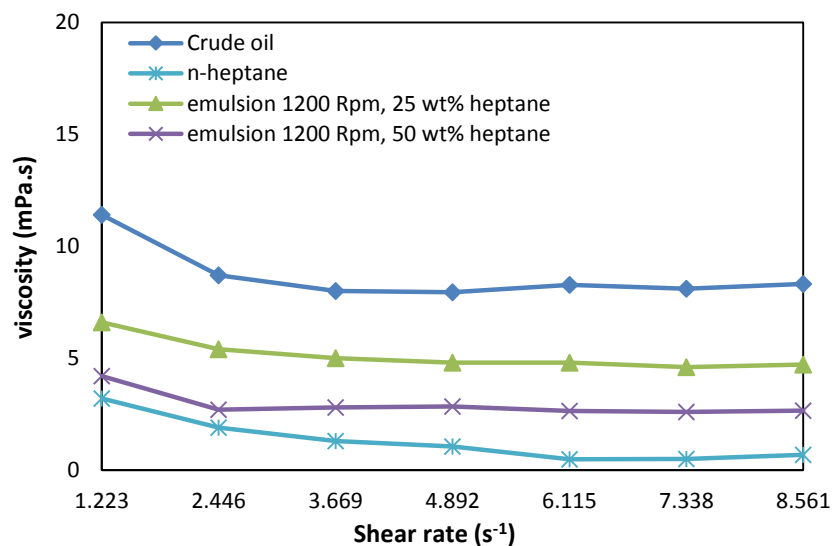


Figure 4-24 Effect of heptane addition on the viscosity of crude oil dispersions

4.5 Conclusions

Potential of ultrasonic based technology to monitor emulsion stability and track changes in emulsion characteristics have been demonstrated through extensive testing with mineral oil and crude oil samples and data analysis. The effects of higher mixing speed and emulsifier concentration on emulsion composition are pointed out and the ability of the technique to distinguish the effects are shown with simultaneous measurements of attenuation and acoustic velocity. Higher attenuation is recorded in emulsions with finer droplet distribution thus quickly pointing to higher emulsion stability. Thus more stable emulsions created with increase in asphaltenes concentration in the crude oil samples are easily detected by the technique. Similarly effects of fine solid particles in the dispersion and effects of dilution effects on the emulsion stability are captured with ease. It is also

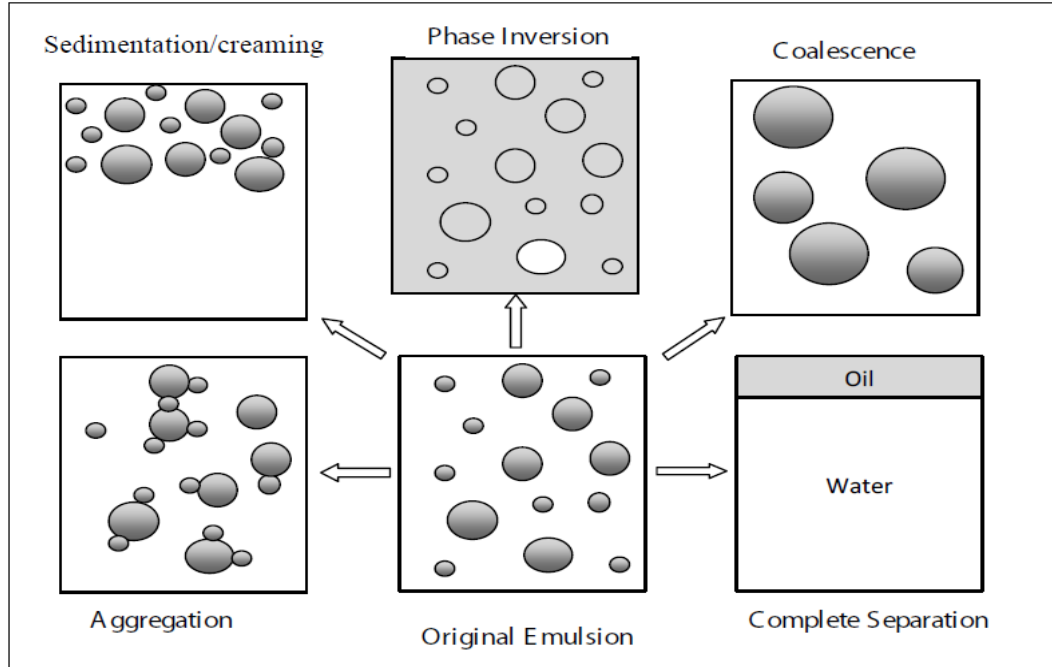
demonstrated that a calibration curve based on acoustic velocity measurements can be generated to estimate water fraction in emulsion phase at any point.

References

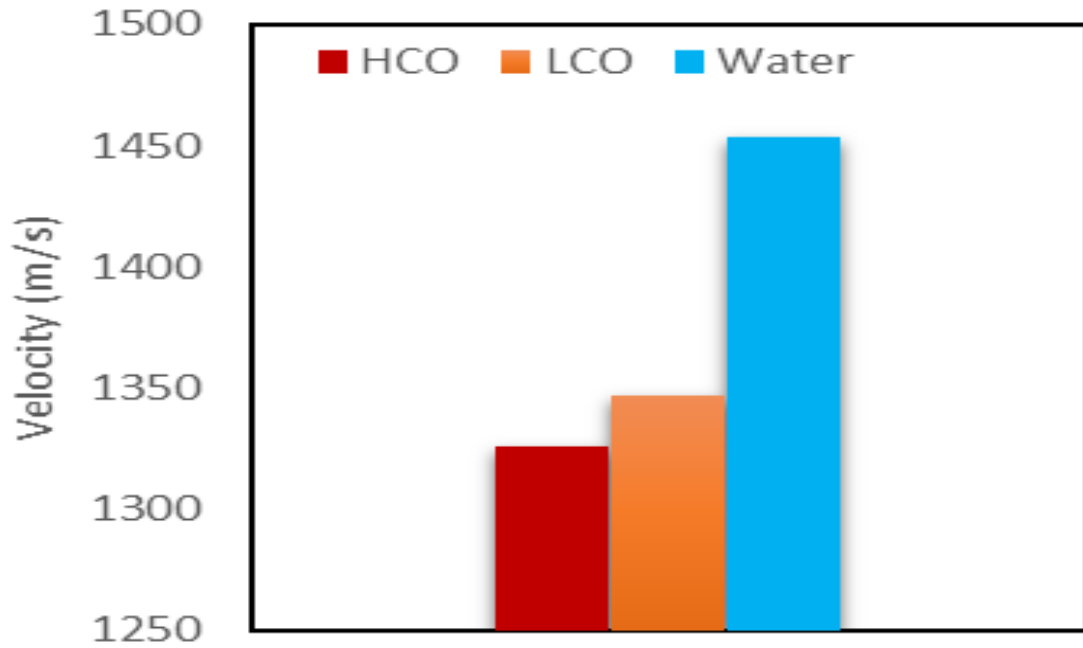
- AL Hadabi, I., Sasaki, K., Sugai, Y. 2016. Effects of Kaolinite Clay on Omani Heavy-Oil Rheology in Considering Enhanced Oil Recovery by Steam Injection. *International Journal of Earth Sciences and Engineering*, 9 (1), 22–24.
- Alwadani, M.S. 2010. Characterization and rheology of water-in-oil emulsion from deepwater fields. Master's Thesis, Rice University.
- Ariffin, T., Yahya, E., Hussin, H. 2016. The Rheology of Light Crude Oil and Water-In-Oil-Emulsion. *Procedia Engineering*, 148 (14), 1149–1155.
- Atkinson, C.M., Kytömaa, H.K. 1992. Acoustic Wave Speed and Attenuation in Suspensions. *International Journal of multiphase flow*, 18 (4), 577-592.
- Aveyard, R., Binks, B.P., Clint, J.H. 2003. Emulsions stabilized solely by colloidal particles. *Advances in Colloid and Interface Science*, 11 (100-102), 503-546.
- Azodi, M., Nazar, A. 2013. An Experimental Study on Factors Affecting the Heavy Crude Oil in Water Emulsions Viscosity. *Journal of Petroleum Science and Engineering*, 106 (11), 1-8.
- Binks, B.P., Kirkland, M. 2002. Interfacial structure of solid-stabilized emulsions studied by scanning electron microscopy. *Physical Chemistry Chemical Physics*, 4 (15), 3727-3733.
- Chevalier, Y., Bolzinger, M. 2013. Emulsions Stabilized with Solid Nanoparticles: Pickering Emulsions. *Colloids and Surfaces A: Physicochemical and Engineering Aspects*, 439 (14), 23–34.
- Coupland, J.N., McClements, J. 2001. Droplet Size Determination in Food Emulsions : Comparison of Ultrasonic and Light Scattering Methods. *Journal of Food Engineering*. 50 (2), 117–20.

- Derkach, S.R. 2009. Rheology of emulsions. *Advances in Colloid and Interface Science*, 151 (1-2), 1-23.
- Ensminger, D., Bond, L.J. 2012. Ultrasonics – Fundamentals, Technologies and Applications, 3rd ed., *CRC Press*, 765.
- Lim, J., Wong, S., Law, M., *et al.* 2015. A Review on the Effects of Emulsions on Flow Behaviours and Common Factors Affecting the Stability of Emulsions. *Journal of Applied Sciences*, 15 (2), 167–172.
- McClements, D.J. 1996. Principles of Ultrasonic Droplet Size Determination in Emulsions. *Langmuir*, 12 (14), 3454–3461.
- Mendes, R., Vinay, G., Ovarlez, G. 2015. Modeling the rheological behavior of waxy crude oils as a function of flow and temperature history. *Journal of the Society of Rheology*, 59 (3), 703-732.
- Moradi, M., Alvarado, A., Huzurbazar, S. 2011. Effect of Salinity on Water-in-Crude Oil Emulsion: Evaluation through Drop-Size Distribution Proxy. *Energy & Fuels*, 25 (1), 260-268.
- Pal, R., Rhodes, E. 1989. Viscosity/Concentration Relationships for Emulsions. *Journal of Rheology*, 33 (7), 1021-1045.
- Shukla, A., Prakash, A., Rohani, S. 2010. Online Measurement of Particle Size Distribution during Crystallization Using Ultrasonic Spectroscopy. *Chemical Engineering Science*, 65 (10), 3072–3079.
- Su, M., Xue, M., Cai, X., *et al.* 2008. Particle Size Characterization by Ultrasonic Attenuation Spectra. *Particuology*, 6 (4), 276-281.

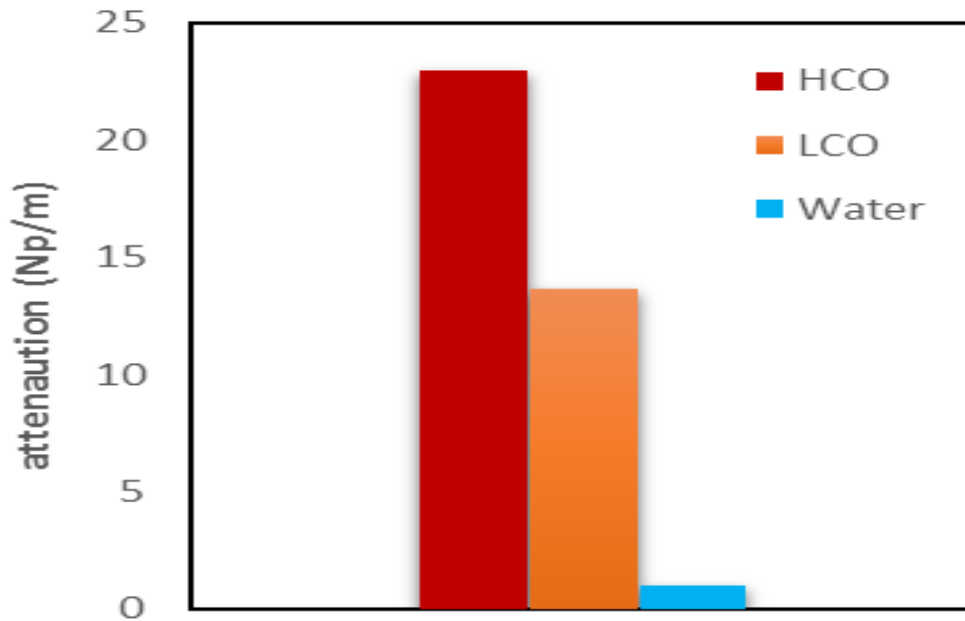
Appendix B



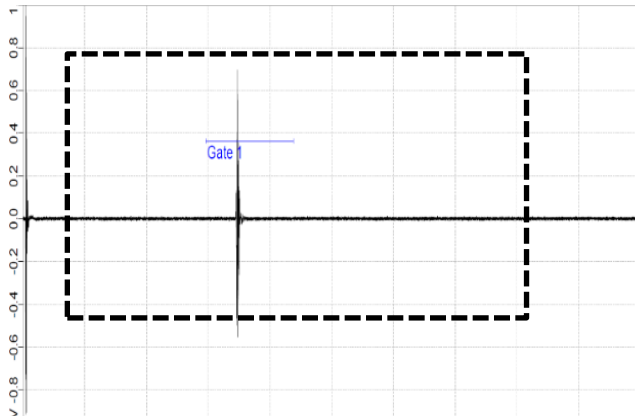
Appendix B 1 Stability mechanism



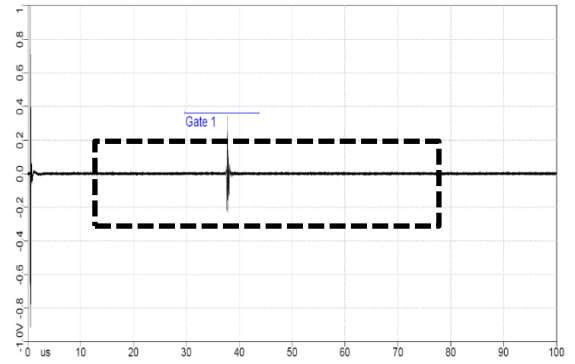
Appendix B 2 Compression of acoustic velocity of heavy and light crude oil



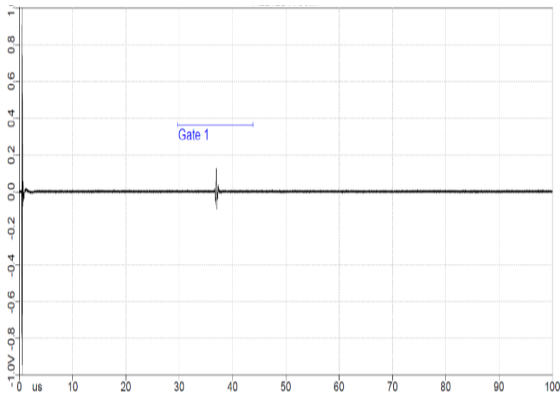
Appendix B 3 Compression of attenuation of heavy and light crude oil



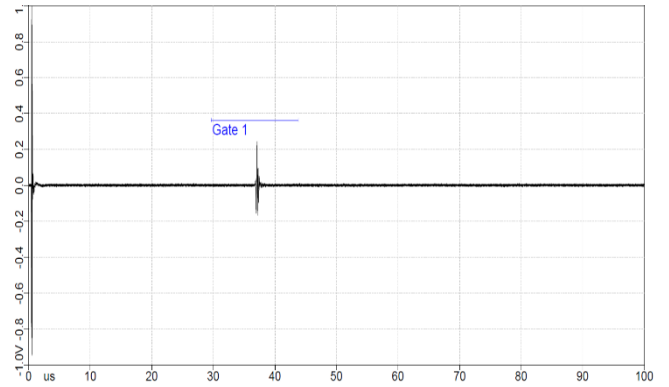
Appendix B 5 Ultrasonic signal in water.



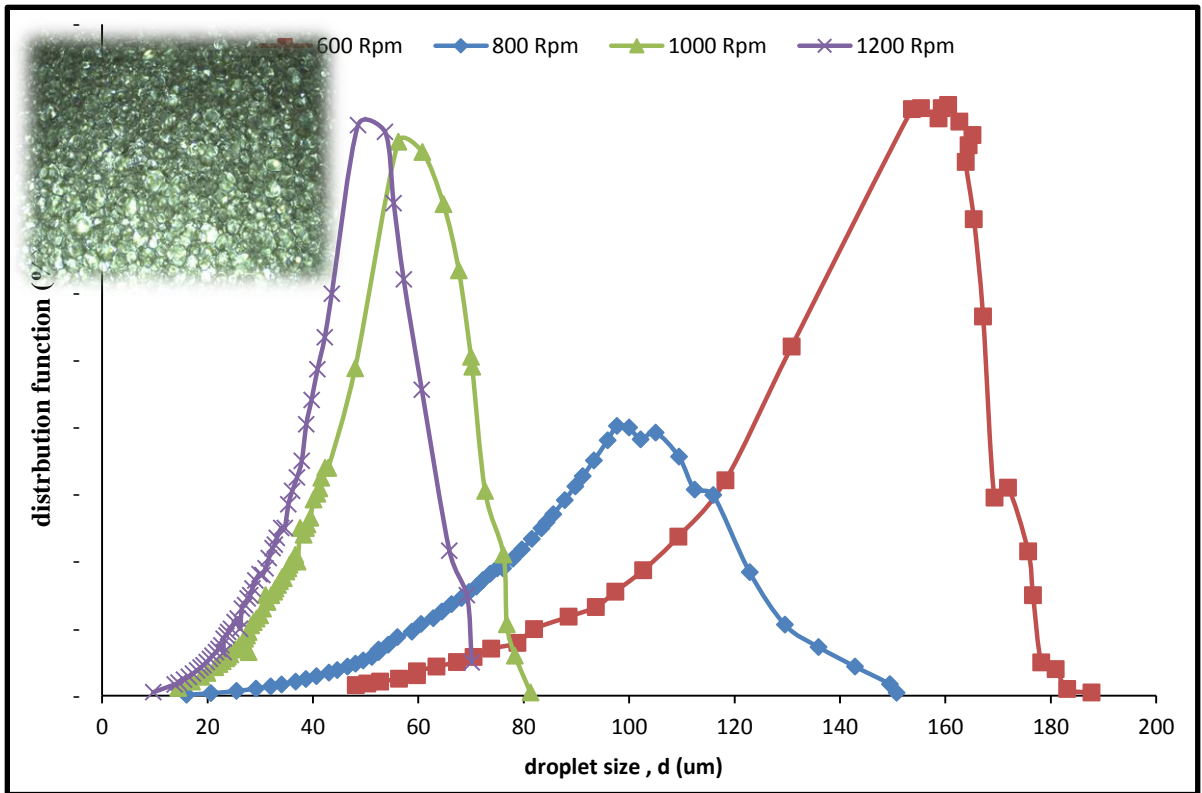
Appendix B 4 Ultrasonic signal in light crude



Appendix B 7), Ultrasonic signal in fresh emulsion 1200 Rpm after 24 hr

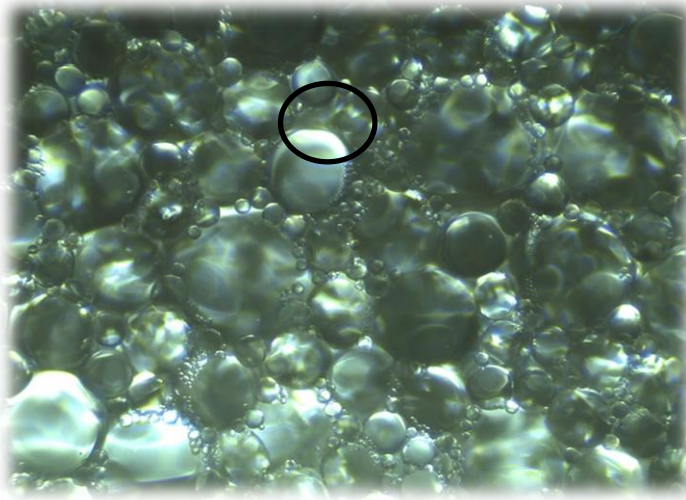


Appendix B 6 Ultrasonic signal in emulsion of 1200 Rpm

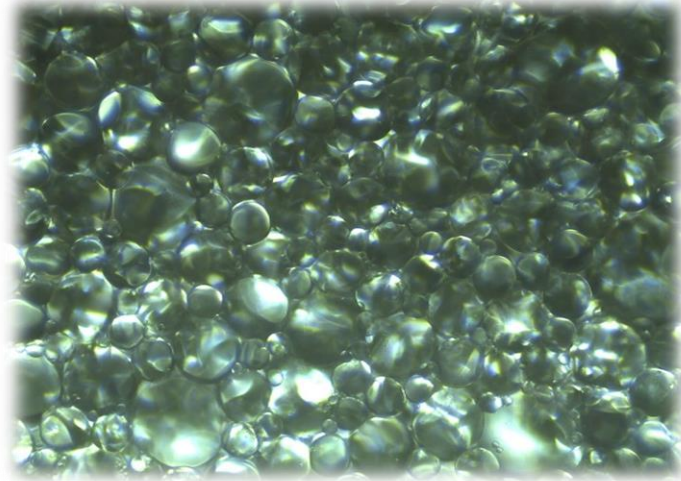


Appendix B8 droplet size distribution for light mineral oil

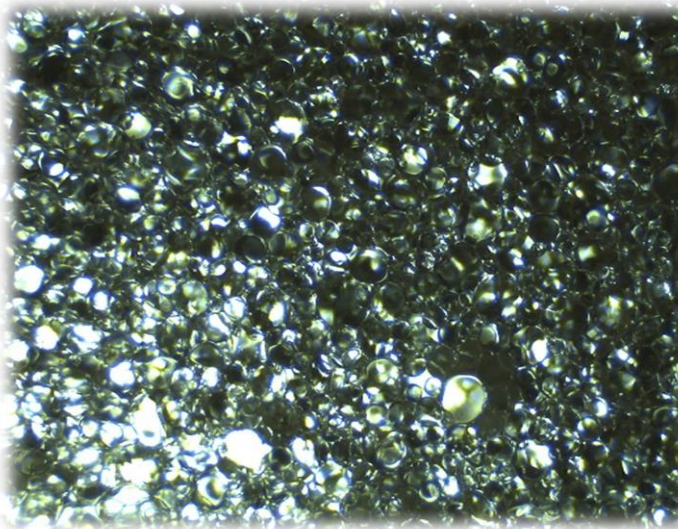
600 rpm



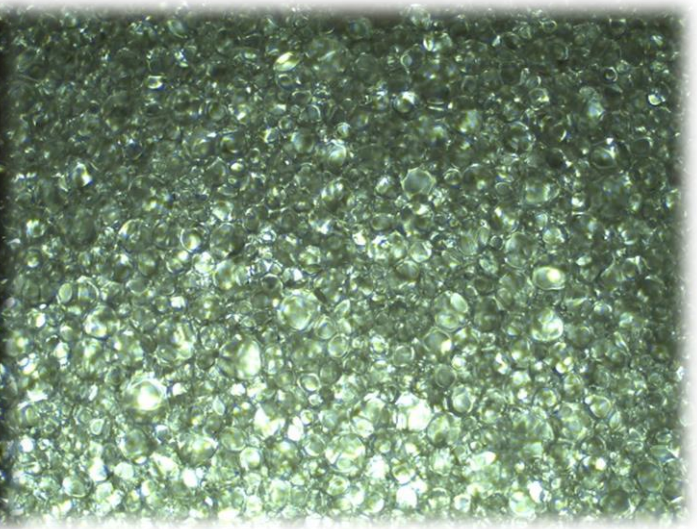
800 rpm



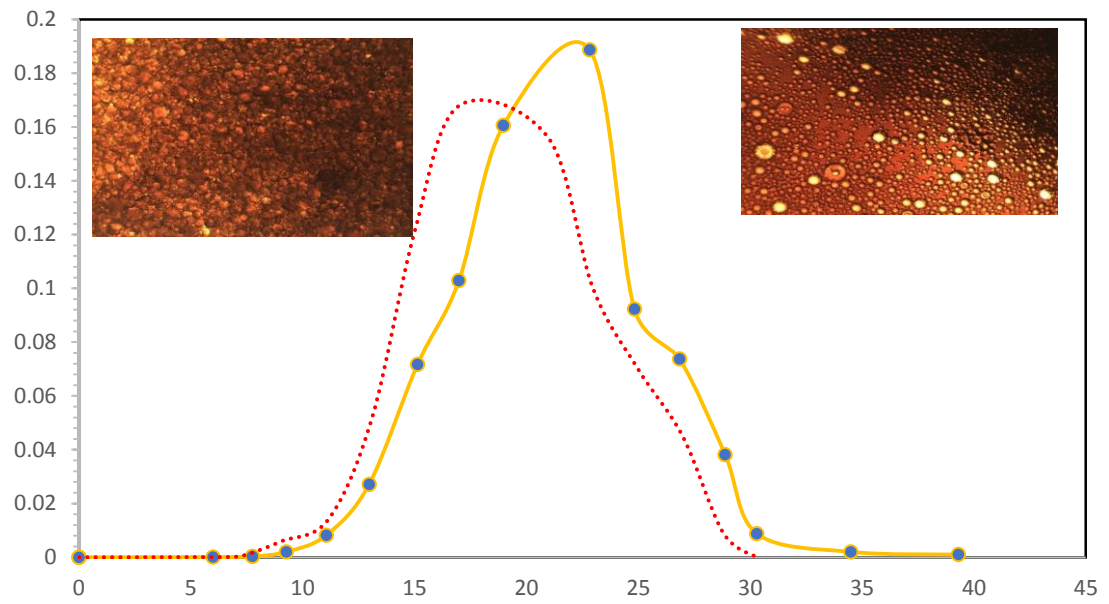
1000 rpm



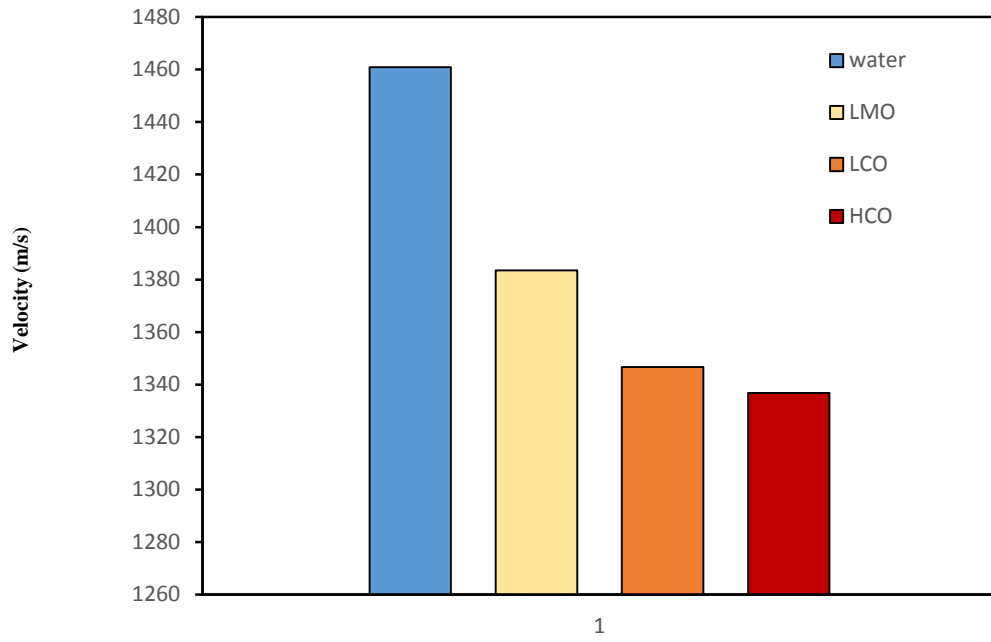
1200 rpm



Appendix B 9 Photomicrographs of freshly prepared water-in-oil emulsions at 10x.



Appendix B10 Comparison of droplet size distribution before and after settling process



Appendix B 11 Comparison of acoustic velocity



MASTERSIZER



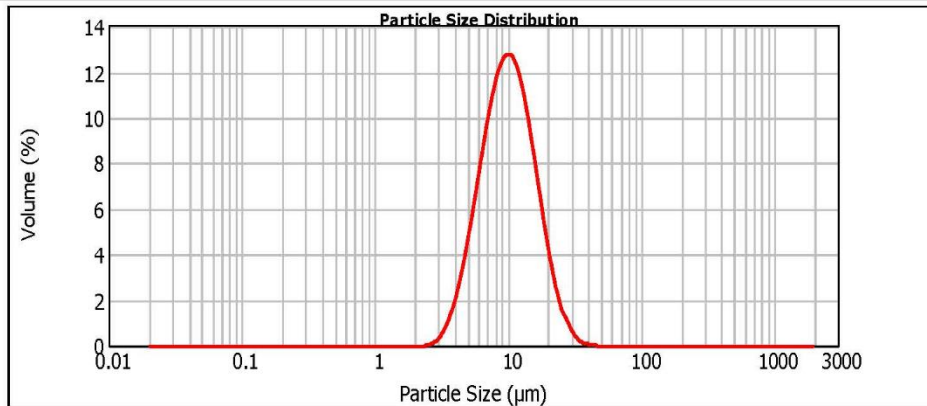
Result Analysis Report

Sample Name: 20170427-30:50
Sample Source & type: Works
Sample bulk lot ref: A
SOP Name:
Measured by: Marivel
Result Source: Measurement
Measured: Friday, April 28, 2017 11:38:18 AM
Analysed: Friday, April 28, 2017 11:38:19 AM

Particle Name: Glutamic acid
Particle RI: 1.468
Dispersant Name: Water
Accessory Name: Hydro 2000MU (A)
Absorption: 0
Dispersant RI: 1.330
Analysis model: General purpose
Size range: 0.020 to 2000.000 um
Weighted Residual: 2.113 %
Sensitivity: Normal
Obscuration: 16.77 %
Result Emulation: Off

Concentration: 0.0214 %Vol
Specific Surface Area: 0.673 m²/g
Span : 1.250
Surface Weighted Mean D[3,2]: 8.919 um
Uniformity: 0.394
Vol. Weighted Mean D[4,3]: 10.967 um
Result units: Volume

d(0.1): 5.441 um **d(0.5):** 9.923 um **d(0.9):** 17.847 um



— 20170427-30:50, Friday, April 28, 2017 11:38:18 AM

Size (µm)	Volume In %	Size (µm)	Volume In %	Size (µm)	Volume In %	Size (µm)	Volume In %	Size (µm)	Volume In %	Size (µm)	Volume In %
0.010	0.00	0.105	0.00	1.096	0.00	11.482	10.64	120.226	0.00	1258.925	0.00
0.011	0.00	0.120	0.00	1.259	0.00	13.183	9.06	138.038	0.00	1445.440	0.00
0.013	0.00	0.138	0.00	1.445	0.00	15.196	7.07	158.489	0.00	1659.587	0.00
0.015	0.00	0.158	0.00	1.660	0.00	17.378	4.98	181.970	0.00	1905.461	0.00
0.017	0.00	0.182	0.00	1.905	0.00	19.953	3.14	206.930	0.00	2187.762	0.00
0.020	0.00	0.209	0.00	2.188	0.00	22.909	2.09	239.883	0.00	2511.886	0.00
0.023	0.00	0.240	0.00	2.512	0.00	26.303	1.73	275.423	0.00	2884.032	0.00
0.026	0.00	0.275	0.00	2.884	0.12	30.200	0.83	316.228	0.00	3311.311	0.00
0.030	0.00	0.316	0.00	3.311	0.39	34.674	0.31	363.078	0.00	3801.894	0.00
0.035	0.00	0.363	0.00	3.802	1.05	39.811	0.11	416.869	0.00	4365.158	0.00
0.040	0.00	0.417	0.00	4.365	2.05	45.709	0.02	478.630	0.00	5011.872	0.00
0.046	0.00	0.479	0.00	5.012	3.50	52.481	0.00	549.541	0.00	5754.399	0.00
0.052	0.00	0.550	0.00	5.754	5.26	60.256	0.00	630.957	0.00	6606.904	0.00
0.060	0.00	0.631	0.00	6.607	7.21	69.183	0.00	724.436	0.00	7585.776	0.00
0.069	0.00	0.724	0.00	7.586	9.07	79.433	0.00	831.764	0.00	8709.636	0.00
0.079	0.00	0.832	0.00	8.710	10.58	91.201	0.00	954.993	0.00	10000.000	0.00
0.091	0.00	0.955	0.00	10.000	11.43	104.713	0.00	1096.478	0.00		
0.105	0.00	1.096	0.00	11.482	11.46	120.226	0.00	1258.925	0.00		

Operator notes:



MASTERSIZER



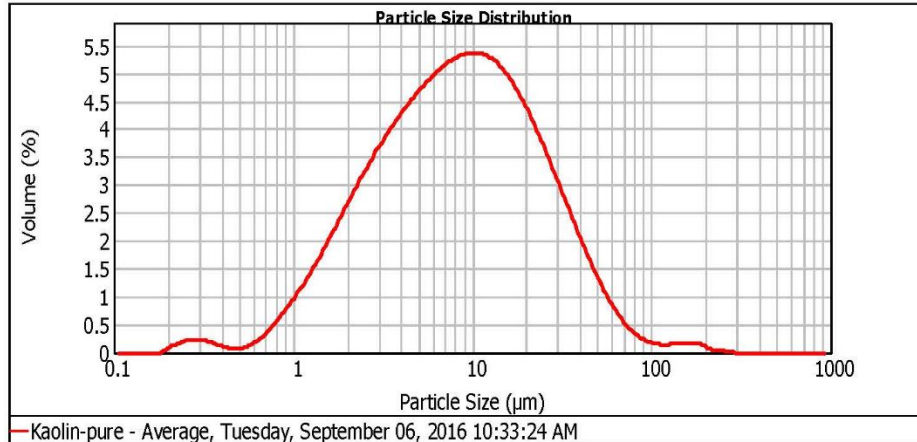
Result Analysis Report

Sample Name: Kaolin-pure - Average	SOP Name: Default2	Measured: Tuesday, September 06, 2016 10:33:24 AM
Sample Source & type: Factory = Paris	Measured by: Bahar	Analysed: Tuesday, September 06, 2016 10:33:25 AM
Sample bulk lot ref: 123-ABC	Result Source: Averaged	

Particle Name: Default	Accessory Name: Hydro 2000MU (A)	Analysis model: General purpose	Sensitivity: Enhanced
Particle RI: 1.520	Absorption: 0.1	Size range: 0.100 to 1000.000 um	Obscuration: 10.41 %
Dispersant Name: Water	Dispersant RI: 1.000	Weighted Residual: 0.924 %	Result Emulation: Off

Concentration: 0.0058 %Vol	Span : 3.523	Uniformity: 1.21	Result units: Volume
Specific Surface Area: 1.43 m ² /g	Surface Weighted Mean D[3,2]: 4.209 um	Vol. Weighted Mean D[4,3]: 14.053 um	

d(0.1): 1.911 um d(0.5): 8.336 um d(0.9): 31.280 um



Size (µm)	Volume In %	Size (µm)	Volume In %	Size (µm)	Volume In %	Size (µm)	Volume In %	Size (µm)	Volume In %	Size (µm)	Volume In %
0.010	0.00	0.105	0.00	1.096	1.17	11.482	4.78	120.226	0.13	1258.925	0.00
0.011	0.00	0.120	0.00	1.259	1.46	13.183	4.64	138.038	0.15	1445.440	0.00
0.013	0.00	0.138	0.00	1.445	1.78	15.136	4.43	158.489	0.16	1659.587	0.00
0.015	0.00	0.158	0.00	1.660	2.11	17.378	4.14	181.970	0.12	1905.461	0.00
0.017	0.00	0.182	0.04	1.905	2.45	19.953	3.79	208.930	0.04	2187.782	0.00
0.020	0.00	0.209	0.14	2.188	2.77	22.909	3.39	239.883	0.03	2511.896	0.00
0.023	0.00	0.240	0.20	2.512	3.09	26.303	2.96	275.423	0.00	2884.032	0.00
0.025	0.00	0.275	0.20	2.884	3.38	30.200	2.52	316.228	0.00	3311.311	0.00
0.030	0.00	0.316	0.20	3.311	3.65	34.674	2.08	363.078	0.00	3801.894	0.00
0.035	0.00	0.363	0.17	3.802	3.89	39.811	1.66	416.869	0.00	4365.158	0.00
0.040	0.00	0.417	0.12	4.365	4.12	45.709	1.27	478.630	0.00	5011.872	0.00
0.046	0.00	0.479	0.07	5.012	4.32	52.481	0.92	549.541	0.00	5754.399	0.00
0.052	0.00	0.550	0.14	5.754	4.50	60.256	0.63	630.957	0.00	6606.934	0.00
0.060	0.00	0.631	0.26	6.607	4.65	69.183	0.41	724.436	0.00	7585.776	0.00
0.069	0.00	0.724	0.45	7.586	4.76	79.433	0.26	831.754	0.00	8709.636	0.00
0.079	0.00	0.832	0.66	8.710	4.83	91.201	0.17	954.993	0.00	10000.000	0.00
0.091	0.00	0.955	0.90	10.000	4.84	104.713	0.13	1096.478	0.00		
0.105	0.00	1.096		11.482		120.226		1258.925	0.00		

Appendix B 8 Particles size distribution of Iron and clay

Chapter 5

5. Characterization of rheological properties of Water-in-Oil Emulsion

5.1 Introduction

Emulsions are mixtures of two kinetically stable immiscible liquids which are thermodynamically unstable. Even though they have multiple applications in food, cosmetics and pharmaceutical industries, they are not always desirable. Oil-water emulsions are commonly encountered at various stages of crude oil production and processing. Most of the emulsion in crude oil processing is generated by the dispersion of water droplets in oil phase and stabilized by the impurities associated with crude oil. A major problem in petroleum industry originates when water oil mixture is agitated leading to the formation of a stable water-in-oil emulsion. These emulsions are found in the desalting process used to remove salts, which poison the refinery catalysts and enhance corrosion. It leads to increase in viscosity of crude oil and significant increase in transportation and pumping costs. While the large droplets are easy to remove with physical methods as gravitational settling or centrifugation, the separation of small micron-sized droplets require further methods to separate. Inorganic solid particles like clays, silicas, and iron oxides act as stabilising agents through surface modifications while crude oil species such as resins and asphaltenes are adsorbed on the surface of these particles and make them interfacially active.

Rheological behaviour of emulsions is important field of study for scientific understanding and industrial applications. This can be Newtonian or non-Newtonian based upon its composition which constitutes of solid particle, organic additives and emulsifying agents.

A study of the stabilisation mechanism and factors affecting the stabilisation has been performed by various authors (Mingyuan et al., 1992; McLean and Kilpatrick, 1997b; Gafonova and Yarranton, 2001; Li et al., 2002; Havre 2003; Ese and Kilpatrick, 2004). Stability of water emulsion comes from a rigid protective film of surfactants encapsulating the water droplets (McLean and Kilpatrick, 1997a,b; Yarranton et al., 2000). These surfactants contain resin, asphaltenes and fatty acids (Sjöblom et al., 1992; Spiecker and Kilpatrick, 2004). The accumulation of these surfactants at the surface hinders coalescence and causes phase separation.

The present work studies the rheological behavior of various emulsions in terms of providing a better understanding. Effects of several factors including mixing speed, shear rate, shear stress, temperature, pH, salt content; solid particle, addition of surfactants concentration, and droplet average diameter have been studied. It has been designed in order to provide a better understanding of water-in-oil emulsion behavior and contribute to technological developments specific to oil production problems.

5.2 Materials and methods

5.2.1 Materials

The light mineral oil (LMO) was purchased from VWR International, and has density of 858.8 kg /m³ and viscosity 60 mPa.s at room temperature. Light and heavy crude oil samples were supplied by Imperial Oil Ltd. Triton X-100 (polyethylene glycol octyl phenol ether) with the chemical formulation of C₃₃H₆₀O₁₀, used as emulsifier was obtained from VWR International. This surfactant is a non-ionic hydrophilic, it has a density of 1065

kg/m³, HLB (Hydrophile-Lipophile Balance) 13.5, viscosity of 240 mPa.s at 25°C, and surface tension is about 3100 dyne/cm. The commercial non-ionic hydrophilic surfactant Tween 20 (Polyoxyethylene-20-sorbitan Monolaurate) with the chemical formulation of C₅₈H₁₁₄O₂₆, density of 1100 kg/m³, viscosity of 450 cP at 25°C, and HLB of 16.5 is used as de-emulsifier. Brookfield digital Rheometer was employed to determine the rheology of the emulsion at different temperatures controlled by water bath thermostat. Density measurements were conducted using SG-Ultra Max Ex Petrol Density Meter, by Eagle Eye Power Solutions, LLC. IKA mechanical mixer model RW 20 D, with a four blade stainless steel propeller type stirrer was used to homogenized the mixtures. A Seven Excellence PH meter supplied from Mettler Toledo Company was used to monitor and adjust the PH values of aqueous solution. Dispersed phase (water) droplets in the oil phase for different emulsions were visualized using optical microscopy (OMAX) with 10x objective and the diameter of droplets were measured using Impulse 7 software. Measurements acoustic parameters (velocity and attenuation) in emulsions have been carried out over a frequency range of 1 to 5 MHz with probes obtained from CD International Technology.

5.2.2 Apparatus and experimental procedure

A schematic diagram of the emulsion characterization system is represented in **Figure 5.1**. The experiments in this work were performed using an IKA mechanical mixer model RW 20 D for emulsion agitation. For most experiments, the operation temperature and pressure were maintained constant at ambient condition. The rheological properties were measured using Brookfield Rotational Digital Rheometer model LV/DV-III with ULA spindle over a temperature over a temperature range of 25-55°C. Meanwhile, a small amount of the emulsion was transferred to a glass slide to observe the emulsion's droplets structure via

the optical microscope (OMAX) with 10x objective; later, the taken picture was analyzed by Impulse 7 software. For stability evaluation, the prepared w/o emulsions were placed in graded cylinder of 1000 ml and left for settling by gravity forces at room temperature for 24 h..

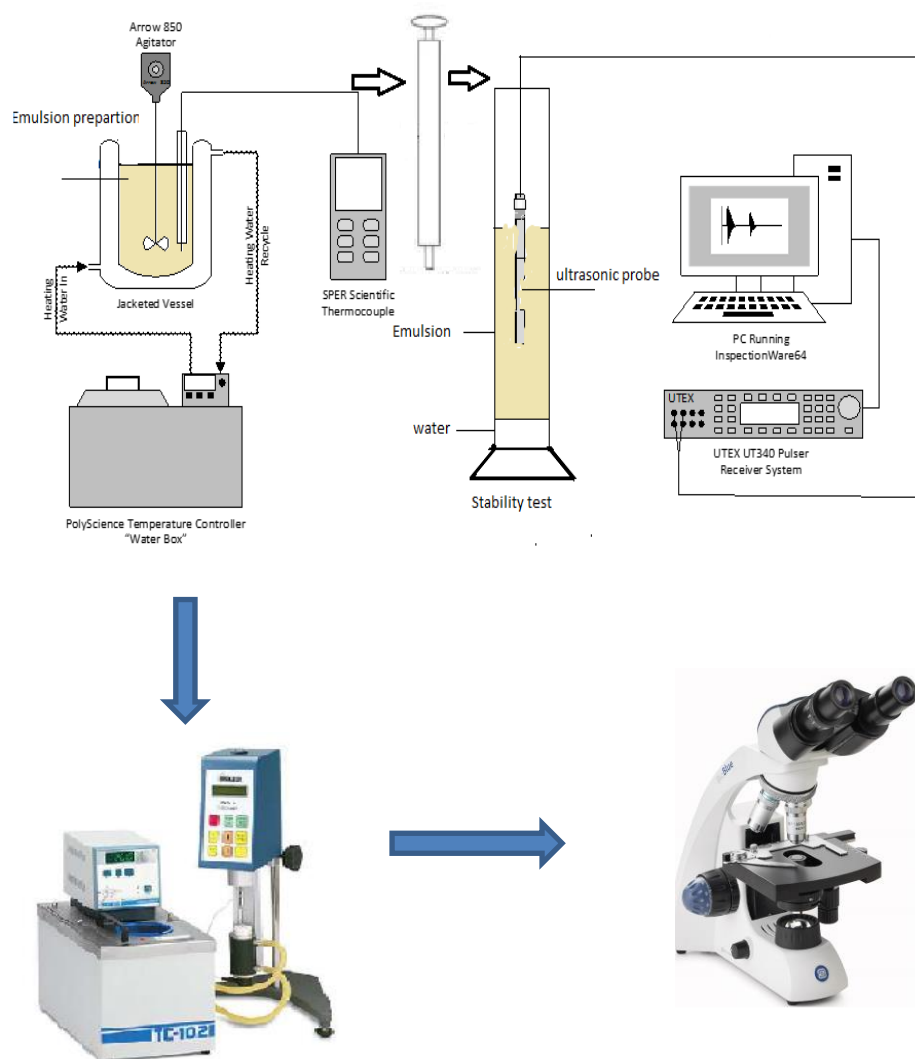


Figure 5-1 Schematic diagram of the experimental setup for emulsion characterization.

5.2.3 Asphaltene Extraction

Asphaltene was precipitated from crude oil samples based on ASTM D2007-80 Standard procedure with some modifications. *N*-heptane was added to each crude oil sample in a 1000 ml conical flask using a solvent-to- crude oil ratio of 5:1 (cm³/g). Following that, the flask was covered with an aluminum foil to prevent solvent evaporation and its content agitated for 45 minutes using a magnetic stirrer under ambient conditions to obtain a homogeneous mixture. The mixture was then left in the fume-hood for 48 hours, after which it was slowly vacuum-filtered (-15 psi) through a 0.22µm filter paper funnel assembly as shown in **Figure 5.2**. The filter paper containing the asphaltene residue was allowed to dry in the fume-hood until a constant weight was accomplished (approximately 5 days). The dried asphaltene transferred into a glass vial. A multispeed pump was used to transfer the filtrate to another container, from which the *n*-heptane was recovered via a rotavap. The weight of the asphaltenes calculated by:

$$\text{Asphaltene content (g/100ml)} = \frac{\text{weight of dried asphaltene (g)}}{\text{crude oil volume (ml)}} \quad (5.1)$$

5.2.4 Blending of crude oil samples

Upon the blending ratios, the heavy crude oil (HCO) was placed in 1000 ml beaker, which is covered with aluminum foil to avoid any evaporation or splashing. The light crude (LCO) oil was gradually introduced to the HCO, where it is homogenized at 600 rpm with an IKA mechanical mixer model RW 20 D for 30 mint at room temperature. The blended samples were placed in glass baker for two days to achieve the stabilization constancy by monitoring the mixture's density.



Figure 5-2 Schematic diagram of the experimental setup for asphaltene extraction.

Table 5-1 Physicochemical properties of different oil samples

Physical property	Light Mineral Oil (LMO)	Light Crude Oil (LCO)	Heavy Crude Oil (HCO)	Blended Crude oil (A)	Blended Crude oil (B)
Sp. gravity @ 60 F ⁰	0.8688	0.8699	0.9129	0.886	0.893
Density (kg/cm ³)	868.8	869.9	912.9	886.02	893.10
API ⁰	—	31.17	23.5	28.21	26.95
Kinematic viscosity (cP)@ 25 ⁰ C	60	11	33.60	23.40	31.80
Asphaltene content (wt%)	0	1.45	9.01	2.45	3.90

(A) 50 HCO: 50 LCO

(B) 70 HCO: 30 LCO

5.2.5 Preparation of Emulsion

The light mineral oil was used to prepare six emulsions according to stirring speed (600 rpm, 800rpm, 1000rpm, and 1200rpm increments). With the purpose of preparing various of water- in- oil emulsions, the constant volume fraction 80 (v/v) of LMO was placed in 1000 ml beaker, 0.2 wt% of Triton X-100 surfactant (calculated on oil amount), was added to oil phase and stirring for 5 mint to ensure the mixing solution become homogenous, 1 wt% of sodium chloride (calculated on oil amount), were dissolved in distilled water to adjust the phase salinity. The pH buffers were employed to adjust the pH of the aqueous phase and Seven Excellence PH meter was used to, the aqueous solution was gradually introduced to the LMO, where it is homogenized with an IKA mechanical mixer model RW 20 D for 30 mint at room temperature. Brookfield Rotational Digital Rheometer model LV/DV-III with ULA spindle was used to determine the rheological measurements for all the samples at different temperatures controlled by water bath thermostat connected to Rheometer, spindle type ULA was used for all measurements, this device was capable to afford the shear rate, shear stress, and apparent viscosity. The Rheometer was calibrated using Brookfield Standards fluid (4.9 – 48- 98 – 490 cP at 25°C) and systematically cleaned between measurements of different samples.

5.3 Results and discussion

5.3.1 Rheological Properties of Mineral Oil Emulsions

To study the flow behavior of oil samples and their water-in-oil emulsions the relation between shear stress and shear rate were investigated over a temperature range of 25°C to 65°C. It can be noticed in **Figures 5.3** that shear stress versus shear rate curves are essentially linear but not passing through the origin. This indicates that the flow behavior is not Newtonian. As expected, viscosity of the oil decreased with increasing temperature and the behavior is coming closer to Newtonian fluid. The viscosity of the oil can be obtained from the ratio of shear stress to shear strain curves. Since the relationship is linear, the viscosity values are essentially independent of shear rate as presented in **Figure 5.4**.

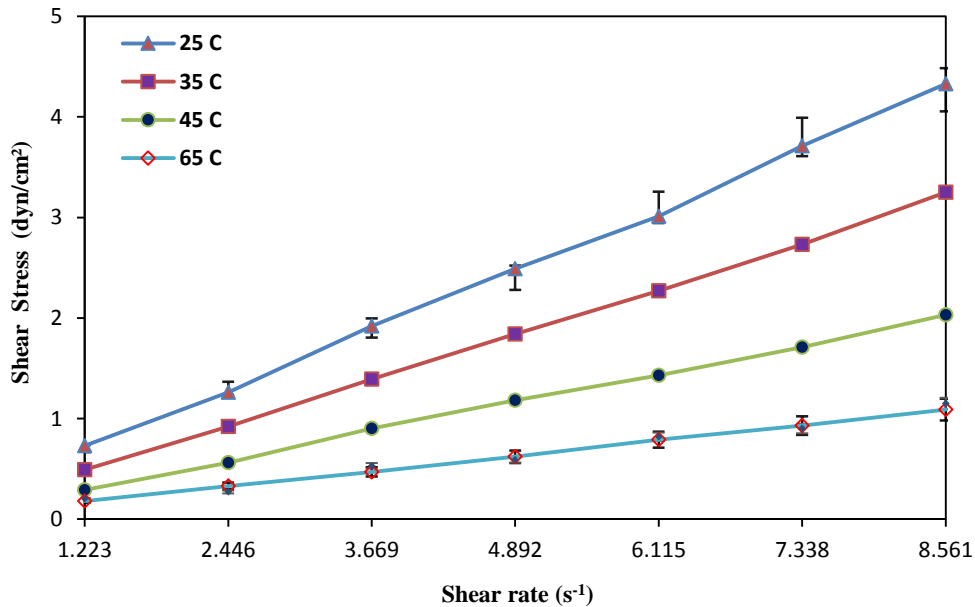


Figure 5-3 Rheo-gram of mineral oil at different temperatures.

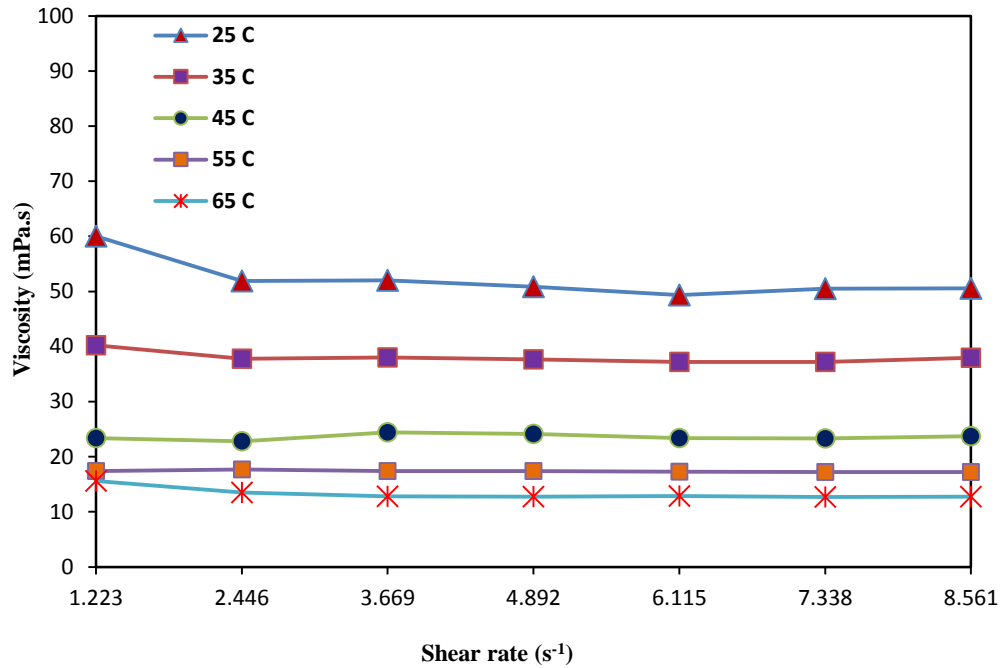


Figure 5-4 Relationship between viscosity and shear rate obtained in mineral oil.

Rheological behavior of real fluids can fall into different categories depending on the nature and composition of the fluid or dispersion. **Figure 5.5** presents different types of rheological behaviors encountered with real systems. It can be noticed that the rheological properties of mineral oil are close to Bingham plastic which show initial resistance to flow until the yield stress is reached. However, for higher temperatures, there is tendency for fluid to approach Newtonian behavior. The rheograms obtained in emulsions of mineral oil created at different mixing speeds and temperature are presented in **Figures 5.6 a to d**. It can be noticed that, the emulsions prepared at higher mixing speed depict higher shear stress for a given shear rate. A comparison with **Figure 5.5** shows that the emulsions rheological properties are closer to Herschel-Bulkley model. The corresponding viscosity versus shear rate curves are presented in **Figures 5.7 a to d**.

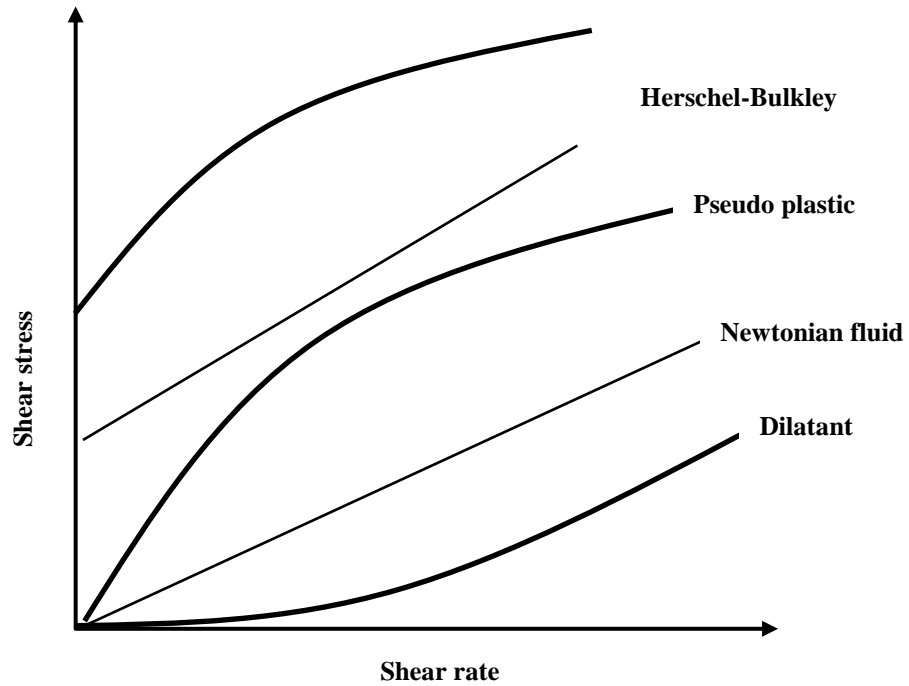
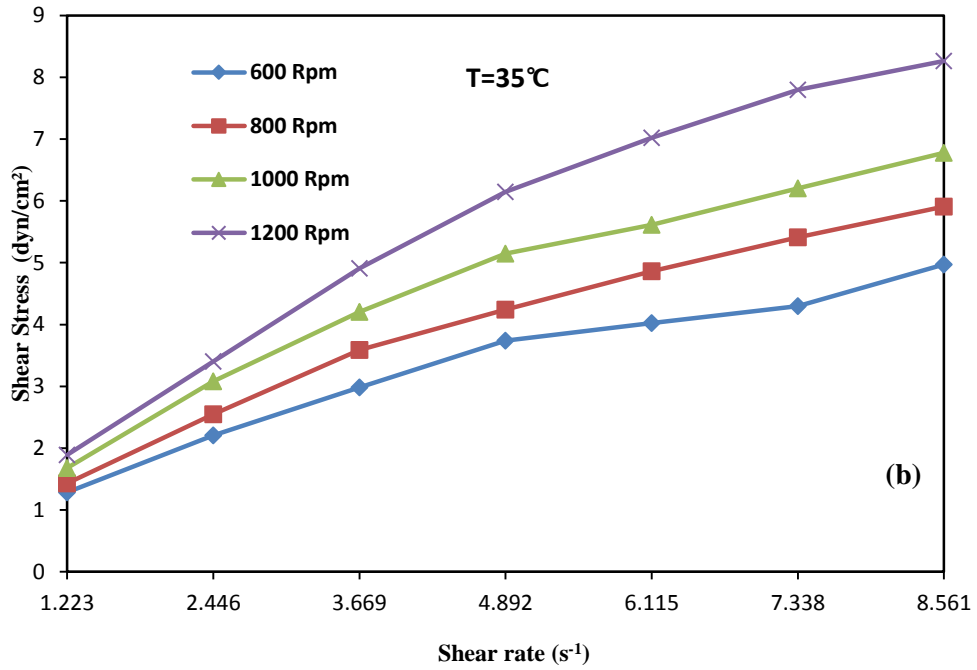
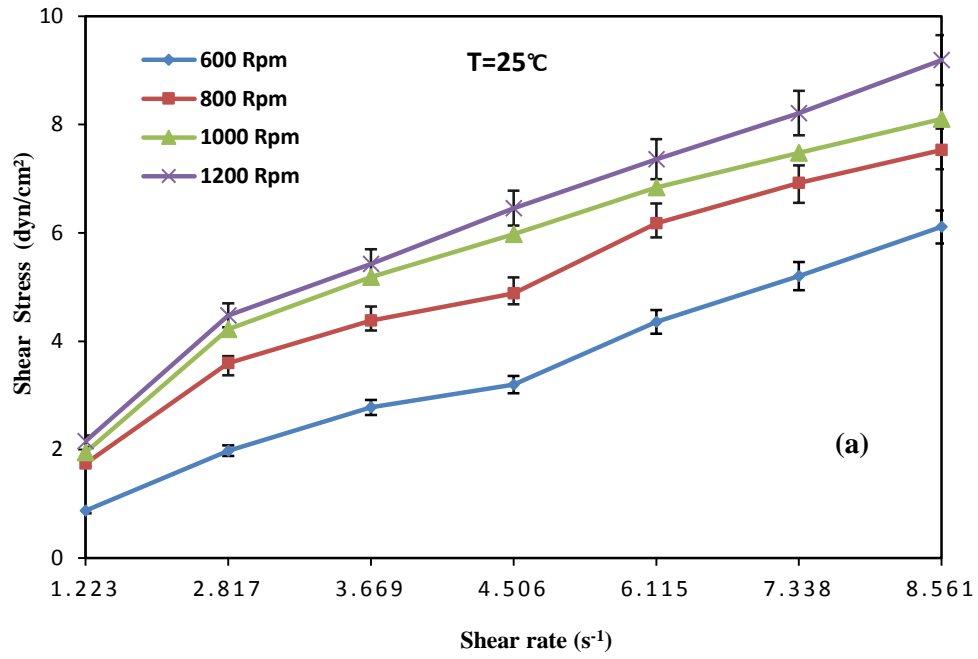


Figure 5-5 Shear stress versus shear rate for different types of fluids

Following observations can be made from Figures below:

1. Emulsion viscosity decreases with increasing shear rate.
2. Viscosities of emulsions are higher than mineral oil for all temperatures.
3. Higher viscosities are obtained in emulsions prepared at higher rpm



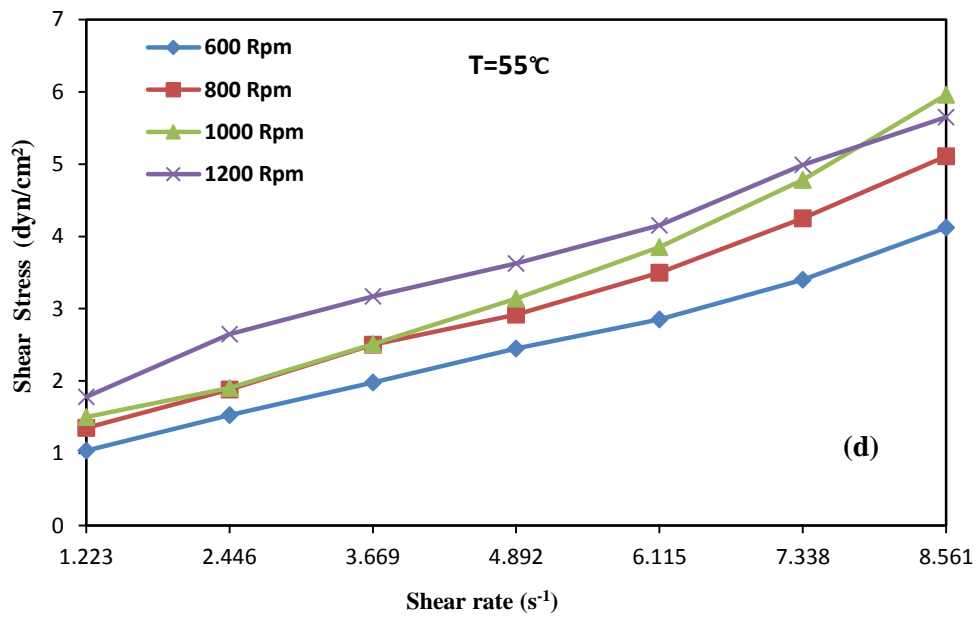
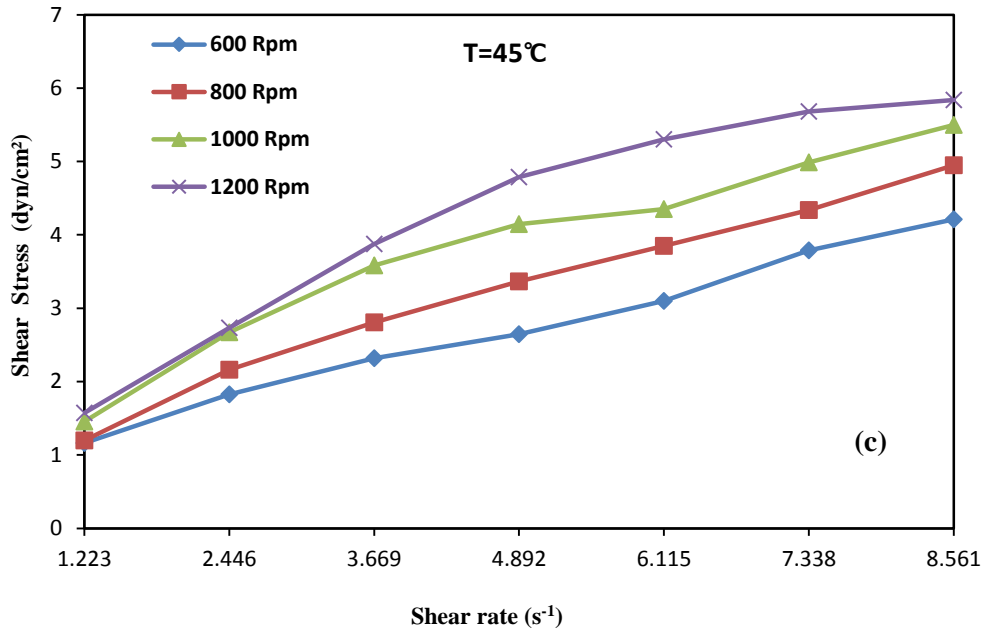
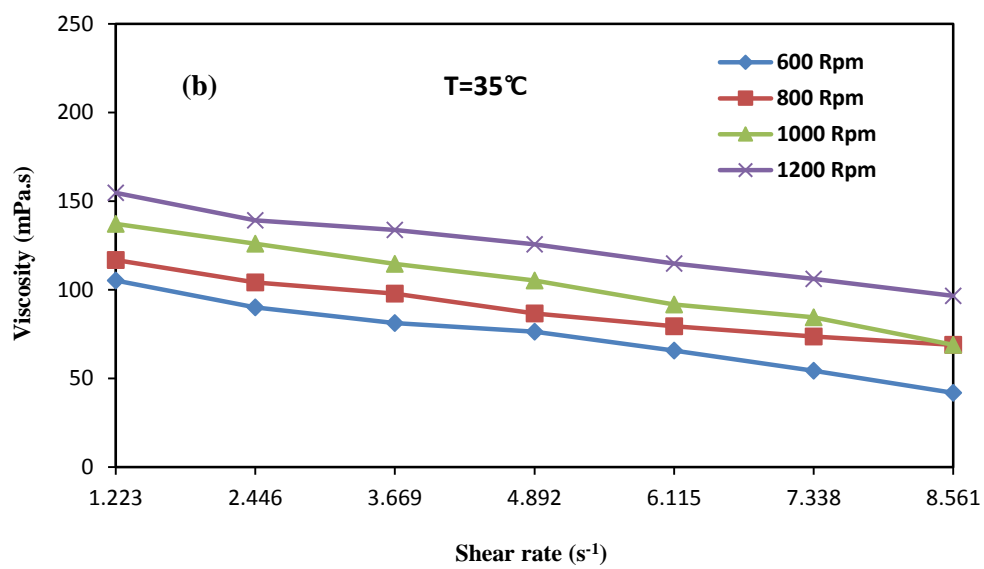
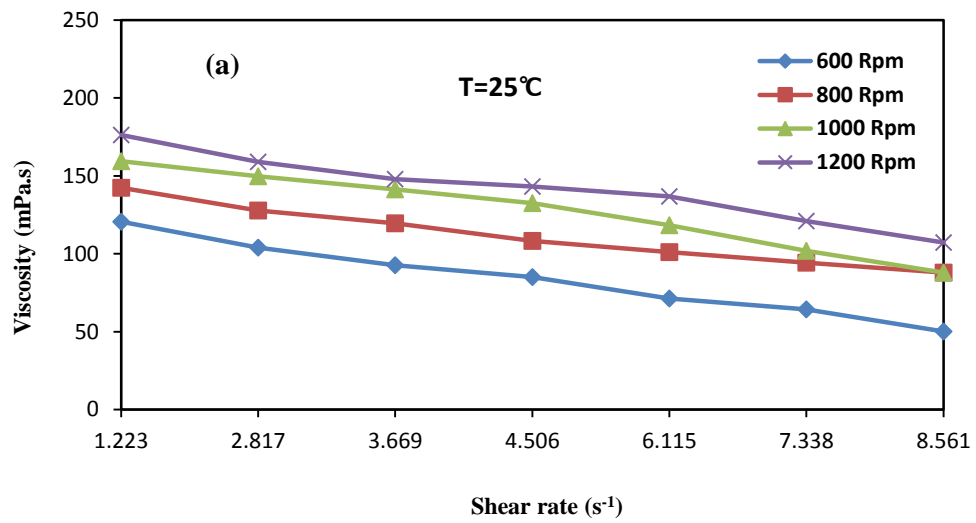


Figure 5-6 Rheo-grams of water-in-mineral oil emulsions for different temperatures and mixing speed



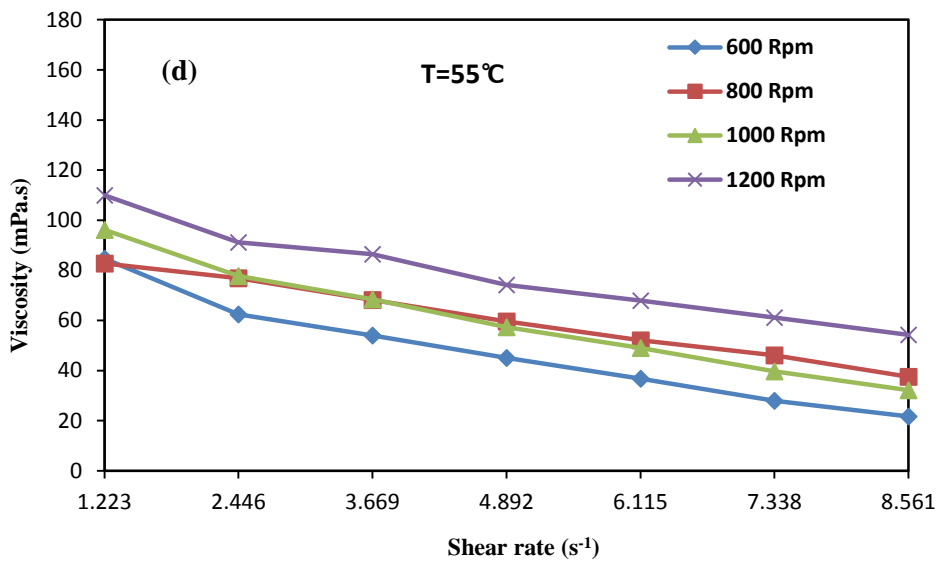
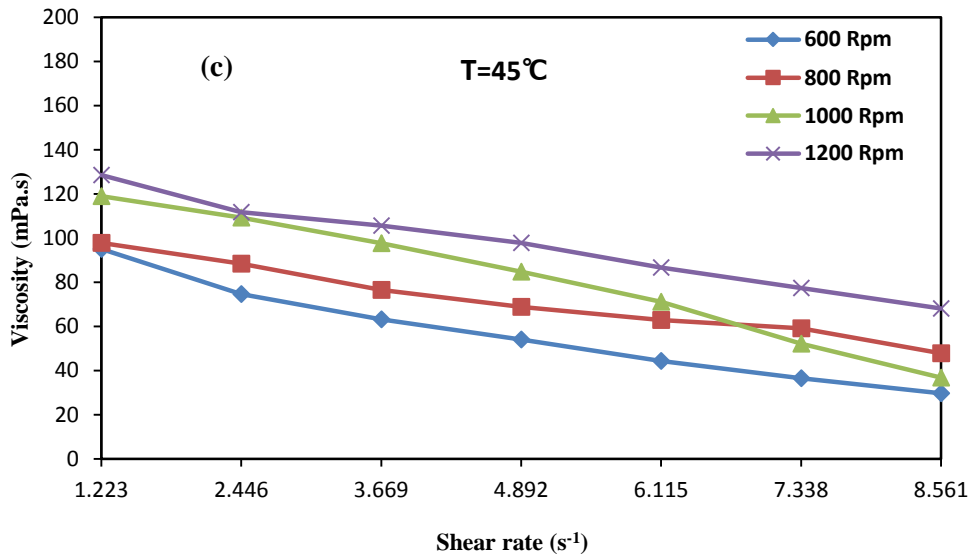


Figure 5-7 Relationship between shear rate and viscosity in emulsions of mineral oil at different temperatures.

5.3.2 Effect of mixing speed on droplet size

Change in mixing speed used for emulsion preparation would alter the droplet size distribution which can influence the emulsion rheology. For each stirring speed, the droplet size distribution was determined with the help of an optical microscope and associated

image analysis. It can be seen in **Figure 5.8**, that the average size of mineral oil emulsion droplets gradually decreased from 160.5 to 28.6 μm with an increase in the mixing speed from 600 to 1200 rpm, at the highest rpm, the droplet size distribution curve is within a narrow band and it becomes wider as the stirring speed declines. The increase in emulsion viscosity with increasing mixing speed can be attributed to decrease in observed droplet size. The images of emulsion samples shown in **Figure 5.9** clearly point to densification of the emulsion droplets. At high rpm, there is tendency for the fine droplets to flocculate which can enhance emulsion viscosity. **Figure 5.10** summarizes the results showing relationship between droplet size and emulsion viscosity.

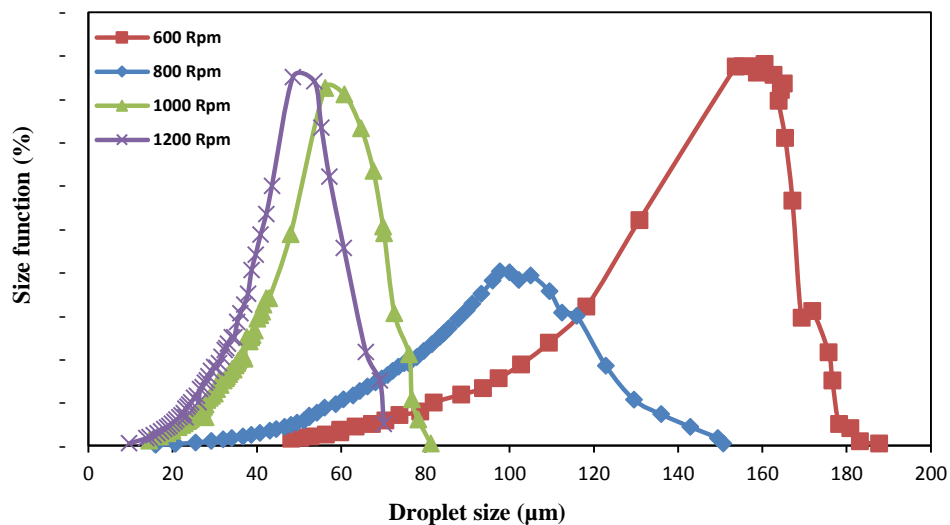


Figure 5-8 Droplet size distribution in water-in-mineral oil emulsions prepared at different mixing speeds (20 wt% water in oil).

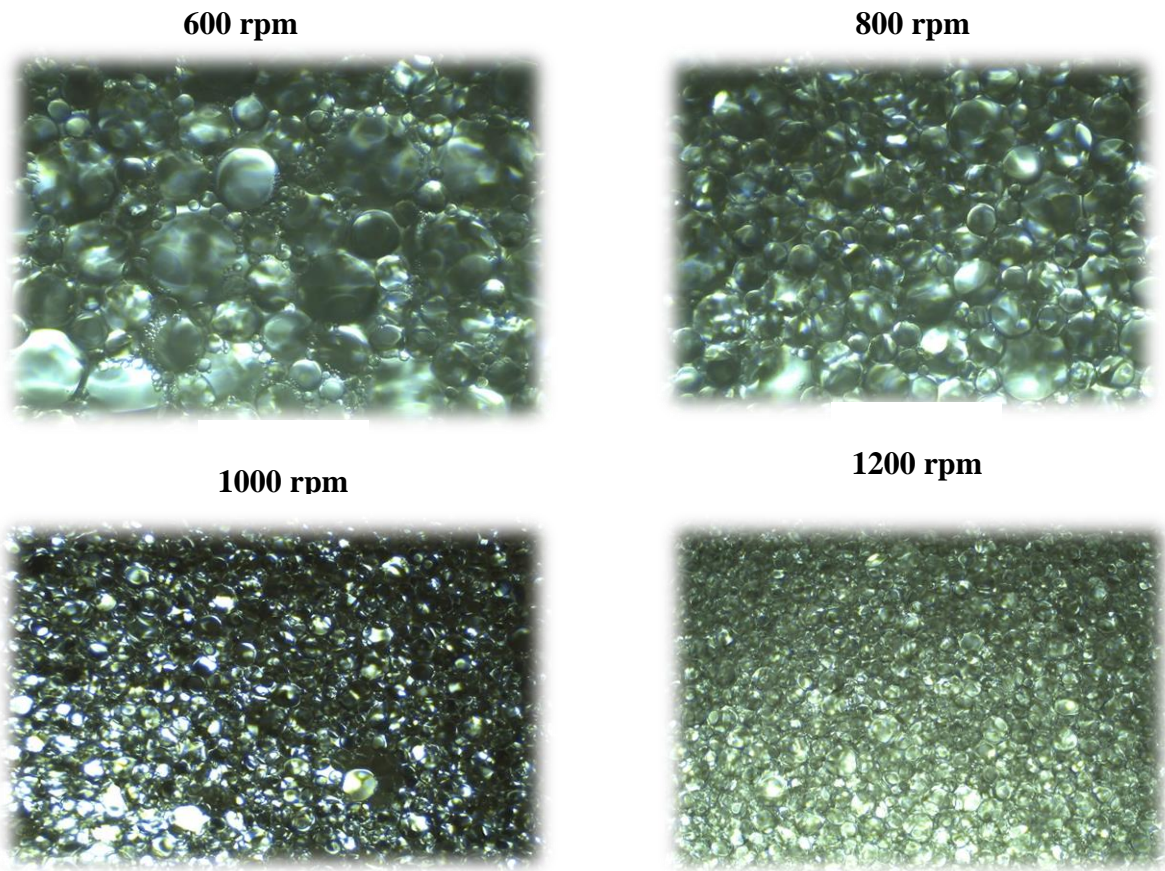


Figure 5-9 Images of mineral oil emulsion samples prepared at different mixing speeds (20 wt% water in oil)

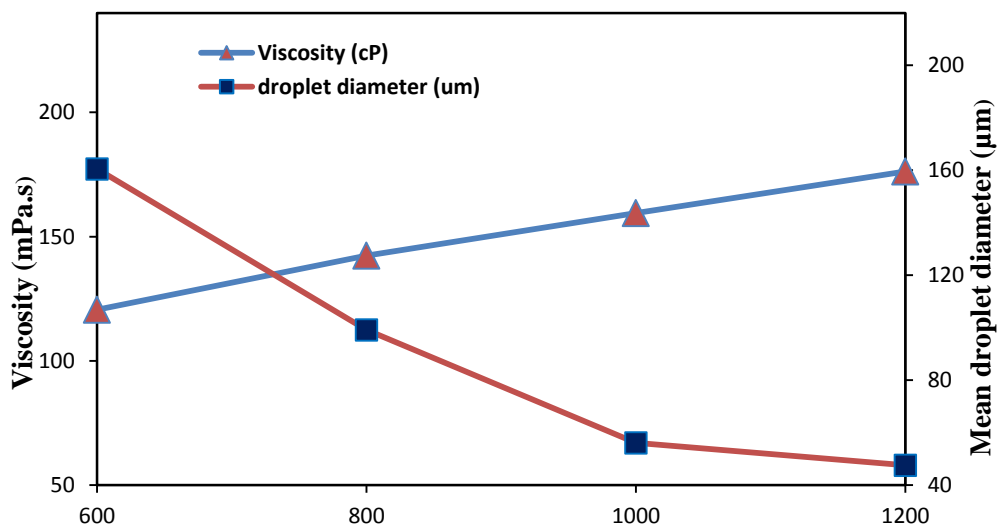


Figure 5-10 Effects of droplet size (mixing speed on mineral oil emulsion viscosity)

The dominant effect of droplet size distribution on viscosity of water-in-oil emulsions has been observed by other literature studies (Parkinson et al, 1970; Pal, 1996; Ashrafizadeh and Kamran, 2010; Abdurahman et al, 2012; Azodiand Solaimany, 2013). On other hand, only a slight effect of dispersed droplet size on viscosity of oil-in-water emulsions has been reported (Stachurski and MichaŁek, 1996; Zaki, 1997). These observations point to a more comprehensive investigation of this phenomenon.

5.4 Rheological properties of crude oil emulsions

Figure 5.11 presents relationship between shear stress and shear rate for light crude oil samples over a temperature range of 25°C to 65°C. It can be noticed that shear stress versus shear rate curves are essentially linear but not passing through the origin. This indicates that the flow behavior is similar to Bingham fluids. There is also a larger difference between 45 and 55 °C curves indicating possible effects of oil’s molecular composition on viscosity variations.

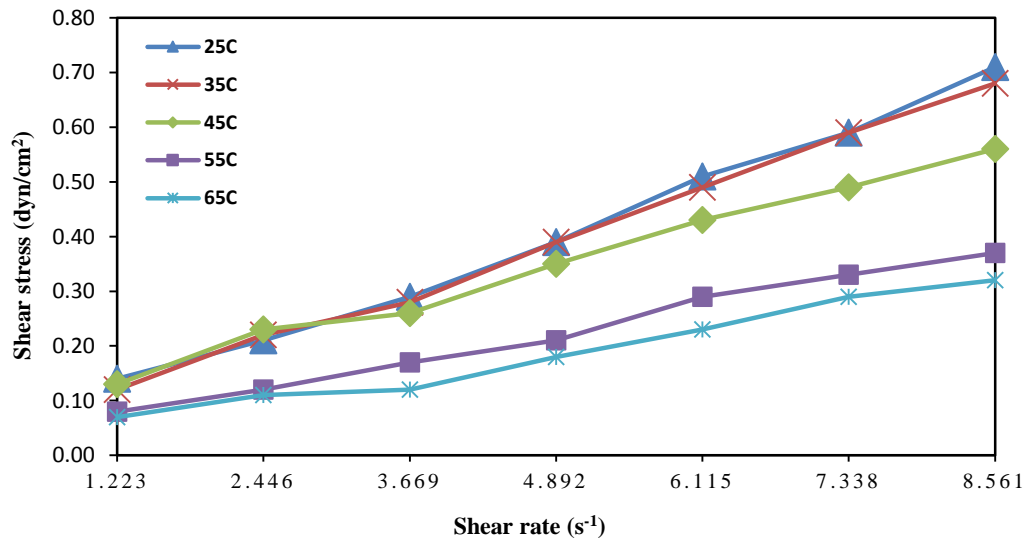


Figure 5-11 Rheogram of light crude oil at different temperatures.

As expected, viscosity of the oil decreased with increasing temperature (Figure 5.12). It is observed that above shear rate of $3.7 \text{ (s}^{-1}\text{)}$, there is essentially no effect of shear rate on the measured viscosity of crude oil. Rheograms of water-in-crude oil emulsions obtained at different mixing speeds and temperatures are presented in Figures 5.13 a to d. The linearity of the curves indicates Bingham flow behavior for these emulsions. The non-Newtonian flow behavior of crude oil emulsions has been reported in literature studies (Ariffin et al., 2016)

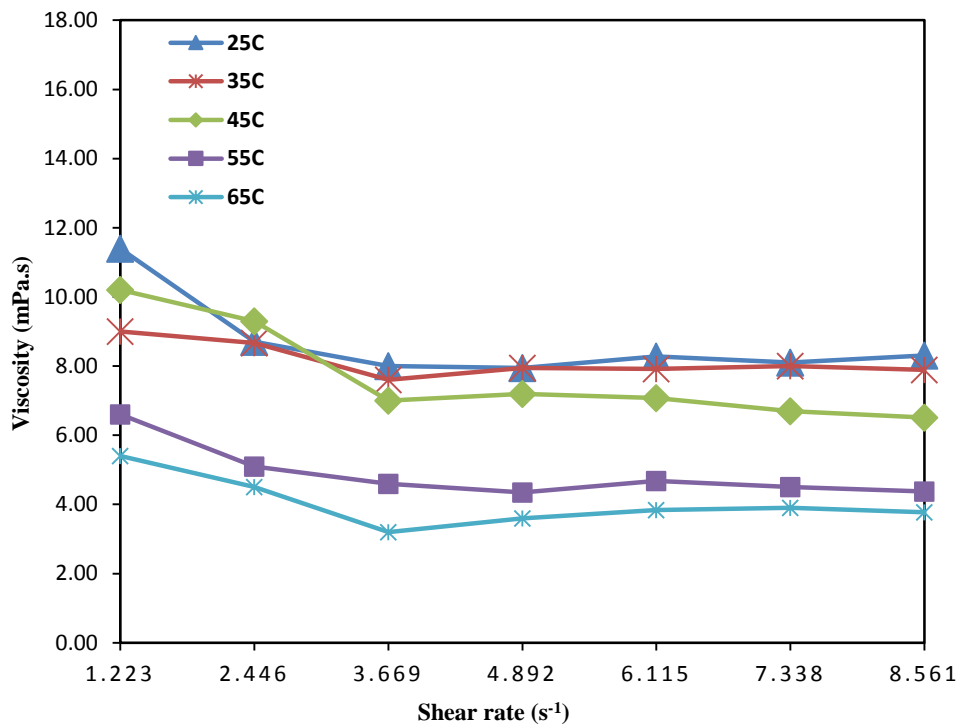
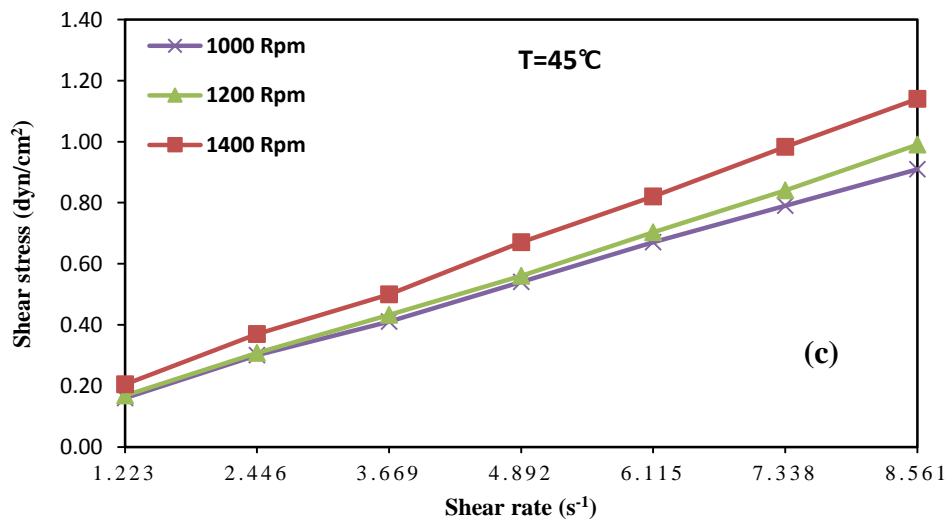
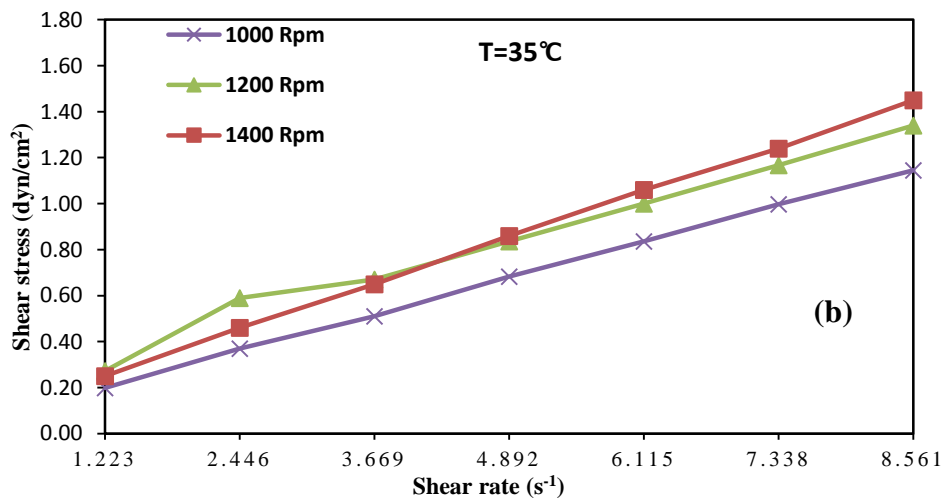
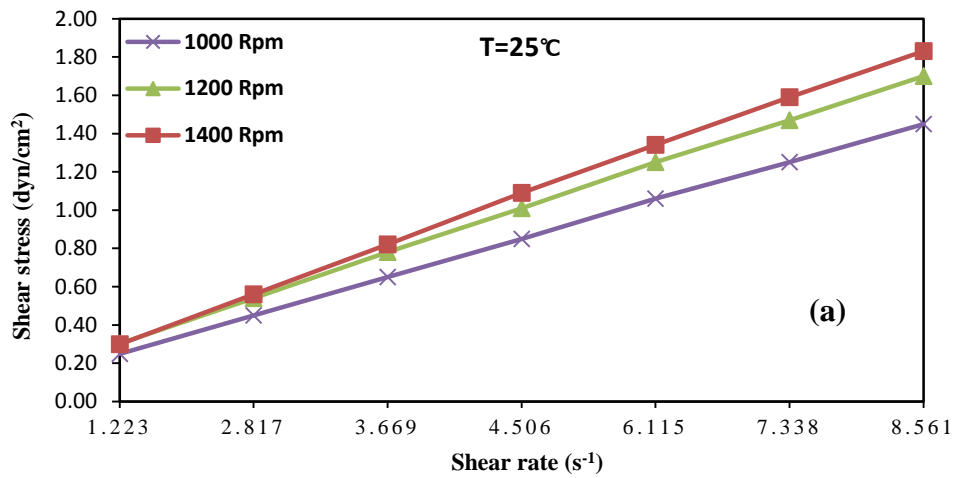


Figure 5-12 Relationship between viscosity and shear rate obtained in light crude oil samples



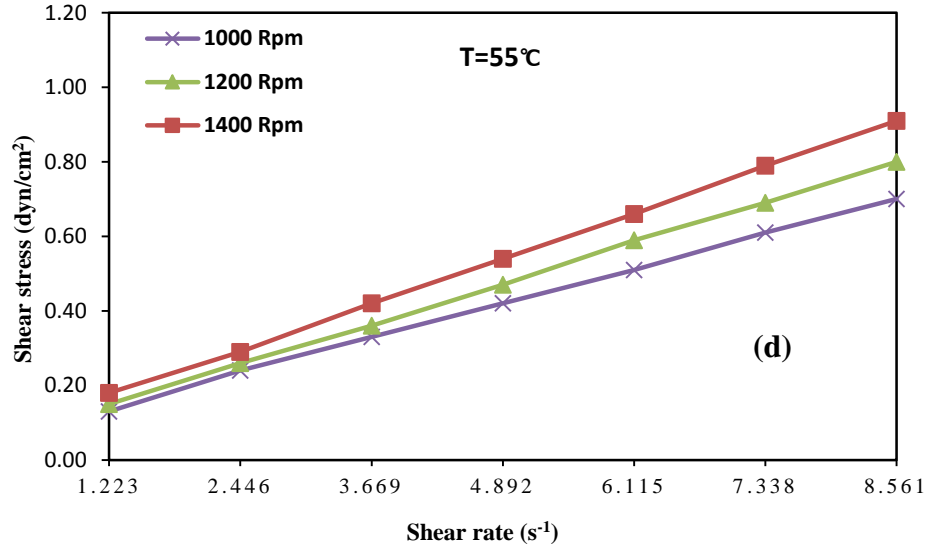


Figure 5-13 Rheograms of water-in-crude oil emulsions at different temperatures and mixing speeds

As observed in Figure 5.14, viscosity of the crude oil emulsions increase with mixing speed and decreased with increasing temperature. It may be noted however, that the viscosity for 1200 and 1400 rpm emulsions are similar at 25 and 35 °C, but at 45 and 55 °C the viscosity of 1200 rpm become closer to 1000 rpm. This behavior may be due to complexity of crude oil composition and resulting thermal impact on rheology. For all sets, It is observed that above shear rate of 3.7 (s⁻¹), there is essentially no effect of shear rate on the measured viscosity of crude oil at different temperatures.

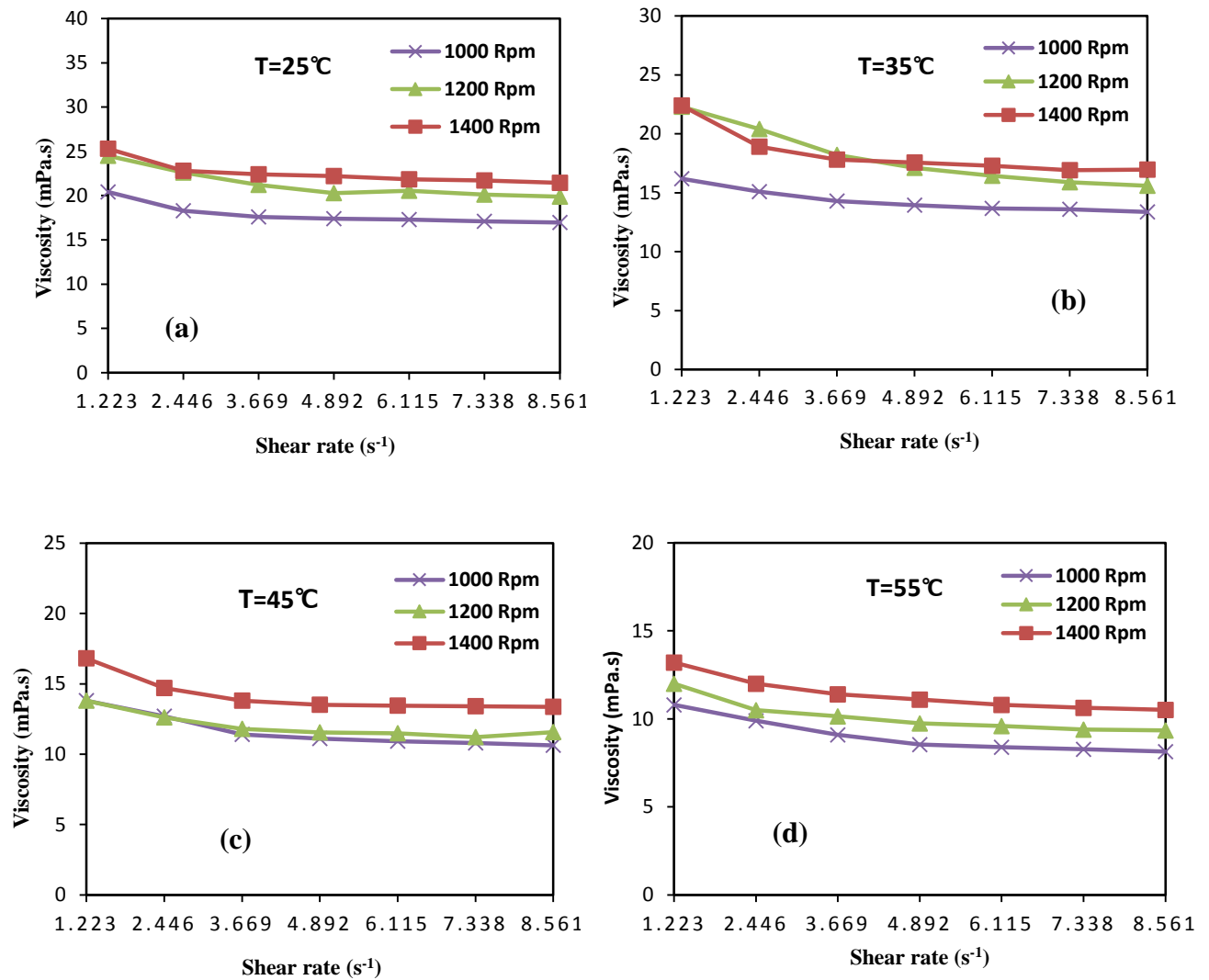


Figure 5-14 Relationship between viscosity and shear rate for light crude oil emulsions

Droplet size distribution in crude oil emulsions was measured to determine influence of changes in mixing speed (Figures 5.15 to 5.17). At higher rpms of 1200 and 1400, the droplet size distribution curve are within a narrow band and it becomes wider as the stirring speed declines to 1000 rpm.

The average droplet size decreased from 30 to 20 micron with increase in rpm from 1000 to 1400 as emulsion viscosity increases (Figure 5.17). These droplet sizes are much smaller compared to those obtained in mineral oil emulsions at similar rpm. This again points to the important effects of crude oil composition on emulsion rheology.

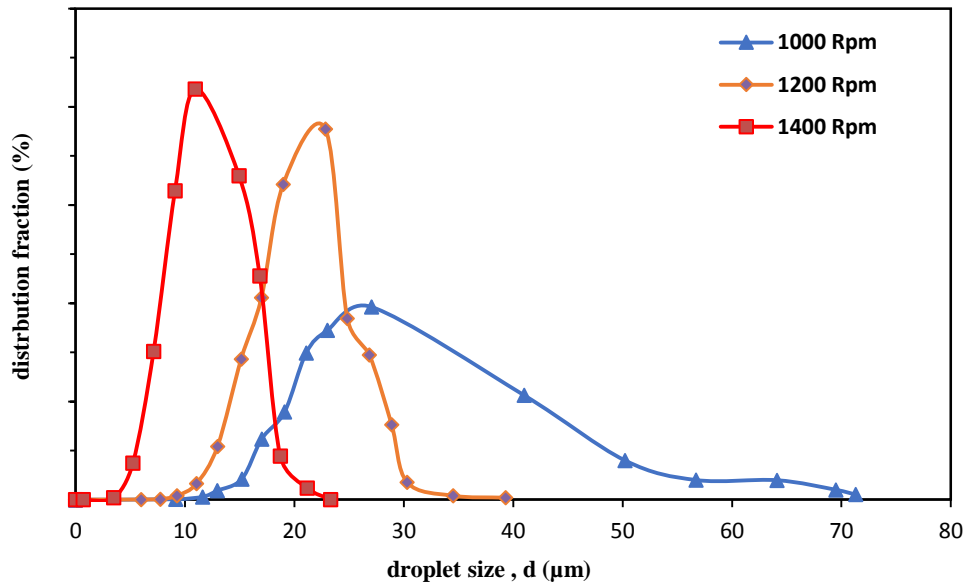


Figure 5-15 Droplet size distribution in water-in-crude oil emulsions prepared at different mixing speeds (20 wt% water in crude oil).

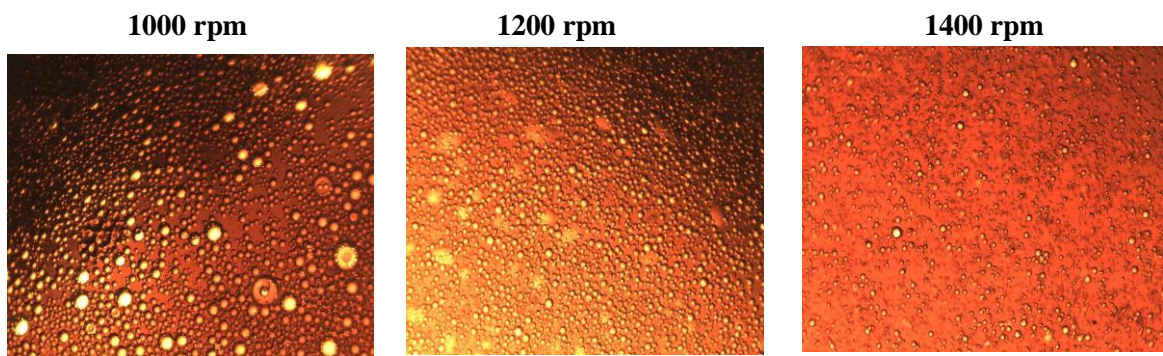


Figure 5-16 Images of crude oil emulsion samples prepared at different mixing speeds (20 wt% water in crude oil)

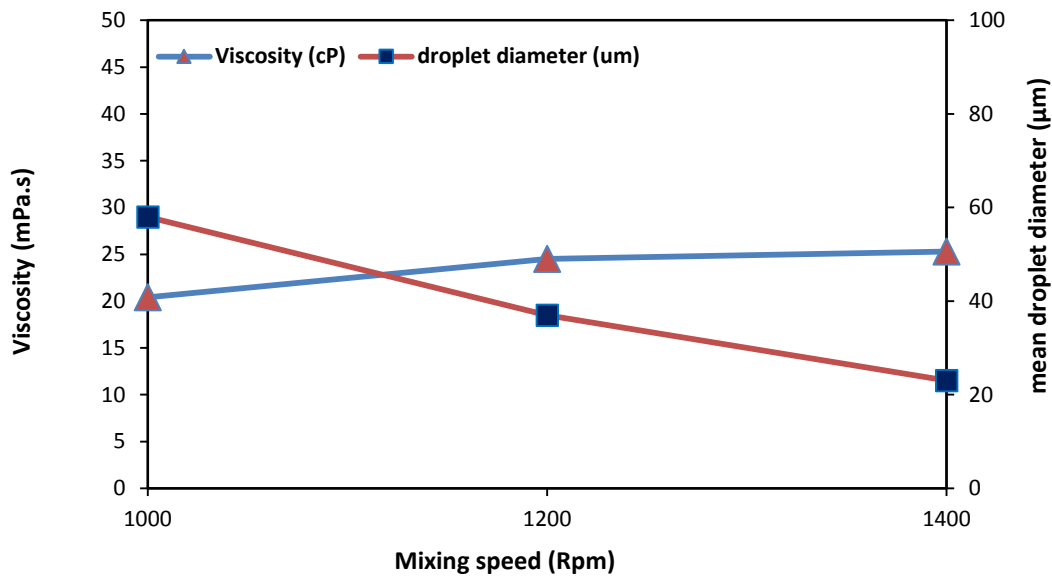
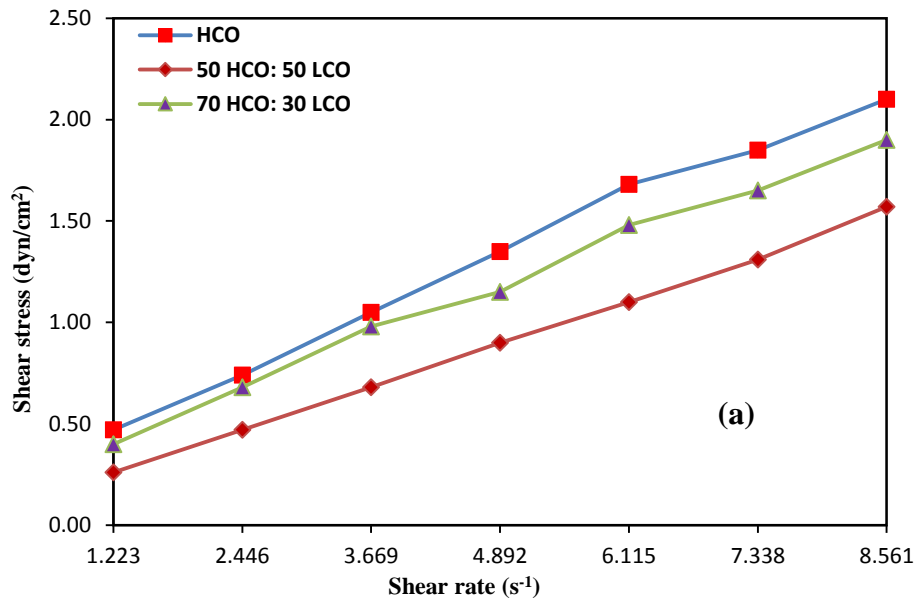


Figure 5-17 Effects of droplet size (mixing speed) on light crude oil emulsion viscosity

5.4.1 Emulsions of light and heavy crude oil mixtures

The rheology of heavy crude oil (HCO) and its mixtures with light crude oil (LCO) and their emulsions were also investigated over a temperature range of 25°C to 65°C. As can be seen in **Figure (5-18a)**, the heavy crude oil develops higher shear stress for a given shear rate compared to its mixtures with lighter crude which show decreasing tendency with increase in light crude fraction in the mixture. The decrease in shear rate recorded with temperature (in Figure 15.18b) relates to drop in viscosity with temperature. It is observed that there is tendency for a slower drop with temperature with increasing fraction of heavy oil. Similar behavior was observed with emulsions HCO and its mixtures with LCO

prepared at rpm of 1200 (**Figure 15.19a**). The effect of temperature is summarized in Figure 15.19b for these emulsions. It can be seen that shear stress decreased with increase of temperature and at 35 °C, there is a sharp change of slope with higher fractions of HCO in the mixture. This behaviour could be a result of high molecular weight compounds such as resins and asphaltenes in the heavy oil. The observed effect of temperature and shear stress are comparable to those reported in literature studies (Abid et al., 2014; Hasan et al., 2010).



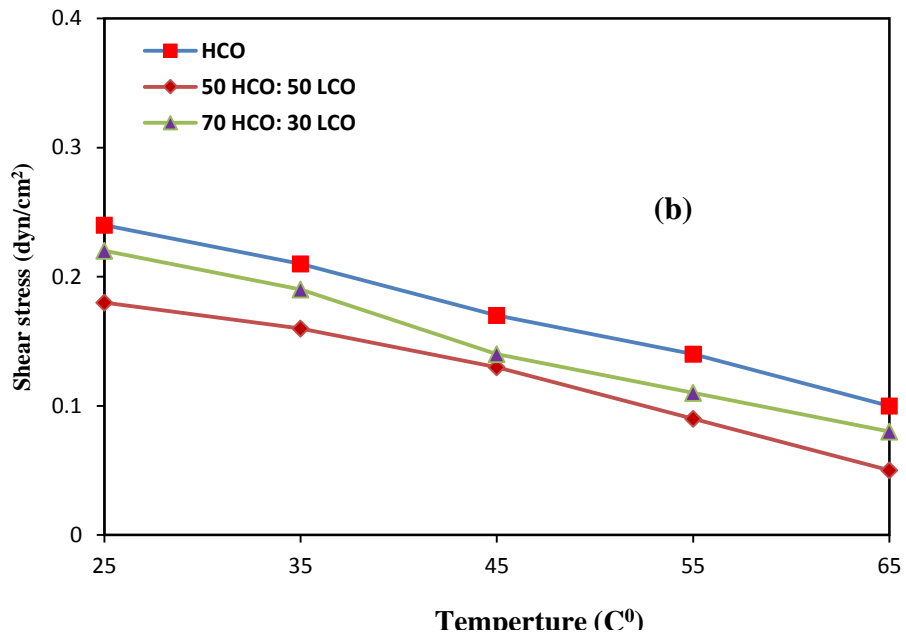
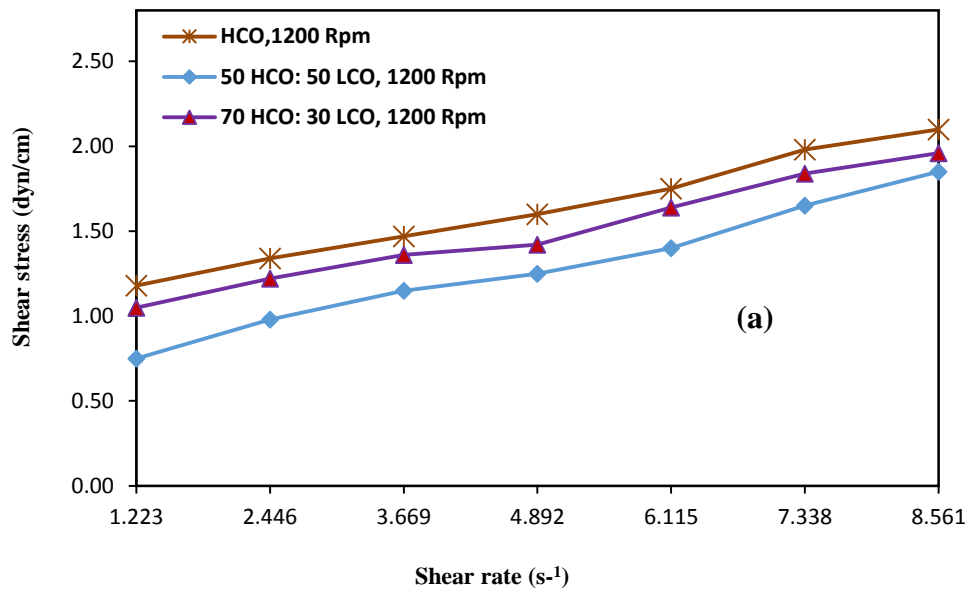


Figure 5-18 Rheogram of crude oil mixtures at different temperatures and shear rates.



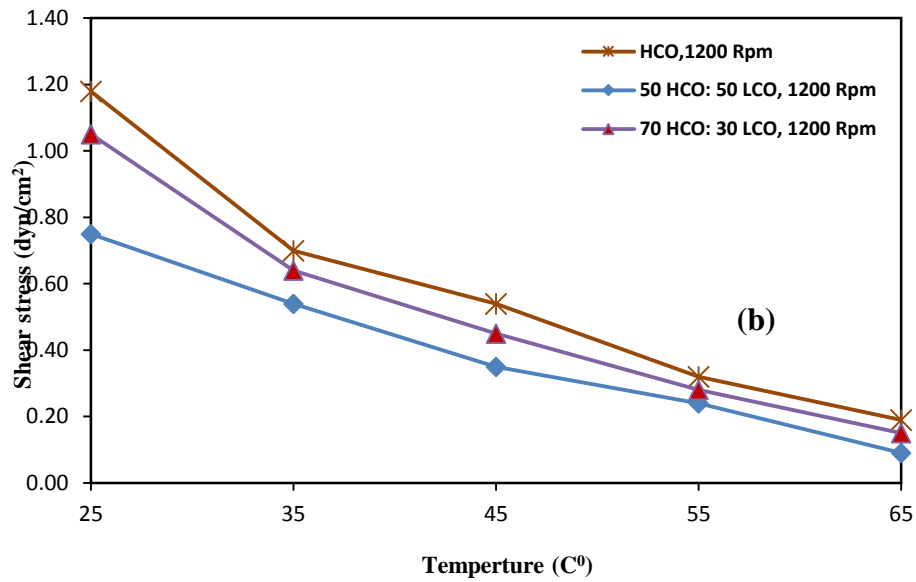


Figure 5-19 Rheograms of water-in-heavy crude oil mixtures emulsions

The droplet size distributions obtained in emulsions of heavy crude oil are shown in **Figure 5.20** for mixing speeds of 1200 and 1400 and the corresponding images are presented in **Figure 5.21**. The droplet size becomes smaller and the distribution narrower and there is a significant concentration of smaller droplets in the dispersions.

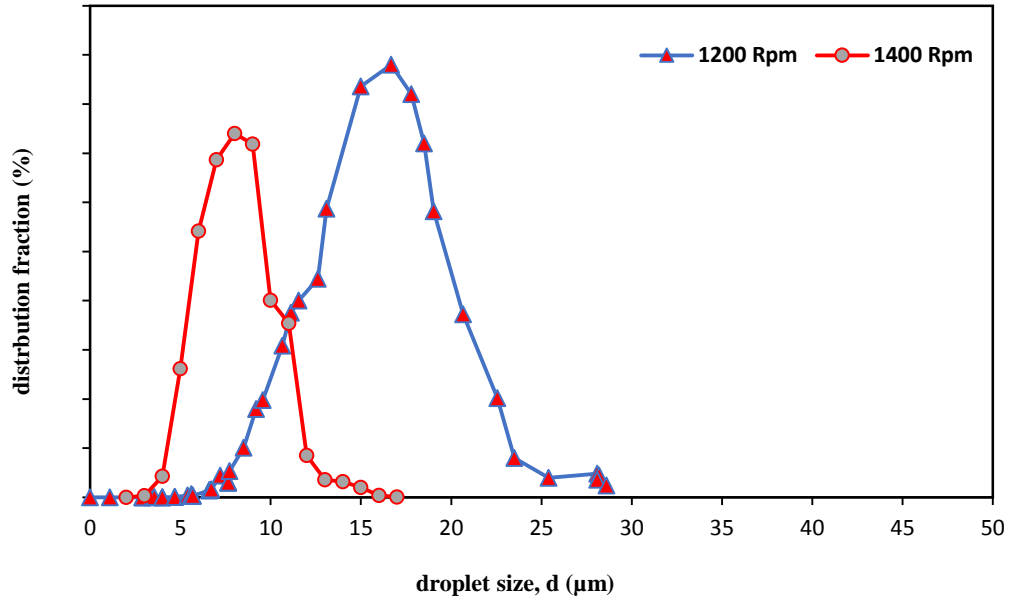


Figure 5-20 Droplet size distribution in water-in- heavy crude oil emulsions prepared at different mixing speeds (20 wt% water in crude oil).

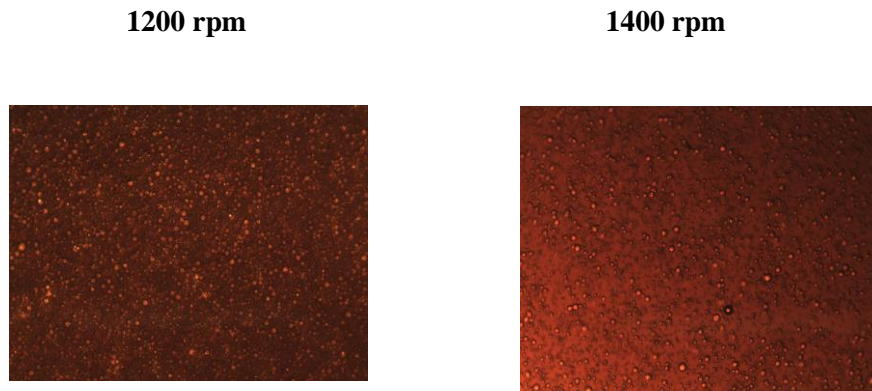


Figure 5-21 Images of heavy crude oil emulsion samples at different mixing speed

The mean droplet size in the emulsions of heavy crude oil are lower compared to light crude oil emulsions for the same mixing speed. The droplet size is about 20 μm at 1200 rpm and decreases to about 10 μm at 1400 rpm (**Figure 5.22**). The corresponding values in light crude oil emulsions were 35 and 20 μm respectively. The decrease in droplet size distribution of heavy crude emulsions can be attributed to high asphaltene content since these large molecules tend to stabilize the droplets and prevent their coalescence.

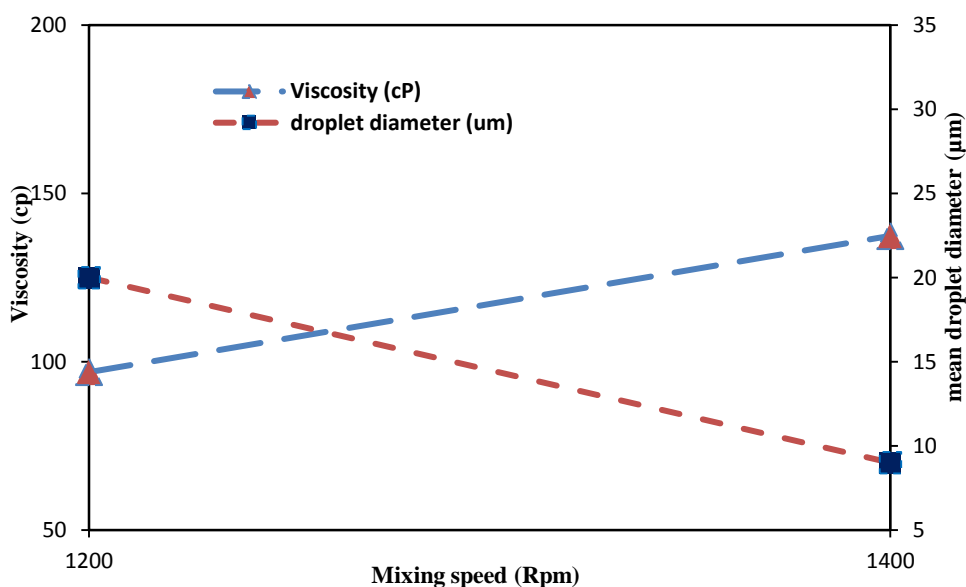


Figure 5-22 Effects of droplet size (mixing speed) on heavy crude oil emulsion

5.4.2 Effect of dispersed phase volume fraction

The influence of dispersed phase volume fraction on the rheological properties of light crude oil emulsions was studied by varying the water fraction from 0.1 to 1. Emulsions were prepared at mixing speed of 1200 Rpm, and surfactant concentration of 0.2 wt%. It can be seen in **Figure 5-23** that an increase in water content increased the viscosity and shear stress of emulsions up to 40% water followed by a decline at higher water content. It may be noted that at water content higher than 40 vol%, the emulsion is converted to oil-in-water. where

the emulsion viscosity and shear stress significantly decreased due to the phase inversion point.

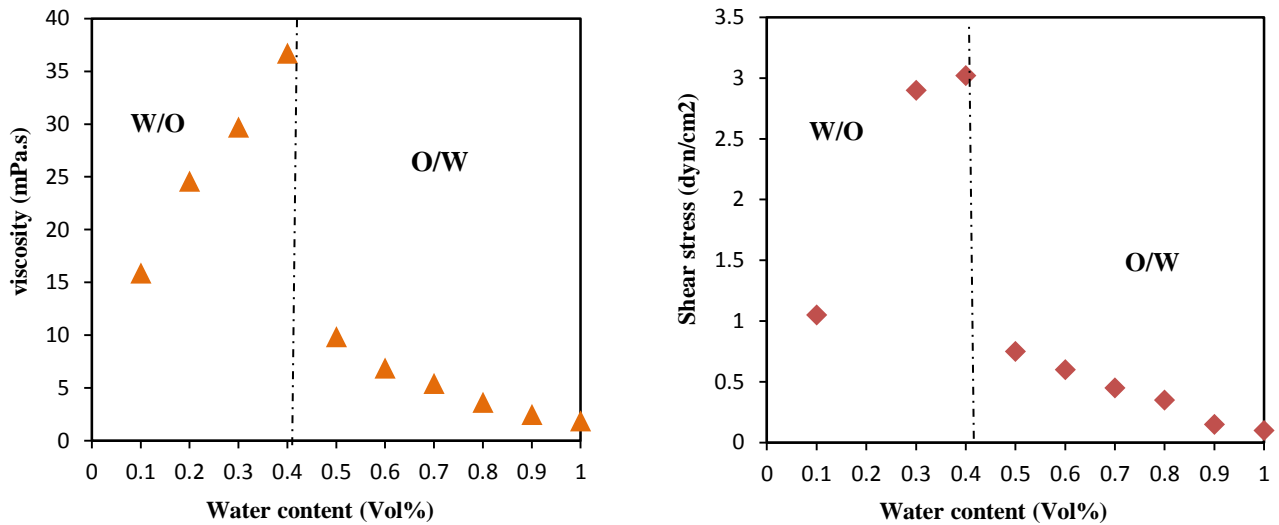


Figure 5-23 Effect of water volume fraction on emulsion viscosity and shear stress @ 1.223 s⁻¹

5.4.3 Effect of fine solid particles

The effect of the presence of fine solids particles on rheology of light crude oil and its emulsions was investigated with kaolinite clay and iron particles of 10 micron. The w/o emulsions were prepared using of 80 vol% of light crude oil and solid particles concentration (clay/iron) of 1 wt%. Mixing speed and duration were 1200 rpm and 30 min respectively and the pH of the dispersed phase was adjusted 7. The results of the measurements are presented in **Figure 5-24 (a to d)**. It can be seen from Figures 5.24a and b that the presence of the particles in light crude oil led to increase in shear stress and viscosity in crude oil/particles suspension at different shear rate. However, presence of the fine particles has opposite effect in its emulsions where the viscosity and shear stress decreased due to

particles addition. The effect is larger with clay particles compared to iron particles. The effectiveness of solids in stabilizing emulsions depends on several factors, including their concentration, density, size distribution, and surface properties. This type of adsorption leads to a stabilized water droplet only if the adsorbed particle is small relative to the water droplet. Hence, the solids that potentially lead to stable films are in the 100 nm to 1 μ m size range (Yan *et al.*, 1999). In fact, to be effective emulsion stabilizers, solid particles must be at least ten times smaller than the droplet (Aveyard *et al.*, 2002; Binks and Kirkland, 2002). The particles used here were not that much larger than the water droplets, These larger particles could not stabilize the smaller droplets which contribute to higher viscosity of emulsion phase. This may explain the lowering of emulsion viscosity observed here. The particle density and shape can also be important in emulsion stability. Emulsions created with denser particles are expected to be less stable than those created with less dense particles (Schulman and Leja, 1954; Gelot *et al.*, 1984). There is a need for a more systematic study to determine the particles-droplet interactions in emulsions specially in presence of surface active compounds/impurities in the oil phase.

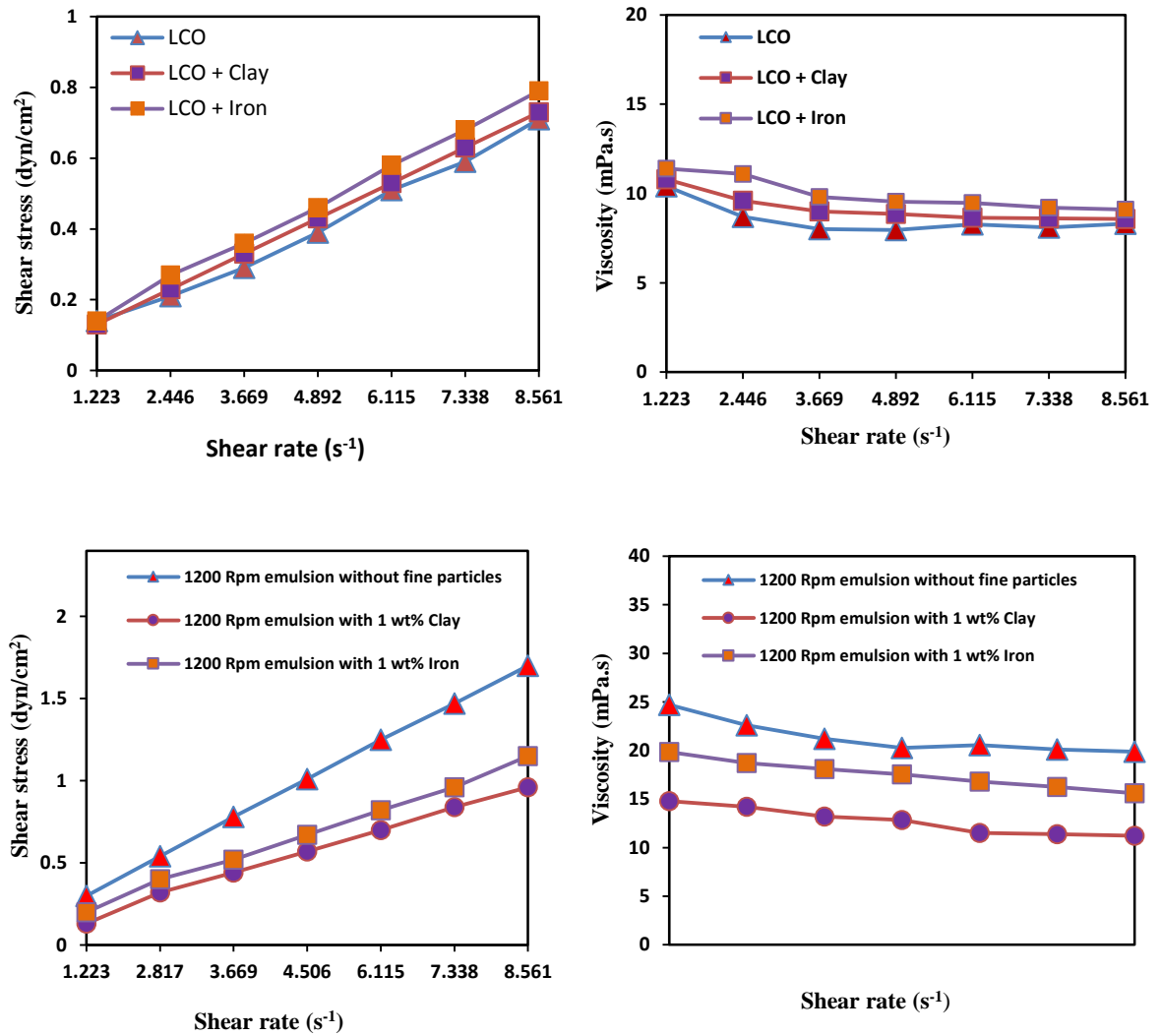


Figure 5-25 Effect of fine solid particles on LCO emulsions rheology

5.4.4 Effect of Surfactant concentration

Surfactants are largely used to reduce the interfacial tension between oil and water, which could form a stable film of emulsion between these two immiscible fluids. The effect of Triton X-100 emulsifier concentration on the viscosity and emulsion stability was investigated at constant shear rate of 3.669 (s⁻¹). **Figure 5-25** demonstrates the influence of emulsifier concentration on the emulsion viscosity. The emulsions were prepared with 20

wt% water in oil and mixing speed was varied from 600 rpm to 1200 rpm for 30 min, respectively. The surfactant concentration calculated based on oil amount was varied from 0 - 0.5 wt%. It is noticed that increase in emulsifier concentration causes increase in the emulsion's viscosity. This can be attributed to combined effects of decrease in droplet size and higher viscosity of the surfactant. The surfactant used (Triton X-100) is viscous liquid and its increasing concentration in the oil phase would enhance viscosity. Moreover, increasing of surfactant concentration would result in smaller droplets due to lower interfacial tension. Thus an optimum concentration of emulsifier need to be determined for a given application. In this study emulsifier concentration was maintained at 0.2 wt% based on the tests.

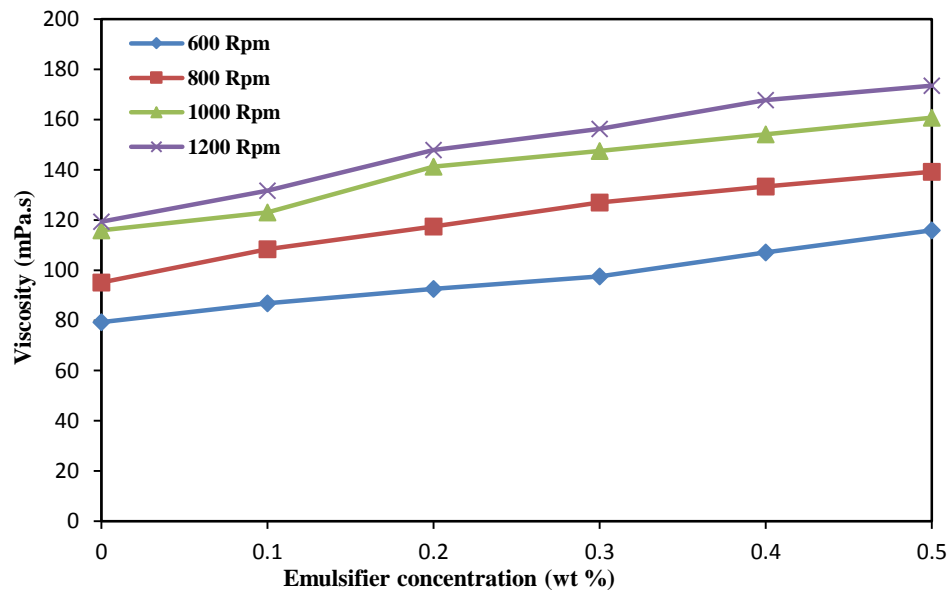


Figure 5-25 Effect of Triton X-100 concentration on emulsions viscosity of 600-1200 Rpm @3.669 s⁻¹

5.5 Modelling of emulsion flow behavior

5.5.1 Estimation of non-Newtonian models parameters

In order to find the appropriate model for the experimental data, the modelling investigation was conducted using three models suggested by Ostwald de Waele, Herschel-Bulkley, and Casson to designate the emulsion with different water fraction. These models were discussed in detail in the literature review section (Chapter # 2) and the Table 2.2 summarizing the model equation is reproduced below.

Table 5-2 Some flow models for describing shear stress (τ) versus shear rate ($\dot{\gamma}$).

$\tau = \eta \dot{\gamma}$	Newtonian model
$\tau = [\eta_{\infty} \dot{\gamma} + K_s \dot{\gamma}^{n_s}]$	Sisko model for high shear rate with respect to η_{∞} .
$\tau = k \dot{\gamma}^n$	Power model used for Non-Newtonian
$\tau - \tau_0 = \eta \dot{\gamma}$	Bingham model
$\tau - \tau_0 = k \dot{\gamma}^n$	Herschel- Bulkley model
$\tau^{0.5} = k_{0c} + k_c (\dot{\gamma})^{0.5}$	Casson model
$\tau^{0.5} - \tau_{0m} = k_M \dot{\gamma}^n$	Mizrahi and Berk (1972) model is a modification of the Casson model

Majdidet.al stated that by using these models, emulsion with different water fractions could be characterized through model parameters such as (behavior index, n and consistency factor, k). The flow consistency index (k) and the flow behavior index (n) were determined for both models with different shear rates ranging of $1.223 - 8.561 \text{ s}^{-1}$.

Table 5-3 Different types of water –in- oil emulsions used in this study

Emulsion Set	Water – oil volume ratio	Type of Emulsion
Set#1^a	20:80	600 Rpm
Set#2^a	20:80	800 Rpm
Set#3^a	20:80	1000 Rpm
Set#4^a	20:80	1200 Rpm
Set#5^b	20:80	1000 Rpm
Set#6^b	20:80	1200 Rpm
Set#7^b	20:80	1400 Rpm

Note, (a) for mineral oil emulsions, where (b) represents crude oil emulsions.

The suggested models parameters were determined using the equations mentioned in art-review. The plot of log shear rate versus log of shear stress gives a straight line with a slope of n and intercept of k. As it can be seen in **Table 5-3**, that all sets of water-in-oil emulsions were exhibit non-Newtonian flow behavior (shear thinning) in the shear rate ranging of $1.223 - 8.561 \text{ s}^{-1}$. The flow behavior index (n) were variation from 0.8331 to 0.920. The pseudo-plastic (shear thinning) phenomena is due to the emulsion droplet aggregation and structural of breakdown during shearing. Furthermore, the emulsion pseudoplasticity is influenced by mixing speed, the flow behavior index (n) for set 1,2and 3 increases with

increasing of mixing speed. While the flow consistency index (k) of all sets decreases with an increasing of mixing speed.

For crude oil emulsions, a straight-line result of plotting the square root of shear rate ($\dot{\gamma}$)^{0.5} against the square root of shear stress (τ)^{0.5}, with slope K_c and intercept K_{0c} . Remarkably, most sets of water-in-crude oil emulsions were exhibit non-Newtonian flow behavior (shear thickening) in the shear rate ranging of 1.223 – 8.561 s⁻¹. The Casson yield stress (K_{0c}) was variation from 0.0175 to 0.0207. Notably, both parameters of Casson behaviour were affected by agitation speed.

Table 5-4 Determination of n and k values for both model.

Emulsion set	Shear rate s⁻¹	Ostwald de Waele		Herschel-Bulkley		Casson model	
		n	k (Pa.sⁿ)	n	k (Pa.sⁿ)	K_C	K_{0C}
Set#1	1.223 - 8.561	0.8331	0.0788	0.8552	0.0551	—	—
Set#2	1.223 - 8.561	0.9200	0.0427	0.9447	0.0175	—	—
Set#3	1.223 - 8.561	0.9113	0.0657	0.9351	0.0415	—	—
Set#4	1.223 - 8.561	0.8841	0.0853	0.9067	0.062	—	—
Set#5	1.223 - 8.561	—	—	—	—	0.1229	0.0207
Set#6	1.223 - 8.561	—	—	—	—	0.1314	0.0278
Set#7	1.223 - 8.561	—	—	—	—	0.1406	0.0175

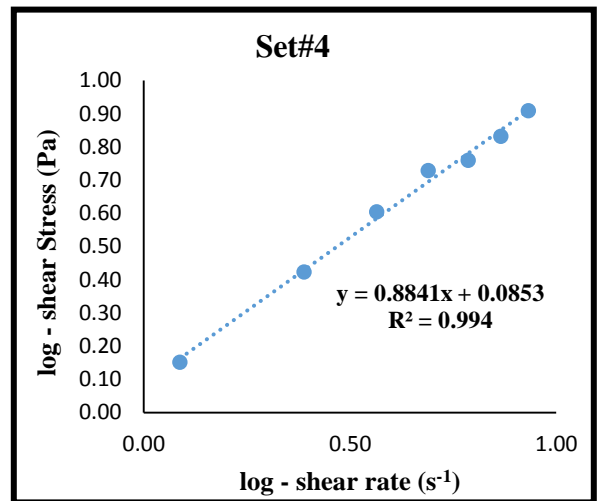
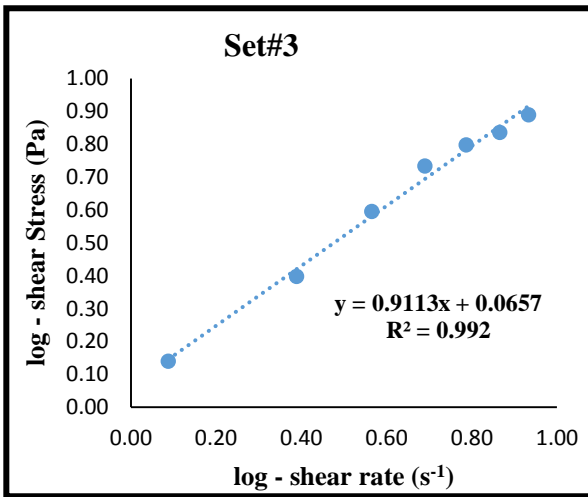
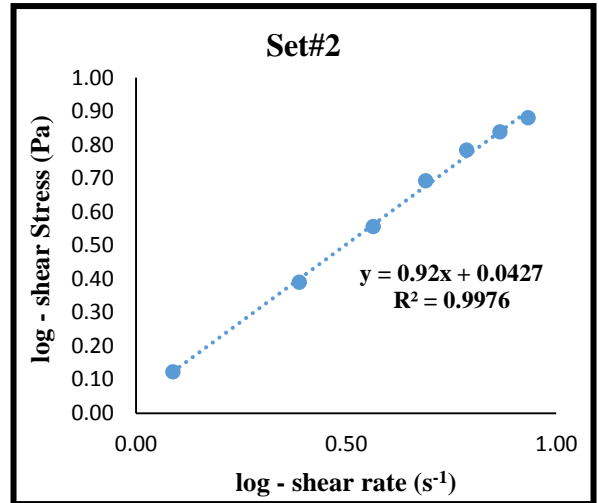
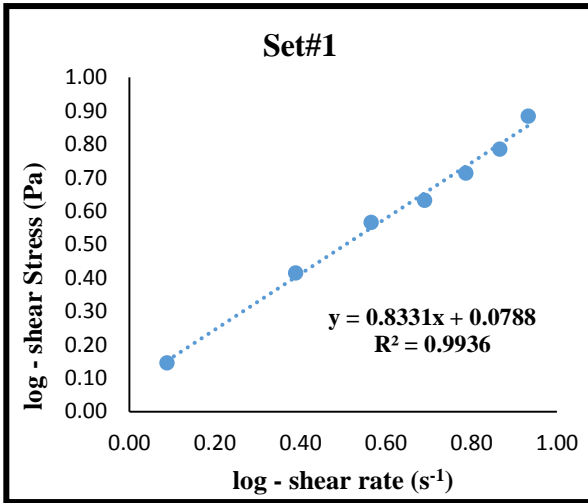


Figure 5-26 Estimation of non-Newtonian parameters for power law model

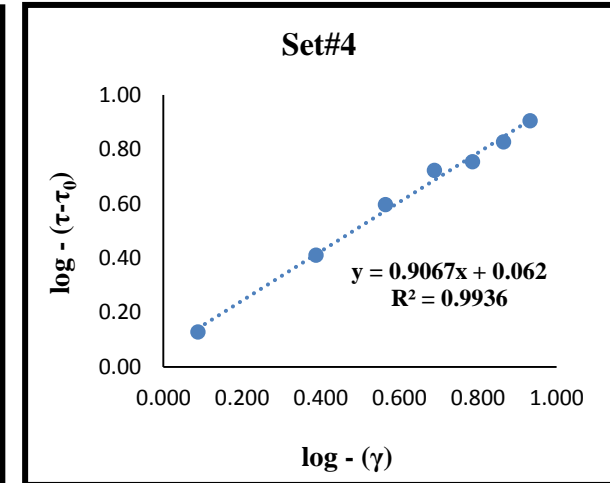
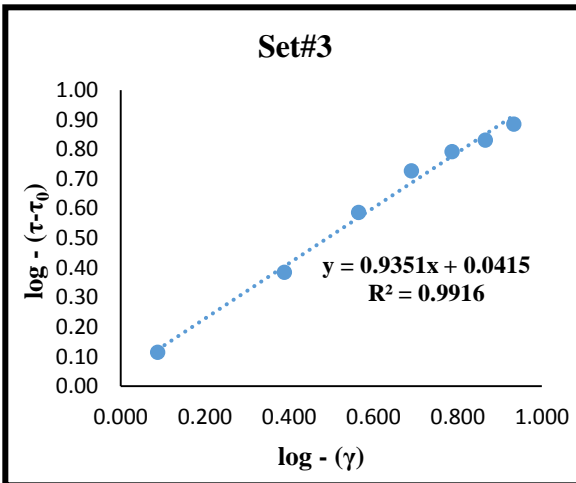
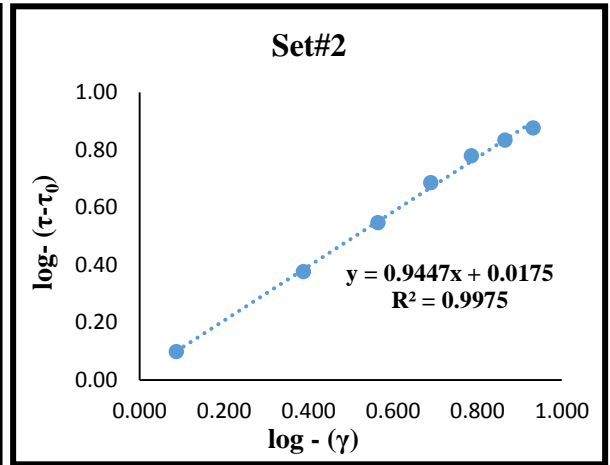
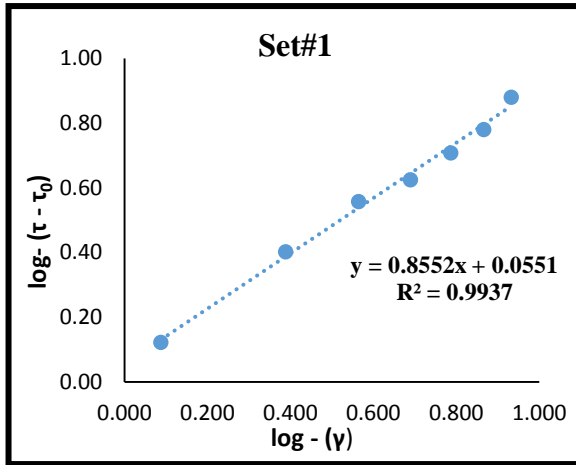


Figure 5-27 Estimation of non-Newtonian parameters for Herschel-Bulkley model.

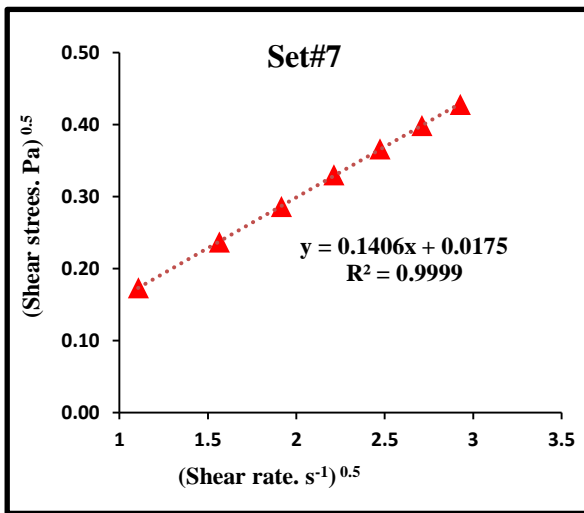
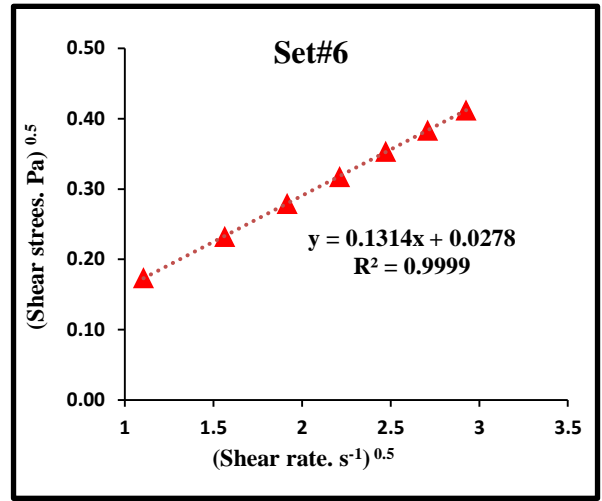
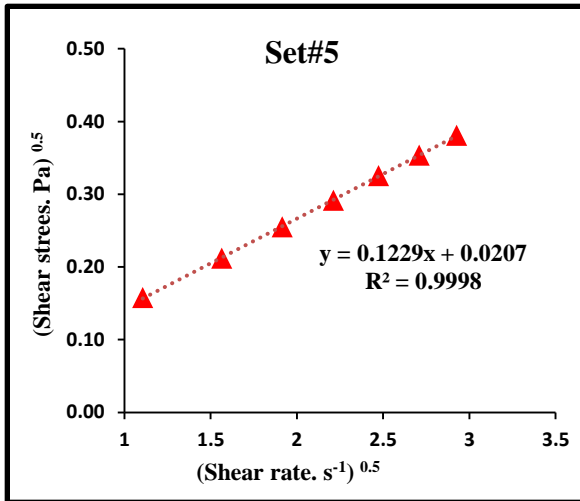


Figure 5-28 Estimation of non-Newtonian flow behavior parameters for Casson model

5.5.2 Comparison of predicted and experimental data

The goodness of proposed models (power law and Herschel-Bulkley) were performed by comparing the experimental values with the ones predicted by models.

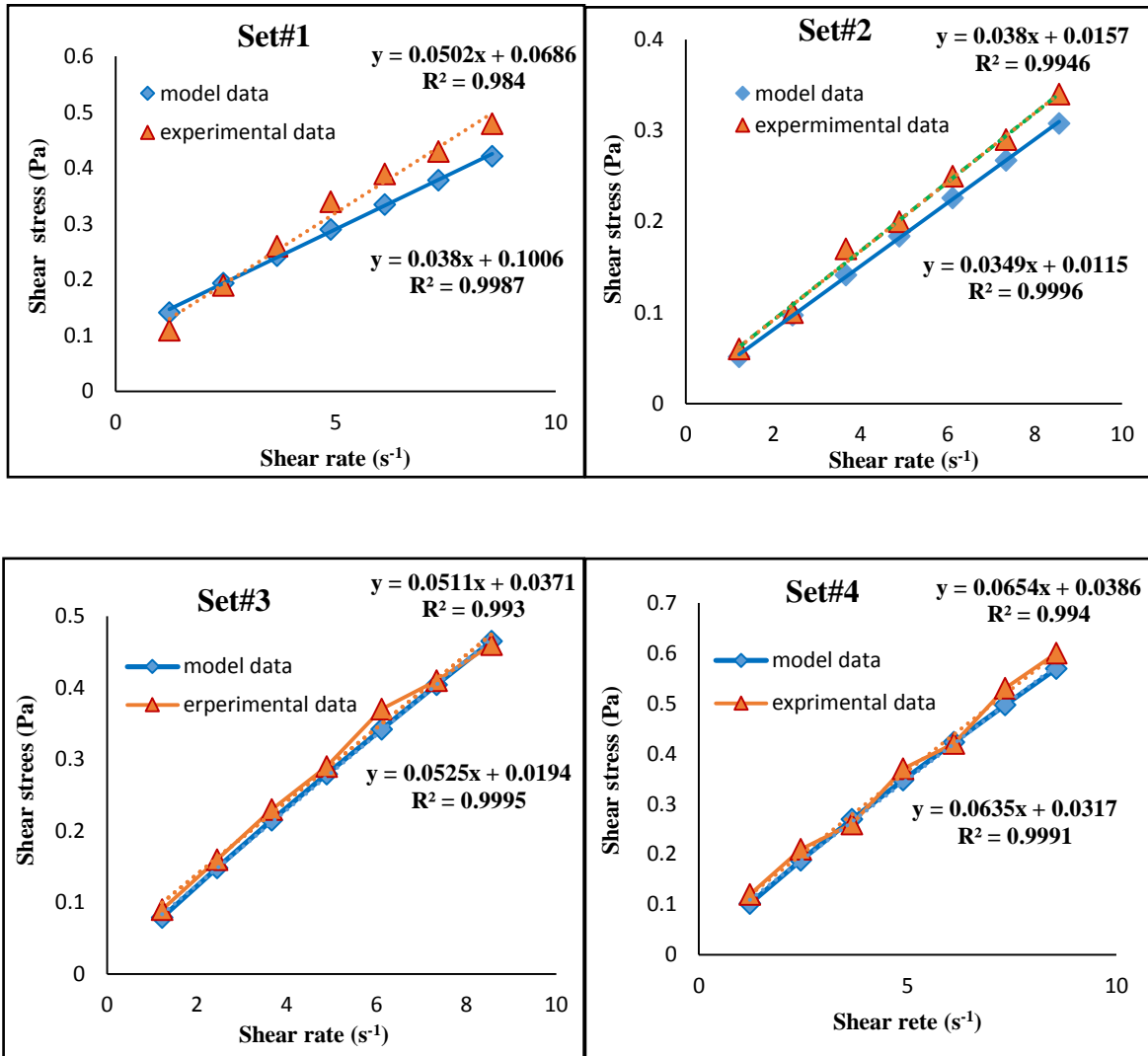


Figure 5-29 Comparison of predicted and experimental data of power law model.

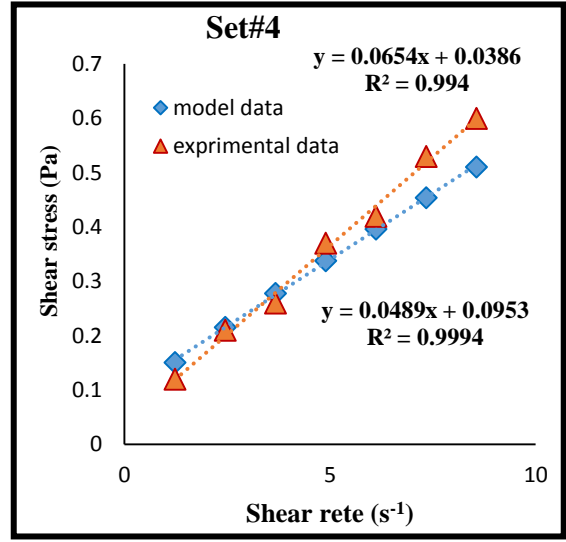
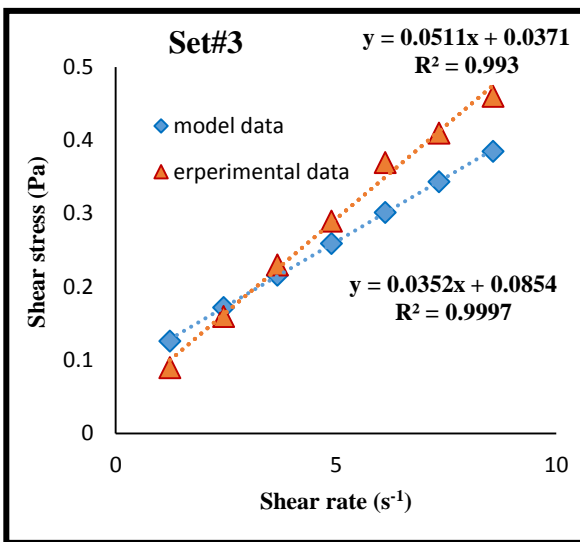
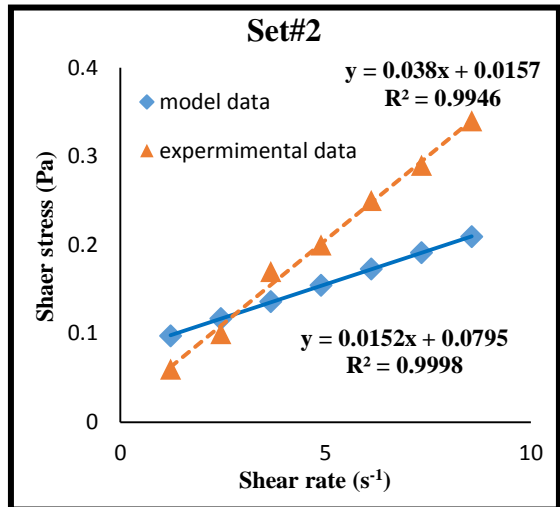
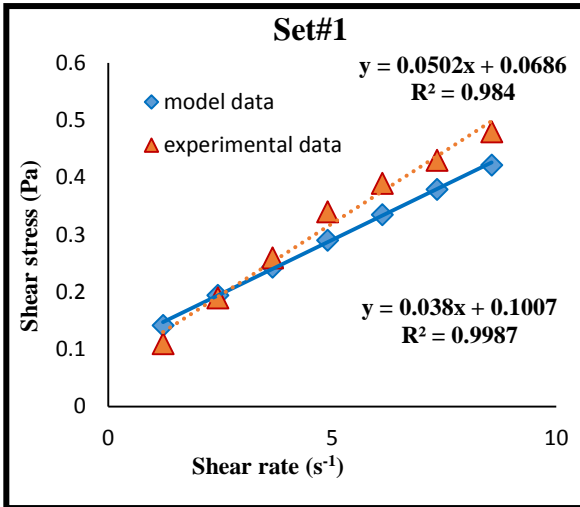


Figure 5-30 Comparison of predicted and experimental data of HB model.

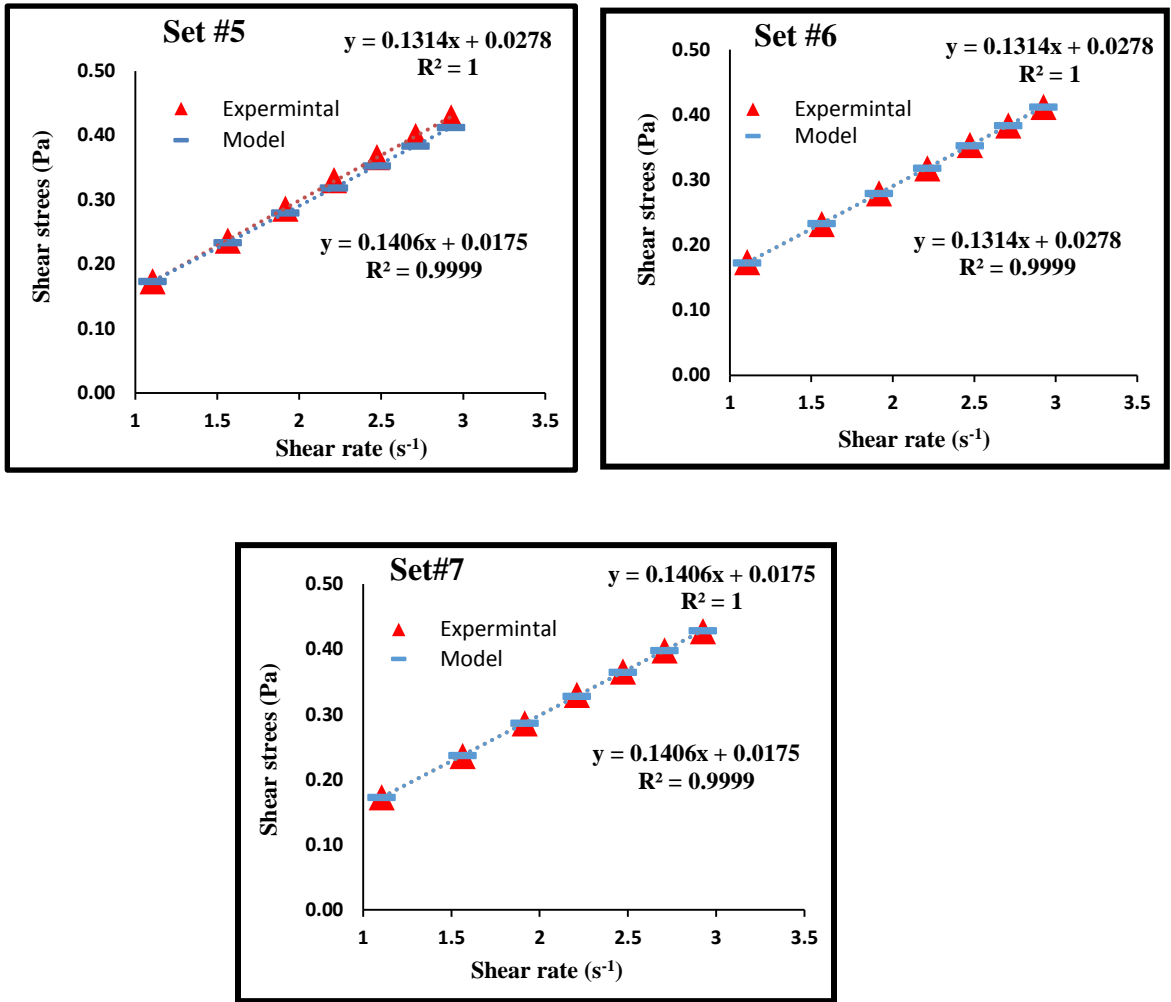


Figure 5-31 Comparison of predicted and experimental data of Casson model

5.5.3 Validation of the Results

Analyzing the model coefficients and matching them with experimental data is the common technique to determine the validity of regression model. (Montgomery *et al*, 1982), concluded that the coefficient with unexpected values are often referred to models which either unstable or poor in estimation of the impact of variables that have been carried out. The best-fit model was selected based on the regression coefficient (R^2), standard error of estimate (SEE), and the sum of square errors (SSE) between experimental and calculated data (Allen, 1974; Ronningsen, 1995; Tarpey, 2000).

The regression co-efficient (R^2) defined by:

$$R^2 = 1 - \frac{\sum_{i=1}^{i=n} (y_i - \hat{y}_i)^2}{\sum_{i=1}^{i=n} (y_i - \bar{y}_i)^2} \quad (5.2)$$

Standard error of estimate (SEE) as the following equation:

$$SEE = \sqrt{\frac{\sum (y_i - \hat{y}_i)^2}{p}} \quad (5.3)$$

The sum of square errors (SSE) were determined as below:

$$SSE = \sum_{i=1}^{i=n} (y_i - \hat{y}_i)^2 \quad (5.4)$$

Where y_i , \hat{y}_i and \bar{y}_i are the experimental and predicted results by the regression model and the average of the experimental results, respectively. Where P is the number of fitted data. As it can be seen in **Table 5.4**, that the highest values of regression correlation coefficient, R^2 were varied from 0.9452 to 0.9861 for the power law model comparing with R^2 values of Herschel-Bulkley, which were ranging of 0.3783 – 0.9075. However, the power law

model was the effective model to describe the experimental data of mineral oil emulsions over different shear rates. On the other hand, the Casson model was effective to describe crude oil emulsions behaviors.

Table 5-5 Validation of the results of power law, HB, and Casson models.

Emulsion Set	Ostwald de Waele			Herschel-Bulkley			Casson model		
	R ²	SSE	SEE	R ²	SSE	SEE	R ²	SSE	SEE
Set#1	0.9534	0.0007	0.01	0.8815	0.0018	0.01611	—	—	—
Set#2	0.9452	0.0005	0.008	0.3783	0.0054	0.02774	—	—	—
Set#3	0.9861	0.0002	0.005	0.8435	0.0025	0.01875	—	—	—
Set#4	0.9856	0.0003	0.007	0.9075	0.0024	0.01844	—	—	—
Set#5	—	—	—	—	—	—	0.9998	0.8e-6	0.00034
Set#6	—	—	—	—	—	—	0.9999	0.36e-6	0.00022
Set#7	—	—	—	—	—	—	0.9991	0.59e-6	0.00092

5.6 Conclusions

- The viscosity of emulsion phase increased with the mixing speed used to prepare the emulsions. This is attributed to decrease in droplet size with increasing mixing intensity.
- Higher asphaltene content in the heavier crude oil samples led to lower droplet size in the emulsion phase attributed to stabilizing effects of large asphaltene molecules on the dispersed droplets.
- The water-in-oil emulsions exhibited non-Newtonian flow (shear thinning) behavior. The behavior is close to Herschel-Bulkley model. Shear stress increased with shear rate while the emulsion viscosity gradually decreased with increasing of shear rate.
- When the water content is varied, the viscosity of emulsion increased up to 40% water and decreased thereafter as the inversion from water-in-oil to oil-in-water occurs.

References

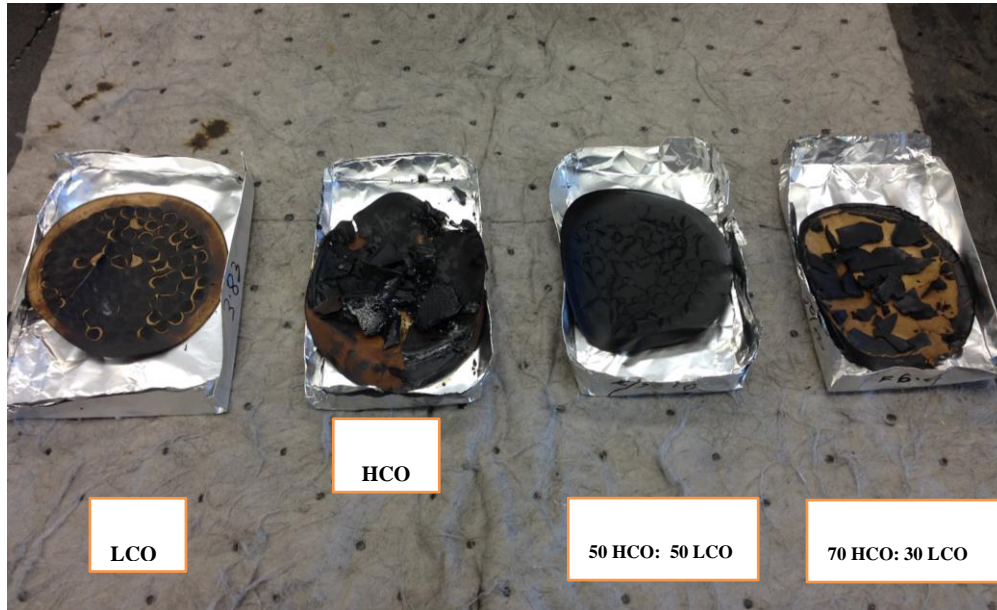
- Abd, R.M., Nour, A.H., Sulaiman, A.Z. 2014. Experimental Investigation on Dynamic Viscosity and Rheology of Water-Crude Oil Two Phases Flow Behavior at Different Water Volume Fractions. *American Journal of Engineering Research (AJER)*, 3 (3), 113-120.
- Abdolmaleki, K., Amin, M., Mohammadi, R. 2016. The Effect of pH and Salt on the Stability and Physicochemical Properties of Oil-in-Water Emulsions Prepared with Gum Tragacanth. *Carbohydrate Polymers*, 140 (2016), 342–348.
- AL HADABI, I., SASAKI, K., SUGAI, Y. 2016. Effects of Kaolinite Clay on Omani Heavy-Oil Rheology in Considering Enhanced Oil Recovery by Steam Injection. *International Journal of Earth Sciences and Engineering*, 9 (1), 22–24.
- Al-Wahaibi, T., Al-Wahaibi, Y., Al-Hashmi, A., *et al.* 2015. Experimental Investigation of the Effects of Various Parameters on Viscosity Reduction of Heavy Crude by Oil/water Emulsion. *Petroleum Science*, 12 (1), 170–176.
- Ashrafizadeh, S.N., Kamran, M. 2010. Emulsification of Heavy Crude Oil in Water for Pipeline Transportation. *Journal of Petroleum Science and Engineering*, 71 (3–4), 205–211.
- Azodi, M., Nazar, A. 2013. An Experimental Study on Factors Affecting the Heavy Crude Oil in Water Emulsions Viscosity. *Journal of Petroleum Science and Engineering*, 106 (11), 1-8.
- Daaou, M., Bendedouch, D. 2012. Water pH and Surfactant Addition Effects on the Stability of an Algerian Crude Oil Emulsion. *Journal of Saudi Chemical Society*, 16 (3), 333–337.
- Ekott, E.J., Akpabio, E.J. 2010. A Review of Water-in-Crude Oil Emulsion Stability, Destabilization and Interfacial Rheology. *Journal of Engineering and Applied Sciences*, 5 (6), 447–452.

- Hasan, S.W., Ghannam, M.T., Esmail, N. 2010. Heavy crude oil viscosity reduction and rheology for pipeline transportation. *Fuel*, 89 (5), 1095-1100.
- Jeon, T.Y., Hong, J.S. 2014. Stabilization of O/W Emulsion with Hydrophilic/hydrophobic Clay Particles. *Colloid and Polymer Science*, 292 (11), 2939–2947.
- Kundu, P., Kumar, V., Mishra, I.M. 2015. Modeling the Steady-Shear Rheological Behavior of Dilute to Highly Concentrated Oil-in-Water (O/w) Emulsions: Effect of Temperature, Oil Volume Fraction and Anionic Surfactant Concentration. *Journal of Petroleum Science and Engineering*, 129 (11), 189–204.
- Lim, J.S., Wong, S.F., Law, M.C., *et al.* 2015. A Review on the Effects of Emulsions on Flow Behaviours and Common Factors Affecting the Stability of Emulsions. *Journal of Applied Sciences*, 15 (2), 167–172.
- Liu, C., Li, M., Han, R., *et al.* 2016. Rheology of Water-in-Oil Emulsions with Different Drop Sizes. *Journal of Dispersion Science and Technology*, 37 (3), 333–344.
- Liyana, M.S., Nour, H.A., Rizauddin, D., *et al.* 2014. Stabilization and Characterization of Heavy Crude Oil-in-Water (O/W) Emulsions. *IJRET: International Journal of Research in Engineering and Technology*, 3 (2), 2319-1163.
- Nadirah, L., Nour, H.A., Rizauddin, D. 2014. Rheological Study of Petroleum Fluid and Oil-in-Water Emulsion. *Nadirah International Journal of Engineering Sciences & Research Technology*, 3 (1), 129-134.
- Pal, R. 1996. Effect of Droplet Size on the Rheology of Emulsions. *AIChE Journal*, 42 (11), 3181-3190
- Suriya, T., Ariffin, T., Yahya, E., Husin, H. 2016. The rheology of light crude oil and water-in-oil-emulsion, *Procedia Engineering*, 148 (2016)., 1149-1155.
- Vafajoo, L., Ganjian, K., Fattahi, M. 2012. Influence of Key Parameters on Crude Oil Desalting: An Experimental and Theoretical Study. *Journal of Petroleum Science and Engineering*, 12 (90-91), 107–111.

Wang, X., Vladimir, A. 2011. Kaolinite and Silica Dispersions in Low-Salinity Environments: Impact on a Water-in-Crude Oil Emulsion Stability. *Energies*, 4 (12), 1763–1778.

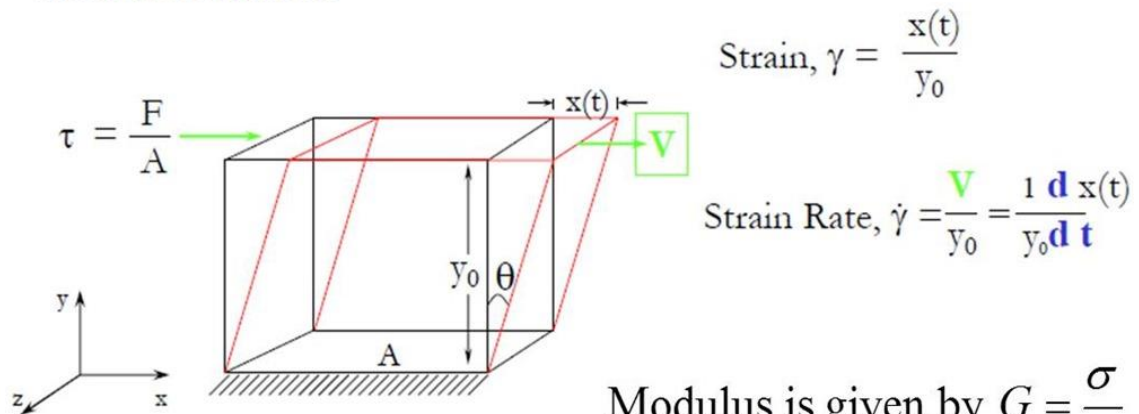
Yan, N., Gray, M., Masliyah, J. 2001. On Water-in-Oil Emulsions Stabilized by Fine Solids. *Colloids and Surfaces A: Physicochemical and Engineering Aspects*, 193 (1–3), 97–107.

Appendix C



Appendix C 1 Asphaltene contents for different crude oil samples

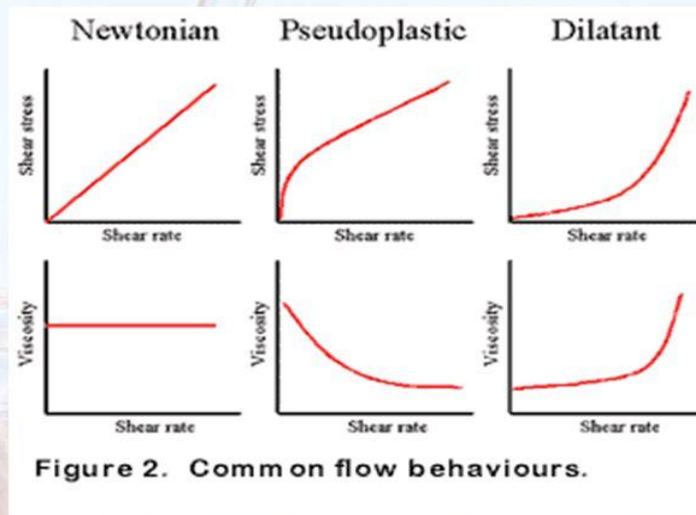
Shear Deformation



$$\dot{\gamma} = \frac{\Delta\gamma}{\Delta t}$$

Viscosity is given by $\eta = \frac{\sigma}{\dot{\gamma}}$

Emulsion rheology



Appendix C 2 Brookfield digital Rheometer calibration with fresh water @ room Temp

Rheocalc T 1.2.19

Data Report

Brookfield Engineering Labs Inc.

Sample Information:		Sample Name: water Ref_11	
Tester Name:	TK: 0.09375	Sample Notes: The calibration was done by fresh water at 25C.	
Run Time: 30/06/2016 1:04:00 PM	SMC: 0.64	Water Viscosity: 0.98 cp	
Serial Number: 8691741	SRC: 1.22		
Torque Range: LV	YMC: 0		

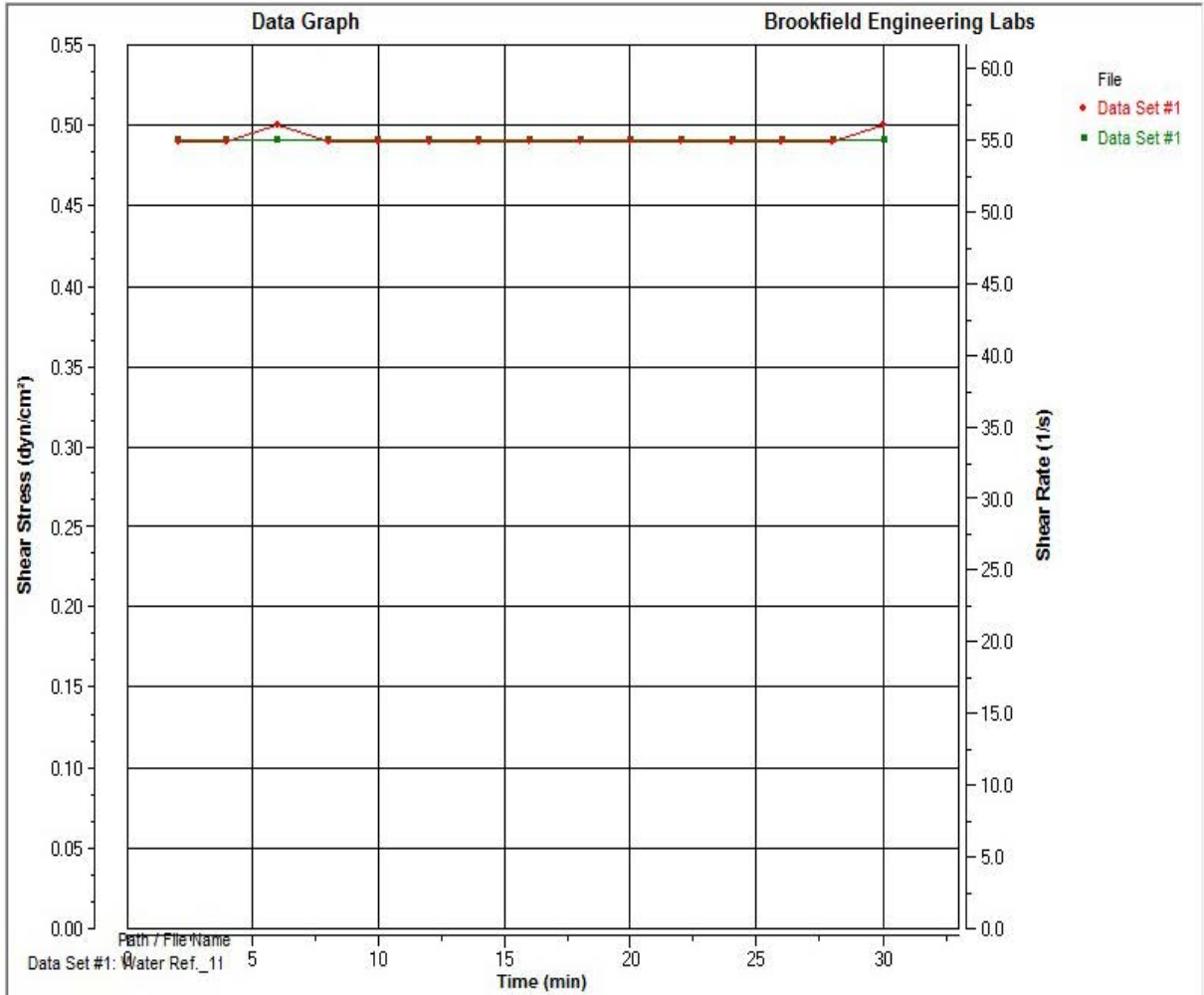
Test Method:		Test Name: {unsaved test}	
Saved on: 30/06/2016 1:04:00 PM	XAxis: Time	Instructions:	
Spindle: ULA	YAxis: Viscosity		
# of Steps: 1	Y2Axis: Time		
# of Loops: 0	ShowY2: False		
Math Model: Bingham	Avg. Steps: False		
Calc Yield: False	Avg. Test: False		
Auto Inc: True	Default Data Path:		

Step (#)	Speed (RPM)	Inc Speed	Use Temp	Temp (°C)	Inc Temp	Data Type	Data Int (hh:mm:ss)	Avg Dur (hh:mm:ss)	Point at End	End Type	End Value	End Tol	Density (g/cm³)	QC Type	QC Low	QC High	In Test Avg	
1	45	False	False	0.0	False	Multi Pt	00:02:00.0	00:00:00	False	Time	1800.0 sec	0.0	0.0000	None	0	0	%	False

Loop (#)	Step (#)	Point (#)	Viscosity (cP)	Speed (RPM)	Torque (%)	Shear Stress (dyn/cm²)	Shear Rate (1/s)	Temp (°C)	Bath (°C)	Time (hh:mm:ss)	Stress (dyn/cm²)	Strain (rad)	Density (g/cm³)
0	1	1	0.89	45	6.7	0.49	55.04	25.1	EEEE	00:02:00.1	----	----	----
0	1	2	0.89	45	6.7	0.49	55.04	25.1	EEEE	00:04:00.1	----	----	----
0	1	3	0.91	45	6.8	0.50	55.04	25.1	EEEE	00:06:00.1	----	----	----
0	1	4	0.89	45	6.7	0.49	55.04	25.1	EEEE	00:08:00.1	----	----	----
0	1	5	0.89	45	6.7	0.49	55.04	25.1	EEEE	00:10:00.1	----	----	----
0	1	6	0.89	45	6.7	0.49	55.04	25.2	EEEE	00:12:00.1	----	----	----
0	1	7	0.89	45	6.7	0.49	55.04	25.1	EEEE	00:14:00.1	----	----	----
0	1	8	0.89	45	6.7	0.49	55.04	25.1	EEEE	00:16:00.1	----	----	----
0	1	9	0.89	45	6.7	0.49	55.04	25.1	EEEE	00:18:00.1	----	----	----
0	1	10	0.89	45	6.7	0.49	55.04	25.1	EEEE	00:20:00.1	----	----	----

Appendix C 3 Shear rate and shear stress versus the time for fresh water sample

Data Graph:



Appendix C 4 Brookfield digital Rheometer calibration with standard fluid of 49 cP@ room Temp

Rheocalc T 1.2.19

Brookfield Engineering Labs Inc.

Data Report

Sample Information: **Sample Name:** Standard fluid 49

Tester Name: TK: 0.09375 **Sample Notes:**
Run Time: 12/07/2016 3:29:00 PM **SMC:** 0.64
Serial Number: 8691741 **SRC:** 1.22
Torque Range: LV **YMC:** 0

Test Method: **Test Name:** {unsaved test}

Saved on: 12/07/2016 3:29:00 PM **XAxis:** Time **Instructions:**
Spindle: ULA **YAxis:** Shear Stress
of Steps: 1 **Y2Axis:** Shear Rate
of Loops: 0 **ShowY2:** True
Math Model: Bingham **Avg. Steps:** False
Calc Yield: False **Avg. Test:** False
Auto Inc: True **Default Data Path:**

Step (#)	Speed (RPM)	Inc Speed	Use Temp	Temp (°C)	Inc Temp	Data Type	Data Int (hh:mm:ss)	Avg Dur (hh:mm:ss)	Point at End	End Type	End Value	End Tol	Density (g/cm³)	QC Type	QC Low	QC High	In Test Avg	
1	7	False	False	0.0	False	Multi Pt	200	.	False	Time	600.0 sec	0.0	0.0000	None	0	0	%	False

Averaging:

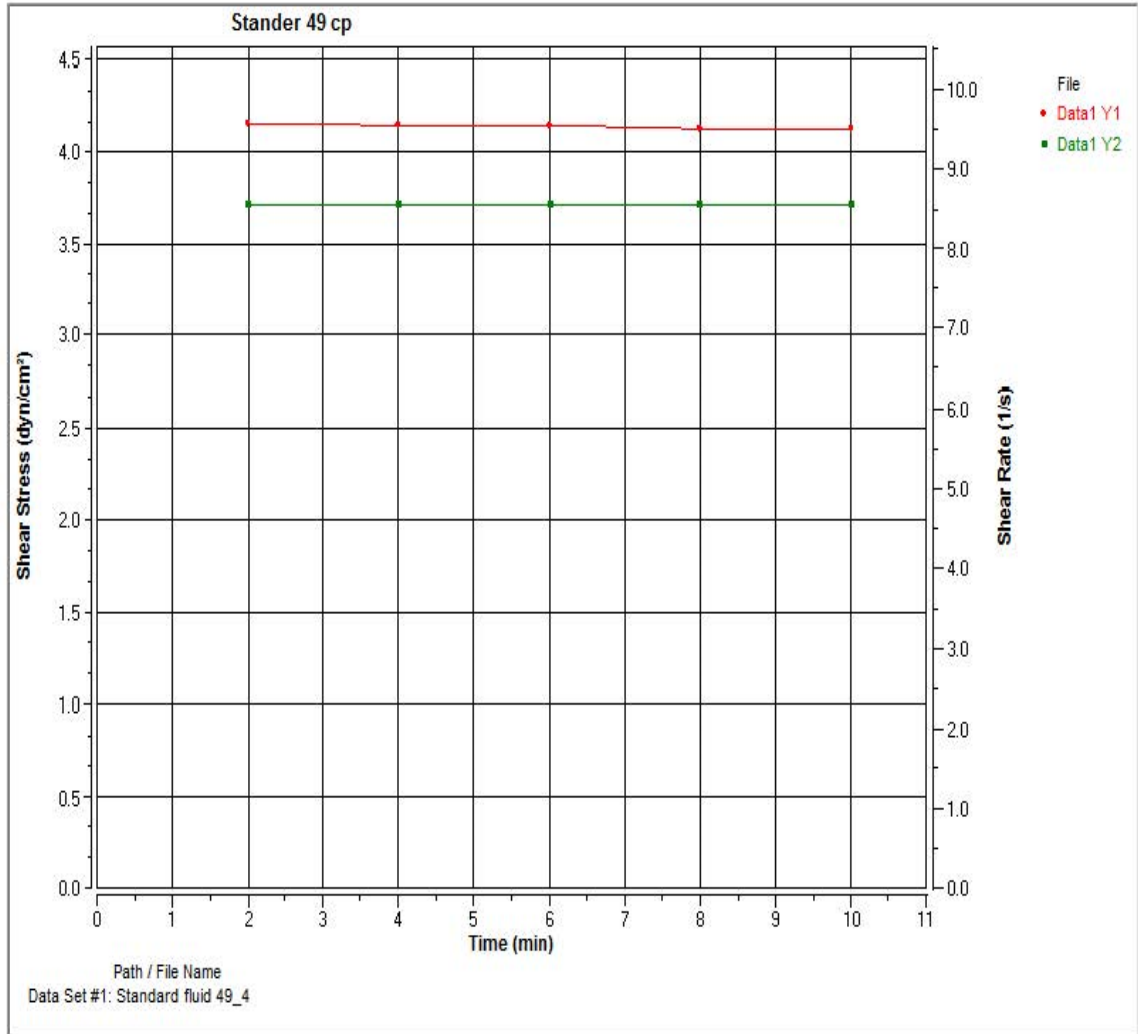
Step (#)	Viscos (cP)	Speed (RPM)	Torqu (%)	Shear (dyn/cm²)	Shear (1/s)	Tempe (°C)	Bath (°C)	Densit (g/cm³)
0	Averag	49.00	0	0.0	4.14	8.561	0.0	0.0
0	Standa	0.00	0	0.0	0.00	0.00	0.0	0.0

Data:

Loop (#)	Step (#)	Point (#)	Viscos (cP)	Speed (RPM)	Torque (%)	Shear (dyn/cm²)	Shear (1/s)	Temp (°C)	Bath (°C)	Time (hh:mm:ss)	Stress (dyn/cm²)	Strain (rad)	Densit (g/cm³)
0	1	1	49.00	7	56.6	4.15	8.561	25.1	EEEE	00:02:	----	----	----
0	1	2	49.00	7	56.4	4.14	8.561	25.1	EEEE	00:04:	----	----	----
0	1	3	49.00	7	56.4	4.14	8.561	25.1	EEEE	00:06:	----	----	----
0	1	4	49.00	7	56.3	4.13	8.561	25.1	EEEE	00:08:	----	----	----

Appendix C 5 Shear rate and shear stress versus the time for standard fluid of 49 cP

Data Graph:



Appendix C 6 Brookfield digital Rheometer calibration with standard fluid of 98 cP@ room Temp

Rheocalc T 1.2.19

Brookfield Engineering Labs Inc.

Data Report

Sample Information: Sample Name: Standard fluid 98

Tester Name: TK: 0.09375
 Run Time: 12/07/2016 4:13:00 PM SMC: 0.64
 Serial Number: 8691741 SRC: 1.22
 Torque Range: LV YMC: 0

Sample Notes:

Test Method: Test Name: {unsaved test}

Saved on: 12/07/2016 4:13:00 PM XAxis: Time
 Spindle: ULA YAxis: Shear Stress
 # of Steps: 1 Y2Axis: Shear Rate
 # of Loops: 0 ShowY2: True
 Math Model: Bingham Avg. Steps: False
 Calc Yield: False Avg. Test: False
 Auto Inc: True Default Data Path:

Instructions:

Step (#)	Speed (RPM)	Inc Speed	Use Temp	Temp (°C)	Inc Temp	Data Type	Data Int (hh:mm:ss)	Avg Dur (hh:mm:ss)	Point at End	End Type	End Value	End Tol	Density (g/cm³)	QC Type	QC Low	QC High	In Test Avg	
1	3	False	False	0.0	False	Multi Pt	200		False	Time	600.0 sec	0.0	0.0000	None	0	0	%	False

Data:

Loop (#)	Step (#)	Point (#)	Viscos (cP)	Speed (RPM)	Torque (%)	Shear (dyn/cm²)	Shear (1/s)	Temp (°C)	Bath (°C)	Time (hh:mm:ss)	Stress (dyn/cm²)	Strain (rad)	Densit (g/cm³)
0	1	1	98.00	3	49.0	3.60	3.669	25.1	EEEE	00:02	----	----	----
0	1	2	97.60	3	48.8	3.58	3.669	25.1	EEEE	00:04	----	----	----
0	1	3	97.60	3	48.8	3.58	3.669	25.1	EEEE	00:06	----	----	----
0	1	4	97.60	3	48.8	3.58	3.669	25.1	EEEE	00:08	----	----	----
0	1	5	97.60	3	48.8	3.58	3.669	25.1	EEEE	00:10	----	----	----

Figure C.3 Shear rate and shear stress versus the time for standard fluid of 98 cP.

Data Graph:

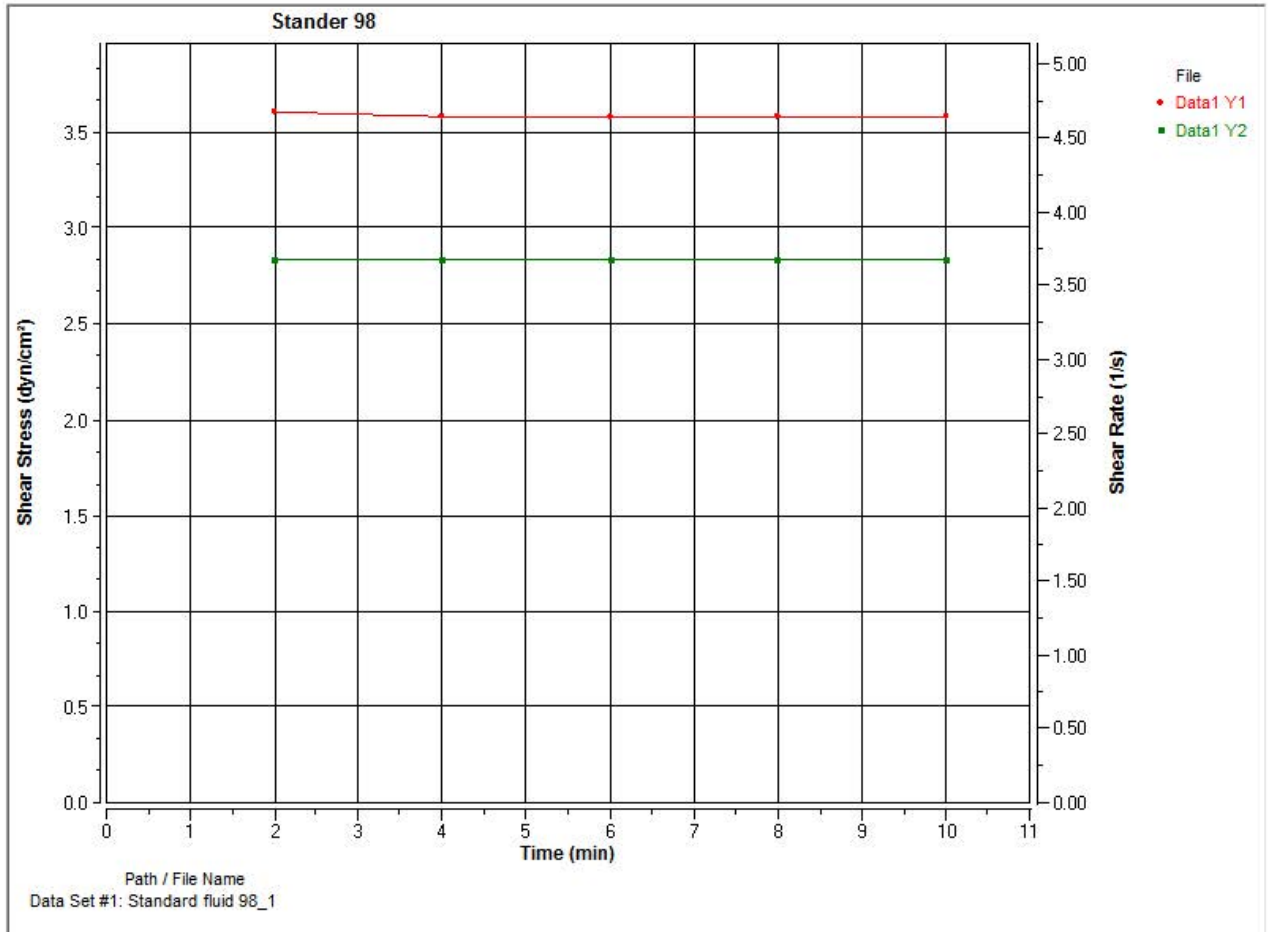


Table C.4 Brookfield digital Rheometer reading of light mineral oil @ room Temp

Rheocalc T 1.2.19

Brookfield Engineering Labs Inc.

Data Report

Sample Information: Sample Name: Light Mineral Oil

Tester Name: TK: 0.09375
 Run Time: 01/07/2016 2:18:00 PM SMC: 0.64
 Serial Number: 8691741 SRC: 1.22
 Torque Range: LV YMC: 0

Sample Notes:

Test Method: Test Name: (unsaved test)

Saved on: 01/07/2016 2:18:00 PM XAxis: Time
 Spindle: ULA YAxis: Shear Stress
 # of Steps: 1 Y2Axis: Shear Rate
 # of Loops: 0 ShowY2: True
 Math Model: Bingham Avg. Steps: False
 Calc Yield: False Avg. Test: False
 Auto Inc: False

Instructions:

Default Data Path:

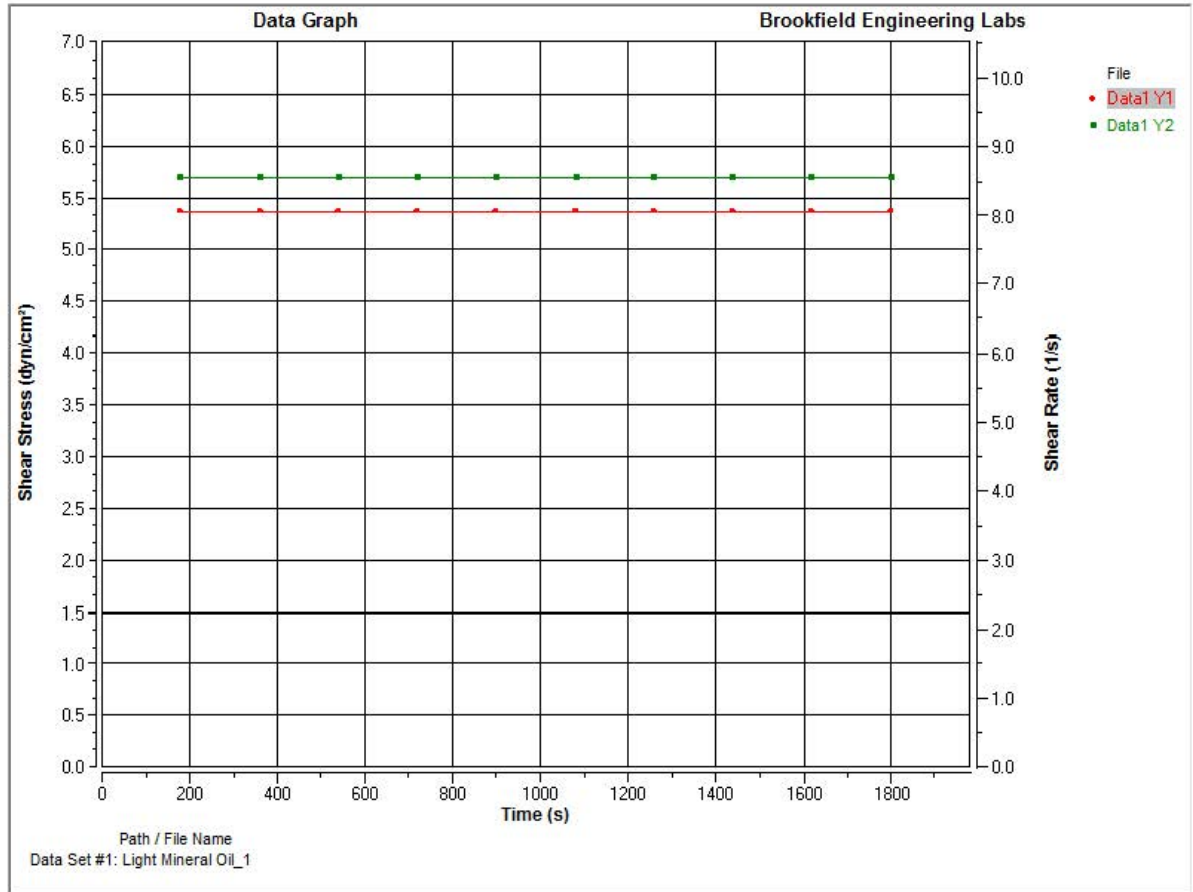
Step (#)	Speed		Temp		Data Int		Avg Dur		Point at End	End Type	End Value	End Tol	Density			In Test Avg		
	(RPM)	Inc Speed	Use Temp	(°C)	Inc Temp	Data Type	(hh:mm:ss)	(hh:mm:ss)					(g/cm³)	QC Type	QC Low		QC High	
1	7	False	False	0.0	False	Multi Pt	300	.	False	Time	1800.0 sec	0.0	0.0000	None	0	0	%	False

Data:

Loop (#)	Step (#)	Point (#)	Viscos (cP)	Speed (RPM)	Torque (%)	Shear (dyn/cm²)	Shear (1/s)	Temp (°C)	Bath (°C)	Time (hh:mm:ss)	Stress (dyn/cm²)	Strain (rad)	Densit (g/cm³)
0	1	1	62.74	7	73.2	5.37	8.561	25.1	EEEE	00:03:	----	----	----
0	1	2	62.74	7	73.2	5.37	8.561	25.1	EEEE	00:06:	----	----	----
0	1	3	62.74	7	73.2	5.37	8.561	25.1	EEEE	00:09:	----	----	----
0	1	4	62.74	7	73.2	5.37	8.561	25.1	EEEE	00:12:	----	----	----
0	1	5	62.74	7	73.2	5.37	8.561	25.1	EEEE	00:15:	----	----	----
0	1	6	62.74	7	73.2	5.37	8.561	25.1	EEEE	00:18:	----	----	----
0	1	7	62.74	7	73.2	5.37	8.561	25.1	EEEE	00:21:	----	----	----
0	1	8	62.74	7	73.2	5.37	8.561	25.1	EEEE	00:24:	----	----	----
0	1	9	62.74	7	73.2	5.37	8.561	25.1	EEEE	00:27:	----	----	----
0	1	10	62.74	7	73.2	5.37	8.561	25.1	EEEE	00:30:	----	----	----

Figure C.4 Shear rate and shear stress versus the time for standard fluid of 98 cP.

Data Graph:



Chapter 6

6 Conclusions and Recommendations

6.1 Conclusions

- The potential of utilizing ultrasonic based techniques to monitor emulsion layer in separation vessels such as crude oil desalter operation has been demonstrated through a series of tests and detailed analysis of data. It is demonstrated that a high degree of confidence in the measurements is achievable with simultaneous measurements of acoustic velocity, attenuation and statistical analysis of the acquired data.
- The applicability of ultrasonic techniques to monitor emulsion stability has been demonstrated with emulsions of different crude oils. The emulsion stability can be easily tracked by recording changes in attenuation and acoustic velocity.
- Higher attenuation were recorded in emulsions prepared at higher mixing speed (rpm). This was attributed to decrease in droplet size with increasing agitation speed.
- Higher stability of heavier crude emulsions can be attributed to its higher asphaltene content which stabilize small droplets and increase their concentration in the emulsion phase.
- Shear stress significantly increased with shear rate and the emulsion experienced the non-Newtonian flow behavior while the emulsion viscosity was gradually decreased with increasing of shear rate.

6.2 Recommendations

- Ultrasonic technique can be further developed to predict droplet size distribution in emulsions to help further characterize emulsions due to significant influence of droplet size on both emulsion rheology and stability. This would require analyzing frequency spectrum and application of mechanisms contributing to attenuation.
- There is a need to systematically study effects of solid particles size and properties, covering the range from micron to submicron and nano-size particles on emulsion stability.
- The technique can be used to determine optimum concentrations of emulsifier/de-emulsifier for a given application and minimize their consumption.
- There is also need to study interactions of surfactant molecules and aspltenes with nano particles toward the emulsion stability.
- There is need to further investigate emulsion rheology aimed at development of optimum probe design to cover wider range of applications.

Curriculum Vitae

Name: Embark Alshaafi

Post-secondary Education and Degrees: The University of Western Ontario
London, Ontario, Canada
2015-2017 M.Sc.

Higher Institute of Engineering Technology
Zliten, Zliten, Libya
2007-2012 B.Sc.

Petroleum training Qualified Institute
Qerqarish, Tripoli, Libya
2003-2006 B. Tech.

Honours and Awards: Libyan ministry of higher education
and scientific research Scholarship
2014-2017

Highly Qualified Professionals (HQP)
Biofuel Net Canada BFN, Vancouver
2016

Related Work Experience

Research Assistant & Teaching Assistant
The University of Western Ontario
2015-2017

Petroleum Engineer
Eni oil & Gas Company
Libya, 2006-Present

Technical support Engineer & Data Acquisition Supervisor
Gas & Oil fields services company
Kuwait, 2013-2014

Publications:

Ultrasonic Techniques to Characterize and Monitor Water-in-Oil Emulsion, Oral and technical presentation in 19th International Conference on Oil and Gas Research, May 2017. Montreal, Canada.

Ultrasonic Techniques to Characterize and Monitor Water-in-Oil Emulsion, Oral presentation for Imperial Oil Company, Western Ontario University, May 2017. London, Canada.